Cape Peninsula University of Technology

A Comparison between Volumetric Modulated Arc Therapy and 3D Conformal Radiotherapy of Stage 3 and 4 Carcinoma of the Larynx.

By

Theresa Binz - Nat Dip (T) (CPUT), B Tech (T) (CPUT)

Thesis submitted in fulfilment of the requirements for the degree

Master of Science in Radiography

in the Faculty of Health and Wellness Sciences

at the Cape Peninsula University of Technology

Supervisor:	Ms. B. Wyrley-Birch (M.Tech: Rad)
Co-supervisors:	Dr. L. Hudson (Doctor of Radiography: D Rad)
Co-supervisor and clinical advisor:	Dr. S. Dalvie MBChB and FC (Radiation Oncology)
	Mr. C. Trauernicht M Sc. (Med) in Medical Physics

Bellville

Date submitted 14 / 12 / 2020

DECLARATION

I, Theresa Binz, declare that the contents of this thesis represent my own unaided work, and that the thesis has not previously been submitted for academic examination towards any qualification. Furthermore, it represents my own opinions and not necessarily those of the Cape Peninsula University of Technology.

14 / 12 / 2020

Signed Date

ABSTRACT

Abstract Title:

A Comparison between Volumetric Modulated Arc Therapy and 3D Conformal Radiotherapy of Stage 3 and 4 Carcinoma of the Larynx.

Introduction:

The introduction of advanced radiation therapy equipment that has the ability to deliver modulated radiation therapy that can replace conventional three-dimensional conformal radiation therapy (3DCRT) methods means that comparisons are needed to understand the clinical impact for the patient. The radiation therapy treatment planning of stage 3 and 4 cancer of the larynx is challenging owing to the proximity of organs at risk (OAR) to the large tumour volume. The International Commission of Radiation Units and Measurements (ICRU) recommend that the dose to the Planning Target Volume (PTV) and the Planning Organ at Risk Volume (PRV) must be reported. The purpose of this research study is to determine the accuracy and reproducibility of the treatment set-up to enable the calculation of the Clinical Target Volume (CTV) to PTV and OAR to PRV margins that should be used for patients treated in the head and neck area. The study also compared the 3DCRT plans to the VMAT plans where the evaluation was based on the doses the OAR received and the conformity and homogeneity of the dose to the PTV.

Method:

In order to determine reproducibility of the treatment setup all patients, those who were treated over a period of 1 year with a thermoplastic mask, and who had a minimum of 5 image sets were studied. Thirty-three (33) patients were treated in both the head and neck area, and 36 patients were treated in the head area only. In each case the Digitally Reconstructed Radiography (DRR) created from the planning Computer Tomography (CT) images were compared to the weekly Electronic Portal Imager Devices' (EPID) images. The van Herk's equation was used to determine the expansion margins in 3 directions: superior to inferior, left to right and anterior to posterior.

As these expansion margins were unknown at time of the study, the current departmental practice of a 5mm margin was applied for the treatment plan comparisons. The plan data sets of 10 patients with stage 3 and 4 cancer of the larynx was used to re-create comparative plans. As some OAR were omitted at the original planning process for the treated Volumetric Modulated Arc Therapy (VMAT) plans (labelled "*RA treat*"), a secondary RA plan was created where all the OAR was present (labelled "*RA study*"), and these plans were compared to the 3DCRT plans (labelled 3DCRT). Each of the 10 patient-data sets had 3 plan groups.

OAR criteria were recorded for the brainstem, spinal cord, parotids, cochlea, temporomandibular joints, oral cavity, and mandible.

The homogeneity index (HI), conformity index (CI) and lesion coverage factor measurements were compared for all plan data sets to determine the impact of each planning technique to the dose to the PTV.

Results:

In terms of treatment accuracy and reproducibility 227 image sets were used to calculate the expansion margins needed of patients treated in both the head and neck area. The use of van Herk's equation indicated that the CTV to PTV expansion was 5.6 mm in the anterior to posterior direction, 6.9 mm in the superior to inferior direction and 6.5 mm in the left to right direction. For those treated in only the head area, 273 image sets were evaluated and resulted in 5.1 mm in the anterior to posterior direction, 6.1 mm in the superior to inferior direction and 4.9 mm in the left to right direction.

For the comparison between VMAT and 3DCRT, a custom plan score system was developed to record results between the planning techniques. The score for the doses to the OAR when comparing the 3DCRT technique to the *RA treat* group indicated equal scores. The 3DCRT compared to the *RA study* group, resulted in 8 (of the 10) patients in the *RA study* group achieving better OAR sparing. In the comparison of the *RA treat* and the *RA study* group, 7 of the 10 patients achieved better OAR sparing with the *RA study* group with 1 of the 10 patients an equal score.

The score results for the PTV dose (coverage, homogeneity, and conformity) indicated no statistical significance between the *RA study* and *RA treat* groups. Comparing the 3DCRT group to the *RA treat* group, 9 of the 10 patients had worse dose results for the 3DCRT plans. Comparing the 3DCRT group to the *RA study* group, all 3DCRT plans scored worse for PTV dose quality.

Conclusion:

This study indicates that current PTV and PRV expansion margins are too small. As this information was previously unclear, the results of this study could be used as a baseline, and a tool to implement more rigorous checks and imaging protocols to lessen these margins.

The results of the dose to normal tissue when comparing 3DCRT to VMAT plans did not indicate large differences, however the score results of the PTV dose, indicated that VMAT offers large improvements compared to the 3DCRT technique.

ACKNOWLEDGEMENTS

Dr. Sameera Dalvie (Radiation Oncologist Consultant) for all the contour, plan and EPID checks as well as scrutinising this thesis and her continuous support.

Senior Radiation Therapists at the Radiation Oncology department for all the independent checks of the EPID images matching results.

Mr. Chris Trauernicht (Chief Physicist) for hours of calculation checks, consultations, and support to enable this research to be completed successfully. Your positive contribution and feedback were more that I could ask for, and I am grateful.

Dr. Corrie Uys (Statistician at CPUT) for your dedication and assistance in the search for a statistical analysis tool, to evaluate the results of this research. You went over and above to assist me, and I am grateful.

Supervisors from Cape Peninsula University of Technology Ms. B. Wirley-Birch and Dr. L. Hudson.

DEDICATION

To my dearest husband Matthias Binz, my rock, who enable me to pursue the career that I love.

To my children Luca and Leon, who always understand when Mamma is busy with her studies. I love you dearly. May you one day enjoy research as much as I.

Most importantly, to the almighty God, who protect and guide me, and have provided me with this calling and the talent to be able to create radiation therapy plans, for each of our wonderful patients.

To all the oncologists, physicists and fellow radiation therapists who have mentored me over the years at Groote Schuur Hospital, especially Prof. Claire Stannard, who have inspired me to do this research.

In loving memory of my mother who passed on during the conclusion of this thesis. You would have enjoyed reading this.

Thank you

TABLE OF CONTENTS

ACKNOWLEDGEMENTS v
DEDICATION vi
TABLE OF CONTENTS vii
LIST OF FIGURES xiv
LIST OF TABLES xxi
LIST OF EQUATIONS xxii
LIST OF APPENDICES xxiii
GLOSSARY xxiv
CHAPTER 1 Introduction and Rationale 1-1
1.1 Introduction 1-1
1.2 Purpose of this study 1-2
1.3 Statement of the problem and research question 1-2
1.3.1 Statement of the problem 1-2
1.3.2 Research question 1-3
1.4 The study-site 1-3
1.5 Research methodology 1-3
1.5.1 Sub-question 1 1-3
1.5.2 Sub-question 2 and 3 1-4
1.6 Rationale 1-4
1.7 Overview of thesis 1-5
1.7.1 Chapter 2 Theoretical Research and Background Information 1-5
1.7.2 Chapter 3 The Clinical Research Process 1-5
1.7.3 Chapter 4 Research Results 1-6
1.7.4 Chapter 5 Conclusion and Recommendations 1-6
CHAPTER 2 Theoretical Research and Background Information 2-1
2.1 Introduction 2-1
2.2 Larynx cancer 2-1
2.2.1 Anatomy of the larynx and the significance of the surrounding lymphatics . 2-1
2.2.2 Larynx cancer staging 2-3
2.2.3 Recommended treatment methods 2-5
2.2.4 Statistics of laryngeal cancer in South Africa and the world 2-8

2.2.5 Risk factors for larynx cancer 2-9
2.3 Immobilisation and stability 2-10
2.3.1 Literature survey of immobilisation devices and accuracies 2-11
2.3.2 Construction of the thermoplastic mask 2-14
2.4 Anatomical modelling & contouring 2-16
2.4.1 The purpose of the anatomical modelling process 2-16
2.4.2 Computed Tomography and patient positioning 2-16
2.4.3 Guidelines for the contouring of the tumour and therapeutic margins. 2-17
2.4.4 Guidelines for the contouring of organs at risk 2-21
2.4.5 Contouring of the organs at risk in this study 2-25
2.4.5.1 Brain and brainstem 2-25
2.4.5.2 Spinal cord and posterior neck structure 2-25
2.4.5.3 Cochlea 2-26
2.4.5.4 Temporomandibular joint and mandible 2-27
2.4.5.5 Oral cavity 2-28
2.4.5.6 Parotids 2-30
2.4.5.7 Shoulders 2-31
2.4.5.8 Contrast 2-32
2.4.5.9 Immobilisation devices 2-34
2.5 Radiation therapy and therapeutic advances 2-35
2.5.1 Improvement in CT imaging 2-35
2.5.2 Improvement in radiation therapy planning and treatment 2-36
2.5.3 Improvement in patient image guidance at treatment 2-37
2.6 Treatment uncertainties and positioning set-up errors 2-39
2.7 Image matching 2-44
2.7.1 Imaging during radiation therapy treatment 2-44
2.7.2 Imaging for the patient receiving radiation therapy to the head and neck region 2-45
2.7.3 Imaging for the patient receiving radiation therapy to the head region 2-46
2.8 Conclusion 2-47

CHAPTER 3 The Clinical Research Processes 3-1
3.1 Introduction 3-1
3.2 Research strategy 3-1
3.2.1 Research design 3-1
3.2.2 Method of analysis 3-2
3.3 Data collection, production, and analysis 3-2
3.3.1 The clinical research process for sub-question 1: How accurate and reproducible is the treatment set-up? 3-2
3.3.1.1 Patient numbers and inclusion criteria 3-2
3.3.1.2 Data preparation for the head and neck matching 3-5
3.3.1.3 Head and neck DRR contouring 3-7
3.3.1.4 Data preparation for the head matching - CT interpolation 3-11
3.3.1.5 Head DRR contouring 3-14
3.3.1.6 The data collection process and measurements 3-17
3.3.1.6.1 Digital matching 3-17
3.3.1.6.2 Manual matching 3-17
3.3.1.6.3 Rotation measurements 3-18
3.3.1.6.4 Peer review 3-20
3.3.1.7 Case study demonstration: Why it is important to apply a rotation in head and neck matching 3-21
3.3.1.8 Uncertainties during data collection 3-24
3.3.1.8.1 Interpolation 3-24
3.3.1.8.2 Verification uncertainty 3-28
3.3.1.8.3 Limited data of anatomical site 3-29
3.3.1.8.3.1 Head and neck radiation therapy example 3-30
3.3.1.8.3.2 Head only radiation therapy example 3-31
3.3.1.8.4 DRR quality 3-33
3.3.1.8.5 Mismatch in treatment area vs verification area 3-33
3.3.1.8.6 Auto match failure 3-34
3.3.1.8.7 DRR of children 3-35
3.3.1.8.8 Total anatomical miss-match 3-36

3.3.1.8.9 Immobilisation devices or CT bed included in DRR creation 3-38
3.3.2 The clinical research process for sub-question 2: What are the critical organ doses for the two planning techniques? 3-39
3.3.2.1 Organ at risk creation 3-39
3.3.2.2 Contouring PRV and “help” contours 3-41
3.3.2.3 Dose recording 3-44
3.3.3 The clinical research process for sub-question 3: Which planning technique offers the best dose coverage and dose homogeneity 3-45
3.3.3.1 Diagnosis 3-45
3.3.3.2 Creation of the treatment plans 3-45
3.3.3.3 Data recording 3-47
3.4 Conclusion 3-47
CHAPTER 4 Research Results 4-1
4.1 Introduction 4-1
4.2 Research results for sub-question 1: How accurate and reproducible is the treatment set-up 4-1
4.2.1 *Head and neck* patient imaging information 4-1
4.2.2 *Head and neck* imaging results 4-4
4.2.3 Head patient imaging information. 4-7
4.2.4 Head imaging results 4-10
4.2.5 In summary 4-13
4.3 Research results for sub-question 2: What are the critical organ doses for the two planning techniques? 4-14
4.3.1 Patient demographics and plan evaluation score system 4-14
4.3.2 Brainstem 4-16
4.3.3 Spinal cord 4-21
4.3.4 Parotids 4-23
4.3.5 Cochlea 4-26
4.3.6 Lungs 4-27
4.3.7 Temporomandibular Joints 4-28
4.3.8 Oral cavity 4-30

4.3.9 Mandible 4-33
4.3.10 Shoulders 4-36
4.3.11 Summary of plan scoring results for all the organs at risk 4-37
4.4 Research results for sub-question 3: Which planning technique offers the best dose coverage and dose homogeneity of the PTV 4-39
4.4.1 Dose coverage 4-39
4.4.2 Conformity index scoring system 4-41
4.4.3 The lesion coverage factor 4-42
4.4.4 Lesion coverage results 4-43
4.4.5 Homogeneity index 4-44
4.4.6 Plan scoring results for homogeneity and conformity and coverage of dose to the PTV 4-46
4.5 Summation of research results for both sub-question 2 and 3 4-48
4.6 Conclusion 4-50
CHAPTER 5 Conclusion and Recommendations 5-1
5.1 Introduction 5-1
5.2 Conclusion of Sub-question 1: How accurate and reproducible is the treatment set-up 5-1
5.3 Recommendations to sub-question 1: How accurate and reproducible is the treatment set-up 5-5
5.3.1 Introduction 5-5
5.3.2 Including the vertex of skull in the planning CT 5-5
5.3.3 DRR Quality and Creation 5-6
5.3.3.1 Thinner CT slice thickness 5-6
5.3.3.2 Standardise greyscale selection 5-6
5.3.3.3 Cropping the CT data to exclude the CT bed artefact when creating the DRR 5-7
5.3.3.4 Standardise anatomical levels for EPID imaging 5-7
5.3.3.5 Imaging margins for patients receiving RT in both the head and neck area 5-7
5.3.3.6 Imaging margins for patients receiving RT to the head area. 5-8

5.3.4 Contouring on DRR 5-9
5.3.4.1 Bi-lateral structure contouring 5-9
5.3.4.2 Contouring at least three anatomical structures for each matching direction 5-9
5.3.5 EPID image acquisition 5-10
5.3.5.1 Double exposure adds little value 5-10
5.3.5.2 Include bilateral anatomy on the anterior image 5-11
5.3.5.3 Include anterior, posterior and where possible the vertex on the lateral image 5-12
5.3.5.4 Measure and correct rotation of anatomy 5-12
5.3.5.5 Standardise and then imaging frequency 5-12
5.3.6 Systematic error correction 5-12
5.3.7 Role expansion for RTTs, regular protocol and audit requirements, and further investigations required 5-14
5.3.7.1 Current immobilisation devices should be investigated 5-14
5.3.7.2 Strict imaging protocols should insure that all imaged data are evaluated and approved 5-14
5.3.7.3 Imaging protocols should stipulate exact anatomical contours needed on DRR's for each treatment site 5-14
5.3.7.4 RTT role expansion as imaging specialist is needed 5-14
5.3.7.5 RTT skills auditing 5-15
5.3.7.6 Yearly imaging audits of set-up accuracy 5-15
5.3.7.7 Rotational errors should be investigated 5-15
5.4 Conclusion of sub-questions 2 and 3 5-16
5.5 Recommendations to sub-question 2 and 3 5-19
5.5.1 Organs at risk 5-19
5.5.1.1 Recommended mandatory OAR contours that should be included for advanced stage larynx cancer 5-19
5.5.1.2 Brainstem and brain contour to be included for one (very high dose) phase of treatment planning 5-19
5.5.1.3 Lung contours not mandatory for late stage larynx cancer 5-19

5.5.1.4 More prospective research needed for OAR tolerance doses in VMAT planning 5-20
5.5.1.5 Contrast agent administration protocol to be investigated to lesser density of contrast in subclavian vain 5-20
5.5.2 Verification of shoulder positioning needs further research 5-20
5.5.3 Peer review needed for OAR contouring 5-21
5.5.4 Better OAR sparing demonstrated when they were contoured before planning 5-21
5.5.5 Multiple phases of treatment increase OAR sparing 5-21
5.5.6 GTV, CTV and PTV contouring 5-21
5.5.7 3DCRT for late stage larynx cancer 5-22
5.5.8 Therapeutic indexes are not useful in evaluation of late stage larynx planning 5-22
5.5.9 Plan score results 5-23
5.6 Conclusion to this research study 5-23
List of References ..... a

LIST OF FIGURES

Figure 2.1: Male (blue) and female (pink) larynx cancer incidence from 2004 to 2014 in South Africa (Cancer in South Africa 2003-2014 Full Report, 2014) 2-8
Figure 2.2: Average age specific Incidences of larynx cancer from 2004-2014 for males (blue) and females (pink) in Sough Africa (Cancer in South Africa 2003-2014 Full Report, 2014) . 2-8
Figure 2.3: Box Label of mask system used on all patients Included in this study 2-13
Figure 2.4: Klarity RG461-4S 3.2mm mask system on the S-frame base that fasten to the treatment couch. (KlarityMedical, 2013) 2-13
Figure 2.5: Graphical example of the GTV, CTV and PTV expansions of a head and neck cancer patient with a intact tumour and metastatic nodal spread to the left cervical nodes (illustration produced by author) 2-19
Figure 2.6: Graphic representation of a post-surgical head and neck cancer patient, where no GTV is present (illustration produced by author) 2-19
Figure 2.7: Organ at Risk 1 (OAR1) that is expanded to create the Planning Risk Volume 1 (PRV 1), and overlaps with the PTV-N. OAR 2 represents the Spinal Cord and is expanded to the PRV2, and does not overlap with any PTV (illustration produced by author) 2-22
Figure 2.8: Dose distribution of a 3DCRT plan on the Left, and a VMAT plan on the Right, indicating the relative difference of dose distribution around the parotids OAR (enlarge image of left parotid can be seen in Figure 2.9 (illustration produced by author)..... 2-24
Figure 2.9: Enlarged image of the dose distribution around the left parotid and PRV of the patient illustrated in Figure 2.8. Annotation A indicates the slow dose fall-off seen in the 3DCRT plan inside the parotid, and annotation B indicates the rapid dose fall-off that can be obtained using VMAT planning inside the left parotid and PRV (illustration produced by author)..... 2-24
Figure 2.10: Contouring of the brain (purple), brainstem and brainstem PRV (brown) (illustration produced by author) 2-25
Figure 2.11: Illustration of the spinal cord PRV (mint green) and the posterior neck dose avoidance structure (light blue) (illustration produced by author) 2-26
Figure 2.12: Right cochlea (black), and left cochlea (blue), both expanded by 5mm to create the PRV (illustration produced by author) 2-27
Figure 2.13: Illustration of the right temporomandibular joint (Pink) that includes the head of the mandible as well as the whole mandibular fossa (illustration produced by author) 2-27
Figure 2.14: The right TMJ (pink) expanded by 5mm to create the PRV (illustration produced by author) 2-28
Figure 2.15: The mandible contour (yellow) expanded by 5 mm to create the PRV. The right side demonstrates the cropped PRV structure, with a gap of 5 mm between the PTV (red) and the PRV (yellow) (illustration produced by author) 2-28

Figure 2.16: The oral cavity (yellow) is contoured superiorly from the hard palate and includes the whole oral cavity (illustration produced by author) 2-29
Figure 2.17: The oral cavity's (light brown) posterior border was kept at 5 mm anterior to the most anterior extent of the PTV (red) (illustration produced by author) 2-29
Figure 2.18: The right parotid (bright green) and left parotid (mint green) were contoured in their entirety. Both were expanded by 5 mm to create the PRV. This PRV was cropped to create an avoidance structure, and a gap of 3 mm was placed between this avoidance structure and the PTV (red) (illustration produced by author) 2-31
Figure 2.19: The right shoulder contour (light purple) was contoured 2cm lateral to the most lateral extent of the PTV and included all soft-tissue of the shoulder superiorly. This contour was then cropped to be inside the body contour (Right sided image) (illustration produced by author) 2-32
Figure 2.20: An illustration of the inferior extent of the right and left shoulder contour (purple) that extends inferiorly until at least 3cm inferior to the PTV (red) (illustration produced by author) 2-32
Figure 2.21: Hounsfield values and Mass Density measurement in the right internal carotid artery (top image), vertebral body (middle image) and contrast filled left subclavian vain (illustration produced by author) 2-33
Figure 2.22: The external contour includes the body of the patient, the mask system as well as the S-frame base plate used during CT scanning and treatment. The right image shows a 3D representation of the whole external contour, and the middle sagittal image shows the exclusion of the CT-bed from this contour (illustration produced by author) 2-35
Figure 2.23: Random and Systematic Uncertainty (illustration produced by author) 2-41

Figure 3.1: Patient numbers and cancer site, included in study who received treatment of the head and neck region (figure produced by author) 3-4
Figure 3.2: Patient numbers and cancer site included in study who received treatment of the head region (figure produced by author) 3-4
Figure 3.3: Guiding contours found on patient data. (a) Anterior vertebral bodies demarcated, as well as crosses and lines on spinous and transverse processes. (b) Crosses on bony structures of the vertebral bodies. (c) Line indicating mandibular body and base of skull (occipital bone). (d) Spinous process contoured as well as a cross on the uncinate process and zygapophyseal joint (illustration produced by author) 3-5
Figure 3.4: Illustration of applying auto matching of the head and neck patient's anterior isocentre verification image. Guiding contours have been drawn on the DRR (a), and projected onto the EPID image (b), to verify the auto matching algorithm that was applied inside the red block drawn on the EPID image (b) (illustration produced by author) 3-6

Figure 3.5: Enlargement of Figure 3.4b to indicate gross miss-alignment of EPID image and DRR image after performing auto matching. (a) Base of skull miss-match, (b) Mandibular angle, ramus, and body miss-match (c) Spinous process of cervical vertebra miss-match (illustration produced by author) 3-6
Figure 3.6: Anterior (a) and left lateral (b) DRR with no filter (illustration produced by author) 3-8
Figure 3.7: Anterior (a) and left lateral (b) DRR with dynamic filter (illustration produced by author) 3-8
Figure 3.8: Anterior (a) and left lateral (b) DRR with content filter (illustration produced by author) 3-8
Figure 3.9: Anterior DRR with invert filter (illustration produced by author) 3-9
Figure 3.10: (a) Perspex base of radiopaque headrest visible on DRR. (b) Dense metal bracket on CT bed included in DRR creation (illustration produced by author) 3-10
Figure 3.11: Anterior DRR of a head and neck patient, illustrating manual bony landmarks drawn to facilitate matching with EPID image (illustration produced by author) 3-10
Figure 3.12: Illustration of manual contours drawn on left lateral DRRs for matching with EPID images. Image b demonstrates how a mandible prosthesis can also be used as an anatomical matching tool (illustration produced by author) 3-11
Figure 3.13: Interpolation artefacts contoured on a lateral head DRR (illustration produced by author) 3-12
Figure 3.14: Illustration of interpolation of a very thin oblique bone (orbital plate) (illustration produced by author) 3-13
Figure 3.15: Illustration of interpolation of a very thin oblique bone (superior orbital margin) and a thick oblique bone (skull vertex) (illustration produced by author) 3-13
Figure 3.16: Contours found on the baseline head DRR's. 3-14
Figure 3.17: Illustration of manual contours drawn on anterior DRRs for use during image matching with EPID image (illustration produced by author) 3-16
Figure 3.18: Illustration of manual contours drawn on left lateral DRRs for use during matching with EPID image (illustration produced by author) 3-16
Figure 3.19: Matching results in centimetres (cm) after manual matching of EPID image with DRR. The DRR is considered the correct image, and the matching of the EPID image to the DRR is done to determine the shift / corrections needed for correct patient positioning (Screenshot from ARIA system) 3-18
Figure 3.20: Rotational error recorded for the anterior Image, but not for the lateral image (Screenshot from ARIA system) 3-18
Figure 3.21: Anterior rotation (illustration produced by author) 3-19
Figure 3.22: Positive and negative angle measurement on lateral image (illustration produced by author) 3-20

Figure 3.23: Measurement of 2.6 degrees of rotation in a negative direction (illustration produced by author)..... 3-20
Figure 3.24: Anterior DRR (left) compared to anterior EPID image (right) (illustration produced by author) 3-21
Figure 3.25: (a) Lateral DRR (b) Lateral EPID Image without applying any shift (c) Lateral EPID Image applying rotational corrections, and a 0.3cm longitudinal shift (Illustration produced by author)…….. 3-22
Figure 3.26: Inter-observer error in matching (illustration produced by author) 3-23
Figure 3.27: When rotations are corrected multiple body landmarks will agree and a true x, y, z offset can be measured (illustration produced by author) 3-24
Figure 3.28: Contours done as exact replica of interpolated data..... 3-25
Figure 3.29: Projection of interpolation contours (left) on actual EPID image (right) (illustration produced by author)..... 3-25
Figure 3.30: Left DRR image, Right EPID image 3-26
Figure 3.31: Measurements on skull vertex on the DRR (left) and EPID image (right) on an anterior image set (illustration produced by author) 3-27
Figure 3.32: Measurements of the skull and orbital plates on a DRR (left) and EPID image (right) of a left lateral image set (illustration produced by author) 3-27
Figure 3.33: Enlarged image of an anterior image set, with measurements of the superior orbital margin on a DRR (left) and an EPID image (right) of an anterior image set (illustration produced by author)..... 3-28
Figure 3.34: Verification uncertainty due to posterior and vertex of skull not being visible on EPID image (right) (illustration produced by author)..... 3-29
Figure 3.35: Nasopharynx radiation therapy with limited Anatomy of skull (illustration produced by author) 3-29
Figure 3.36: No base of skull or maxilla anatomy visible on EPID image to verify head position (illustration produced by author)..... 3-30
Figure 3.37: Not enough anatomy inferiorly to verify rotation of patient to correct for set-up error (illustration produced by author) 3-31
Figure 3.38: Comparison of two EPID images of patients receiving radiation therapy to the head only (illustration produced by author) 3-32
Figure 3.39: Comparison of DRR quality between two patients' data sets. The DRR created for patient a shows no facial anatomy, while the DRR for patient b has very good contrast between soft tissue and bony structures, making it ideal for comparison with EPID image (illustration produced by author)..... 3-33
Figure 3.40: Disagreement between anatomy imaged and treatment area (illustration produced by author) 3-34

Figure 3.41: Auto matching failing, although search range was limited to a small part of anatomy (illustration produced by author). 3-35
Figure 3.42: DRR quality of young children (illustration produced by author) 3-36
Figure 3.43: Arrows indicating shift of head and spine in opposite directions (illustration produced by author) 3-37
Figure 3.44: Arrows indicating a shift of head and spine in opposite directions (illustration produced by author) 3-37
Figure 3.45: Visualisation of CT bed re-enforcement and the Headrest Baseplate on the DRR. The CT bed re-enforcement is not visible on the EPID image (illustration produced by author) 3-38
Figure 3.46: Incorrect location of cochlea on left image, and corrected on right image (illustration produced by author) 3-40
Figure 3.47: Purple parotid contour and corrected green contours on an orthogonal and coronal image (illustration produced by author) 3-40
Figure 3.48: List of original patient OARs (left). List of the OARs after anatomical data preparation (right) (illustration produced by author) 3-41
Figure 3.49: Body contour created to include headboard and mask (illustration produced by author) 3-42
Figure 3.50: Contrast contoured, and density corrected (purple contour) (illustration produced by author) 3-43
Figure 3.51: Posterior neck helper contour drawn in blue (illustration produced by author) ..... ….3-43
Figure 3.52: (Left) Mandible expanded to create the PRV (yellow) (Right) PRV cropped away from the PTV (illustration produced by author) 3-44

Figure 4.1: Calendar days from planning CT to start of treatment for *Head and Neck* patients 4-2
Figure 4.2: Calendar days from start of treatment to end of treatment for *Head and Neck* patients 4-2
Figure 4.3: Fractionation schedule for *Head and Neck* patients 4-3
Figure 4.4: Imaging days for patients in the *Head and Neck* group 4-3
Figure 4.5: Imaging sets per patient for the *Head and Neck* group 4-4
Figure 4.6: Distribution of set-up error 4-4
Figure 4.7: Calendar days from Planning CT to Start of Treatment for *Head* patients 4-8
Figure 4.8: Calendar days from Start of treatment to End of Treatment for the *Head* patients 4-8
Figure 4.9: Fractionation schedule for *Head* patients 4-9

Figure 4.10: Imaging days for patients in the *Head* group 4-9
Figure 4.11: Imaging sets per patient for the *Head* group 4-10
Figure 4.12: Distribution of set-up error across population 4-11
Figure 4.13: Dose prescriptions for planned patients, note that patient 5 had only one phase of treatment 4-15
Figure 4.14: Score allocation system developed by the researcher to quantify the results of both the PTV and OAR doses 4-15
Figure 4.15: Maximum dose for the brainstem recorded per patient 4-16
Figure 4.16: Maximum dose for the brainstem PRV per patient 4-17
Figure 4.17: Brainstem Dmax dose range per planning technique for all patients 4-18
Figure 4.18: Dose increase from brainstem Dmax to brainstem PRV Dmax observed on 50 Gy plans (*RA study* only). 4-19
Figure 4.19: Dose increase from brainstem Dmax to brainstem PRV Dmax observed on 50 Gy plans (3DCRT plans only). 4-19
Figure 4.20: Score results of the brainstem and brainstem PRV Dmax per patient 4-20
Figure 4.21: Lowest, highest and average Dmax (EQD2) recorded over all 10 plans per planning technique for the spinal cord 4-21
Figure 4.22: Lowest, highest and average Dmax (EQD2) recorded over all 10 plans per planning technique for the spinal cord PRV 4-22
Figure 4.23: Score results of the spinal cord and spinal cord Dmax per patient 4-23
Figure 4.24: Mean dose to parotids Combined 4-24
Figure 4.25: Mean dose to parotids combined PRV 4-24
Figure 4.26: Parotids plan scores 4-25
Figure 4.27: Mean dose to the right and left cochlea per planning technique for total population 4-26
Figure 4.28: Cochlea PRV plan score results 4-27
Figure 4.29: Mean lung dose per plan type (note: the whole lungs were not included in the CT data set, but these doses can be used to compare mean lung dose per patient comparing plan types) 4-28
Figure 4.30: Maximum doses to the right and left temporomandibular joints PRV 4-29
Figure 4.31: Scoring Results for the TMJ 4-30
Figure 4.32: Dmax to the Oral Cavity per patient 4-30
Figure 4.33: Average Dmax over total population per planning technique 4-31
Figure 4.34: Recorded minimum and maximum mean doses to the oral cavity per planning technique 4-32
Figure 4.35: Scoring results for the oral cavity 4-33
Figure 4.36: Maximum doses to the mandible 4-34

Figure 4.37: Maximum doses to the Mandible PRV cropped from the PTV with a 5mm gap ..... …4-34
Figure 4.38: Scoring results for the mandible 4-35
Figure 4.39: Shoulders contour 4-36
Figure 4.40: Mean doses to the shoulders 4-36
Figure 4.41: Maximum doses recorded for the patient population per planning technique 4-37
Figure 4.42: OAR plan results 4-38
Figure 4.43: Conformity for 3DCRT and RA plans 4-40
Figure 4.44: Results of conformity index scoring system 4-42
Figure 4.45: Results of Lesion Coverage scoring system 4-43
Figure 4.46: Homogeneity Index plan scores comparison for all 19 plans 4-45
Figure 4.47: Plan score results for the PTV per patient 4-47
Figure 4.48 Plan score results for the OAR per patient 4-48
Figure 4.49 Plan score results for the PTV per patient 4-49
Figure 4.50 Summation of OAR and PTV planning score results per patient 4-49

Figure 5.1: Illustration of the vertex skull bone that is not in agreement on the EPID image (right side). This will be an indication that a rotation of the head will be seen on the lateral image (image created by author). 5-6
Figure 5.2: Imaging area for the Anterior image (left) and the Lateral image (right) for the patient receiving treatment to both the head and the neck area (illustration produced by author). .. 5-8
Figure 5.3: Imaging area for Anterior image (left) and the lateral image (right) for patients receiving RT to the head (illustration produced by author). 5-8
Figure 5.4 Left DRR image, Right EPID image 5-9
Figure 5.5 Manual contour drawn on the DRR before Portal imaging (illustration produced by author). 5-10
Figure 5.6: Reference DRRs prepared and contoured on the left, and comparable EPID images on the right. The red arrow indicates valuable missing anatomy not imaged and blue arrow indicates imaging information not adding value (illustration produced by author). 5-11
Figure 5.7: The image on the left (3DCRT), middle (RA treat) and right (RA study) indicate different dose gradients (image created by Author) 5-18

LIST OF TABLES

Table 3.1: Examples of plans used in the study where patient 4 had two dose levels, and patient 5 only one dose level (table produced by author).....3-46

Table 4. 1: Mean and Standard Deviation calculated for 33 patients in the head and neck group 4-6
Table 4.2: Results of van Herk's equation (CTV to PTV expansion parameters).....4-7
Table 4.3: Mean and Standard Deviation calculated for 36 patients in the head group 4-12
Table 4.4: Results of Van Herk's equation (CTV to PTV expansion parameters) 4-13
Table 4.5: Plan scoring allocation for the brainstem.....4-20
Table 4.6: Plan scoring allocation for the spinal cord 4-22
Table 4.7: Plan scoring allocation for the parotids.....4-25
Table 4.8: Plan scoring allocation for the cochlea PRV.....4-27
Table 4.9: Plan scoring allocation for the TMJ.....4-29
Table 4.10: Plan scoring allocation for the Oral Cavity.....4-32
Table 4.11 Plan scoring allocation for the Mandible.....4-35
Table 4.12: OAR plan score allocation.....4-38
Table 4.13: Conformity index score allocation.....4-41
Table 4.14: Lesion coverage factor score allocation 4-43
Table 4.15: Homogeneity Index score allocation.....4-44
Table 4.16: Pairwise comparison results for HI calculations.....4-46
Table 4.17: The PTV score allocation table.....4-47

Table 5.1: Example of data collected from three patients. Random errors have been greyed, and the systematic errors that should have been adjusted are shown in white areas (Table produced by author).....5-13

LIST OF EQUATIONS

Equation 2.1 The van Herk equation used to calculate the PTV margin (Van Herk et al., 2000) 2-40

Equation 4.1: Conformity Index equation from Feuvret et al. (2006)..... 4-41
Equation 4.2: The Lesion Coverage Factor equation from Freuyet et al. (2006)..... 4-42

LIST OF APPENDICES

Appendix A: Data collected for Head and Neck image matching..... m
Appendix B: Data Collected for Head image matching..... t
Appendix C: Dose recorded to OAR ..... aa
Appendix D: Dose recorded for Plan comparison..... jj
Appendix E: The Plan Scoring system and Result ..... mm
Appendix F: Ethics approval xx

GLOSSARY

3DCRT:	Three-Dimensional Conformal Radiation Therapy
4DCT:	Four-dimensional computed tomography
CBCT:	Cone Beam Computer Tomography
CI:	Conformity Index
CT:	Computed Tomography
CTV:	Clinical Target Volume
CVF:	(Lesion) Coverage Factor
Dmax:	Dose maximum for specific Photon Energy
Dmean:	Mean Dose
DNA:	Deoxyribonucleic acid
DVH:	Dose Volume Histogram
DRR:	Digitally Reconstructed Radiograph
EPID:	Electronic Portal Imaging Device
EPID images:	Electronic Portal Imaging Device Images
ESTRO:	European Society for Radiotherapy and Oncology
FDG:	Fluorodeoxyglucose
FOV:	Field of view
GTV:	Gross Tumour Volume
HI:	Homogeneity index
HU:	Hounsfield Units
IMRT:	Intensity Modulated Radiation Therapy
ITV:	Internal Target Volume
LET:	Linear Energy Transfer
LINAC/S:	Linear Accelerator/s
LMIC:	Lower to middle-income countries
MLC:	Multi-leaf Collimator
MRI:	Magnetic Resonance Imaging
OAR:	Organ/s At Risk
PET:	Positron Emission Tomography
PET/CT:	Positron Emission Tomography-Computed Tomography
PRV:	Planning Organ at Risk Volume
PTV:	Planning Target Volume
QA:	Quality Assurance
RA:	Rapid Arc (Term used by Varian equipment for VMAT)
RA Study:	Term constructed for purpose of study referring to RA plans constructed for this study
RA Treat:	Term constructed for purpose of study referring to RA plans that was used for patient treatment and retrospectively analysed.
RT:	Radiation Therapy
RTT:	Radiation Therapy Technologist (Radiation Therapist)
TMJ:	Temporomandibular Joint
VMAT:	Volumetric Modulated Arc Therapy
V50:	Volume receiving 50Gray
WHO:	World Health Organisation

CHAPTER 1 Introduction and Rationale

1.1 Introduction

In 1911 Marie Curie received her second Nobel Prize to recognise her work in radioactivity and her worked contributed greatly to the use of radiation therapy for cancer care (Gasinska et al., 2015). During the twentieth century radiation therapy became a standard treatment modality within radiation oncology along with a variety of treatment interventions available to the cancer patient. It is estimated that approximately 50% of all cancer patients will receive radiation therapy during their course of treatment (Baskar et al., 2012).

Ongoing advances in radiation therapy treatment techniques, and improved understanding of the biology of cancer cells and their response to radiation, enables the radiation oncology team to continue working towards the increased survival of cancer patients and the potential of reduced side effects during and after radiation therapy.

With three-dimensional radiation therapy techniques being well established as convention, the development of new, expensive equipment, enabling a different treatment technique to be used namely volumetric modulated arc therapy. This has led to many questions: What are the differences in these techniques? Does it add value to the care of the patient? Are patients' treatments better? Can treatment side-effects be decreased, while still offering curative treatment?

As responsible healthcare providers we must ensure that we understand how technological improvements affect the care given to patients, what the differences are, and if the financial investment in these technologies is improving the care to the patients, or if it remains the same, but even more importantly, that it is not to the patient's detriment.

According to the World Cancer Report 2014, laryngeal cancer is the 14th most common cancer among men globally (Wild & Steward, 2014). The purpose of this research was to determine the difference that two radiation therapy planning techniques offered to a patient with advanced stage cancer of the larynx. This treatment has the intent to provide curative treatment with high radiation doses to a large treatment site, surrounded by many organs at risk, that have the potential to lead to significant side effects to normal tissue and long term morbidity.

1.2 Purpose of this study

This study aimed to compare two radiation treatment techniques that was used for treatment of patients with stage 3 and 4 cancer of the larynx. The three-dimensional conformal radiation therapy technique (3DCRT) was compared to the Volumetric Modulated Arc Therapy (VMAT) technique, also called Rapid-Arc (RA). This comparison had two purposes: the first was to compare the dose to the organs at risk, and the second to compare the dose to the PTV.

This study also compared DRRs to EPID images of patients in the immobilisation position to calculate the CTV to PTV expansion as well as the OAR to PRV expansion needed for planning volume expansions during above mentioned planning, as these were unknown, and a vital part of the plan creation process.

1.3 Statement of the problem and research question

1.3.1 Statement of the problem

The introduction of new technology into the radiation oncology department, resulted in a disruption of established procedures, and an urgent need to understand the impact of a new treatment technique on the patient. As responsible healthcare providers this researcher's aim was to investigate the difference between the established 3DCRT treatment technique, compared to the VMAT treatment technique for patients with cancer of the larynx.

The 3DCRT technique for late stage larynx cancer is one of the most challenging planning techniques due to the anatomical location of the larynx in the midline of the patient and just anterior of the spinal cord, a very radiation sensitive organ at risk. Furthermore the horse shoe shaped PTV that is sculpted towards the left and right side of the patients neck, due to the location of the lymph nodes just adjacent to the spinal cord, poses great difficulty in achieving a high radiation dose to the PTV as well as ensuring a safe dose to the spinal cord.

The high level of control that the radiation therapy planner has in the selection of the beam energy, beam direction and shielding, during 3DCRT, is greatly challenged when inverse planning is used. During the inverse planning process, the planner utilizes a single radiation energy and beam arcs to sculp the dose, and therefore the dose is spread out to the tissue surrounding the head and neck area.

These two treatment techniques were compared in terms of the dose to the organs at risk and the dose to the PTV.

According to the ICRU 83 guidelines (2010) the expansion of structures during the planning process is vital to ensure safe planning and delivery of the radiation dose. As this expansion

margin was unknown, this research investigated the treatment accuracy (systematic and random) to enable these margins to be applied during the planning process.

1.3.2 Research question

How does Volumetric Modulated Arc Therapy compare to 3D Conformal Radiation Therapy for patients with stage 3 and 4 cancer of the larynx? The following sub-questions assisted the researcher to address the main research question:

1. How accurate and reproducible is the treatment set-up?
2. What are the critical organ doses for the two planning techniques?
3. Which planning technique offers the best dose coverage, dose conformity and homogeneity to the PTV?

1.4 The study-site

All the data collection was done at a radiation oncology department in a tertiary hospital in the Western Cape Province of South Africa.

Data was collected retrospectively during 2017, and included patients treated in the department during 2016.

1.5 Research methodology

1.5.1 Sub-question 1

The clinical research process is explained in detail in subsection 3.1.

All patients who were treated in 2016 with the head and neck mask as immobilisation devices were retrospectively reviewed, to enable the treatment accuracy to be determined. The Digitally Reconstructed Radiograph (DRR) produced from the planning Computer Tomography (CT) images acquired for the planning of the radiation therapy treatment, was compared to the Electronic Portal Images (EPID) acquired on the treatment units.

With a minimum of 5 imaging sets per patient, the recorded disagreements in three dimensions was recorded and the van Herk's equation used to calculate the expansion margins applicable to this patient population (Van Herk, 2004).

The patient population was further subdivided into those receiving treatment only to the *head*, and those receiving treatment to both the *head and neck* area, as these anatomical sites posed significant challenges during the image matching process.

1.5.2 Sub-question 2 and 3

A total of ten patients, who received radiation therapy to the head and neck for late stage larynx cancer, were identified from the 2016 patient population.

All 10 patients had completed radiation therapy, and their CT data was used retrospectively to construct the comparative treatment plans.

1.6 **Rationale**

Literature shows (Hong et al., 2005; Cho, 2018b; Bhide & Nutting, 2010) that IMRT has been extensively researched as a clinical tool for cancer treatment and proven to be clinically relevant and safe for use. It has been shown that clinically 42% of all cancers treated with radiation therapy in the United States are done using IMRT (Smith & Smith, 2020).

Radiation therapy machine producers announced in 2008 the first two clinical sites that had installed equipment with VMAT capability (Elekta, 2008). This was followed by a global council formed to research the clinical use of VMAT technology (Varian, 2008). Therefore, IMRT has been in use for over 3 decades and VMAT, as an alternative method of the delivery of radiation dose, has been used for just over 1 decade (Cho, 2018a).

Teoh et.al (2011) stated that VMAT has a definite place for treatment of many tumours, but that each case must be evaluated on an individual basis and the most appropriate RT technique that provides optimal results for the patient selected. Currently phase III trials proving the long term clinical benefit of VMAT compared to other radiation therapy methods are still absent. Clinical comparisons of VMAT to 3DCRT for head and neck cancers are also not that prevalent (Teoh et al., 2011).

At the research site, the introduction of VMAT technology meant that fixed field IMRT was never introduced as a RT modality, and the shift was made directly from 3DCRT to VMAT. This research study aim is to directly compare the clinical impact of these two treatment techniques in terms of accuracy and reproducibility, OAR doses and dose coverage to the PTV.

Radiation therapy to the head and neck region is considered as one of the most technically challenging treatment planning sites. This is due to the number of targets and the shape thereof, the complex patient anatomy and the close proximity of many OARs (Shang et al., 2015).

The difference in the dose distribution produced by 3DCRT compared to VMAT poses complex clinical decision making and a shift in the thinking of the treatment planner. Craft et al (2016) suggested that, somewhat counter-intuitively, allowing the dose inside the target to be increased, allows the dose to OAR to be reduced, and this is opposing to the historic 3DCRT method of planning (Craft et al., 2016). With the planner having full control of the radiation beams, energy, modulation and weighting, the inverse planning module used in VMAT changes the planner's tools, where the dose to normal tissue is manipulated with multiple other tools and relies fully on the capabilities of the algorithm to apply plan parameters.

It is therefore critical to do such plan comparisons in the institution where it is used and to research the capabilities of treatment modalities depending on institution specific tools, systems, and abilities.

1.7 Overview of thesis

1.7.1 Chapter 2 Theoretical Research and Background Information

Anatomical information of the larynx as well as the staging, treatment recommendations, statistics and risk factors for larynx cancer are discussed. Thereafter literature survey of immobilisation devices used during RT and the specific mask system used in this study is discussed.

The anatomical modelling during the RT process consisting of positioning during CT, contouring of both the tumour and OAR and their therapeutic margins have been supported by the advances in radiation therapy that have enabled the development of complex planning and treatment techniques. These sections have been subdivided into the development of the CT, followed by planning and treatment technology. Lastly the uncertainties in positioning set-up errors and image matching for both the patients receiving RT to the head and the head and neck region are discussed.

1.7.2 Chapter 3 The Clinical Research Process

This chapter discusses each of the three sub-questions individually. Sub question 1 dealt with the accuracy and reproducibility of the treatment set-up. The inclusion criteria for this sub question, contouring and data preparation for both the head and head and neck group is given. Thereafter the data collection process and measurements done is set out and uncertainties and trends discussed with clinical examples and a case study.

Sub question 2 explains the clinical research process of determining the OAR doses comparing the two planning techniques: 3DCRT compared to VMAT. The creation of the OAR, contouring of the PRV and other normal tissue contours, and the recording of the doses are explained.

Sub question 3 explains the clinical research process to determine the dose to the PTV when comparing 3DCRT to VMAT. The inclusion criteria for this patient population, the creation of the treatment plans and recording of specific dose parameters are described.

1.7.3 Chapter 4 Research Results

This chapter provides the research results for each of the sub questions. Sub-question 1 provides the validation of the inclusion criteria to enable the accuracy and reproducibility of treatment to be calculated. Furthermore, the results for both the head and neck, and head image matching are shown resulting in a quantified treatment accuracy measurement in the three anatomical directions, namely: anterior to posterior, left to right and superior to inferior.

The results of sub-question 2 regarding the critical organ doses for the two planning techniques are provided for each OAR individually using a custom-made plan scoring system, as well as the OARs together, resulting in a score for each planning technique for each of the 10 patients.

The results of sub-question 3 where evaluating the dose to the PTV when comparing the two planning techniques are given through calculation of the conformity index, lesion coverage and homogeneity index. The results are quantified in the custom-made plan scoring system and a result is given for each planning technique for each of the 10 patients. Finally, the scoring results of sub-question 2 and 3 are combined to provide an overall plan score where both the doses to the OAR and PTV are added together to give an overall plan score for each planning technique for each of the 10patients.

1.7.4 Chapter 5 Conclusion and Recommendations

The research results given in chapter 4 is discussed and used by the author to link this research study to other similar studies to enable comparative analysis and the scientific relevance of this study.

The clinically relevant findings in this study and issues encountered during the data collection process aids in the compilation of recommendations for each sub-question. The recommendations for sub-question 1 are aimed in improving set-up accuracy for this patient population. The recommendations for sub-question 2 and 3 are aimed to improve the quality of planning practices with a detailed understanding of the comparison of 3DCRT with VMAT planning.

.

CHAPTER 2 Theoretical Research and Background Information

2.1 Introduction

This chapter is an overview of the literature researched to substantiate the research study. It provides an overview of larynx cancer related to the anatomical location, staging, treatment methods, risk factors and statistics of larynx cancer in South Africa. Furthermore, it addresses immobilisation of patients treated in the head and neck area both historically and the current method used at the tertiary hospital where the study was conducted.

The radiation therapy process related to the planning CT, planning and treatment is discussed referring to the evolution of technology, and the exact OAR and tumour contouring used globally as well as in this research study. Lastly, treatment uncertainties are addressed and followed by the image matching process and the determination of treatment accuracy.

This research site utilised VARIAN equipment, including the ARIA Oncology information system and the Eclipse planning system version 10.

2.2 Larynx cancer

2.2.1 Anatomy of the larynx and the significance of the surrounding lymphatics

The larynx is situated in the upper and anterior part of the neck, immediately inferior to the root of the tongue and hyoid bone. The larynx forms part of the respiratory system as air passes through the larynx where the vocal cords produces sound for speech. The epiglottis closes the larynx during swallowing to prevent food or drink passing through to the trachea and into the lungs.

For the purpose of clinical staging for larynx cancer, the larynx is sub-divided into three regions: supraglottis, glottis and subglottis (Fleming & Cooper, 1999).

The subsites for the supraglottis are the suprahyoid epiglottis, infrahyoid epiglottis, aryepiglottic folds, arytenoids, and ventricular bands (false cords). The incidence of supraglottic cancer has been reported to be approximately 35% (Brady et al., 2011).

The supraglottis has a rich and bilaterally interconnected lymphatic network. Therefore, primary supraglottic cancers are commonly accompanied by regional nodal spread. These malignancies commonly spread to upper and mid jugular nodes, occasionally to retropharyngeal nodes, but rarely to submental or submandibular nodes (AJCC, 2010).

For the purpose of radiation therapy localisation and contouring, the global consensus on the lymph node levels in the head and neck was published and has been used since 2003, and has been recently updated in 2014 (Grégoire et al., 2003; Grégoire et al., 2014).

For supraglottic cancers the percentage of lymph node involvement for ipsilateral nodes are as follows (Brady et al., 2011):

Level I: 1%

Level II: 39%

Level III: 26%

Level IV: 8%

Level V: 5%

And for contralateral nodes:

Level I: 0%

Level II: 12%

Level III: 5%

Level IV: 3%

Level V: 3%

The glottis region is composed of the true vocal cords, and includes the anterior and posterior commissures, superior and inferior surfaces. It occupies a horizontal plane, 1cm thick, extending inferiorly from the lateral margins of the ventricle (Fleming & Cooper, 1999).

The true vocal cords are nearly devoid of lymphatics and a tumour of this site alone rarely spreads to regional nodes. The late staged glottic tumours may spread to adjacent soft tissue, and thence to pre-laryngeal, pre-tracheal, para-laryngeal, paratracheal, upper, mid and lower jugular nodes (AJCC, 2010).

Primary tumours of the glottis compromise approximately 65% of all larynx cancers (Brady et al., 2011).

The uncommon subglottic primary tumours represent less than 1% of laryngeal cancer cases (Brady et al., 2011). The cancer spreads first to the adjacent soft tissue and pre-laryngeal, pre-tracheal, para-laryngeal and paratracheal nodes, and thereafter to mid and lower jugular nodes. The spread to contralateral lymphatics is also very common (Fleming& Cooper 1999).

The radiation therapy treatment volume for the treatment of stage 3, 4a and 4b cancer of the larynx, often includes the nodal levels 2, 3 and 4, but depending on the extent of the lymph nodes involved, further levels may also be included.

The radiation dose prescribed by the oncologist is subdivided and dependent on the risk per treatment site. The high-risk areas can be treated to a dose of 66Gy to 70Gy. Intermediate-risk areas to a dose of 60 to 63Gy and low risk areas from 54 to 56 Gy (Chamberlain et al., 2017).

It has been reported by Pfister et.al. (2012) that doses as low as 44Gy can be given for prophylactic nodal areas, with a fraction size of 1.6Gy to 2Gy per fraction, depending on the fractionation schedule. If a simultaneous integrated boost technique is used, the fraction size to the prophylactic nodal area will be closer to 1.6Gy per fraction, where the higher dosed areas will be receiving approximately 2.25Gy per fraction (Pfister et al., 2012).

2.2.2 Larynx cancer staging

Specific rules for the classification of larynx cancer has been defined by the American Joint Committee on Cancer (AJCC). As per the AJCC (1997) definition, for the purpose of clinical staging, a thorough inspection of the larynx must be performed using indirect mirror and direct endoscopic examination. The tumour must thereafter be confirmed histologically. Radiological studies must be used to supplement the clinical examination and to determine the nodal extent. For T1 and T2 lesions, imaging studies are used to confirm the staging. For T3 and T4 lesions, advanced radiological studies such as magnetic resonance imaging (MRI) are essential to assess the tumour erosion and the infiltration of adjacent tissue, as palpation and endoscopy are often unable to identify the extent of the primary disease (AJCC, 2018).

Due to resource constraints at the centre where this research study was conducted, diagnostic investigations are only requested by the oncologist, if there is any doubt in the staging assessment.

Pathologic staging will require the information obtained from clinical staging, as well as the histologic study of the surgical resected specimen. The surgeon’s evaluation of the gross unresected residual tumour must also be included in this staging process (AJCC, 2010).

The tumour, node and metastasis (TNM) classification is the standard used for laryngeal cancer (see table 2.1) and is complex due to the subgroups of the larynx, that must be very accurately identified to enable appropriate treatment.

The staging of cancer provides a mechanism that permits an assortment of tumour groups that have similar prognosis to be grouped. This facilitates comparisons of outcomes after therapy. The staging of laryngeal cancer can be seen Table 2.2.

The inclusion criteria for this research includes stage 3 and 4A & 4B laryngeal cancer.

Table 2.1: TNM Classification for Larynx Cancer (AJCC, 2018)

Stage	Description
T-Staging	**Supraglottis**
T1	Tumour limited to 1 subsite of Supraglottis, with normal vocal cord mobility
T2	Tumour invades mucosa of more than 1 adjacent subsite of Supraglottis or glottis or region outside the Supraglottis, without fixation of the larynx
T3	Tumour limited to larynx with vocal cord fixation and/or invades any of the following: post cricoid area, preepiglottic space, paraglottic space, and/or inner cortex of thyroid
T4a	Moderately advanced local disease: Tumour invades through the thyroid cartilage and/or invades tissues beyond the larynx
T4b	Very advanced local disease: Tumour invades prevertebral space, encases carotid artery, or invades mediastinal structures
	Glottis
T1a	Tumour limited to 1 vocal cord (may involve anterior or posterior commissure) with normal mobility
T1b	Tumour involves both vocal cords (may involve anterior or posterior commissure) wit normal mobility
T2	Tumour extends to supraglottis and/or subglottis, and/or with impaired vocal cord mobility
T3	Tumor limited to the larynx with vocal cord fixation and/or invasion of paraglottic space, and/or inner cortex of the thyroid cartilage
T4a	Moderately advanced local disease: Tumour penetrates the outer cortex of the thyroid cartilage and/or invaddes tissues beyond the larynx
T4b	Very advanced local disease: Tumor invades prevertebral space, encases carotid artery, or involves mediastinal structures
	Subglottis
T1	Tumour limited to subglottis
T2	Tumour extends to vocal cord(s) with normal or impaired mobility
T3	Tumour limited to larynx with vocal cord fixation
T4a	Moderately advanced local disease: Tumour invades cricoid or thyroid cartilage and/or invades tissues beyond the larynx
T4b	Very advanced local disease: Tumour invades prevertebral space, encases carotid artery, or invades mediastinal structures
N-Stage	**Regional lymph nodes (N)**
Nx	Regional lymph nodes cannot be assessed
N0	No regional lymph node metastasis
N1	Metastasis in a single ipsilateral lymph node ≤ 3cm in greatest dimension
N2a	Metastasis in a single ipsilateral lymph node, > 3cm but < 6cm in greatest dimension
N2b	Metastasis in multiple ipsilateral lymph nodes, none>6cm in greatest dimension
N2c	Metastasis in bilateral or contralateral lymph nodes, none >/= 6cm in greatest
N3	Metastasis in a lymph node, >6cm in greatest dimension
M-Stage	**Distant Metastasis (M)**
M0	No distant metastasis
M1	Distant metastasis

Table 2.2: Staging for Larynx Cancer (AJCC, 2018)

Anatomic stage/ Prognostic groups			
Stage	**T**	**N**	**M**
I	T1	N0	M0
II	T2	N0	M0
III	T3	N0	M0
	T1	N1	M0
	T2	N1	M0
	T3	N1	M0
IV A	T4a	N0	M0
	T4a	N1	M0
	T1	N2	M0
	T2	N2	M0
	T3	N2	M0
	T4a	N2	M0
IV B	T4b	Any N	M0
	Any T	N3	M0
IV C	Any T	Any N	M1

The histopathological grading of squamous carcinoma of the larynx is recommended as part of the staging process (AJCC, 2010). The degree of closeness to the deviation from squamous epithelium in mucosal sites is defined as well differentiated, moderately differentiated, and poorly differentiated. This grade is subjective and uses a descriptive as well as numerical form. Also recommended by the same authors (AJCC,2010), is a qualitative evaluation of depth of invasion of the primary tumour and the presence or absence of vascular and perineural invasion. This grading is not included in the staging criteria but aids the oncologist in determining appropriate treatment options.

2.2.3 Recommended treatment methods

Local laryngeal lesions (T1) incapable of spread are reported to be treated with: external beam radiation therapy (EBRT), endoscopic laser surgery or in select circumstances surgery (Brady et al., 2011). A single modality of treatment should suffice for this patient group. In a retrospective review of patients treated at a single institution for T1 glottic cancer that compared endoscopic CO_2 laser surgery and EBRT (30 fractions of 2Gy per fraction, 5 fractions per week or 25 fractions in 2.4Gy per fraction,5 fractions per week), Sjogren et al. (2008) reported that in T1a patients the number of local recurrences was more than double for the radiotherapy group versus the laser surgery group. (21% vs. 10%). The authors (Sjogren et al., 2008) commented that there seemed to be a shortfall in the current T-stage referencing method specifically for the T1 stage, as the only differentiation in this staging level is the involvement of one (T1a) or two (T1b) vocal cords. There is no specification regarding the

depth of infiltration, or the involvement of the anterior commissure and many patients were referred for EBRT after thorough investigation. This staging system seemed to lack the ability to effectively stage and therefore this lack of accurate information made the prediction for outcomes more challenging (Sjogren et al., 2008).

A large meta-analysis published in 2019 also commented that there is a lack of randomized control trials for the T1 group comparing RT and CO_2 laser surgery. The meta-analysis however, concluded that laser surgery is the superior modality of treatment in terms of overall survival, disease specific survival and laryngeal preservation (Vaculik et al., 2019).

The main aim of treatment for the larynx is always to preserve the structure to enable speech to continue. Multiple publications reported on comparisons using radiation therapy together with chemotherapy to surgery. The ESMO guidelines from 2010, stated that for stage I and II, either conservative surgery or radiation therapy is the most appropriate treatment modality, as it gives similar loco-regional control, although all data is based on retrospective studies only (Gregoire et al., 2010).

With larger laryngeal tumours, the involvement of lymph nodes is of great concern. The challenge is to not compromise the function of the larynx, when radical surgery was the historic treatment of choice, or whether, other modalities can aid in larynx preservation with similar survival rates than surgery only. This type of surgery is debilitating and dangerous, and the question has arisen whether routine bilateral neck dissection is necessary in management of N0 staged patients. Dequanter et al. (2011) retrospectively analysed surgical specimens of patients with advanced head and neck disease, who received bilateral neck dissection as the primary intervention. Of the 28 patients who had T4 staged larynx cancer, all patients with clinical and radiological N+ disease had involved lymph node metastases. All patients who were staged clinically and radiologically N0, had no involved cervical lymph nodes. But in those patients staged clinically N0 and radiologically N+, 8/12 had positive cervical nodes, and 50 % of those had bilateral nodes (Dequanter et al., 2011).

Due to post-surgical morbidity, patients might refuse surgery or may be found to be not eligible for surgery because of other co-morbidities, therefore other modes of treatment have been investigated. The RTOG 9111 trial compared three non-surgical treatment strategies to preserve the larynx for locally advanced larynx cancer. Stage III and IV patients were randomly assigned to three arms of the study: induction cisplatin/fluorouracil followed by RT, concomitant cisplatin with RT, or RT alone. The primary endpoint was laryngectomy-free survival. Ten-year results showed that the two chemotherapy arms showed similar endpoints for laryngectomy free survival. However, locoregional control and larynx preservation were significantly improved with concomitant cisplatin and RT compared to the other two arms. The

authors comment that this type of treatment has a high level of morbidity, and the search should continue for less morbid treatment options (Forastiere et al., 2013).

For patients with locally advanced tumours with extra laryngeal disease (T4a) or those with advanced destruction of the laryngeal structure and a non-functional larynx, the ASCO (2013) consensus has stipulated that primary total laryngectomy with appropriate neck management followed by adjuvant RT or chemo-RT for patients with positive margins or extracapsular extension should be the standard of care (Cmelak et al., 2013).

These guidelines agree with the ESMO (2010) guidelines, that stipulate that for locally advanced stage III and IV tumours, surgery (including reconstruction) plus postoperative RT should be the standard of care. For those with high risk features, for example R1 resection and/or extracapsular spread, post-operative chemoradiotherapy with single-agent platinum-based chemotherapy is needed (Gregoire et al., 2010).

The Union for International Cancer Control placed cisplatin chemotherapy on the World Health Organisations' (WHO) list of essential medicines in 2014, for the use of locally advanced squamous carcinoma of the head and neck, and this treatment regime is therefore recognized worldwide as the standard of care for this specific sub-group (UICC, 2014).

Current data revealed that microscopic tumour cell aggregates escaping surgical excision repopulate rather quickly before RT completion. It is therefore important to offer surgery and post-operative RT as a combined treatment package, that needs to be delivered in the appropriate time (Ang et al., 2001).

Therefore, practical steps need to be implemented to enable the timely start of RT, for example, teeth should be extracted during tumour surgery to prevent delay in starting RT. The selection of the appropriate treatment is often a complex discussion with the patients within the multidisciplinary treatment group, while weighing up the positive and negative effects linked to each of these complex treatment decisions. When radiotherapy is selected the patient's nutritional status must be corrected and maintained during treatment and dental rehabilitation completed prior to the start of radiation therapy. With an overall treatment time of <11 weeks (surgery and RT) the 5-year locoregional control for patients with high risk features was 76%, compared to 62% for 11-13 weeks and 38% for >13 weeks (Ang et al., 2001).

2.2.4 Statistics of laryngeal cancer in South Africa and the world

The South African National Cancer Registry reports from 2004 to 2014 (latest available) were analysed to determine the prevalence of larynx cancer in South Africa. It indicated that the incidence of male larynx cancer is greater than 7 times higher than for females, see figure 2.1. The male to female ratio was 4:1 (Brady et al., 2011) in the 2009 United States' statistics.

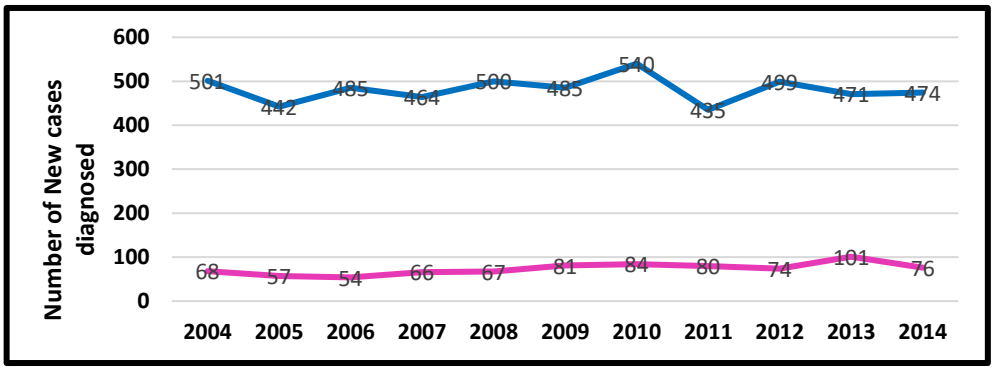

Figure 2.1: Male (blue) and female (pink) larynx cancer incidence from 2004 to 2014 in South Africa (Cancer in South Africa 2003-2014 Full Report, 2014)

The most prevalent age range for females to be diagnosed with larynx cancer in South Africa was found to be 55 to 64 years, and for males 45 to 54 years (see figure 2.2). This difference in age specific incidence poses interesting aetiological questions regarding the reason for this, as the statistics in the United States indicated that the prevalence is mainly after the age of 55, as seen in females in South Africa, but not in males (Brady et al., 2011).

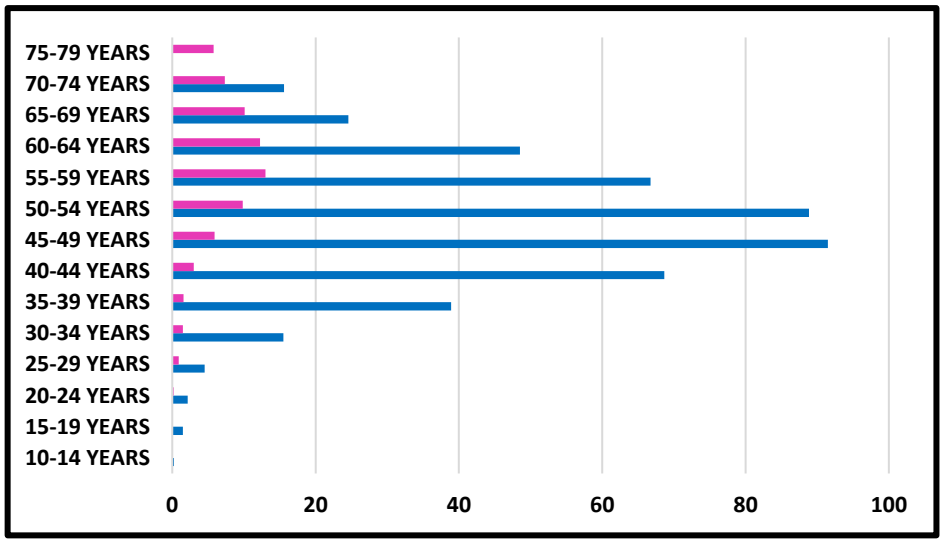

Figure 2.2: Average age specific Incidences of larynx cancer from 2004-2014 for males (blue) and females (pink) in Sough Africa (Cancer in South Africa 2003-2014 Full Report, 2014)

The World cancer report from 2008 reported that worldwide there were 160 000 incidences of larynx cancer per year (Boyle & Levin, 2008). The World cancer report of 2020 reported that the incidence reported in 2018 had risen to 177 000 new larynx cancer cases worldwide. This

incidence is therefore increasing (Wild et al., 2020). Regions with a higher incidence has been identified to be Southern Asia and Central and Southern Europe (Wild et al., 2020).

2.2.5 Risk factors for larynx cancer

Most of the cancers found in the larynx are squamous cell carcinomas histologically. The main risk factor has been identified to be tobacco and alcohol use. The risk has been proven for heavier smokers, long-term smokers and smokers of black tobacco or high-tar cigarettes. Cigar- and pipe smoking also pose a risk, while stopping smoking will decrease the risk of larynx cancer. Smoking of bidis in Asia appears to have a higher risk than smokers of western type cigarettes. Heavy drinkers show a tenfold increase in larynx cancer incidence compared to abstainers or light alcohol drinkers. This risk is unlikely to be related to the alcohol being consumed per unit, but rather the exposure to acetaldehyde, which is an intermediate metabolite of ethanol and is a well-known animal carcinogen. A pooled analysis based on over 10 000 cases and 15 000 controls showed that 86% of larynx cancer can be attributed to exposure to these two factors (Wild et al., 2020).

Patient related factors also include the carcinogenic effects of previous head and neck malignancy, weakened immunity (e.g. AIDS or organ transplant patients) and genetically acquired factors (e.g. Fanconi anaemia and dyskeratosis congenita). Environmental factors that have been identified are exposure to sulfuric acid mist, nickel, wood dust and asbestos (Brady et al., 2011).

Studies using epidemiological data have indicated a correlation between larynx cancer and the socioeconomic profile of patients. A study in Greece (Markou et al., 2013), indicated that most patients with larynx cancer were unemployed or unskilled workers and farmers without basic education. A similar study in Germany (Maier & Tisch, 1997) indicated that from a total of 162 patients with larynx cancer, 10.1 % had basic education, 8.2 % had higher and university education, while the remaining 87.7 % were illiterate or had elementary skills training. Furthermore, 20.3 % lived below the poverty line. The author commented that the increased incidence of tobacco use and alcohol consumption, poor nutritional diet, lack of preventative strategies and poor sanitation are factors that may characterize the poorer socioeconomic population sector involved and this may explain the higher rates of larynx cancer.

A small number of patients (5%) develop larynx cancer with no history of exposure to any known exogenous pathogenetic factor, therefore other mechanisms such as inheritance are possible. Genetic research in Sao Paulo found an association between genetic polymorphisms in DNA mismatch repair-related genes in the risk and prognosis of head and neck squamous cell carcinoma. In the study by Augusto et al. (2015) conducted from 2000 to 2013, 200 of the 450 squamous cell head and neck cancer patients were diagnosed with laryngeal cancer.

Overall survival was worse for patients with MSH3 GG genotype when compared to those with MSH3 GA+AA genotype (42.8% vs 52.5%) Additional observations for the first time identified that squamous cell carcinoma in the head and neck patients with GG genotype of EXO1 had worse recurrence free survival than the carriers of A allele. This was a significant finding as it has previously been observed that osteosarcoma cell lines expressing EXO1 were resistant to ionizing radiation when compared to EXO1-deficient cells (Augusto et al., 2015).

The pending release from the Cancer Genome Atlas Project will set the stage for translating new discoveries into therapies for patients. Squamous cell carcinoma is characterised by substantial heterogeneity at the clinical as well as the molecular level, and this challenges their consideration as a single disease entity. As an example, epidermal growth factor receptor (EGFR) is a member of a family of receptor tyrosine kinases whose receptors play a major role in the regulation of a host of cellular activities, including cell division, differentiation, and migration. A fundamental problem in EGFR-targeted therapy in head and neck squamous cell carcinoma is patient selection, since a consistent mechanism for resistance has not been identified. Molecular biology and patient specific immune therapy may have great potential for the treatment of laryngeal cancer (Psyrri et al., 2013).

The European Journal of Cancer Prevention has published multiple epidemiological studies in the search for causal reasons for head and neck cancer. One such metanalysis reported that those that has never used mouthwash has a odds ratio of 1.01 of ever developing head and neck cancer. Comparing to those who have used it for more than 35 years the odds ratio increase to 1.15, and for those using it more than once per day the odds ratio increased to 1.31 (Boffetta et al., 2016).

Authors publishing in the European Journal of Cancer Prevention, also proved a positive association between the Mediterranean diet and head and neck cancer, and the sub-sites. They found a reduced risk with a odds ratio of 0.64 for larynx cancer when the patient follows a Mediterranean diet. A high consumption of fruit, vegetables and legumes also showed a significant association with a lower risk of larynx cancer (Giraldi et al., 2017).

2.3 Immobilisation and stability

Achieving accuracy of treatment delivery varies with the type of immobilisation used. The material type, fixation method and area of the material in contact with the patient all affect the achievable reproducibility for each patient.

2.3.1 Literature survey of immobilisation devices and accuracies

The compliance of the patient is of utmost importance when focusing on the immobilisation in the head and neck area. The patient may be unable to remain still during treatment, for example, due to a neurological deficit where a patient is physically unable to keep still. It can also be due to nausea from raised intracranial pressure or due to anxiety. Many mask systems cover the whole face and this is problematic for patients who suffer from claustrophobia (Royal College of Radiologists, 2008).

There are a wide variety of immobilisation devices on the market specifically for head and neck radiation therapy. The most aggressive and invasive mask systems were designed to offer the most accurate RT treatment possible. The TALON system uses implanted metal fixtures to the skull to fasten the patient to the RT table (Salter et al., 2001). This product was created for accuracy during single fraction IMRT and was also used in fractionated IMRT. Analysis of the CT scans performed during fractionated RT included nine patients who received a total of 26 CT scans. This revealed that during a 6 week course of treatment, the isocentre shift of x = 0.95 mm +/- 0.55 mm, y = 0.58 mm +/- 0.46 mm and z = 0.51mm +/- 0.38 mm was achieved. This stability showed only slight deterioration during a long course of treatment, compared to the single fraction treatment where the isocentre translation was found to be x = 0.52 mm +/- 0.30 mm, y = 0.56 +/- 0.30 mm and z = 0.46 mm +/- 0.25 mm (Salter et al., 2001).

The Cosman-Roberts-Wells frame (Integra-Radionics, Burlington, MA, USA) system has for many years been considered to be the most reliable and stable platform for pin-point invasive immobilisation system (Sahgal et al., 2016).

This system places four screws into the skull of the patient for immobilisation during stereotactic RT. This system is not appropriate for long term use, and only remains in place for 1 to 5 days. Due to the invasive nature of these devices, the search was for a non-invasive mask-based system that can offer the same level of accuracy. The thermoplastic uniframe (Aquaplast Corporation) offered such an alternative with vacuum fixation bite-block suctioned to the upper hard palate, fastened to the mechanical fixed dental mouth piece and then to the carbon-fibre couch, and was combined with an external thermoplastic head support to the posterior part of the head. These two devices offered comparable immobilisation, but when superior immobilisation is required a single institution study indicated that the pinpoint system is still preferred for single fraction treatment (Babic et al., 2018).

The BrainLab immobilisation system (Brainlab AG) offers the user the ability to produce both a posterior and anterior mask, for the treatment of intercranial stereotactic lesions, and is regarded as a superior non-invasive system for stereotactic treatment. The use of the posterior mask eliminates the use of a standard headrest that could add inaccuracies to the

reproducibility in setting up the patient for treatment. A single institution study (Ali et al., 2010) using kV onboard imaging for the daily treatment of 9 patients totalling 50 imaging sets, indicated that isocentre shifts as large as 4.5mm (anterior to posterior), 5.0mm (right to left) and 8.0mm (superior to inferior) had occurred. Ali et al (2010) showed the value of onboard imaging with the ability to correct for these large random errors, but stipulated that certain systematic errors could not be corrected for, and perhaps the use of a mouth-block could be advantageous together with this mask system (Ali et al., 2010).

Tryggestad et al (2010) compared 4 types of mask systems These all included shoulder immobilisation in order to reduce potential movement of the lower neck. The mask systems were: Type-S IMRT mask from CIVCO with an individualised head cushion, the Uni-frame mask from CIVCO with individualised head cushion and a bluebag body immobilisation, Type-S head and shoulder mask from CIVCO with head and shoulder cushion and the Type-S head and shoulder mask from CIVCO with head and shoulder cushion with a biteplate. The resultant shifts of 1.1+/- 1.2mm, 1.1+/-1.1mm, 0.7+-0.9mm and 0.7+/-0.8mm respectively, indicated that all four systems are suitable for intracranial RT, but that system 4 that included a head and shoulder cushion and biteplate offered the best overall accuracy and stability (Tryggestad et al., 2010).

Improved set-up accuracy using the CIVCO S-frame mask system was achieved by Cronin et.al. (2013) with additional tattoos that were placed on the patient's body, inferior to the mask, with the aim of reducing rotational error during the duration of treatment. The placement of the tattoos for this study was on the level of the xiphisternum and placed anterior, left and right side of the patient. This study indicated an improvement of the set-up error in both the superior to inferior direction, as well as the left to right direction. Additionally, the yaw angle (the shift of the body from left to right in relation to the head) was also reduced (Cronin et al., 2013).

The immobilisation mask system utilised during this research study was from Klarity (Klarity Medical &Equipment Co.Ltd). It is a green coloured S-frame mask system. Figure 2.3 illustrates the mask description on the packaging. This mask system offers moderate mouldability and high rigidity with a forming time of 5 - 6 minutes. The mask can potentially shrink 5 % over 24 hours and is 98 % non-stick (KlarityMedical, 2013).

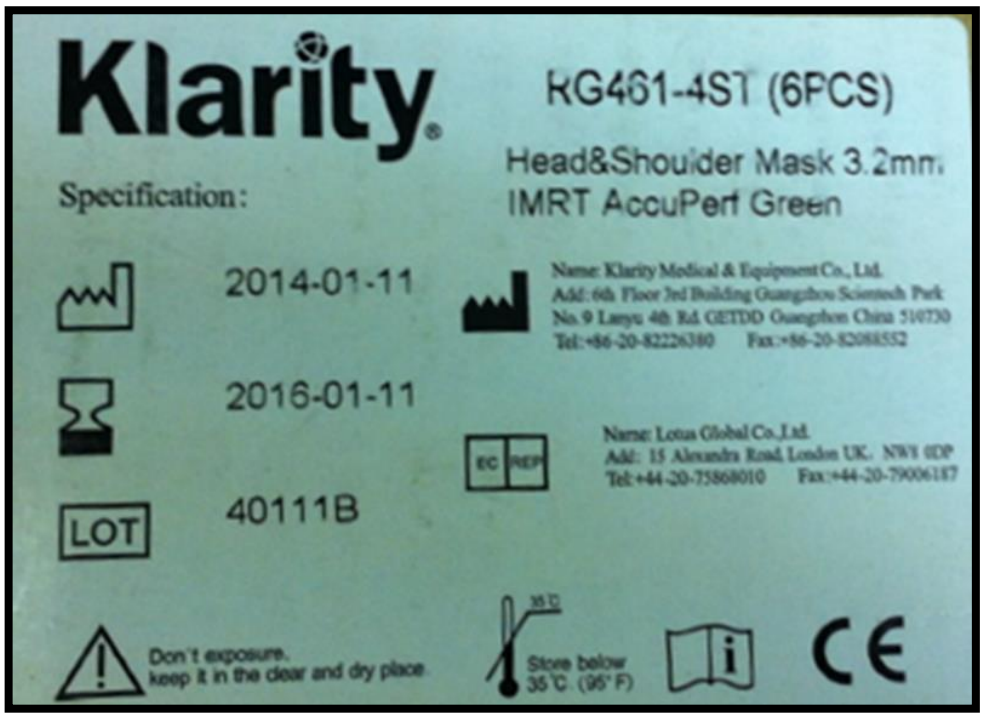

Figure 2.3: Box Label of mask system used on all patients Included in this study

.

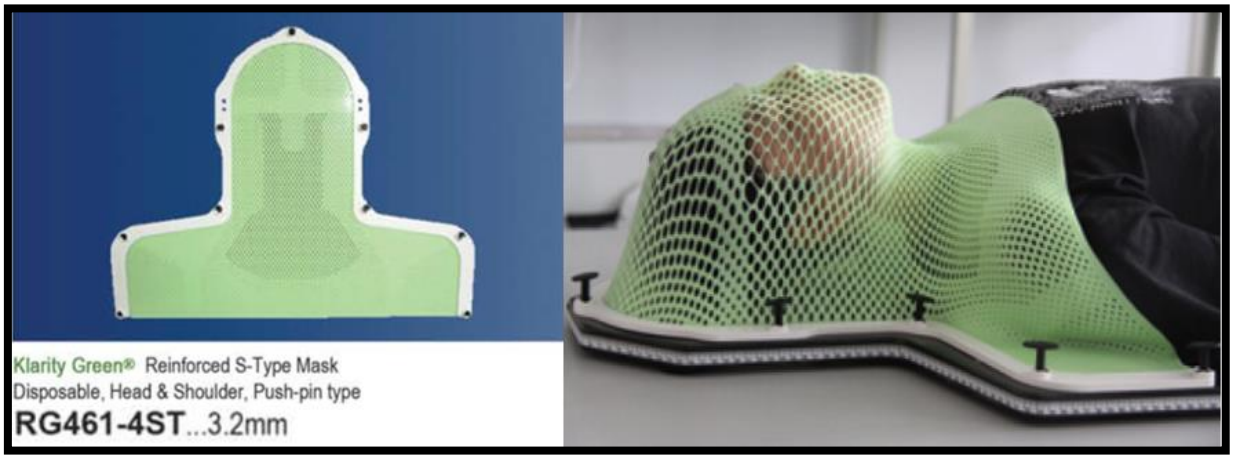

Figure 2.4: Klarity RG461-4S 3.2mm mask system on the S-frame base that fasten to the treatment couch. (KlarityMedical, 2013)

This mask system is used in conjunction with a standard range of head pillows. No individual pillows were produced. This immobilisation mask system offers re-enforced panels over the forehead and nose, as well as less dense material over the face and neck area, as demonstrated in figure 2.4. This head, neck and shoulder immobilisation device was used for all patients, including those receiving treatment to the head/brain and those receiving treatment of the head and neck area.

2.3.2 Construction of the thermoplastic mask

In 2017 the ESTRO ACROP guidelines were published for the positioning and immobilisation of head and neck patients. These guidelines were specifically designed to assist radiation therapists in the treatment of head and neck patients (Leech et al., 2017).

They stipulated the following steps in positioning of the patient prior to production of the mask:

- Identification of patient according to department protocol
- Explanation of the full procedure
- Explain the importance of remaining still and breathing normally throughout procedure
- Emphasise the safety and efficacy of the procedure as well as the mask temperature, and how the patient can alert the RTT if they have difficulty during the procedure
- The patient must be asked to remove all clothing from the waist up
- The patient must remove any dentures, hearing aids, toupees, earrings and any piercings
- Shoes as well as any devices in the trousers' back pocket must be removed
- All makeup must be removed
- Provide a gown for the patient, that will be removed when the procedure starts
- Position patient in prescribed position on the treatment couch, as comfortably and reproducibly as possible
- Use sagittal laser to ensure midline alignment including nasal septum, sternal notch, xiphisternum and symphysis pubis. This minimises rotation.
- All immobilisation devices must be indexed and fixed to the couch. Neck rest must provide adequate support for the head and neck and gaps should not be present underneath the head or neck.
- With inadequate support of the head and neck using conventional neck rests, the position should be adapted using individual customised neck rests.
- The RTT should be aware of the diagnosis of the patient and beam arrangement to enable appropriate neck positioning.
- Care should be taken to ensure the quality of the neck rest.
- Additional support devices such as knee rest or shoulder retractors should be indexed to the treatment couch.
- If a mouth bite is required, it should be present at the production of the mask, and the patient should be given time to grow accustomed to the mouth bite.
- Documentation of all immobilisation devices must be made by one RTT, and verified by a second RTT

- The appropriate mask is selected according to the disease site. Masks should have 3 or more fixation points. If treating the lower neck, a 5-point mask is recommended. If a 3-point mask is used, a device to maintain shoulder position is mandatory.
- Ensure that the patient's airway is not compromised during the mask making procedure. This could necessitate enlarging the nasal and mouth areas in the mask and creating an enlarged gap for the stoma area.

Procedure of construction of the mask

- Adhere to the manufacturer's guidelines with the correct temperature and duration of preparing the mask.
- Absorb excess water from the mask and check the temperature before placing on the patient's skin to avoid burns
- When using a four- or five-point mask, three RTTs should be involved in the process: One RTT superior of the head of the patients and two RTTs on both sides of the patient. When construction a 3-point mask, two RTT's will suffice
- RTTs must work quickly to mould the mask as close as possible to the patients' skin, ensuring no gaps between the skin of the patient and the mask. Constantly ensure that the neck position of the patient remains as required. This process must be completed within 1-2 minutes, as the mask hardening process will then commence
- The RTT superior of the patient must ensure that the head is held still and in position during production of the mask.
- Give specific attention to the forehead, bridge of the nose, chin, and shoulders to ensure adequate immobilisation.
- Allow the material time to harden according to the manufacturer's recommendations. The duration can vary between 5 and 15 minutes. This time can be shortened by using towels from the fridge, cold gel pads or cold air.
- Support and reassure the patient during the production of the mask. Direct the patient to use abdominal breathing that will help them to relax during the procedure
- It is recommended to remove the mask and then re-fit prior to CT scanning to ensure the immobilisation provided is adequate.
- The name of the patient, type of neck rest and all immobilisation devices should be documented on the mask, as well as the patient chart
- Any "cutting out" of masks should be avoided, accept to facilitate respiratory devices or bite blocks.

2.4 **Anatomical modelling & contouring**

2.4.1 The purpose of the anatomical modelling process

The method in acquiring anatomical data of the patient and the process of contouring all relevant anatomical structures forms a large part of this research process. This subsection will address the guidelines, purpose and accuracy required to achieve this.

Each structure contoured for planning purposes in this study is shown, and literature provided to substantiate the use thereof.

2.4.2 Computed Tomography and patient positioning

Computed Tomography (CT) imaging is used to obtain cross-sectional images of the patient anatomy, which in turn are used for treatment planning. A spiral/helical CT is performed of the patient in the treatment position with all the immobilisation devices in place, the same as if during daily radiation therapy treatment. A modern multi-slice CT scanner acquires images within a few seconds. This CT process is considered standard practice worldwide.

The tissue contrast on CT images is directly related to the X-ray characteristics. Each detector that rotates around the patient receives a variable number of X-rays depending on the physical parameters of the incidental kilovoltage and milliamperes per second, and on the specific attenuation characteristics of the patient's tissue. The CT system measures this attenuation coefficient and quantifies it into a numerical value ranging from -1000 to 3000 Hounsfield Units (HU). The calibration of the CT sets 0 HU for water and -1000 HU for air (Gregoire et al., 2004).

This data enables the planner to visualize not only the patient's anatomical data but also all immobilisation devices present and the densities thereof. The HU acquired from the CT is converted to electron density, which is what radiation therapy dose calculation requires. As this CT data is not only used for dose calculation but also for target volume and OAR delineation, it is advantageous to acquire slice thicknesses of 3mm or less for this patient population (Dieterich et al., 2016).

The patients included in this study (sub-questions 2 & 3) with stage 3 and 4 laryngeal cancer following the protocol of the research study site, are positioned supine and immobilised with the appropriate headrest to position the chin clear of the larynx and fixated in a mask. The arms are positioned at the sides, and knees placed on a specialised knee pillow for comfort. The S-frame headboard with headrest is indexed and fastened to the CT table as it would be at the treatment table. Unless patient-specific contra indications are present, the planning CT scan is performed with continuous intra venous contrast media. The contrast is administered with a flow rate of 2ml per second, a bolus is administered 25 seconds prior to CT, and

continued during the CT to a total of 100ml. The CT limits is specified superiorly from the vertex of the skull to 5cm below the sternal notch, but could be extended to the carina, with a slice thickness of 3mm (Dalvie, 2013).

2.4.3 Guidelines for the contouring of the tumour and therapeutic margins.

Contouring of the tumour as well as the organs at risk is by far the most time-consuming part of the whole radiation therapy planning process. There is also a high probability of inter-observer variations, and therefore it is important to always state the method used to identify all relevant structures (Vinod et al., 2016; Riegel et al., 2016). All the contouring is done on the planning CT, as this is the modality used for the calculation of the radiation doses. This however is not a limiting factor as the use of MRI images can easily be integrated into a modern planning system (Nuyts, 2007; Henderson et al., 2018). MRI scans offer superior contrast resolution in comparison to CT, due to the magnetic and radio frequency radiation used that is sensitive to the soft tissues microenvironment (Khan et al., 2016).

The Gross Tumour Volume (GTV) is the initial structure contoured that represent the primary tumour, metastatic lymphadenopathy, or other metastases. This structure is of utmost important to contour as this is the structure that must receive adequate dose for curative treatment. This contour also allows for a measurement of tumour response in relation to the radiation dose (ICRU, 1993).

The shape, size and location of the GTV may be determined by clinical examination. For the larynx patient this will be visual inspection, laryngoscopy and palpation of lymph nodes in the neck. Various imaging techniques could also be used for visualisation and contouring for the larynx patient for example, pre-surgery CT, Ultrasound, MRI and radionuclide methods. For the patient with advanced stage larynx cancer, there might be multiple GTVs to be contoured. The first being the visible primary tumour (GTV-T) and the second metastatic neck nodes (GTV-N) (ICRU, 2010).

The use of PET (Positron Emission Tomography) imaging using FDG has proven to have a sensitivity of 80% and specificity of 80% and this increased to 90% for PET-CT. This is an improvement compared to CT and MRI with sensitivity values of 60% and specificity of 70% in detecting lymph nodes in larynx cancer (Magram et al., 2008).

The GTV must be described and reported in a complete and accurate way and must be in agreement with the TNM classification system (ICRU, 1999). If the tumour has been surgically removed no GTV can be contoured.

The definition of the Clinical Target Volume (CTV) is similar to the concept of a safety margin used at surgery, where a margin of tissue is removed around the tumour to compensate for possible spread. The CTV margin added to the GTV in radiation therapy is purely based on the anatomic-topography and biological considerations. Clinical experience has indicated subclinical involvement of malignant cells which cannot be detected by diagnostic staging procedures. It is recommended in the ICRU 83 report that a CTV is always associated with the GTV for malignant tumours (ICRU, 2010).

In this patient population as illustrated in figure 2.5, the GTV-T representing the primary tumour, was expanded to include sub-clinical disease and labelled CTV-T (tumour). Similarly, the GTV representing the histological positive Neck nodes (GTV-N) is expanded to include sub-clinical disease and labelled CTV-N (nodes). In the postoperative setting, only a CTV is delineated and is based on the knowledge of the anatomical pathways for the tumour infiltration and dissemination (see figure 2.6).

The clinical knowledge and probable pathways of tumour spread for the larynx patient, necessitate the prophylactic treatment of multiple lymph node levels in the neck. These have been extensively described in literature, and atlases assist with clear delineation of these lymph node levels (Grégoire et al., 2014). In this scenario where prophylactic RT needs to be delineated, no GTV exists and a CTV-N will be delineated.

The Planning Target Volume (PTV) is a geometrical concept of CTV expansion and is used for treatment planning purposes. This volume does not define specific tissues or tissue borders. The tissue contained geometrically inside the PTV may not truly receive the planned dose distribution, at least not in the areas closer to the border of the PTV. This is due to the variation of the CTV inside the PTV during a course of radiation (ICRU, 1993).

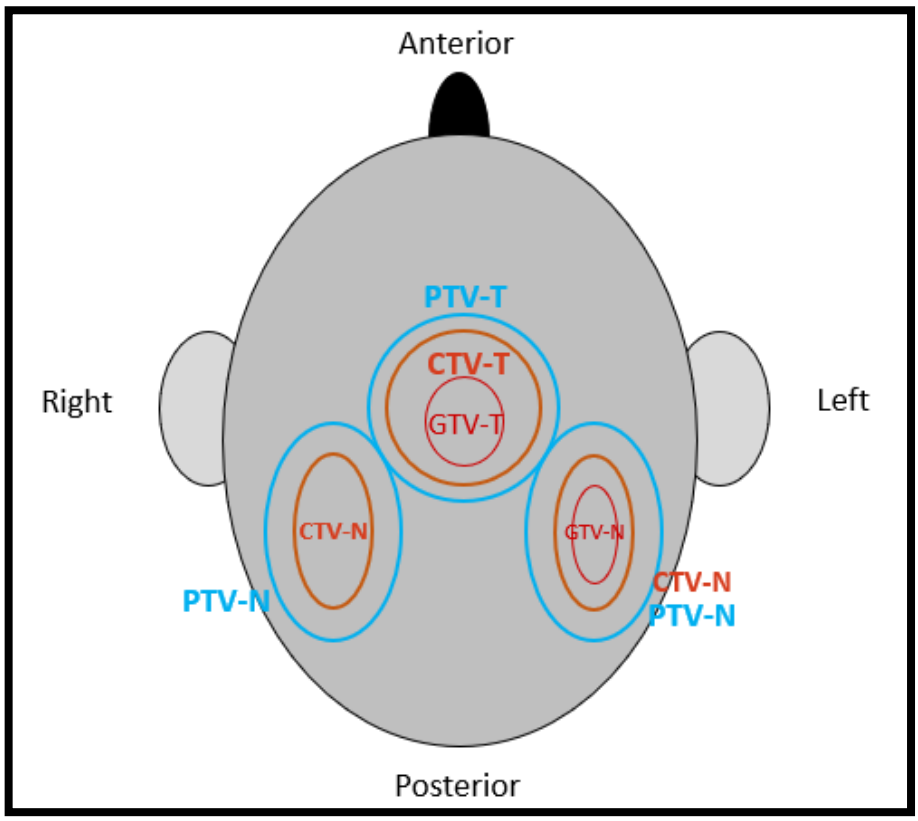

Figure 2.5: Graphical example of the GTV, CTV and PTV expansions of a head and neck cancer patient with a intact tumour and metastatic nodal spread to the left cervical nodes (illustration produced by author)

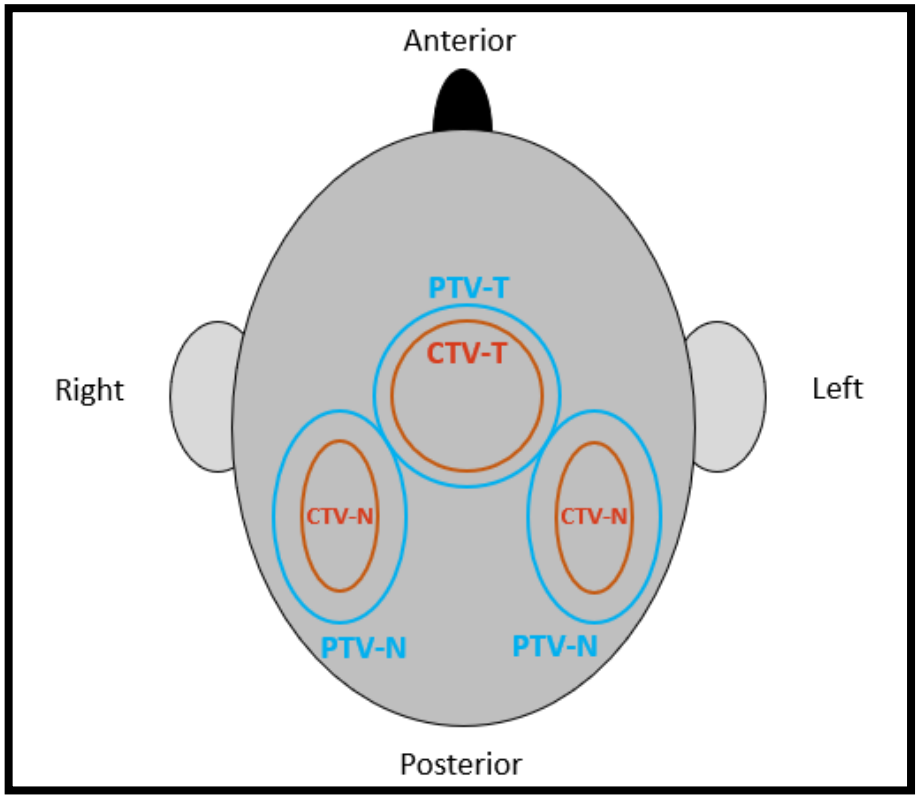

Figure 2.6: Graphic representation of a post-surgical head and neck cancer patient, where no GTV is present (illustration produced by author)

Although the GTV and CTV are the volumes that should receive the whole prescribed dose, there are variations and uncertainties involved in daily treatment. Current planning can only be achieved by a static representation of the patient (the planning CT) and therefore daily uncertainties in the position, size and shapes of both the patient and the tissue involved in the treatment area can differ daily per treatment session (ICRU, 1999).

Many factors are considered when standardising a CTV to PTV margin applicable to the head and neck patient. This must include the uncertainties in patient positioning and alignment of the therapeutic beams during the treatment planning as well as through all treatment sessions. In the early ICRU documents (50 and 62) it was suggested that it would possibly compromise the PTV margin if it encroaches on organs at risk. However, this is no longer recommended due to the use of IMRT and VMAT, where OAR's doses can be better controlled with an improvement in conformity and a sharper dose gradient achievable. The use of the Internal Target Volume (ITV) has been suggested to compensate for internal variations of the CTV. For the intact larynx patient, the movement of the larynx during speech or swallowing should be considered, and a margin could be placed around the CTV before a PTV expansion is done (ICRU, 2010). This, however, could lead to unnecessary large margins but it should be included in the consideration of the extent of CTV to PTV expansion.

External variation factors according to the ICRU 83 document include (ICRU, 2010):

- Patient positioning (could be limited with proper immobilisation and mask production),
- Mechanical and equipment uncertainties (gantry, couch, collimator, multi leaf collimators [MLC]),
- Dosimetric uncertainties (penetration of the beam),
- Data transfer uncertainties linked to the transfer of data from the CT to the linac,
- Human factors (the skill of the radiation therapy professionals involved in various steps of the patients treatment).

These factors will vary from centre to centre and between treatment units, and even more so from patient to patient. Although the mentioned factors may lead to an increase in the CTV to PTV margin, the use of quality assurance programs and image-guidance systems, can significantly reduce the size of the margins required (ICRU, 2010).

Many authors have proposed the calculation of this margin based on systematic and random uncertainties (Strbac & Jokic, 2013; Kanakavelu & Jebaseelan, 2016; Royal College of Radiologists, 2008).

Due to the close proximity of the neck nodes and tumour to the skin of the patient, it is often seen for head and neck patients, that the expansion of the CTV to the PTV could place the

PTV outside or very close to the patient's skin. Current dose computation algorithms cannot accurately compute absorbed dose in the build-up regions close to the skin and this leads to convergence errors (Wang et al., 2018). To solve this problem, sub-divisions of PTV's and relaxation of the dose objectives are often needed during planning, and care should be taken in these situations. The ICRU 83 (2010) document predicts that in the future the concept of a PTV might be utilized in unconventional ways to ensure that the prescribed absorbed dose is delivered to the CTV.

Dose reporting should always be performed for the whole PTV. This ensures that reporting under dosage to the PTV reflects the probability of lesser dose to the CTV (ICRU, 2010).

2.4.4 Guidelines for the contouring of organs at risk

In the ICRU 50 (1993) report, the Organs at Risk (OAR) were defined as the normal tissue whose radiation sensitivity may significantly influence treatment planning and/or prescribed dose. At that point in time the use of 2D and 3D RT were the standard of care, and the presence of the OAR close to the tumour influenced the amount of radiation dose that could be delivered to the tumour. The organs were grouped into three classes:

- Class One where exceeding the organs tolerance dose would lead to severe morbidity or death.
- Class Two were organs where exceeding the organs tolerance will result in moderate to mild morbidity.
- Class Three were organs where exceeding the organs tolerance will result in mild, transient, reversible or no significant morbidity.

Further classification of OARs in the ICRU Report 62 (1999) identified those organs according to their tissue, namely: parallel tissue, serial tissue and mixed serial-parallel tissue. This broadened the understanding of the impact of high doses on normal tissue. Although the OAR is the structure where dose should be limited, uncertainties during daily treatment, similar to those uncertainties applied to the calculation of the expansion of the CTV to PTV expansion should also be applied to the OAR. Therefore, organ motion and set-up uncertainties, etc, needs to be taken into consideration for the OAR as well. This led to the development of the expansion of the OAR that was called the Planning Organ at Risk Volume (PRV) in the ICRU 83 document (ICRU, 2010).

It was suggested by the International Commission on Radiation Units and Measurements (ICRU report 83) that the margin added to the OAR to form the PRV should be similar to the CTV to PTV margin, and is illustrated in figure 2.7 (ICRU, 2010).

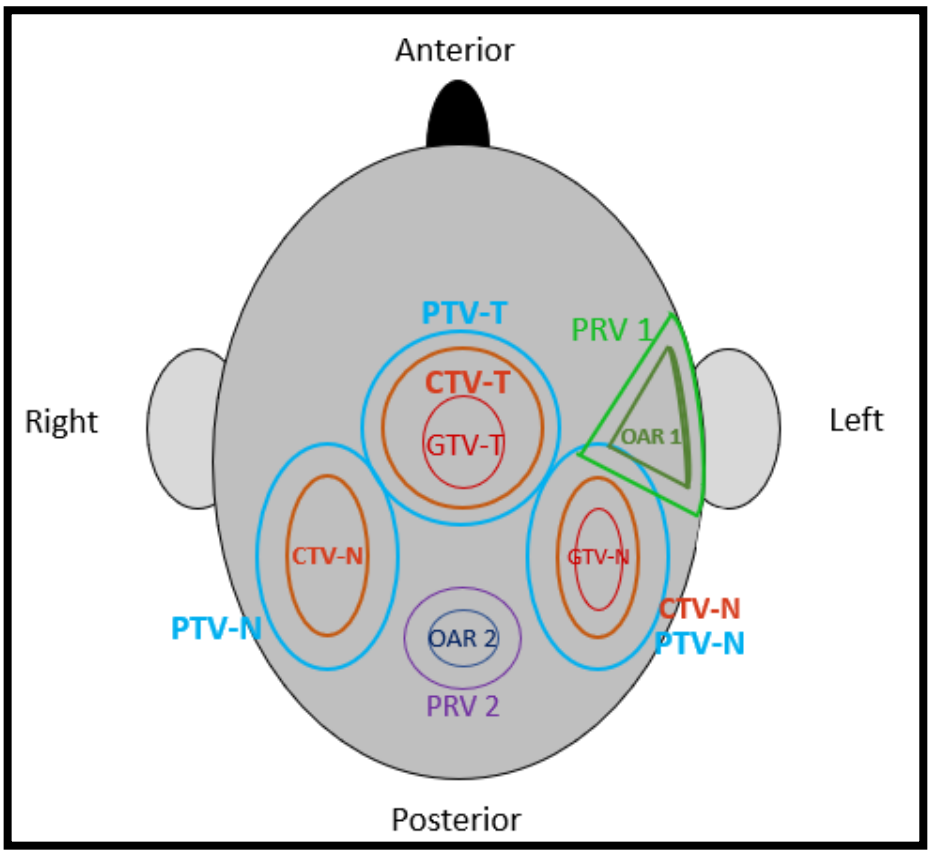

Figure 2.7: Organ at Risk 1 (OAR1) that is expanded to create the Planning Risk Volume 1 (PRV 1), and overlaps with the PTV-N. OAR 2 represents the Spinal Cord and is expanded to the PRV2, and does not overlap with any PTV (illustration produced by author)

With the use of IMRT and VMAT the concept of the OAR and PRV has been raising many questions: especially in head and neck radiation therapy. Structures like the mandible or oral mucosa were standardly not contoured as they were not considered to be organs at risk, and generally did not receive much dose, because with conventional planning methods of the time they were outside the treatment fields. However, with IMRT and VMAT these structures do receive significant absorbed doses due to the radiation being delivered from various angles around the patient's head and neck area, although the tumour might be situated far from these structures. Therefore, these structures need to be delineated to enable the dose to be controlled (by the optimiser) to all areas during the planning process and thereafter quantified and reported with the use of the DVH. IMRT results in more heterogeneous absorbed-dose distribution in normal tissues with larger volumes of normal tissue irradiated and each tissue type presenting with different responses. This has led to an increased level of importance in the understanding of the biological responses of normal tissue (ICRU, 2010).

Most dose-volume constraints for OAR's were retrospectively reported and translated into normal-tissue complication probability (NTCP) curves (Emami, 2013).

Due to this tolerance data being collected retrospectively only, certain dose levels were reported, and this was applicable for 2D and 3D radiation therapy. But the delivery of dose with IMRT has changed the dose deposited in many OARs. For organs with a serial cell structure it is accepted that a maximum dose limit is the upper dose threshold, for example, the spinal cord has a maximum dose limit of 50Gy to the full cord cross section as cited in the Quantec documents (Kirkpatrick et al., 2010). However, the dose-inhomogeneity using IMRT in organs with a parallel-like structure, like the parotid gland, has changed significantly.

The parotid gland is often very close or even overlapping with the PTV in head and neck radiation therapy as demonstrated in figure 2.7. The oncologist has to make a clinical decision whether to spare the parotid and compromise the dose to the PTV, or to exceed the dose to the parotid, leading to xerostomia, a significant debilitating long-term side effect. With the use of IMRT and the planner's ability to modulate the dose inside the parotid, it has become possible to both achieve a curative dose to the PTV, and to stay within the current tolerance doses of the parotids. A VMAT plan can produce a steep dose gradient inside the parotid, as indicated in figure 2.9(B). The clinical challenge with this scenario is that the currently available tolerance doses are specified by Emami (2013) as a mean dose less than 20 Gy to one parotid, or less than 25 Gy to both parotids, which will result in minimal grade 4 xerostomia. Another dose tolerance suggested by Barrett et. al (2009) is V30 < 45 %, and a further publication has stipulated that 50 % of the gland must receive less than 30 Gy (Videtic & Woody, 2015).

As demonstrated in figures 2.8 and 2.9, it is now possible that the medial part of the parotid receives extremely high doses, even though the whole parotid is within the mean dose tolerance. No published data was found on the permitted extent of these high dose regions. More prospective data would greatly improve clinical confidence in setting dose-volume constraints before running the dose optimizer for both the planner and the oncologist.

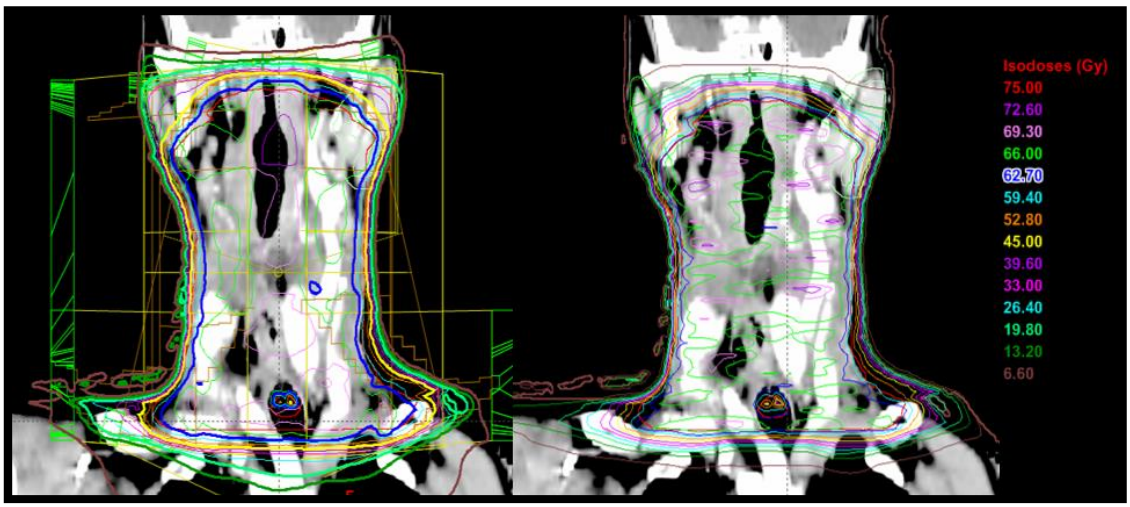

Figure 2.8: Dose distribution of a 3DCRT plan on the Left, and a VMAT plan on the Right, indicating the relative difference of dose distribution around the parotids OAR (enlarge image of left parotid can be seen in Figure 2.9 (illustration produced by author).

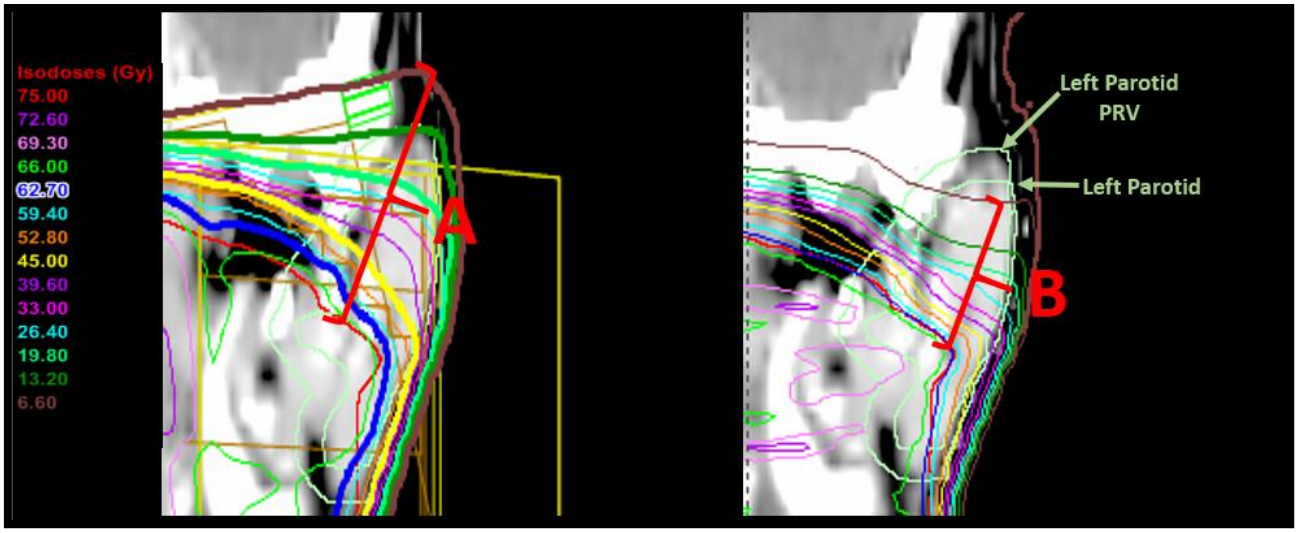

Figure 2.9: Enlarged image of the dose distribution around the left parotid and PRV of the patient illustrated in Figure 2.8. Annotation A indicates the slow dose fall-off seen in the 3DCRT plan inside the parotid, and annotation B indicates the rapid dose fall-off that can be obtained using VMAT planning inside the left parotid and PRV (illustration produced by author)

It is recommended in the ICRU 83 document (2010) that the absorbed dose be reported in the full PRV and PTV, even if overlapping of these expanded structures occur, and rather than changing the margins, different levels of priority should be used for overlapping parts of each structure.

2.4.5 Contouring of the organs at risk in this study

2.4.5.1 Brain and brainstem

The colour of the brain contour was standardised in this research study as purple, and the brainstem, as well as the brainstem PRV, were brown. All substructures of the brain were included in the brain contour, including the brainstem. A contouring atlas was used to guide the contouring process, and although MRI imaging was not used for contouring of these patients, the use of a MRI would add great value to the certainty in contouring of the brainstem. The following guidelines were used to contour the brainstem (Sun et al., 2014):

- Cranial: Optic tract
- Caudal: Foramen magnum
- Anterior: Posterior edge of prepontine cistern or basilar artery
- Posterior: Anterior edge of forth ventricle or mesencephalic aqueduct
- Lateral: Posterior cerebral artery, anterior inferior cerebellar artery, cerebellar peduncle

The Brainstem was expanded by 5mm to create the Brainstem PRV.

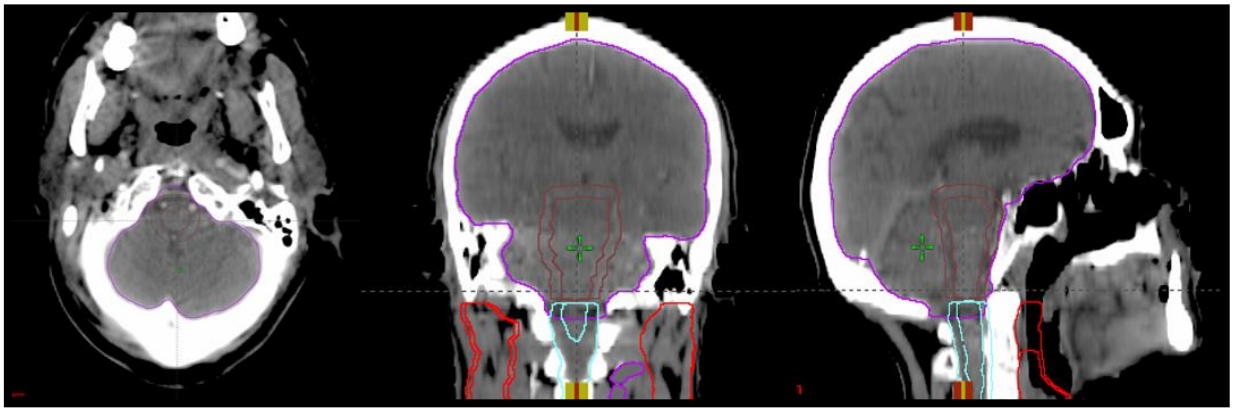

Figure 2.10: Contouring of the brain (purple), brainstem and brainstem PRV (brown) (illustration produced by author)

2.4.5.2 Spinal cord and posterior neck structure

The spinal cord was contoured in mint green. Cranially it was adjacent to the most inferior contour of the brainstem on the level of the foramen magnum and contoured inferiorly on all CT slices.

The spinal cord was expanded by 5 mm on each slice to create the spinal cord PRV structure. As the PTV does not extend posteriorly past the vertebra, an avoidance structure was created and labelled “posterior neck” and contoured in light blue. This avoidance structure was used to limit dose to this area, as it has been shown that muscle fibrosis occurs after radiation therapy, due to an increased release of transforming growth factor beta 1 (TGF-B1) by the muscles, which in turn can lead to severe morbidity (Peng et al., 2016).

The posterior neck structure was directly posterior to the spinal cord PRV and extends posteriorly up to the skin. No gap was allowed between the posterior neck structure and the spinal cord PRV. This structure was also contoured to have the same width as the spinal cord PRV (see figure 2.11).

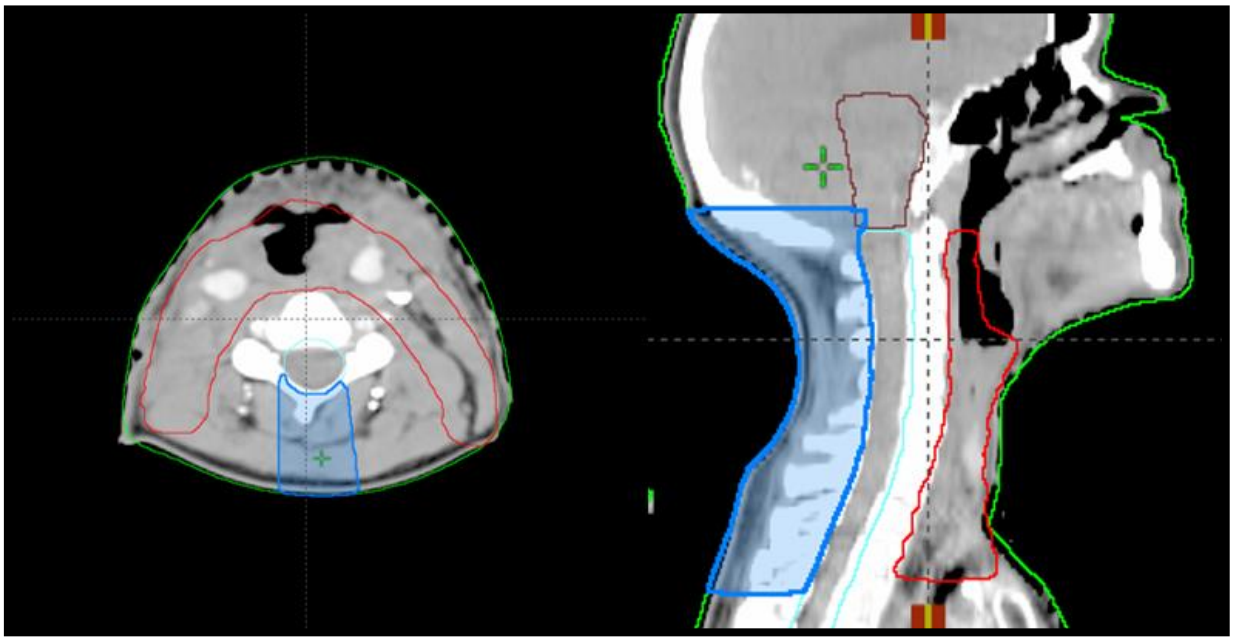

Figure 2.11: Illustration of the spinal cord PRV (mint green) and the posterior neck dose avoidance structure (light blue) (illustration produced by author)

2.4.5.3 Cochlea

The right sided cochlea was coloured black and the left sided cochlea in dark blue. Both structures were expanded by 5 mm to create PRV structures. Figure 2.12 demonstrates these contours. In this clinical case, both cochleae were not visible on the same CT slice, due to slight rotation of the patient’s head.

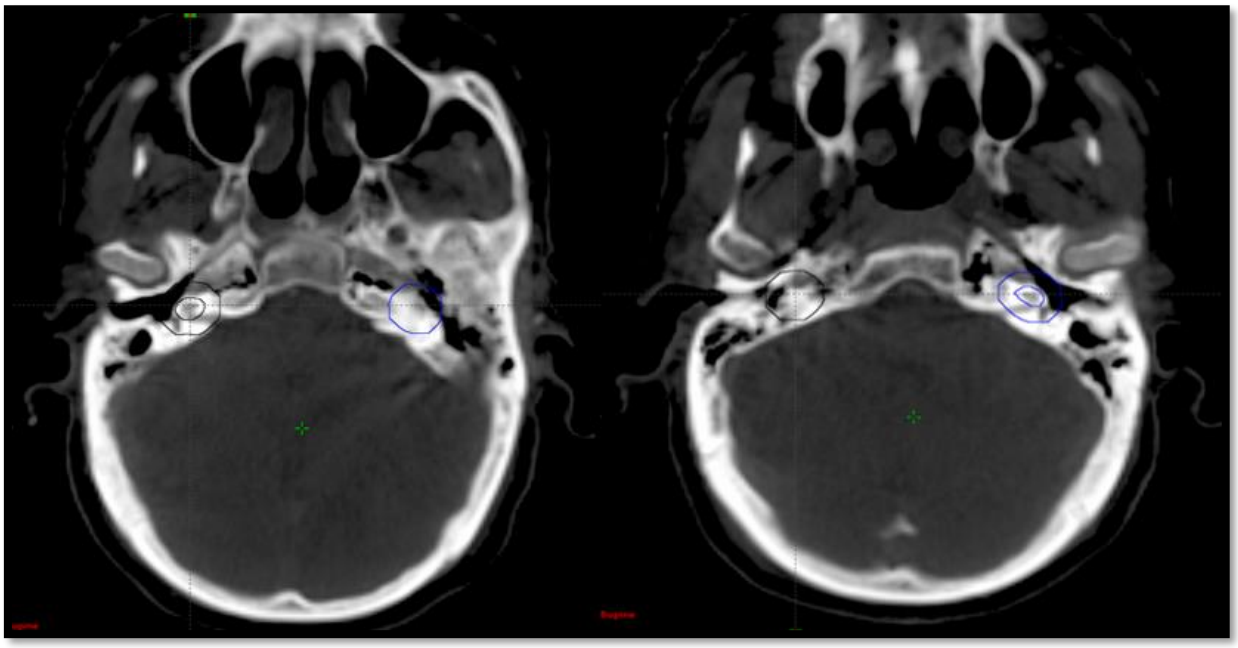

Figure 2.12: Right cochlea (black), and left cochlea (blue), both expanded by 5mm to create the PRV (illustration produced by author)

2.4.5.4 Temporomandibular joint and mandible

The temporomandibular joint (TMJ) was contoured individually, according to the contouring atlas recommendations by Sun et.al. (2014). This contour includes cranially the head of the mandible as well as the whole articular disk and fossa and ends caudally when the sigmoid notch appears. The slice thickness on all the planning CT's was 3mm, and this contour on average was drawn on 4 slices, resulting in an average length of 1.2cm (demonstrated in figure 2.13).

The right sided TMJ was coloured pink and the left side orange. The contour was automatically expanded in 3D by 5mm, to create the PRV (see figure 2.14).

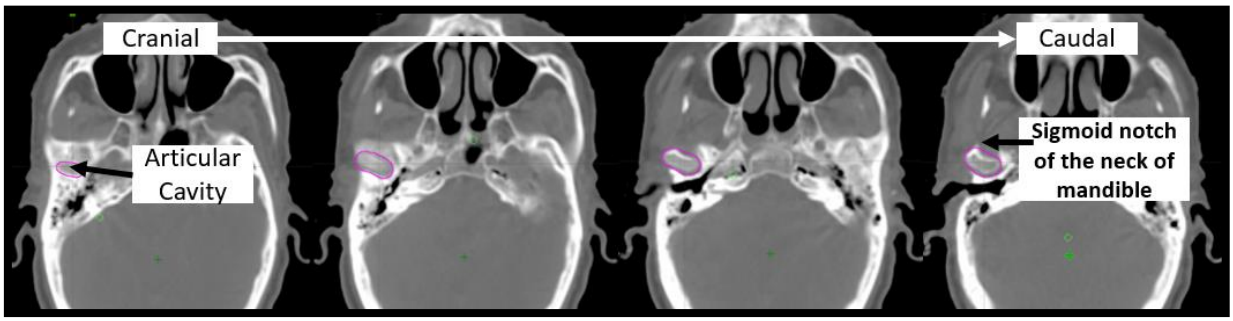

Figure 2.13: Illustration of the right temporomandibular joint (Pink) that includes the head of the mandible as well as the whole mandibular fossa (illustration produced by author)

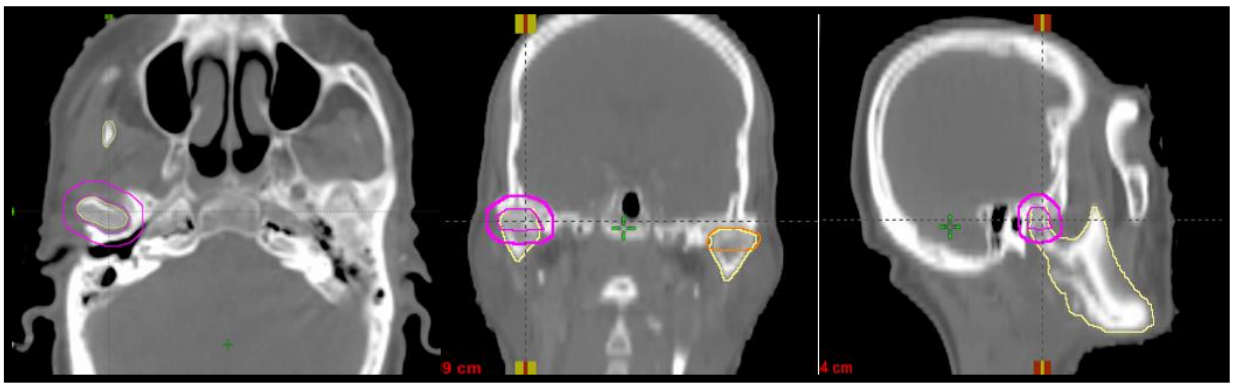

Figure 2.14: The right TMJ (pink) expanded by 5mm to create the PRV (illustration produced by author)

The whole mandible was contoured in yellow, and included all of the alveolar bone, but excluded the teeth. The mandible was expanded by 5mm to create the PRV, and as this structure overlapped the PTV, another structure was created and cropped 5mm from the PTV (see figure 2.15).

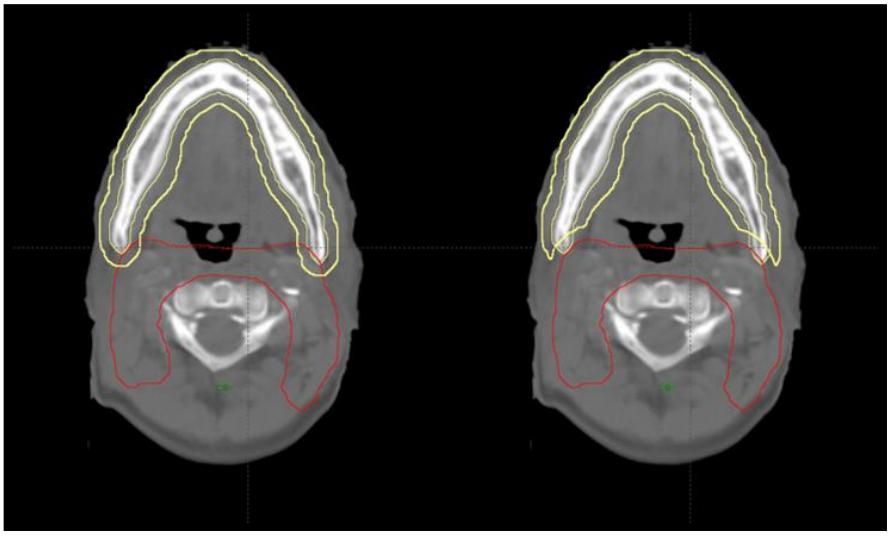

Figure 2.15: The mandible contour (yellow) expanded by 5 mm to create the PRV. The right side demonstrates the cropped PRV structure, with a gap of 5 mm between the PTV (red) and the PRV (yellow) (illustration produced by author)

2.4.5.5 Oral cavity

The oral cavity was contoured in light brown, and included the hard palate, tongue, floor of mouth, and the whole of the oral cavity (see figure 2.16). In this study, the oral cavity was limited posterior by the location of the PTV, and therefore cropped by 5mm from the anterior border of the PTV (see figure 2.17).

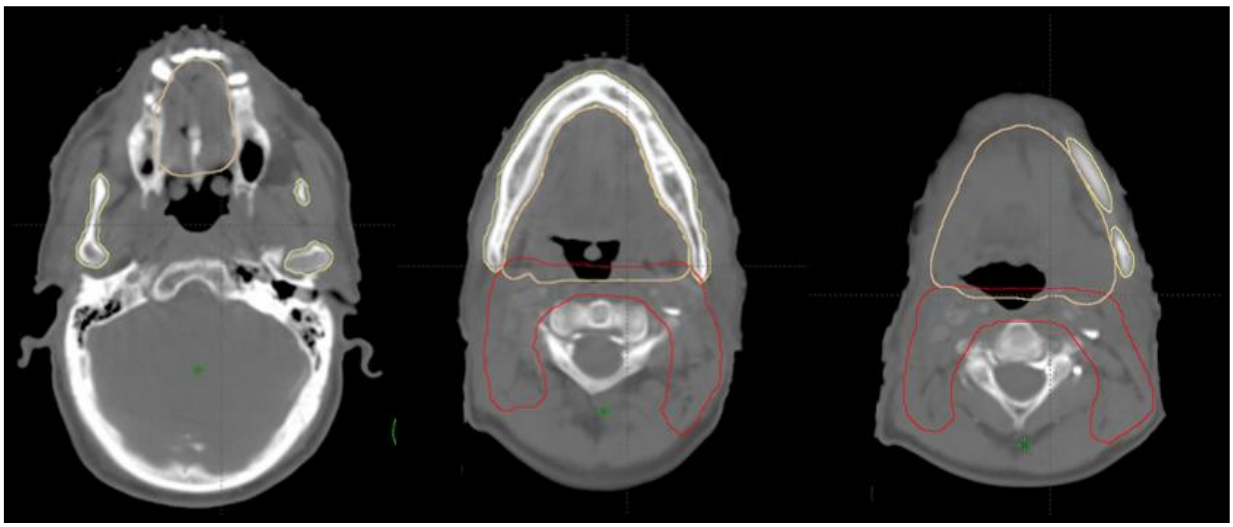

Figure 2.16: The oral cavity (yellow) is contoured superiorly from the hard palate and includes the whole oral cavity (illustration produced by author)

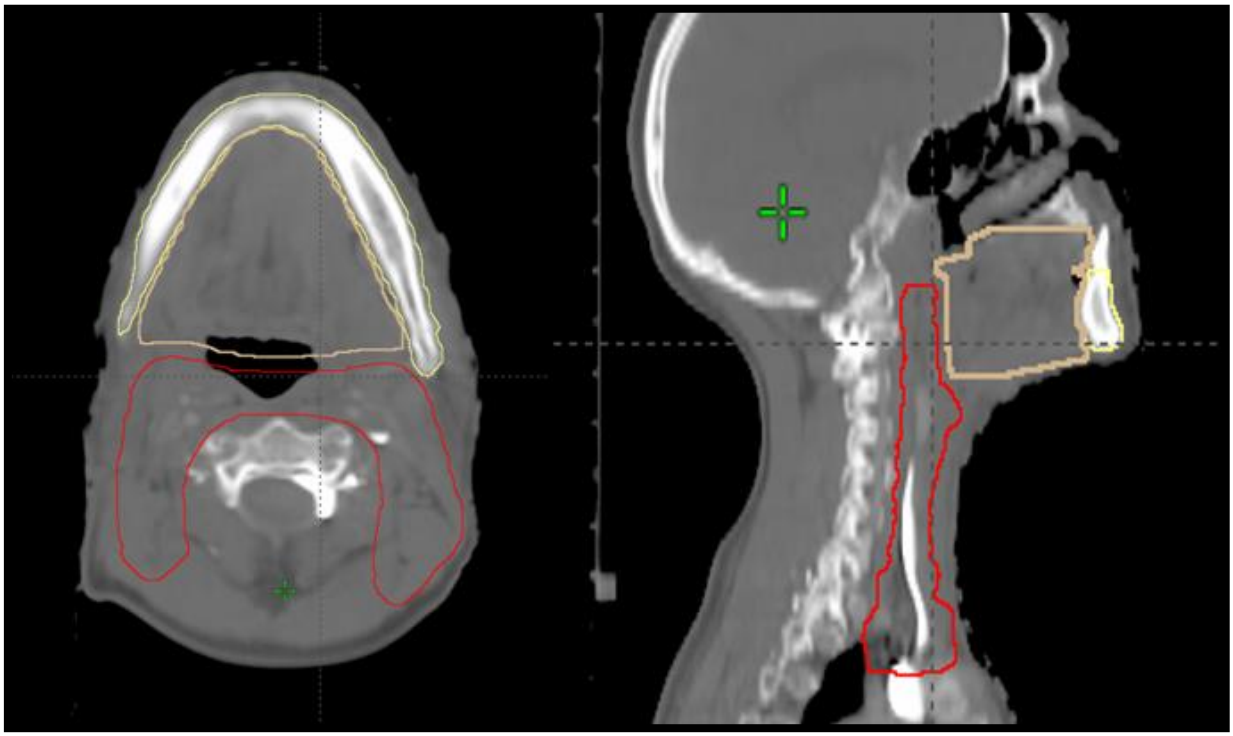

Figure 2.17: The oral cavity's (light brown) posterior border was kept at 5 mm anterior to the most anterior extent of the PTV (red) (illustration produced by author)

The borders of the oral cavity were as follows (Merlotti et al., 2014):

Cranial: Superior aspect of the hard palate,

Caudal: Hyoid bone,

Anterior: Symphysis menti,

Lateral: Mandible, and

Posterior: 5mm anterior to PTV (as illustrated in figure 2.18)

2.4.5.6 Parotids

Both parotid glands were contoured separately in their entirety, according to the contouring atlas from Sun, et.al. (2014).

The borders are defined as follow:

- Cranial: External auditory canal, mastoid process,
- Caudal: Posterior part of the submandibular space,
- Anterior: Posterior of the masseter muscle, medial of pterygoid, posterior border of mandible,
- Posterior: Anterior to the sternocleidomastoid muscle, lateral side posterior from the belly of the digastric muscle, and mastoid process,
- Lateral: Submandibular fat, and
- Medial: Posterior belly of the digastric muscle, styloid process, parapharyngeal space and sternocleidomastoid

Both parotids were expanded by 5 mm to create the PRV. Due to large overlap with the PTV a further avoidance structure was created and labelled, for example, “Left Parotid PRV-3mm”, as this avoidance structure was cropped 3 mm from the PTV. The avoidance structure can be used in the inverse optimizer to limit dose to the parotids (see figure 2.18).

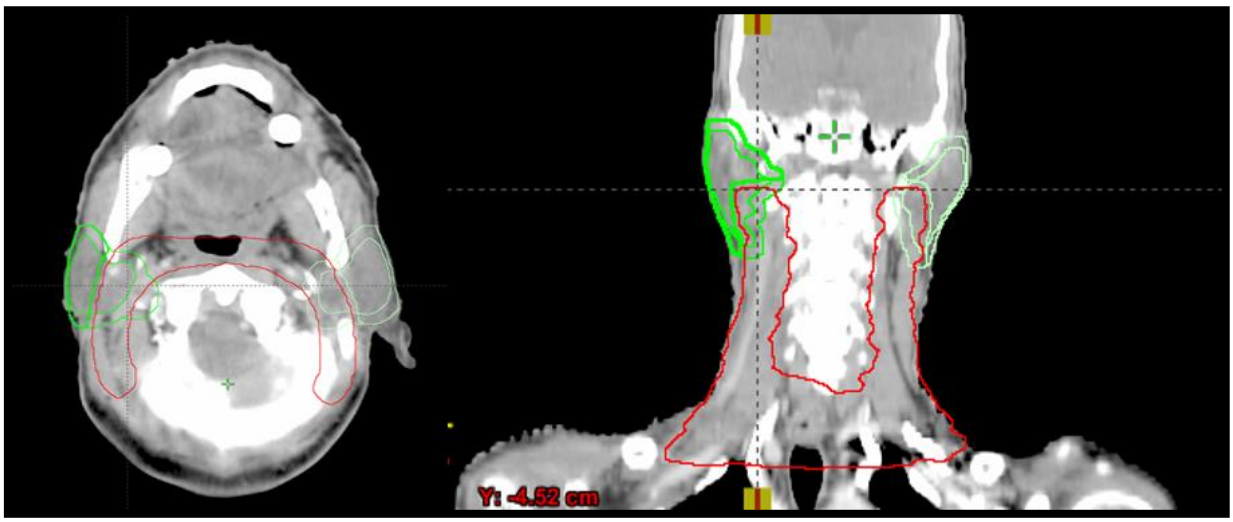

Figure 2.18: The right parotid (bright green) and left parotid (mint green) were contoured in their entirety. Both were expanded by 5 mm to create the PRV. This PRV was cropped to create an avoidance structure, and a gap of 3 mm was placed between this avoidance structure and the PTV (red) (illustration produced by author)

2.4.5.7 Shoulders

The shoulders were contoured because of the large amount of normal tissue lateral of the inferior PTV, where dose will be deposited when treating laryngeal tumours. The shoulder consists of muscular tissue as well as bony structures. The purpose of this shoulder structure is not to use it as a structure to limit dose to, but rather to record the dose that it will receive. Even though the head and shoulders are immobilised in the mask system, the shoulders have been shown, through clinical experience, to be very movable during daily set-up, and it is difficult to reproduce the position inside the mask.

When 3DCRT and VMAT treatments are applied to the patient, and the shoulders are moved inferiorly due to daily set-up requirements and error, it is important to know the amount of absorbed dose traveling through the shoulders, as this dose will increase dose to the organs at risk where the dose limit has already been reached, for example the spinal cord.

To enable consistent contouring practice of the shoulder contour, and as no literature of this contour has been found, in consultation with the oncologist, the following contouring guidelines were decided: a measuring tool was used to determine 2cm lateral to the most lateral extent of the PTV in the shoulder area (see figure 2.19). This lateral offset was used for the medial border of the shoulder contour. All tissue was included from the most superior soft tissue of the shoulder, until 3 cm inferior to the most inferior extent of the PTV (see figure 2.20). This contour was then cropped to be inside the body contour.

Both shoulders were contoured in light purple individually.

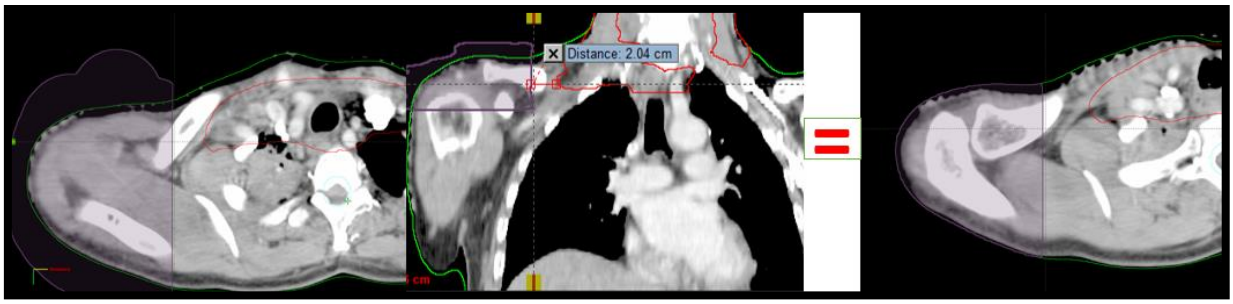

Figure 2.19: The right shoulder contour (light purple) was contoured 2cm lateral to the most lateral extent of the PTV and included all soft-tissue of the shoulder superiorly. This contour was then cropped to be inside the body contour (Right sided image) (illustration produced by author)

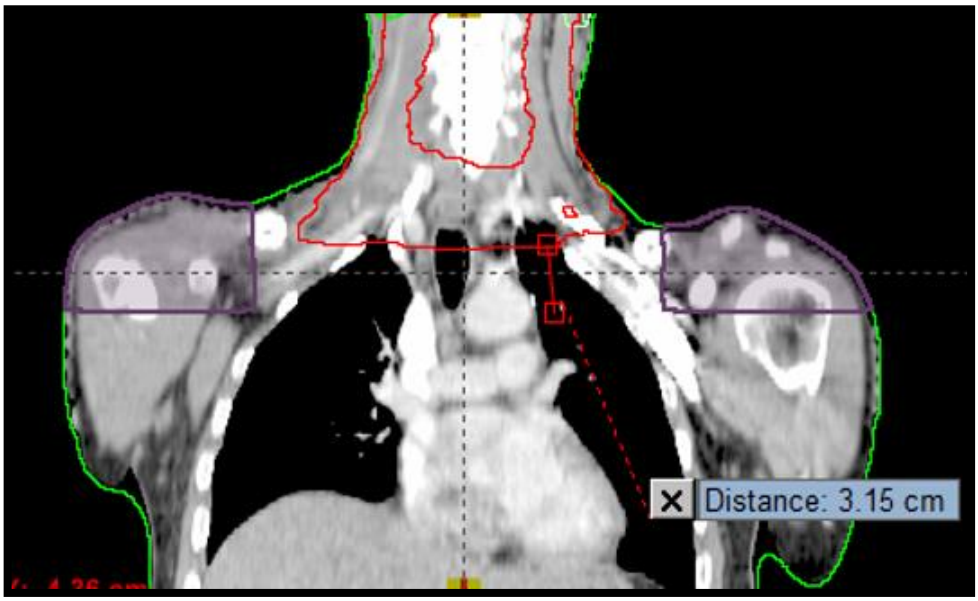

Figure 2.20: An illustration of the inferior extent of the right and left shoulder contour (purple) that extends inferiorly until at least 3cm inferior to the PTV (red) (illustration produced by author)

2.4.5.8 Contrast

The use of contrast media has been proven to add great value to the visualisation of anatomy during the contouring of the tumour volume (Videtic & Woody, 2015). The distribution of the intravenous contrast administered to the studied patient population, has shown a great increase of density of the major blood vessels inside the treated volume, as demonstrated in figure 2.21. The subclavian vain drains blood directly from the left arm where the contrast was injected, and therefore has not been diluted throughout the body.

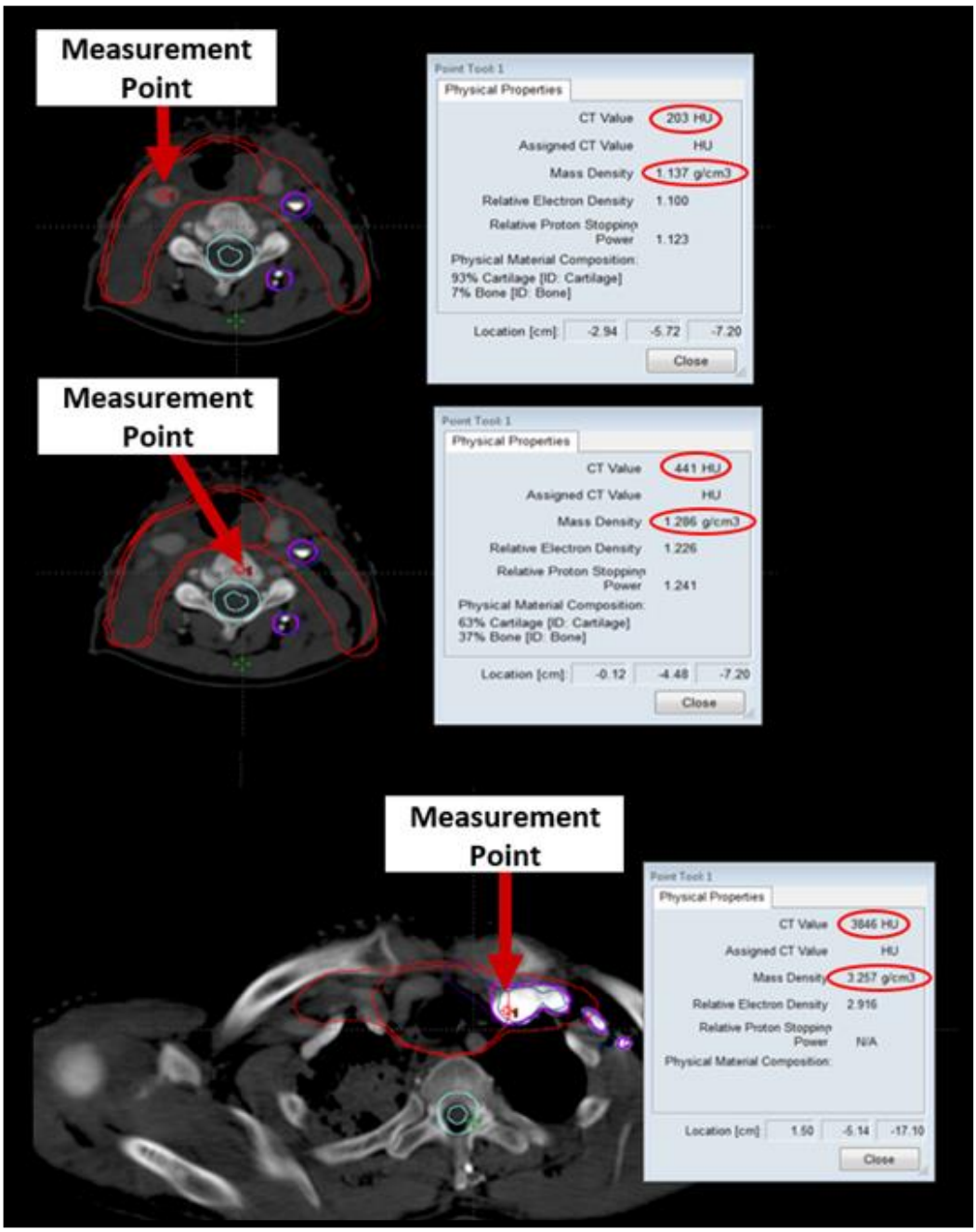

Figure 2.21: Hounsfield values and Mass Density measurement in the right internal carotid artery (top image), vertebral body (middle image) and contrast filled left subclavian vain (illustration produced by author)

Izmirli et. al. (2016) conducted a dosimetric study, comparing four different algorithms and the impact that different diluted densities of contrast media (0 %, 1 %, 2 % and 5 %) had on both the maximum dose (Dmax), and the dose at 5 cm depth with a variety of photon beams. It was shown in all algorithms that, as the contrast ratio increases, the dose values at Dmax and 5 cm depth increased accordingly. The increase of dose resulted in a 3 % - 5 % dose increase and it increased linearly with the increase of contrast concentration. With the correction of the contrast density on the planning system it was shown that all results were equal, therefore proving that correction of density data resulted in correct dose calculation (Izmirli et al., 2016).

Yamada et al.(2014) designed a contrast enhanced phantom that corresponds to a HU value of 270 HU, which is the same as the density of organs in the upper abdomen (e.g. liver, kidney) when IV contrast is administered to the patient. Dose studies comparing this phantom to the measurement in a tissue equivalent phantom indicated a dose increase of 5 % greater than the prescribed dose. The authors experimented with the unconventional use of dual-energy CT scans with two combinations of tube settings, and both using the tin filter. This CT data could then be virtually unenhanced and this was shown to result in more accurate dose calculations, without additional contrast correction being needed (Yamada et al., 2014).

Yamada et al. (2014) used a contrast experiment with 270 HU, and in this research study a density of up to 3846 HU was observed (see values circled in red on figure 2.21). Therefore, in this research study, all contrast media with HU values higher than 200 HU were contoured and corrected to the density of similar tissue.

2.4.5.9 Immobilisation devices

The use of the thermoplastic mask system is a well-established practice in radiation therapy and allow radiation therapists to administer radiation therapy accurately during daily treatment. There are many producers of these mask systems, and each system has its own limitations. Bahl et al. (2012) followed fifty patients during radiation therapy, and although they reported an increase of grade 3 and 4 skin toxicity, this was not a significant increase when comparing it to patients that were treated without a mask (Bahl et al., 2012).

Hadley et al. (2005) measured the change in skin dose, comparing mask systems with small and large holes, as well as the change in thickness when stretched during production of the mask. The thickness of the masks varied from 1.17 mm to 2.39 mm. The increase in skin dose resulted in an increase with a factor of 1.5 in the best-case scenario, and in an increase by a factor of 3.8 in the worst-case scenario (Hadley et al., 2005). This was again shown by Snider et. al. (2015), who also recommended how this bolus effect can be prevented, namely by cutting out the mask re-enforced areas over the neck region and by limiting the skin to PTV distance to 6 mm. With these guidelines the authors managed to reduce the dose to the skin by 26.1% (Snider et al., 2015).

The patients included in this research study had the whole mask system, as well as the S-frame baseplate contoured, to ensure accurate dose calculation close to the surface (see figure 2.22). The headrest under the neck and head was not contoured due to the density being close to the density of air.

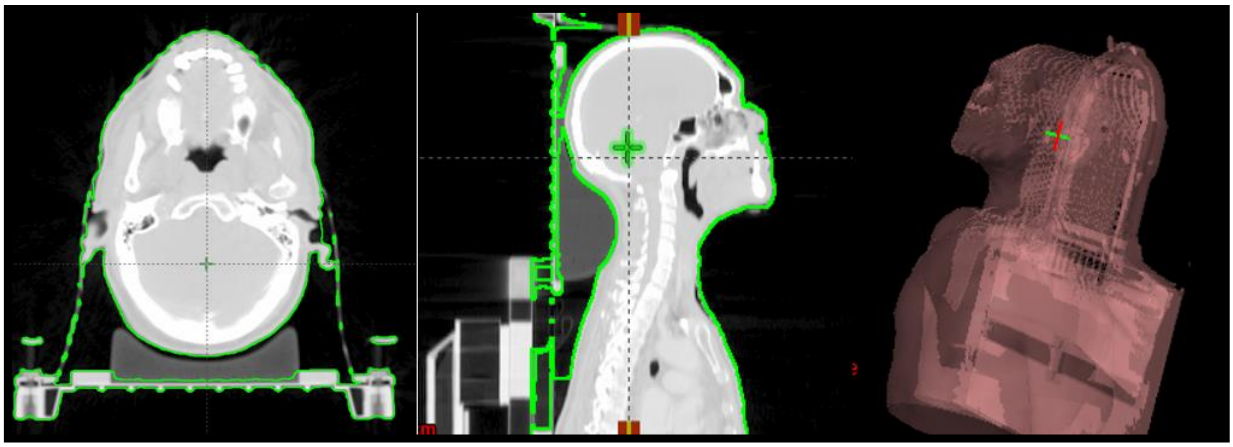

Figure 2.22: The external contour includes the body of the patient, the mask system as well as the S-frame base plate used during CT scanning and treatment. The right image shows a 3D representation of the whole external contour, and the middle sagittal image shows the exclusion of the CT-bed from this contour (illustration produced by author)

2.5 Radiation therapy and therapeutic advances

Cancer cells can be killed by radiation using a variety of mechanisms. The main aim however is to deprive the cancer cell of their multiplication potential and eventually kill the cells. The biological effectiveness (of cell killing) with radiation depends on the linear energy transfer (LET), total dose, fractionation schedule, and radiosensitivity of the targeted cells (Khan et al., 2016).

X-rays are sparsely ionizing radiation and therefore are considered low LET electromagnetic radiation. Although the purpose of the radiation is to deliver a high dose to the tumour cells, it is inevitable that the non-cancerous normal tissues surrounding the tumour, also receive damage from the radiation delivered (Baskar et al., 2012).

2.5.1 Improvement in CT imaging

CT imaging as diagnostic equipment was invented in the early 70's (Bhattacharyya, 2016) and serves as the equipment that acquires baseline data for all subsequent steps in radiation therapy. The CT data set is used to identify and contour the extent of the cancer as well as all other relevant anatomical structures needed for RT planning. The CT needs to have the ability to acquire high quality images, as well as the ability to acquire this data in a very short time, due to the possibility of patient movement as well as organ movement, which may influence the quality of the imaging. Since the invention of the CT scanner, image acquisition times have decreased by more than seven orders of magnitude (Pelc, 2015).

The development of helical scanning, and especially multi-detector row systems facilitated the acquisition of thin slices for volumetric coverage and have allowed the CT to become a 3D imaging modality. The first multi-detector CT's initially acquired 4 slices, followed by 8, 16, 32, and now 320 detector rows are available (Pelc, 2015).

This advancement in CT technology had a direct impact on the contouring and planning capabilities in a RT planning system. It is now possible to do full 3D reconstructions of CT images, which enable the planner to contour not only the transverse slices, but also on sagittal and coronal sections, and in the newest reconstruction software even in other planes. Contouring capabilities in all planes can be a very powerful tool for the planner to visualize certain structures that might not be as easy to contour in the commonly used transverse plane, for example locating bilateral structures if the patient is anatomically skewed during CT.

2.5.2 Improvement in radiation therapy planning and treatment

Head and neck treatment planning for bilateral tumours present many technical challenges, due to the patient's anatomy and multiple target volumes that need to be treated (Shang et al., 2015). With many organs at risk surrounding these tumours, the 3DCRT techniques that were developed by the Bellinzona forward-planning multi-segment technique and the field-in field technique, enabled planners to deliver high doses to the tumour, and the subsequent sparing of OARs (Herrassi et al., 2013).

Intensity modulated radiation therapy was developed during the 1980-1990's, due to the improved computing capability required for inverse planning (Cho, 2018a). In 1994 the first commercial IMRT system became available, and in 1995, 13 patients were treated with the Peacock 3DCRT planning and delivery system utilising conformal RT beams that were utilising intensity-modulated fields (Carol et al., 1996). The first systems used compensators or multisegmented IMRT delivery on the linear accelerators, but they were soon replaced by dynamic multi-leaf collimators (MLC). The aim of IMRT was to firstly, maintain delivery of the high dose inside the tumour, and to lower the dose to normal tissue surrounding the tumour and secondly, to escalate the dose to the tumour while maintaining acceptable normal tissue doses. Hong et al. (2005) noted that it was necessary to apply caution along with the enthusiasm with respect to the use of IMRT. Concerns were raised regarding the acceptance of IMRT as a standard approach, until comparative clinical trials had been done. Nevertheless, the use of IMRT spread dramatically in the field. One concern with IMRT was the increase in integral dose to the patient due to a dramatic increase in monitor units (MU) required for IMRT (Hong et al., 2005). Consequently, the increased radiation leakage from the linear accelerator, raised the total body exposure by 2-3 times. This increase could potentially heighten the rate

of second malignancy from 1% per 10 years to 1.75%, thus almost doubling it (Hong et al., 2005).

The concept of Tomotherapy arose in the late 1980's, and the first paper published in 1993. This was the introduction of the continuously moving slip-rig gantry. The modulating beam was produced by a fan beam and a binary collimator system, without the use of any flattening filter, and with continuous couch movement. The use of this system would eliminate the inaccuracies between treatment plan junctions found in linac based treatment (Mackie, 2006).

In 2008 equipment manufacturer Elekta announced the first two clinical sites using VMAT technology (Elekta, 2008). Prior to this, VARIAN introduced Rapid-Arc technology during the ASTRO congress in 2007, and in 2008 developed a global council of specialists to improve this technology (Varian, 2008). These two companies rapidly developed the planning and treatment equipment to be able to deliver this type of treatment technique. VMAT/ Rapid-Arc (the term used for VMAT by Varian medical systems) is described as a form of single arc IMRT. The delivery technique includes gantry rotation speed modulation, treatment aperture shape via movement of the MLC leaves, and fluctuation of the dose rate. The technological advances in both software and hardware enabled the development of these technologies. The delivery technique of VMAT (Rapid-Arc) is faster than IMRT, with IMRT taking approximately 15 minutes to deliver multiple beams, and VMAT taking only 2 minutes to deliver 2 arcs of treatment and with less monitor units and faster treatment time, a reduction of integral dose was achieved (Teoh et al., 2011).

International clinical studies revealed that VMAT (Rapid-Arc) plans were superior to IMRT for head and neck cancers in dose comparison to the PTV, as well as OAR doses (Fung-Kee-Fung, 2012; Holt et al., 2013). The treatment delivery time and less MUs reduced the risk of intra-fractional patient movement, and along with less dose transmission at the collimator and a reduced risk of secondary malignancies (Krishnan et al., 2015).

As imaging modalities allow for more detailed visualisation of tumours in the head and neck, the shape of the tumours is becoming more accurate and thus, more complex to treat. This is true especially in head and neck RT planning with the presence of multiple tissue densities. Advanced optimization algorithms are essential in reducing dose to the OAR, for example the spinal cord and parotids. These improvements also allow re-irradiation to become easier to manage, as the limiting dose allowed for the spinal cord often prevents re-irradiation, if recurrences happen in the same area (Klippel et al., 2015).

2.5.3 Improvement in patient image guidance at treatment

Accurate reference images and high-quality planning techniques produce acceptable treatment plans and could predict acute and late toxicity for each head and neck patient. Poor

positioning and poor positioning verification procedure, will negatively impact the treatment plan and could lead to increased side effects and less curative dose delivered to the PTV (Leech et al., 2017).

Historic treatment of head and neck cancers in South Africa involved the use of localisation with the use of a simulator (van Wyk et al., 2017) where x-ray images were taken of the target area, and these parameters transferred to the patient skin or mask with a marker pen (Storer & Teljeur, 2006). The patient would then be positioned on the treatment machine and the light field produced, by the machine was aligned to these markings before treatment commenced.

Isocentric laser systems are now used to position the patient for treatment by aligning the markings on the mask system with the lasers. However today radiotherapy imaging allows the alignment of the patient's bony structures to the reference images created from the planning CT.

Megavoltage planar images (portal images, colloquially referred to as EPID images at the research study center) can be used in gantry-based systems. These 2D images are compared to Digitally Reconstructed Radiographs (DRR) created from the planning CT scan. These images are mostly used to compare bony structures. Kilovoltage on-board imaging (OBI) has led to improved planar image quality, and these same systems can now acquire a cone-beam CT that enables soft tissue comparisons to the baseline planning CT directly. Improved matching algorithms allow for automatic fusion of image sets as well as de-formable registration (Dieterich et al., 2016).

Planar stereoscopic kV-imaging systems for example the Exac-Trac system (BrainLab AG, Feldkirchen, Germany) use paired x-ray tubes/ flat panel imagers mounted to the floor and ceiling around the linear accelerator to determine the set-up error relative to the DRR. Dual energy kV systems enable subtraction imaging to enhance soft tissue visualization (Brainlab, 2013).

Linac-based imaging systems enable the RTT to verify the patient positioning in the actual treatment position and to compare the current position to the original position of the planning CT. If there is any difference, corrections can be applied to ensure accurate treatment. This is called image-guided radiotherapy (IGRT). Image guidance must be applied at regular intervals, even daily if clinically required (Nakata et al., 2013).

Three dimensional (3D) surface tracking has also been used in head treatments by utilising infrared reflective markers on the mask of the patient and stereoscopic cameras to align the patient (Brainlab, 2013). Surface guided radiotherapy uses stereo vision technology which tracks the surface of the patient in 3D. It can monitor both setup accuracy as well as motion

management during treatment adding another dimension to patient set-up accuracy (NICE, 2018).

As the mask systems used for immobilisation of the head and neck during treatment are considered uncomfortable and challenging to use for patients with claustrophobia, technology aims to eliminate the use of the mask. One such method is to produce a partial mask, which only immobilizes the forehead and chin. Mouldable pillows can be used for shoulder positioning. These less conventional systems can only be used if advanced imaging modalities are present to verify the correct position (Zhao et al., 2018).

To position a patient accurately for daily treatment requires trained radiation therapists (RTTs). The use of imaging and tracking devices allows the RTT to verify and correct daily inaccuracies that were previously unknown or not accounted for. The author must however acknowledge that the use of these technologies is highly technical and extensive training in their correct use is required. Specialisation towards image interpretation could be advantageous for the increase use of IGRT (Alimonte et al., 2017; Harnett et al., 2018).

2.6 Treatment uncertainties and positioning set-up errors

To ensure correct radiation therapy treatment, the first step in treatment correction is to compare the measured patient position with the treatment plan using a reference image. Image registration tools can co-register the two sets of images, which in turn translate into set-up corrections. There are currently two modalities that can assist the radiation therapist. The first is 2D orthogonal images and the second cone-beam CT images that can be acquired on the linac with the patient in the treatment position. The measured inaccuracies can be corrected by applying the measured shift to the treatment couch on which the patient is positioned. A remote controllable treatment couch reduces errors and should be used, rather than manual corrections, but should always be verified. The use of an automated couch also reduces the time needed for this intervention (IAEA, 2019).

The aim during daily treatment is to always treat the patient in the same position as prescribed by the position the patient had at the planning CT. However, a very complex data-process needs to happen before the patient can start treatment. A number of factors can influence the patient positioning on the day when compared to the planning CT scan, as discussed in section 2.3.2. The planners try to mitigate the level of uncertainty by adding margins to the tumour, in order to ensure that the tumour receives the correct dose. Calculating this margin is a very complex process and can include many uncertainties. When understanding and locating these possible uncertainties, measures can be implemented to reduce them. This will result in

smaller safety margins and a decrease in dose to normal tissue that directly translates to reducing short- as well as long term side-effects (Kung et al., 2019).

The van Herk's equation can be used to estimate the CTV to PTV margin. It incorporates two levels of uncertainty. The first, and the one that has the largest impact on this margin, is the systematic error. The random error, is considered to have less of an impact, but cannot be ignored (Van Herk et al., 2000).

$$\text{PTV Margin} = \underbrace{2.5\Sigma}_{\text{Systematic Error}} + \underbrace{0.7\sigma}_{\text{Random Error}}$$

Equation 2.1 The van Herk equation used to calculate the PTV margin (Van Herk et al., 2000)

This equation can only be used when a patient is receiving a large number of treatment fractions and the result of this equation is to ensure a minimum dose of 95 % to the CTV for 90 % of the patients. This equation only includes translational uncertainties, and excludes rotational errors (roll, pitch, jaw rotations).

Mans et al. (2010) conducted a retrospective study to identify and quantify the level of systematic errors and the use of in vivo dosimetry to prevent these errors. Although rigid QA is performed in radiation therapy prior to the patient starting treatment, some errors are difficult to foresee or recognize. For example, one such error identified was the accidental corruption of a few segments of an IMRT plan. It was found that MLC positions could not be practically verified segment by segment, as the chance of recognizing a missing segment in a beam consisting of 37 segments was impossible. Other systematic errors found included: a change in patient anatomy, accidental plan modification, failed delivery, and sub optimally tuned TPS parameters. Furthermore it was noted that considerable weight loss, recovery from atelectasis, patient contour change and the emptying of a postoperative cavity that was filled during the planning CT, all had considerable dosimetric changes as a result and could not be detected unless dosimetry was done during the actual treatments. These changes all had a radical contribution to systematic errors (Mans et al., 2010).

Such gross errors, transcription errors and software faults must be identified by quality assurance and will not necessary be eliminated by portal imaging during treatment. Dose errors (or deviations) are the difference between the measured value and the expected value obtained, considered to be a reference. Errors in dose, may be errors of commission or omission, and usually reflect deficiencies in the system of care. Although the aim should

always be to minimize them, further discussion in this document does not include dosimetric errors or gross errors.

The van Herk's equation is a measurement tool of accuracy. Accuracy is defined as the closeness of agreement between a result (imaged and measured) and the true value (reference image) (IAEA, 2016). This accuracy involves a combination of random and systematic components (IAEA, 2016).

Examples of systematic errors include the motion of the skin with respect to the internal anatomy during daily treatment set-up (Van Herk, 2004). Rigid immobilisation of the patient receiving RT to the head using a comfortable head rest and rigid mask system could limit the movement of the skin, but if the motion of the larynx during swallowing is not included in the contouring process, this would lead to a systematic error where the internal organ motion is not taken into consideration. A random error for this (mask immobilised) patient could be daily set-up error where the thickness of the lasers and thick pen markings on the mask could lead to small variations in set-up These errors are illustrated in figure 2.23.

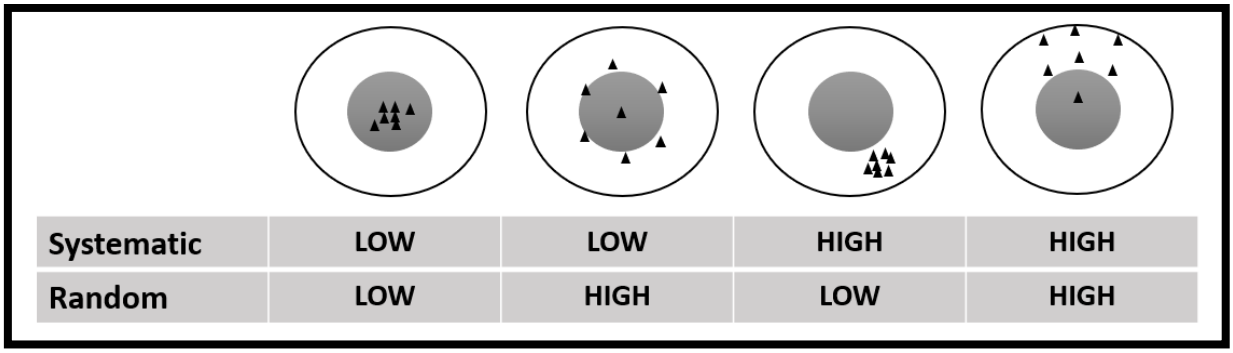

Figure 2.23: Random and Systematic Uncertainty (illustration produced by author)

Set-up errors measured from a single image will contain both systematic and random components. Over a period of acquiring multiple image sets, the systematic part of the measurement will nominally be constant, whereas the random part will vary in an unpredictable way. Gross error is an unacceptably large set-up error, that could underdose a part of the TV or overdose an OAR and should be corrected before any treatment is delivered. The possibility of eliminating gross error due to the valuable contribution of imaging modalities on linacs adds great value to the patient outcome (Royal College of Radiologists, 2008).

The expansion of the CTV to PTV is of cardinal importance to ensure that the CTV receives the treatment dose. The variations that can occur for head and neck patients need to be quantified accurately and should incorporate the possible movement of the CTV and the patient itself, as well as the tissue surrounding the CTV and all the geometric components (e.g.

beam shape, gantry sag). These variations can vary from patient to patient as well as from treatment unit to treatment unit (ICRU, 1993).

The repositioning uncertainties for patients receiving head and neck radiation therapy are dependent on the exact site and the immobilisation device used and could significantly influence random as well as systematic error (Verma et al., 2016). When treating the head and the neck a mask system that covers both sites should be used with marks that are put on these immobilisation devices to indicate the reference CT slice, isocentre and field outlines. The marks must be clear and not too thick. When positioning lasers have to coincide with such markings, thicker lines allow a larger positioning variability. Care must be taken when a second phase of treatment commences, in order to prevent confusion in the location of the treatment area. Some treatment centres prefer different colour marks for the second phase of treatment. If tape is used on the mask it should be secured with minimal creasing in order to facilitate clear marking. Institutional policies must reflect the reference system based on table position and the indexing of immobilisation and positioning devices. After production of the mask, it must be marked with the patient details clearly visible. The mask must be carefully stored to prevent distortion (IAEA, 2016).

Strbac and Jokic (2013) evaluated the set-up errors present in their clinic with the use of a 5-point head and neck Orfit cast system for immobilisation. The departmental protocol indicated that each patient would receive at least 3 sets of portal images in the first week and thereafter, weekly for patients treated with 3DCRT. Those having IMRT were imaged daily. If a mismatch of < 3 mm was observed, no corrective action was taken, but if > 3 mm, the patient was re-positioned, re-imaged and corrected. Using the van Herk's equation, they obtained results of 1.9 mm to 6.16 mm in the three directions, and concluded that the use of a 6 mm CTV to PTV margin remained an acceptable confidence level in their department (Strbac & Jokic, 2013).

The treatment of the head and neck region can pose a challenge, as the shoulders and thorax could potentially be more movable and therefore less reproducible with daily treatment than the head. An audit of set-up reproducibility done by Verma et.al (2016) comparing three mask systems indicated significantly larger set-up errors in the neck and shoulder regions compared to the head. The portal imaging offsets were measured in the medial-lateral (ML), anterior-posterior (AP) and cranio-caudal directions (CC). Using the S-frame system the measurements in the face were 3 mm, 4 mm and 5mm respectively, compared to the neck's 4 mm, 8mm and 5mm in the same directions. When using the S-frame system with the re-enforced chin and nasion region the results were 3 mm, 4 mm and 3mm for the head and 3 mm, 5 mm and 3mm in the neck area respectively. It was concluded that reinforced masks therefore add value in set-up accuracy (Verma et al., 2016).

Gilbeau et. al. (2001) reported that the use of a 5-point head and shoulder immobilisation mask system resulted in 90% of the setup variations in all three directions to be below 4.5mm for the head area and 90% to be below 5.5mm in the neck region.

The increases in the complexity of head and neck treatment and the use of IMRT with very steep dose gradients, it is noted that image guidance is becoming a daily, rather than weekly tool. Nakata et.al. (2013) recognized the challenge in the reproducible set-up of patients receiving RT of both the head and neck area. Using Exac Trac to monitor daily treatments before, during, and after RT, they divided this region of interest (ROI) into two imaging areas. The first was superior to the third cervical spine and included the head, the second inferior to the third cervical spine and included the shoulders. With a six-degree-of-freedom couch, corrections could be applied for the pitch, roll and yaw rotations, as well as the ML, AP and CC directions. They reported that even with the use of IGRT and a mask immobilisation system, it was still not providing sufficient reproducibility of both the head and the comprehensive nodal irradiation area in the neck (Nakata et al., 2013).

To compare the use of EPID images and CBCT in head and neck RT, Kang et al. (2011), indicated that with the use of 2D imaging with a six-degree-of-freedom couch system, the translational set-up error was found to be 3.5 mm +/- 2.2 mm (range 0-8 mm). The further use of CBCT resulted in very small incremental adjustments between 0.8 mm +/- 1.5 mm. They also acquired a CBCT after RT to determine the intrafraction motion, and observed < 3.5 mm for 8 of the 9 patients and < 2 degrees for all patients (Kang et al., 2011).

Intrafraction tumour and OAR motion in the head and neck area has been shown to be significantly less than other body parts where large motion can be observed, for example, the lungs during breathing (Glide-Hurst et al., 2010). In the head and neck area, the larynx can move significantly during swallowing, and the patient should be instructed to not swallow during RT (Matsuo & Palmer, 2009).

With the use of IGRT, interfraction motion has the most significant influence on overall treatment uncertainties. A measurement of interfraction motion of patients treated for nasopharynx cancer resulted in shifts less than 2 mm observed in all directions. It was determined that without the use of online CBCT the required right to left, crania to caudal and anterior to posterior margins are 4.9 mm, 4.0 mm and 6.3 mm respectively. However daily CBCT imaging reduced margins to 1.2 mm in all directions (Lu et al., 2012).

Uncertainties in target volume definition and the certain complicated motion in the patients, cannot be corrected or solved by IGRT. Daily positioning and set-up error of a patient will always be present, therefore radical fractionated radiation therapy can never be successful without safety margins (IAEA, 2016).

Guckenberger et al. (2006) quantified the influence and magnitude of translation and rotational error in radiation therapy. The cranial-caudal length of the PTV for advanced stage head and neck cancer can translate to a large error in the presence of rotations. With a rotational angle of only 2 degrees, at a distance of 10cm from the isocentre the deviation is 3.4 mm, and at 20 cm it is 6.8 mm. This is of clinical significance for high-precision radiotherapy (Guckenberger et al., 2006).

Uncertainties in the planning and treatment process remain a challenge. The continuing research and implementation of clear policies, guidelines and procedures will ensure good treatment practices and patient outcomes. Education and training for routine procedures, as well as new technologies, should be ongoing for all staff, to ensure best practice in each department (IAEA, 2016).

2.7 Image matching

2.7.1 Imaging during radiation therapy treatment

Good quality images are essential for both the reference and the acquired images.

The image quality of the Digitally Reconstructed Radiograph (DRR) is directly related to the slice width of the planning CT. Therefore, the use of standard procedures, to ensure the correct slice with is consistently used is important. It is recommended by the Royal College of Radiologists (2008) that if the DRR is of poor quality, an X-ray simulator reference image should be obtained, but it is noted that this adds the risk of introducing further systematic error by adding an additional step to the RT process. As the X-ray simulators are not widely available, great care should be taken when acquiring the CT. The ideal image quality should have fine spatial resolution and high contrast with a high contrast-to-noise ratio. Thus additional image processing software might be needed to achieve high quality DRR's (Royal College of Radiologists, 2008).

The quality of the reference and treatment image must be of sufficient quality to identify both the isocentre and/or field edges, as well as the tumour surrogate which could be bone, soft tissue, or implanted markers (Cherry & Duxbury, 2009). The use if contrast during acquisition of the CT images, could also add uncertainty to the quality of the DRR, as the density of the contrast is similar to bone, and will be visible on the DRR and not on the linac based 2D image.

The quality assurance component of image matching must include each step in the verification process, from the acquisition of planning data to the subjectivity in decision-making by individuals. The registration techniques and accuracy of different algorithms available and image processing can also affect the measured displacement. The translation of 2D data to 3D movements and the accuracy of the couch movements must be tested with a robust QA

protocol, as this treatment technique process could add uncertainty and must be included in PTV margin calculations (Royal College of Radiologists, 2008).

It is recommended by the Royal College of Radiologists (2008), that patient imaging action levels must be designed for each treatment site, and for each individual radiation therapy centre. It is recommended that gross errors should be immediately acted upon, and that action levels and tolerances depend on the imaging strategy adopted by each centre. Imaging must be conducted at least once per week. All corrections applied to the treatment set-up must be verified by repeated imaging (Royal College of Radiologists, 2008).

2.7.2 Imaging for the patient receiving radiation therapy to the head and neck region

The use of a mask system for head and neck radiation therapy is mandatory. Changes in shape and anatomy are important in head and neck cancer and can be due to weight loss or shrinkage of the tumour. This could lead to an ill-fitting mask and a decrease in treatment accuracy. If this occurs re-masking and re-planning is recommended in the 3rd or 4th week of treatment. The movement of the tongue and larynx are potentially relevant, in anatomical matching, and should be controlled with the use of tongue depressors and coaching to limit swallowing during imaging and treatment.

It is recommended by the Royal College of Radiologists (2008), to image during the first fraction and to correct any gross errors immediately. If field edge verification is needed, specific treatment fields can also be imaged over and above the orthogonal images or CBCT. Images acquired on the 1st, 2nd and 3rd fraction are assessed against the recommended tolerance levels, an overall error level calculated, and applied at the 4th fraction. Further weekly imaging must be assessed and if any isocentre adjustments are needed, these must be verified for at least two further fractions (Royal College of Radiologists, 2008).

The images acquired must be of sufficient size to ensure that the bony anatomy is visible and the appropriate bony landmarks have been identified by the Royal College of Radiologists (2008). These anatomical landmarks include the nasal septum, vertebral bodies, sinuses, maxilla, clavicles, posterior wall of trachea, pituitary fossa, base of skull or any other stable radiopaque structure, for example a dental filling. The same authors recommend that these anatomical structures should be used for matching, whether they fall inside the field arrangement area or not. They recommend that at least three identifiable structures should be used per image and contoured on the reference image.

Tamponi et al. (2014) conducted a retrospective audit of set-up errors in head and neck patients and suggested that the use of the nasal septum, sinuses, maxilla, lateral edge of

vertebral bodies, and clavicles for the matching of the anterior image; and the sinuses, maxilla, pituitary fossa, base of skull, posterior wall of trachea and anterior edge of the vertebral bodies for the evaluation of the lateral image (Tamponi et al., 2014).

The mandible, clivus, C2 vertebra and C7 vertebra were used as surrogate matching structures in use with CBCT in a study by Kung et al. (2018). These structures were 3D contoured on the reference data set and expanded by 3 mm and 5 mm, respectively. Due to multiple translational errors identified during CBCT matching, and the complexity of the matching of both the head and shoulder areas, the use of these surrogate (expanded) structures, achieved more acceptable matching results. It was found that after the use of the 5 mm margin contours, the unacceptable registration decreased from 15 % to 4 %; and with the 3 mm planning target volume margin, the unacceptability decreased from 49 % to 21 % with the use of a six-degrees-of-freedom correction (Kung et al., 2019).

The image interpretation of head and neck during verification CBCT is extremely challenging due to variable rotations that can be present in both the head and the shoulders area separately (Nakata et al., 2013).

2.7.3 Imaging for the patient receiving radiation therapy to the head region

Verification of the target position for tumours in the brain is done by comparing bony anatomy as the tumours are fixed within the confines of the skull. The frequency of imaging will be dependent on the RT method and PTV margins used. The British National Radiotherapy Implementation Group Report on IGRT (2012) recommends that imaging is required for the first 3 fractions using off-line matching to eliminate both systematic and random errors, however online imaging must be used if large variations are seen (e.g. gross errors), followed by weekly imaging to establish for trend over time, that can occur due to the changing fit of the immobilisation devices due to weight increase (due to steroids) or hair loss (Richards, 2012).

These factors agreed with the “On Target” document (Royal College of Radiologists, 2008) and it was pointed out that internal organ motion is very small in this group of patients, and with stable positioning imaging on the first day of treatment might be the only imaging needed. But with steep dose gradients when using IMRT, and the close proximity of some OAR to the PTV, imaging could be done more often. These factors, however, are only applicable to fully fractionated RT, and do not include stereotactic RT. Tumours with very small margins as is common in stereotactic treatments, will require daily verification (Royal College of Radiologists, 2008).

Orthogonal image sets, and a field size that minimises dose to critical organs (where possible) should be standard of care. If field edge verification is needed, each treatment field should be imaged. Although vertex fields cannot be imaged, the field light seen on the patient can be utilised for verification.

As recommended by the Royal College of Radiologists (2008), at least three bony structures visible in each image are outlined on the reference image and are used for matching. The following anatomical structures have been indicated as the most stable features and are recommended for use: on the anterior image: stable radiopaque structures or surgical defects, orbital ridges, nasal septum, inner border of the skull vault, frontal sinuses and zygoma and o the lateral image: the inner border of the skull vault, occiput, pituitary fossa, frontal sinuses and orbital ridges could be used (Royal College of Radiologists, 2008).

2.8 Conclusion

This chapter gave an overview of the literature to substantiate and motivate this research with an understanding of the evolution of technology and the need for treatment accuracy, the radiation therapy process from the CT-planning, contouring, plan calculation and treatment accuracy was discussed. Our responsibility as healthcare workers mandate us to ensure that good radiation therapy practice is based on international guidelines, trusted research and local practice.

Chapter 3 provides the process applied to conduct this research study. The aim being to determine the accuracy and reproducibility of the treatment given to the patient to enable the correct planning margins to be applied at the planning process stage, and comparing 3DCRT radiation therapy to VMAT radiation therapy for patients with late stage larynx cancer, with the comparison of the dose to both the OAR and the PTV.

CHAPTER 3 The Clinical Research Processes

3.1 Introduction

This chapter presents the methodology of the retrospective collection of patient data and the processes used to conduct this study. All sub questions are explained individually. The VARIAN Aria Oncology Information System and Eclipse treatment planning system version 10 using AAA algorithm were used.

Sub-question 1 used the DRR images of all patients treated during the 2016 calendar year using the identical mask system and compared it with the weekly EPID images. As all patients at the research site were treated with the same mask system, the sample size was enlarged to all patients over a one year period (69 patients), rather than only using the 10 patients studied further in subsection 2 and 3, as this result would have an increased statistical significance and representation of population error.

The contouring of the DRR is illustrated and described as well as the image matching processes and peer review of matching results. The uncertainties occurring during data collection has been included to aid the reader in understanding the limitations encountered during the data collection process. This data enabled the calculation of the accuracy and reproducibility of patients when treated with this specific mask system and it is needed to correctly expand the OAR's and CTV's to ensure correct treatment.

The CT data and plans of 10 patients were used for sub-question 2 and 3.

Sub-question 2 illustrates all OAR's and PRV's that were contoured and created as well as the dose recording that was included in this study. This sub-question will enable dose comparisons of the OARs for the respective VMAT and 3DCRT planning techniques.

Sub-question 3 provides information of the creation of the treatment plans and specific PTV data recording parameters. It enables the comparative measurement of dose achieved to the PTV for the two different planning techniques.

3.2 Research strategy

3.2.1 Research design

All data was collected at one research site (a tertiary hospital in the Western Cape), utilising the data from a period of one calendar year (2016). All the data used was collected retrospectively during 2017.

Quantitative data collection was used as the statistical method used for all three sub-questions.

3.2.2 Method of analysis

The van Herk calculation was used to determine the set-up accuracy for sub-question 1 (Van Herk, 2004). Other data was quantitively analysed and the results presented in descriptive statistics format, for example table form as can be seen in sub-section 4.2.2 and 4.2.4.

In sub-question 2, the doses to the OAR and normal tissue structures achieved for each planning technique were compared using the Independent-Sample Kruskal-Wallis Test. This is a rank-based nonparametric test that is used to compare outcomes and statistically significant differences between two or more groups of an independent variables. Therefore it will indicate if one sample doinates on other sample. Where needed, the data was further compared using multiple comparisons (LaMorte, 2017). Each OAR was first analized individually, see subsection 4.3.2 to 4.3.10. Thereafter the whole population was compared using the plan scoring system designed for this research study, see subsection 4.3.11.

For sub-question 3, mathematical equations from Feuvret et al.(2006) was used to calculate the conformity index and, lesion coverage; and homogeneity index was calculated using 4 calculations (Helal & Omar, 2015). These are further described in subsection 4.4.2 to 4.4.5. The results of these calculations were further compared using the Chi-Square test for statistical comparison of the HI results, to determine statistical significance within each planning group (Nihan, 2020). The Kruskal-Walis test was used for statistical significance between planning groups, and where applicable pair comparisons were made. All results were quantified in the plan scoring system that was specifically designed for this research.

As the same 10 patients' data were used for the analysis of sub-question 2 and 3, the results of these two sub-questions were combined to determine the overall plan score and is discussed in subsection 4.5.

3.3 Data collection, production, and analysis

3.3.1 The clinical research process for sub-question 1: How accurate and reproducible is the treatment set-up?

This section will address the data collection and production to answer the first sub-question relating to the accuracy and reproducibility of the treatment set-up, which will ultimately enable the calculation of the expansion margins needed for the CTV in relation to the PTV.

3.3.1.1 Patient numbers and inclusion criteria.

The hospital where the research was conducted provides each new patient with a unique identification number. These numbers are used on the oncology information system for all oncology related data, treatment, and storage. This unique number will always start with the

first four digits of the year of registration, and the following four digits will be consecutive numbers. For example, the first patient that was registered in the year 2016 will be assigned the number 2016.0001, the following patient will be 2016.0002. The patient management system is ARIA which is provided by the VARIAN medical systems company (Varian, n.d.).

As there is no written register to search for a specific patient according to diagnosis, all patients on the system whose registration number starts with 2016, had to be identified. 615 radiation therapy patient registration numbers were found in the radiation therapy part of the department. Each patient's data had to be viewed to enable the identification of patients who receive a CT scan of the head and neck area, and who could have been eligible for radiation therapy.

Of the 615 patients, 134 patients were identified as having received a CT scan of the head and neck area with a thermoplastic mask fitted. The rest of the patients received radiation therapy treatment on other body sites.

Although the 134 patients identified were treated with the same thermoplastic mask system that was covering the head and the neck and shoulder region, the specific treatment area varied. All patients were included as an appropriate sample size was needed of patients being treated with these masks. Patients included in this data collection were not only those suffering of larynx cancer, but all patients treated with the thermoplastic mask system. There were those who only received radiation treatment of the head, and therefore only the head was imaged, and there were those who received treatment of the head and the neck area simultaneously.

Patient inclusion criteria were:

- Five or more imaging sets available for evaluation.
- Radiation treatment administered to the head or head and neck anatomical region.
- Completion of the radiation therapy to enable retrospective data collection.

Sixty-one of the 134 patients identified who had a planning CT with a mask fitted, did not meet the inclusion criteria and were excluded from this study. The reasons for exclusion were ranged as follows:

- 20 patients had no radiation therapy, or no DRR or EPID images.
- 19 patients had less than 5 image sets done during the course of radiation therapy.
- 12 patients were still receiving radiation therapy when the data collection closed on 13 February 2017.
- 2 patients had radiation therapy where the neck and mediastinum were imaged.
- 2 patients had stereotactic radiation therapy.

- 1 patient was a child where only the neck was treated.
- 5 patients had craniospinal radiation therapy where both the head and spine were imaged.

Of the remaining 73 patients, 36 had treatment to the head only (see figure 3.2), and 33 had treatment in the head and neck region (see figure 3.1). Four patients were found to be so grossly miss-aligned, that portal image matching was impossible. In consultation with the responsible oncologist, it was decided that they will not be eligible for this study.

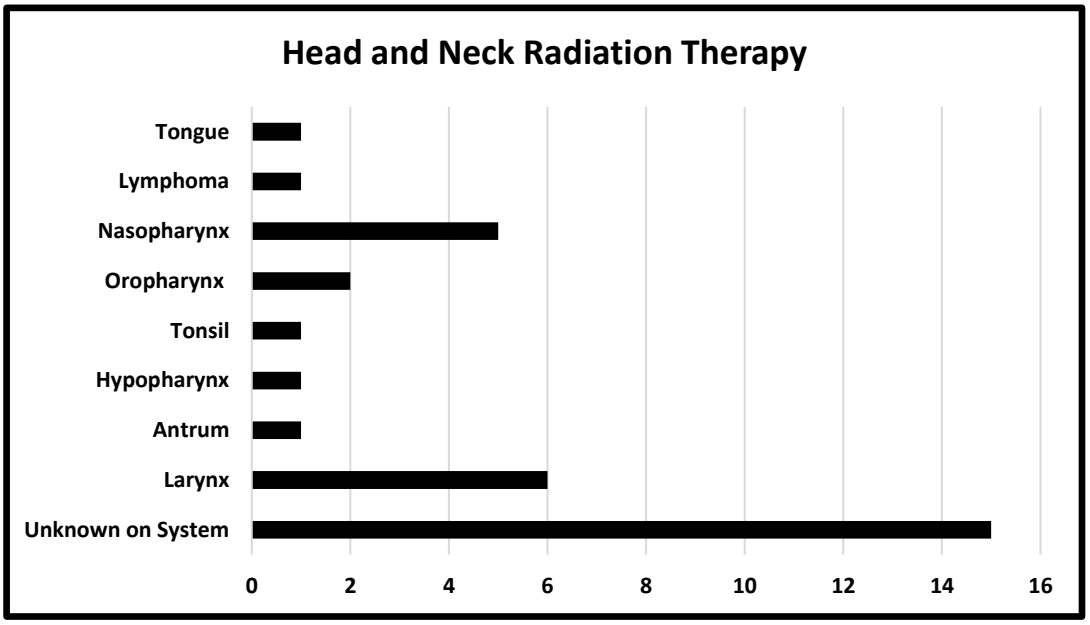

Figure 3.1: Patient numbers and cancer site, included in study who received treatment of the head and neck region (figure produced by author)

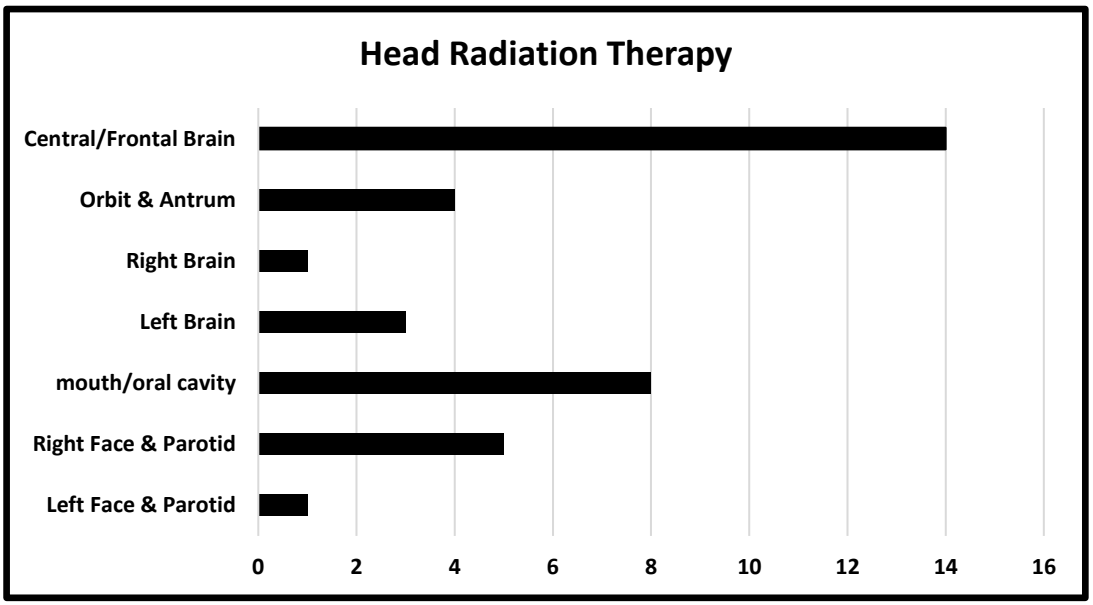

Figure 3.2: Patient numbers and cancer site included in study who received treatment of the head region (figure produced by author)

3.3.1.2 Data preparation for the head and neck matching

During data collection it was found that many image data sets had not been matched at all, and very few, if any, guiding contours had been used to compare the data. Figure 3.3 provides examples of guiding contours that were used in the clinical setting. Most patients had no structures outlined at all.

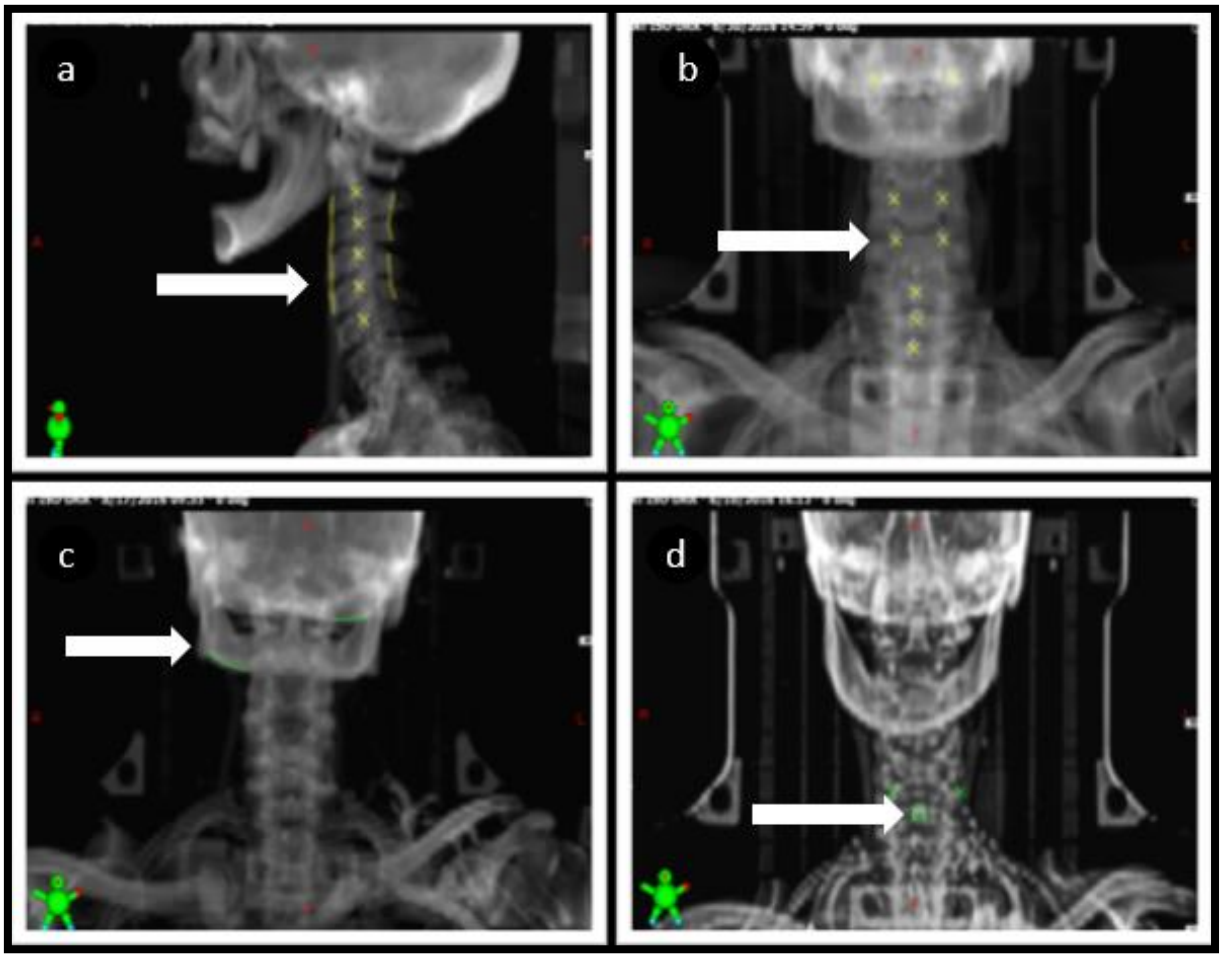

Figure 3.3: Guiding contours found on patient data. (a) Anterior vertebral bodies demarcated, as well as crosses and lines on spinous and transverse processes. (b) Crosses on bony structures of the vertebral bodies. (c) Line indicating mandibular body and base of skull (occipital bone). (d) Spinous process contoured as well as a cross on the uncinate process and zygapophyseal joint (illustration produced by author)

At the research site, when no matching had been performed on an image set, an attempt was made to use the auto matching function, to establish the data match. As the bony anatomy in the head and neck area is complex, it was found that the auto matching functions tended to fail thus manual matching had to be performed. Figure 3.4 illustrates how the automatic matching was completed but shows that there was still no agreement between the two images, and it therefore failed. Figure 3.5 demonstrates the gross miss-alignment found in figure 3.4 after the automatic matching process.

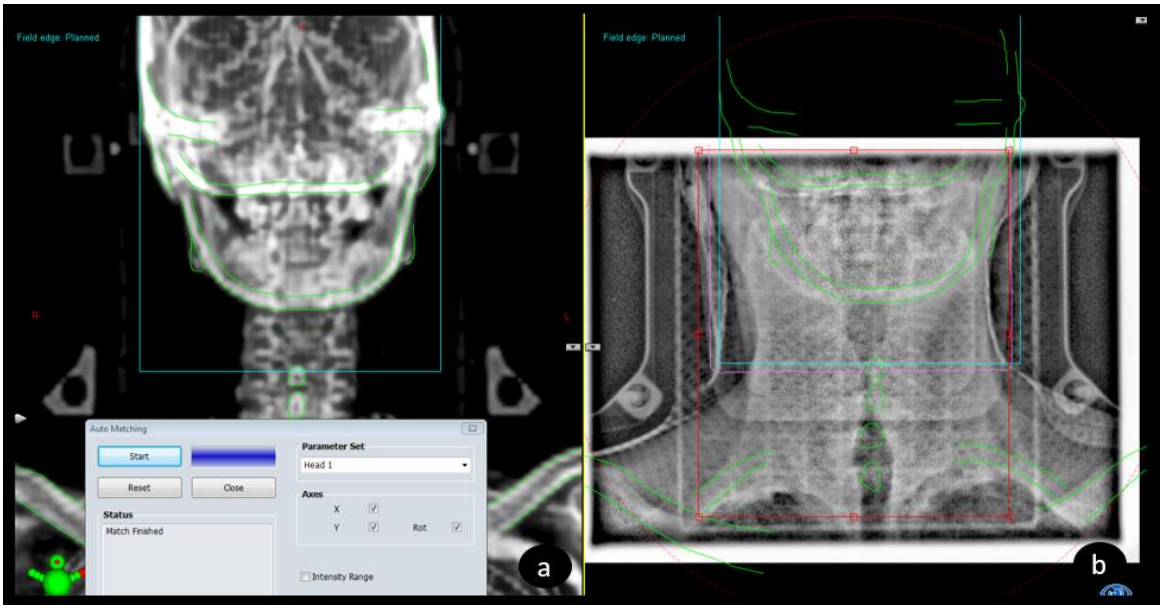

Figure 3.4: Illustration of applying auto matching of the head and neck patient's anterior isocentre verification image. Guiding contours have been drawn on the DRR (a), and projected onto the EPID image (b), to verify the auto matching algorithm that was applied inside the red block drawn on the EPID image (b) (illustration produced by author)

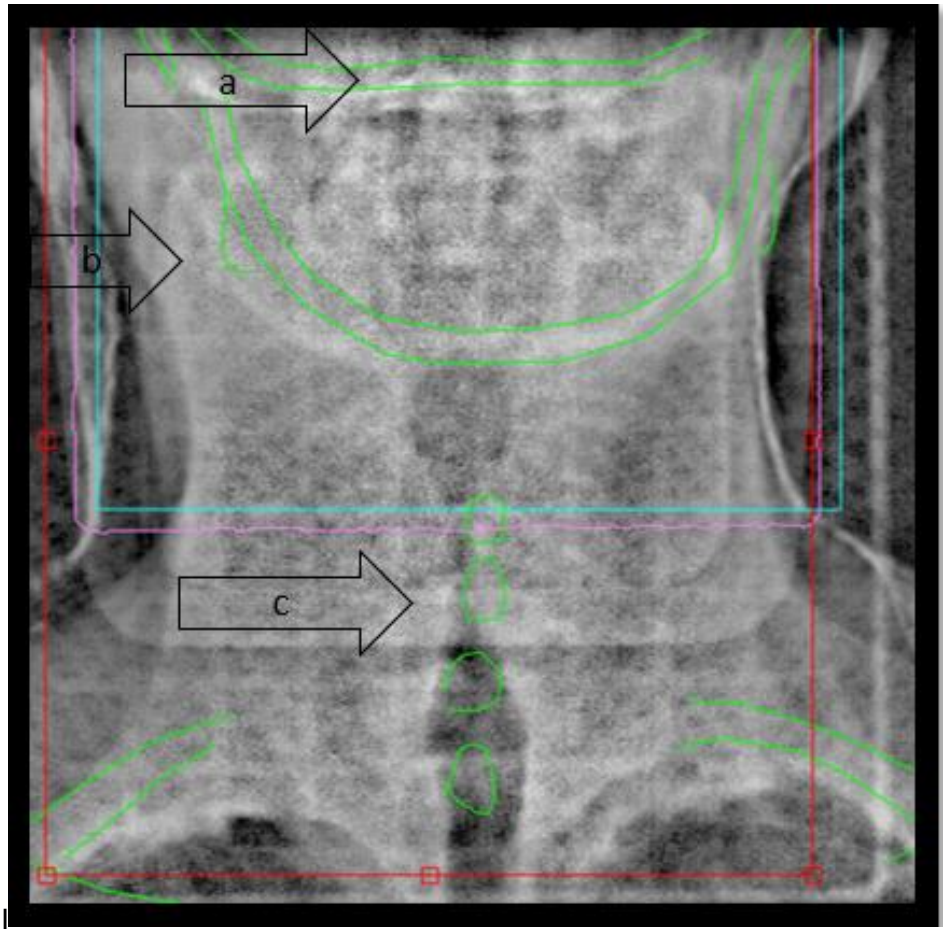

Figure 3.5: Enlargement of Figure 3.4b to indicate gross miss-alignment of EPID image and DRR image after performing auto matching. (a) Base of skull miss-match, (b) Mandibular angle, ramus, and body miss-match (c) Spinous process of cervical vertebra miss-match (illustration produced by author)

A decision was made that in order to accurately verify the matching datasets, guiding structures must be drawn on all DRRs, before a manual comparison with EPID images was to be carried out.

3.3.1.3 Head and neck DRR contouring

The Royal College of Radiologists (2008) report that within the head and neck treatment area, the tongue and larynx may have some movement during treatment due to swallowing. These structures should therefore not be used for anatomical matching (Royal College of Radiologists, 2008).

The report (2008), further noted that at least three structures, that are visible within the field, should be outlined. Bony structures that should be used for anatomical matching which can be visible on both the DRR and EPID images include:

- Nasal septum
- Vertebral bodies
- Sinuses
- Maxilla
- Clavicles
- Mandible
- Pituitary fossa
- Base of skull.

Any other visible bony structures or stable radiopaque structures, for example teeth or implanted prosthesis, as well as the posterior wall of the trachea (from the lateral image), can be helpful when further reference landmarks where needed.

The DRR should be created to enable the visibility of these anatomical landmarks to be identified and contoured. DRR's that are created using only the bony setting do not allow any soft tissue to be identified. Unfortunately, all the DRR's used in this research study were created using the bony setting of the software, and therefore the researcher had to use the limited filters available, in order to create enough anatomical visibility for contouring. The result was that no soft tissue could be identified on the DRRs.

During the contouring process various window/level settings were used to draw structures, as seen in figures 3.6 to 3.9. These window settings greatly enhanced the identification of bony landmarks. All planning CT's were done with a 3 mm slice thickness and from these the DRR's were reconstructed.

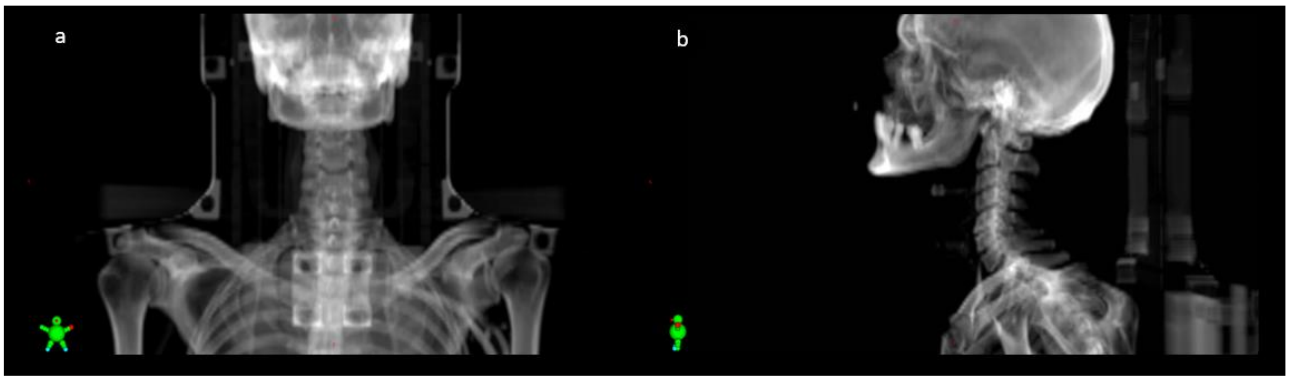

Figure 3.6: Anterior (a) and left lateral (b) DRR with no filter (illustration produced by author)

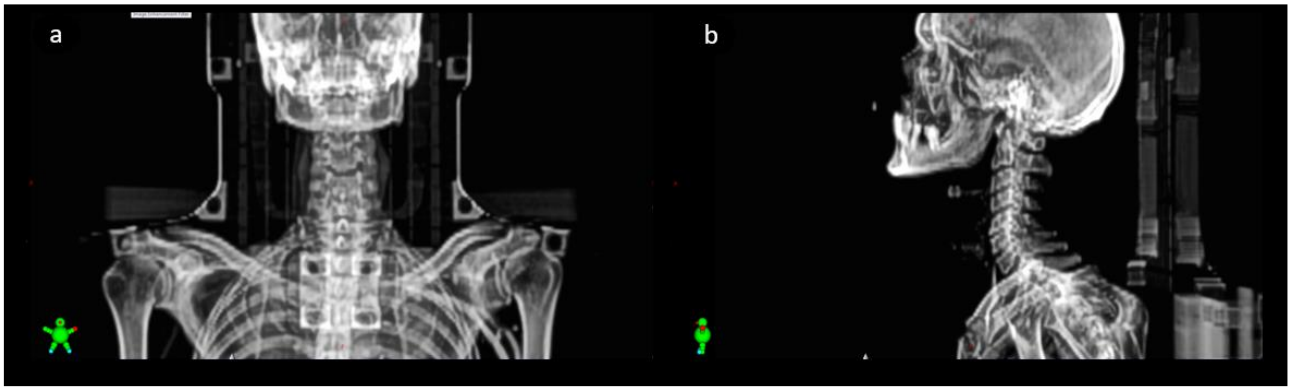

Figure 3.7: Anterior (a) and left lateral (b) DRR with dynamic filter (illustration produced by author)

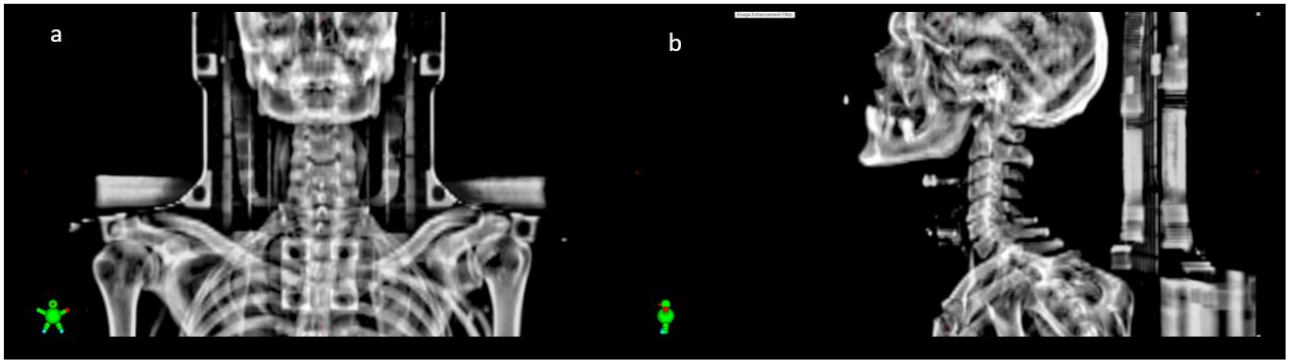

Figure 3.8: Anterior (a) and left lateral (b) DRR with content filter (illustration produced by author)

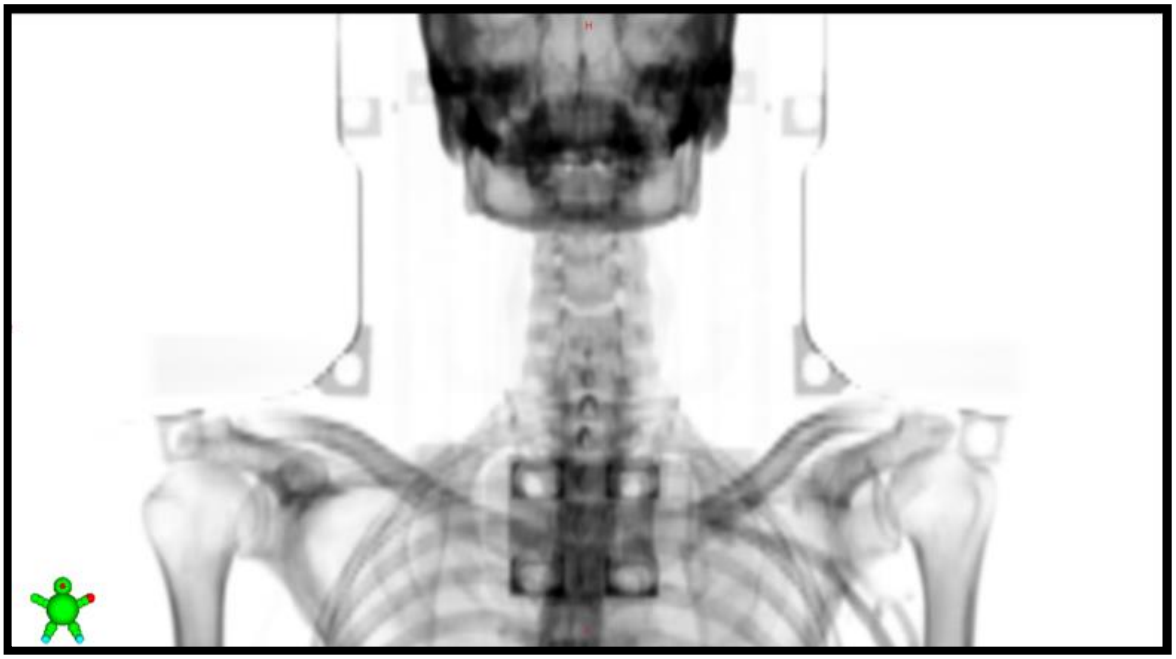

Figure 3.9: Anterior DRR with invert filter (illustration produced by author)

When the DRRs were created before the patients started radiation therapy, the immobilisation devices and CT bed were not cropped out of the CT data. Therefore, the S-frame immobilisation devices, as well as very dense CT bed structures can be seen in the DRRs. It was noted that one should be aware of this, and not confuse them with patient anatomy. Unfortunately, these structures could potentially add uncertainty during the contouring process, and could lead to errors, or block valuable/ useful anatomy. See figure 3.10 for a demonstration of a DRR with CT bed and immobilisation devices included.

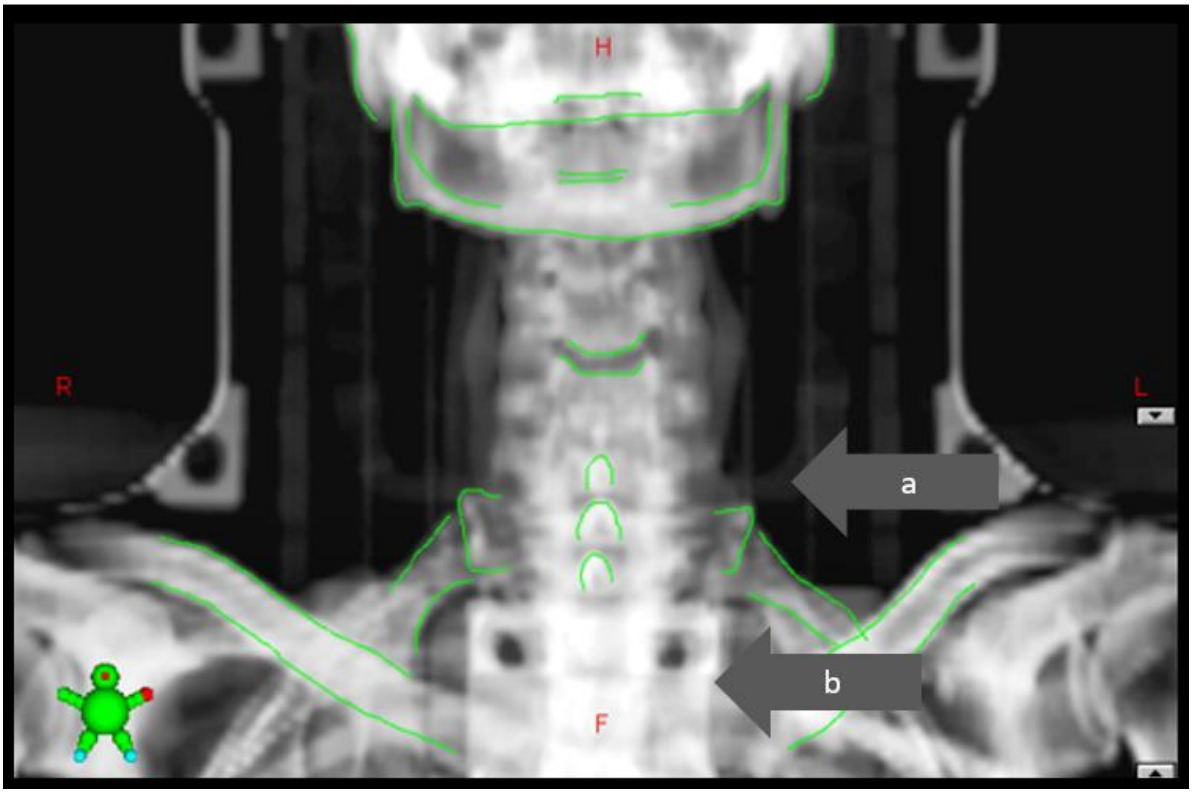

Figure 3.10: (a) Perspex base of radiopaque headrest visible on DRR. (b) Dense metal bracket on CT bed included in DRR creation (illustration produced by author)

Due to the grey scale that was selected during creation of the DRR, it was found that contouring an anatomical landmark on one side was not accurate enough, and therefore, as far as possible and depending on the quality of the anatomical landmark, contouring on both sides of a bone was done by the researcher. Thus, when matching the DRR with the EPID images, irrespective of the greyscale selected, the bony structure could be placed inside the two contours as needed as is illustrated in figure 3.11 and 3.12.

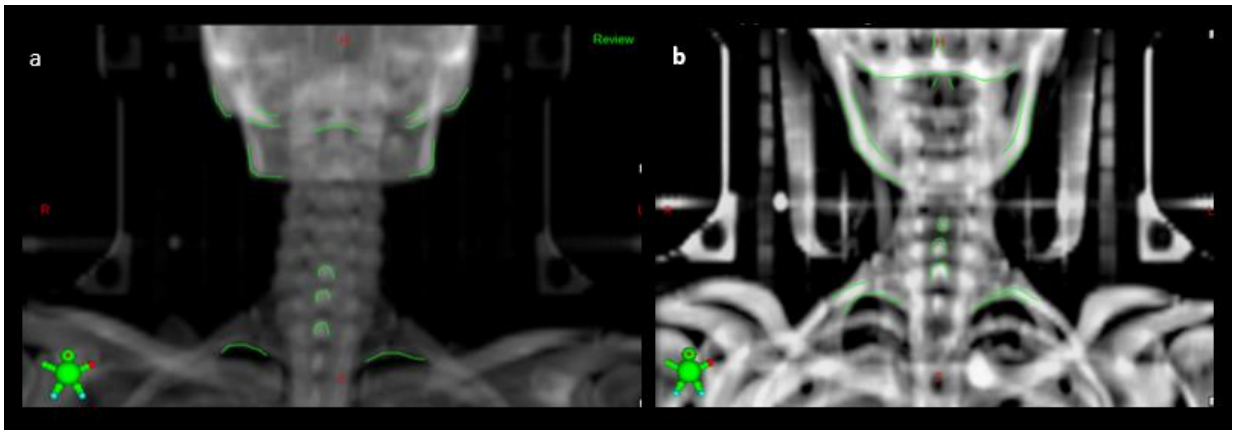

Figure 3.11: Anterior DRR of a head and neck patients, illustrating manual bony landmarks drawn to facilitate matching with EPID image (illustration produced by author)

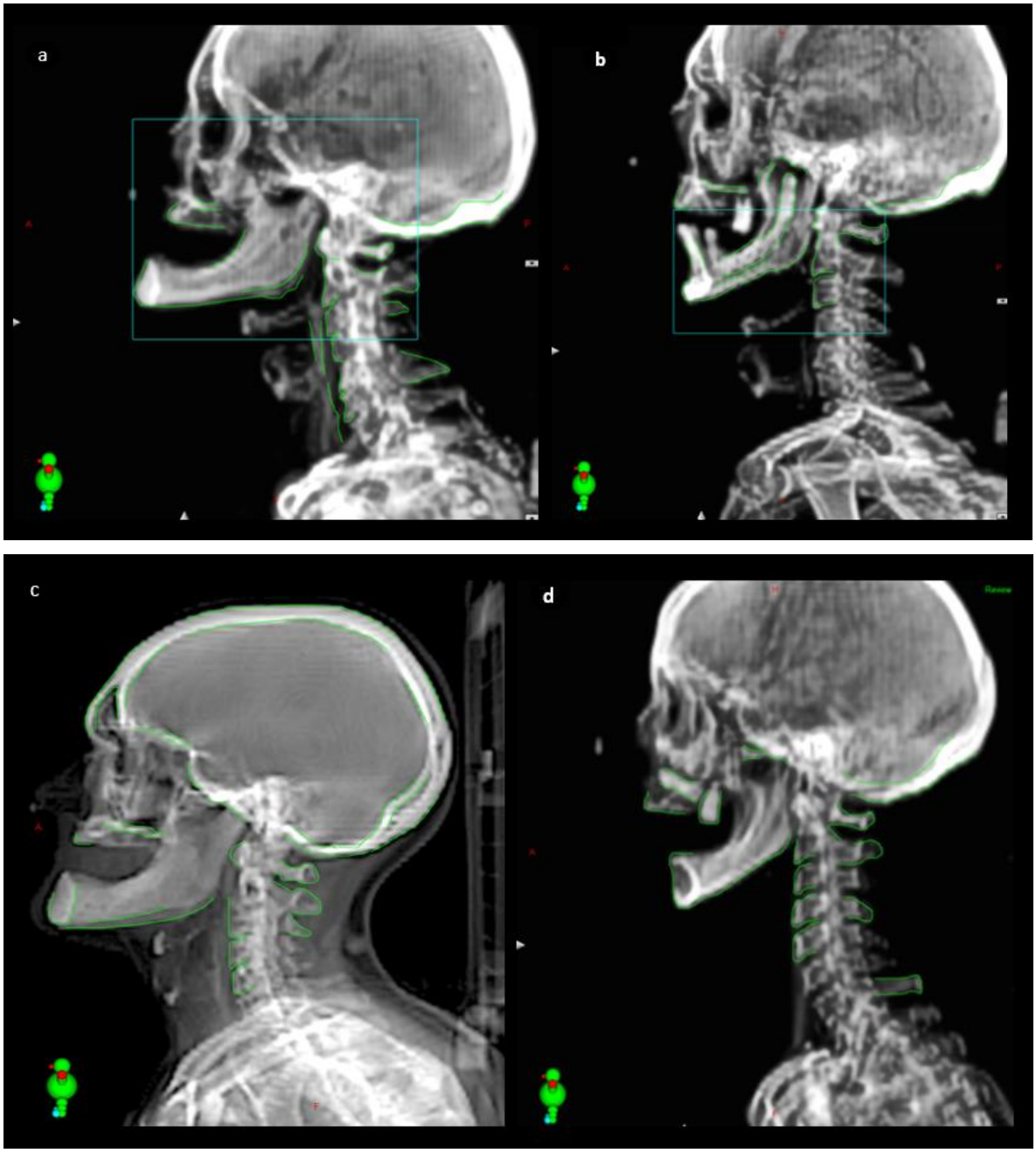

Figure 3.12: Illustration of manual contours drawn on left lateral DRRs for matching with EPID images. Image b demonstrates how a mandible prosthesis can also be used as an anatomical matching tool (illustration produced by author)

3.3.1.4 Data preparation for the head matching - CT interpolation

The planning CT slice thickness for this patient population was reconstructed at 3 mm. Therefore, when DRRs were created by interpolating the CT data and creating a 2D DRR, step artefacts were observed on the DRR as shown in figure 3.13.

With complicated bony anatomy in the head, interpolation of oblique or curved bony structures can lead to artefacts in the DRR. Examples of these bony structures are the skull vertex and superior orbital margin seen from the anterior DRR in figure 3.15. The frontal sinus, maxilla, orbital roof, and greater sphenoid wing, as well as skull vertex and the external occipital protuberance are illustrated in figure 3.13. The challenges with interpolation are illustrated in figure 3.13 and compared to the EPID image in figure 3.14.

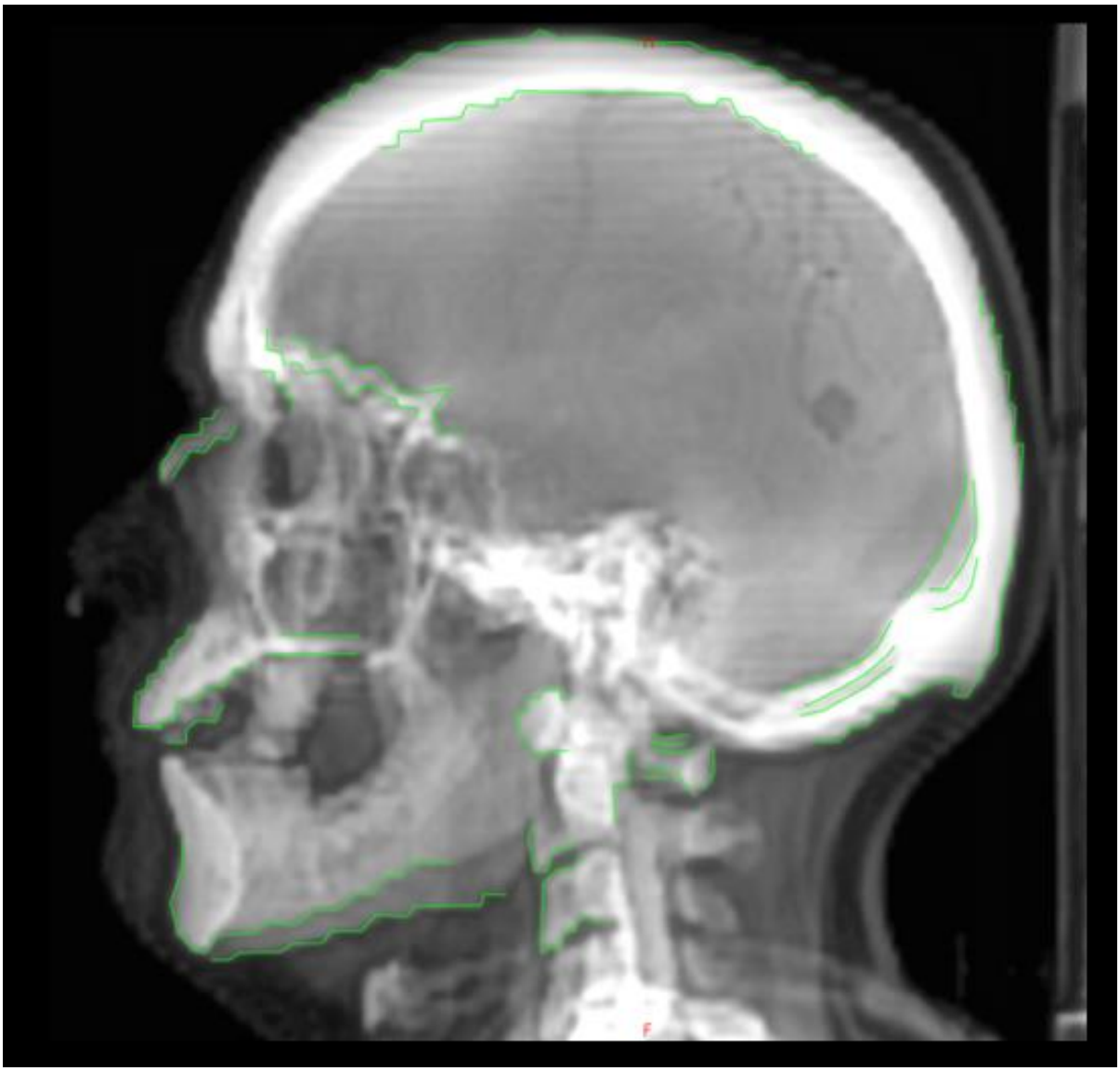

Figure 3.13: Interpolation artefacts contoured on a lateral head DRR (illustration produced by author)

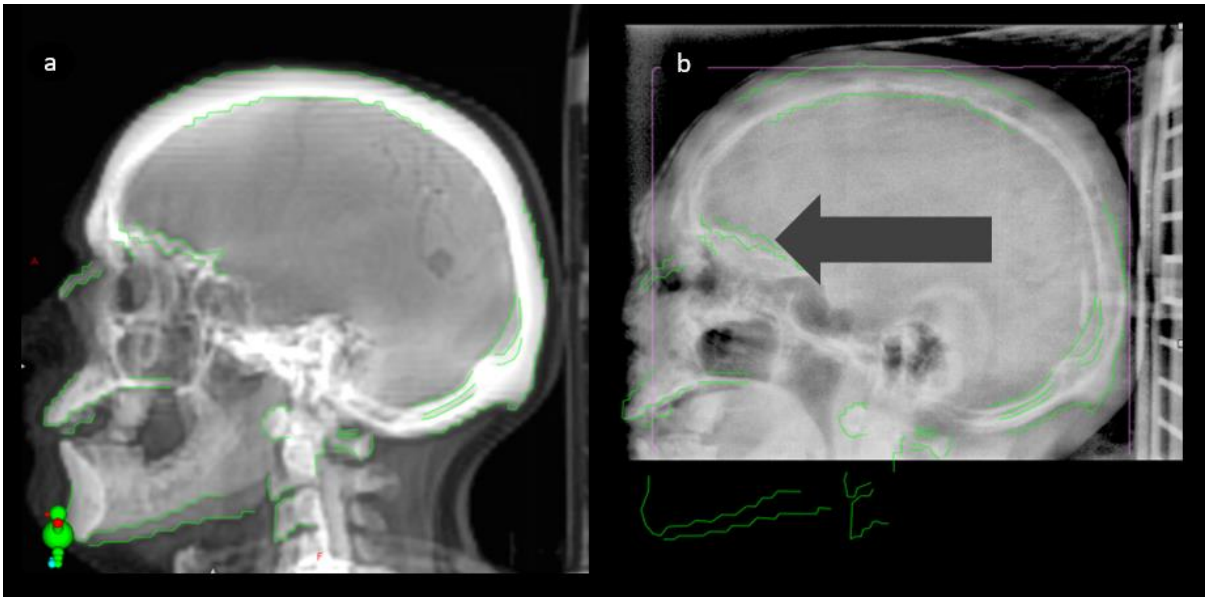

Figure 3.14: Illustration of interpolation of a very thin oblique bone (orbital plate) (illustration produced by author)

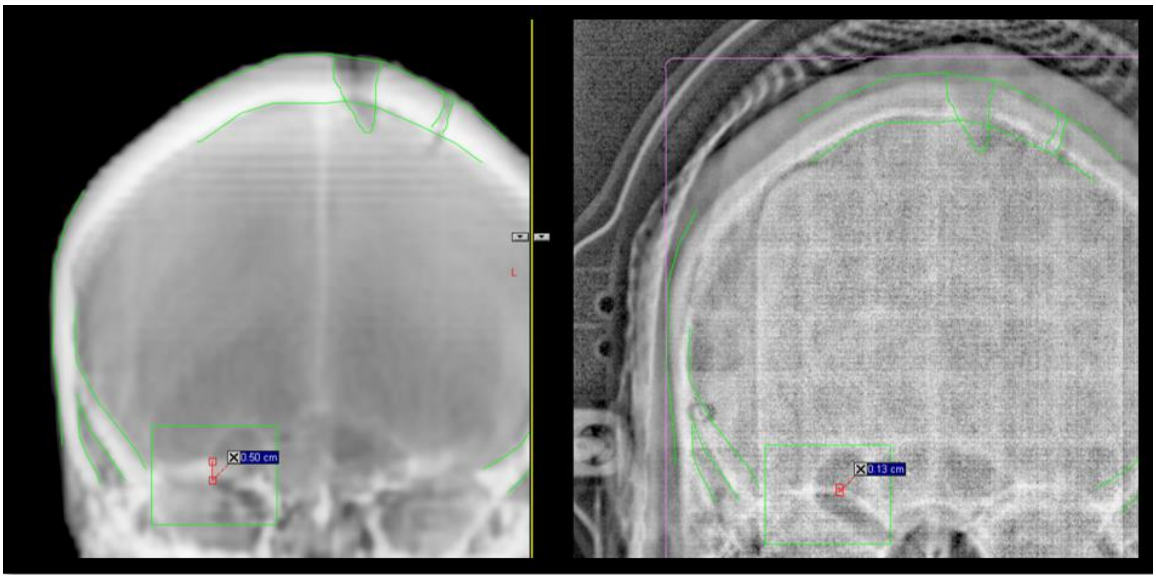

Figure 3.15: Illustration of interpolation of a very thin oblique bone (superior orbital margin) and a thick oblique bone (skull vertex) (illustration produced by author)

The value of contouring bony structures on both sides of the bone to enable the anatomy to be matched with the comparable EPID image is illustrated clearly in Figure 3.15. If these bones were only contoured on the one side of the structure the matching result could be a few millimetres different than intended.

During the data collection it was found that a few image sets had contours drawn on the anatomy to assist with image matching. Examples of these can be seen in figure 3.16.

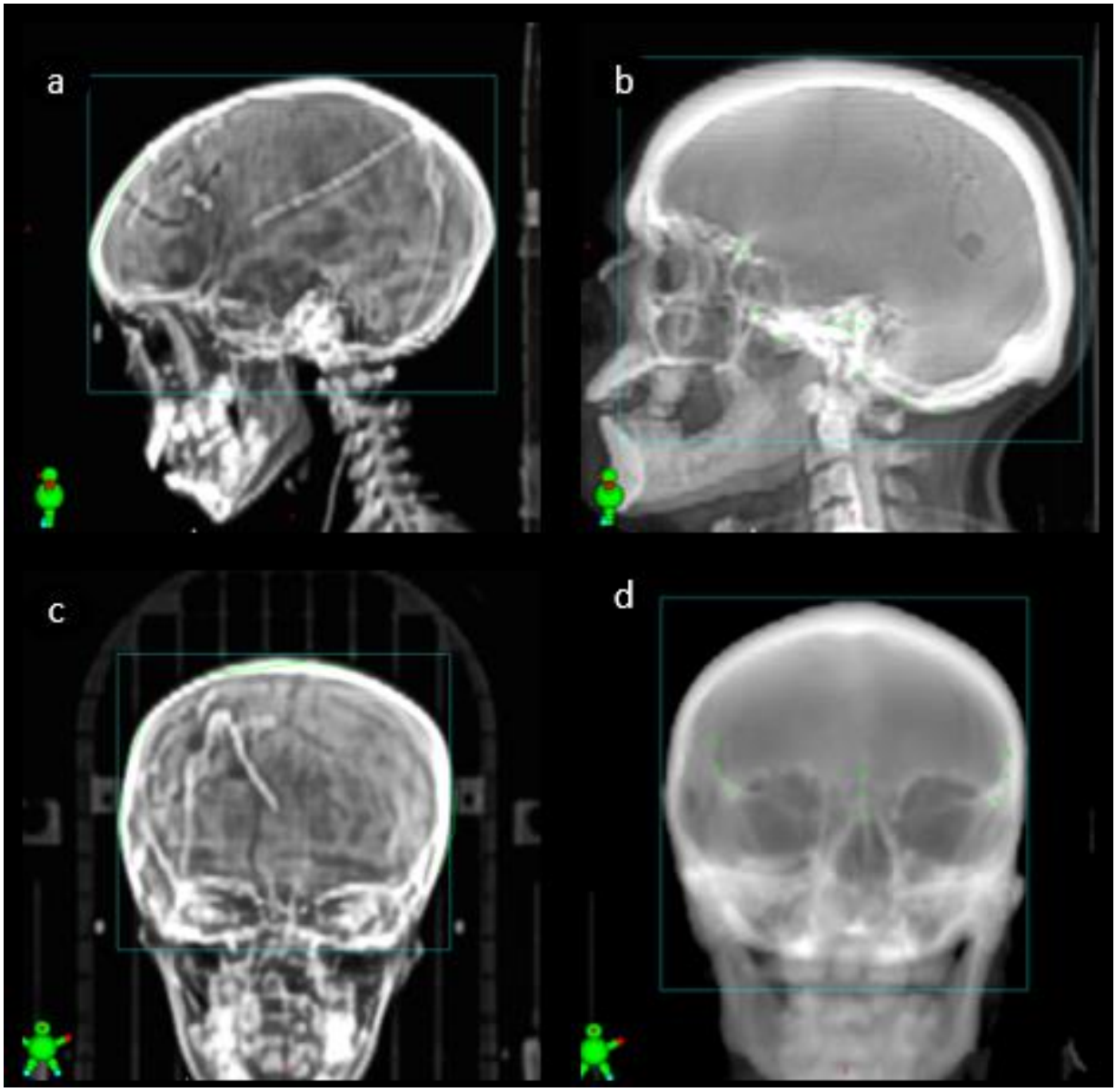

Figure 3.16: Contours found on the baseline head DRR's.
a - green line on frontal bone
b - an array of green crosses on various bony structures
c - a green contour on superior and lateral skull bones
d - green crosses placed on oblique orbital line and crista galli
(illustration produced by author)

3.3.1.5 Head DRR contouring

It was recommended by the Royal College of Radiologists (2008) that at least three anatomical structures should be contoured to assist with image matching. These anatomical landmarks should be used irrespective of the field arrangement chosen for radiation therapy treatment (Royal College of Radiologists, 2008).

On the anterior image the inner border of the skull vault, frontal sinuses, zygoma, nasal septum and orbital ridges were identified. On the lateral image, the inner border of the skull vault, occiput bone, pituitary fossa, frontal sinuses, and orbital ridges were identified. It was also noted that any stable radiopaque structures or surgical defects could be of great value.

Although the mandible and the pedicles of the upper cervical spine and the anterior vertebral bodies were not labelled in the images provided by the Royal College of Radiologists (2008), these structures were also contoured on illustration images shown in their report.

The guidelines from the Royal College of Radiologists (2008), as well as the illustrated value of drawing manual contours on both sides of bony landmarks previously shown by the researcher in figure 3.11 and 3.12, were taken into account for the landmarks contoured during this study and is illustrated in figure 3.17. Most prevalent contours on the anterior images were the orbits, nasal septum, skull vault (superior) as well as teporal and parietal (lateral) bones. These bony structures were used to determine the left to right, and superior to inferior, positioning errors on the EPID image.

Figure 3.18 demonstrates the manual contours that were drawn on the lateral DRRs for matching with EPID images. These contours include bony structures of the skull as well as the first and second cervical spine.

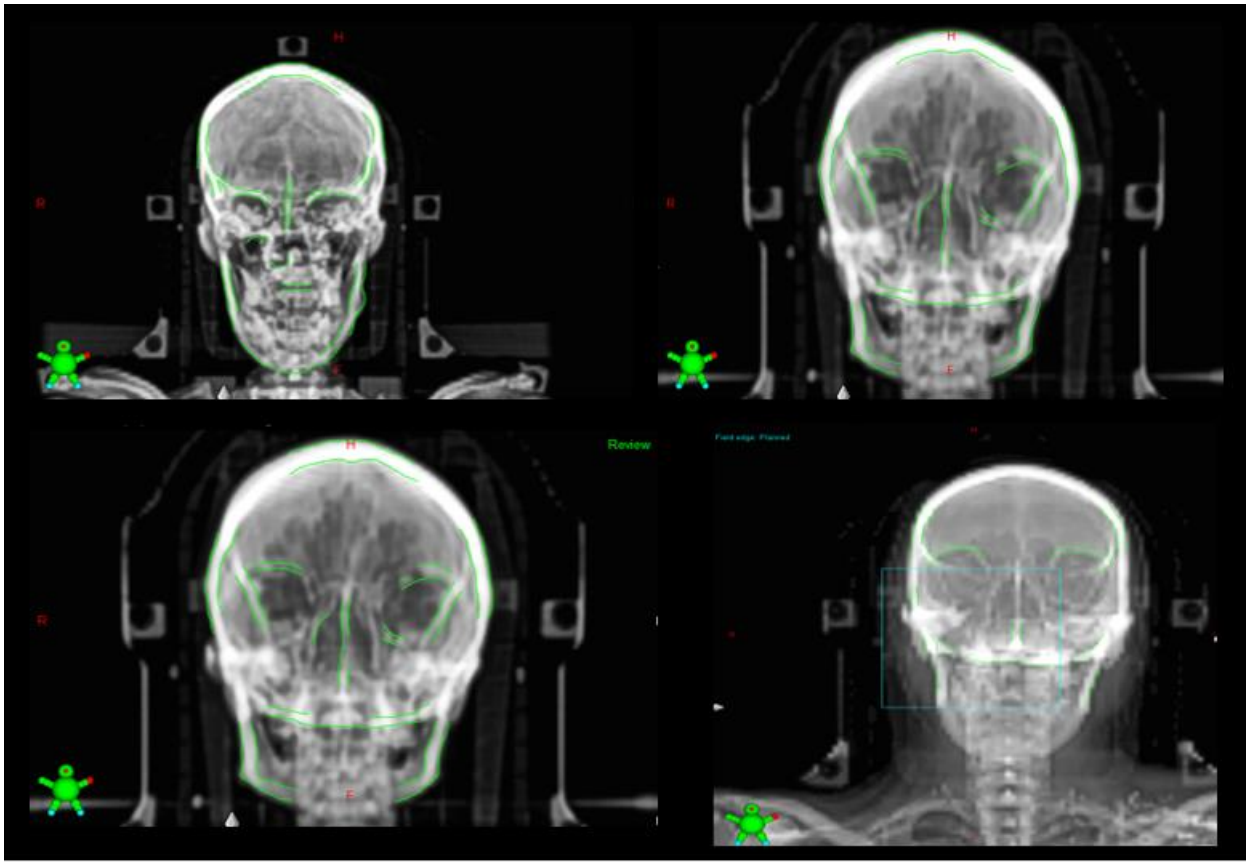

Figure 3.17: Illustration of manual contours drawn on anterior DRRs for use during image matching with EPID image (illustration produced by author)

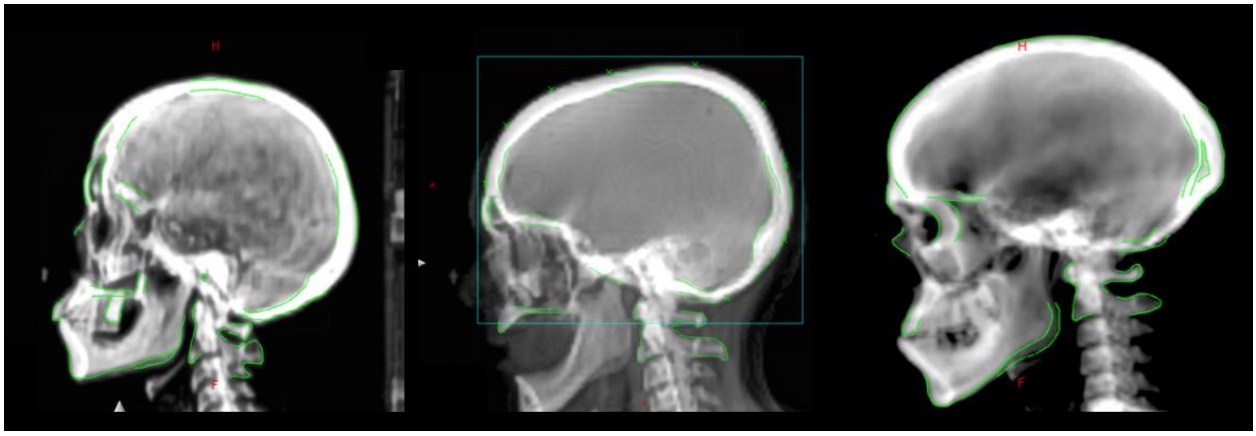

Figure 3.18: Illustration of manual contours drawn on left lateral DRRs for use during matching with EPID image (illustration produced by author)

3.3.1.6 The data collection process and measurements

An Excel spreadsheet was used to record all image matching results and can be seen in: Appendix A for the image matching results for the head and neck matching group, and Appendix B for the image matching results for the head matching group.

3.3.1.6.1 Digital matching

To enable the automatic matching algorithm to be used, a Field of View (FOV) had to be placed around the anatomy of interest. Therefore, all bony anatomy was included in this FOV. In most cases this algorithm failed, as bony landmarks were not in agreement. Based on the researcher's personal experience this is often seen in anatomical sites where complicated bony structures exist.

Complicated 3D anatomy is reconstructed to create 2D DRRs, and if any rotation is present in the patient positioning during the acquisition of the portal images, the bony anatomy may be too different from the original DRR, and the image matching fails.

Therefore, in this research study, bony landmarks were contoured, and manual image matching was done, thus giving confidence that the match results were as good as possible.

3.3.1.6.2 Manual matching

A process of placing two sets of anatomy on-top of each other, allowed the user (researcher) to manually move the contoured anatomy together with the DRR image over the EPID image. This enabled the user to find agreement between anatomical landmarks. When three or more of the landmarks agreed, the image was accepted as matched. The result of the manual matching was digitally recorded in the offline-review program.

Figure 3.19 illustrates the measured results after the matching of two datasets. The lateral offset and longitudinal offsets were measured on the anterior image, and the vertical and longitudinal offsets were measured on the lateral image.

In daily practise this allows the operator to determine the agreement between the planned isocentre and the daily positioned isocentre. When online matching is performed before daily patient treatment any discrepancies can be corrected before delivering the daily treatment dose.

As the treatment couch can be shifted vertically, longitudinally, and laterally, these types of shifts can be corrected for, and will the degree of correction based on clinical protocols.

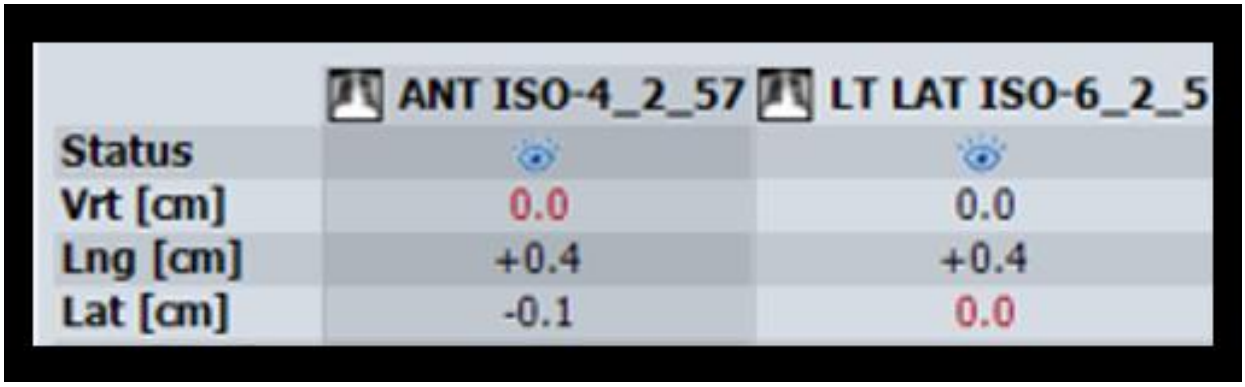

Figure 3.19: Matching results in centimetres (cm) after manual matching of EPID image with DRR. The DRR is considered the correct image, and the matching of the EPID image to the DRR is done to determine the shift / corrections needed for correct patient positioning (Screenshot from ARIA system)

3.3.1.6.3 Rotation measurements

The rotational offset that was observed very often, is an error that cannot be easily compensated for, or corrected, on the linear accelerator. For the head and neck group rotations were observed for 67.1% of the matched images, and in the head group 63.7%. The treatment couch can be moved in three directions to correct translational errors, but the correction for a rotational error is more challenging and is not corrected in routine practice.

The rotational error in 2D matching can only be calculated in the plane of the image. Therefore the rotation measurable for the anterior image (in degrees) can potentially be corrected with the rotation of the couch itself, and therefore is automatically recorded after matching, as illustrated in figure 3.20.

The rotation on the lateral image, however, is not recorded as it cannot be adjusted.

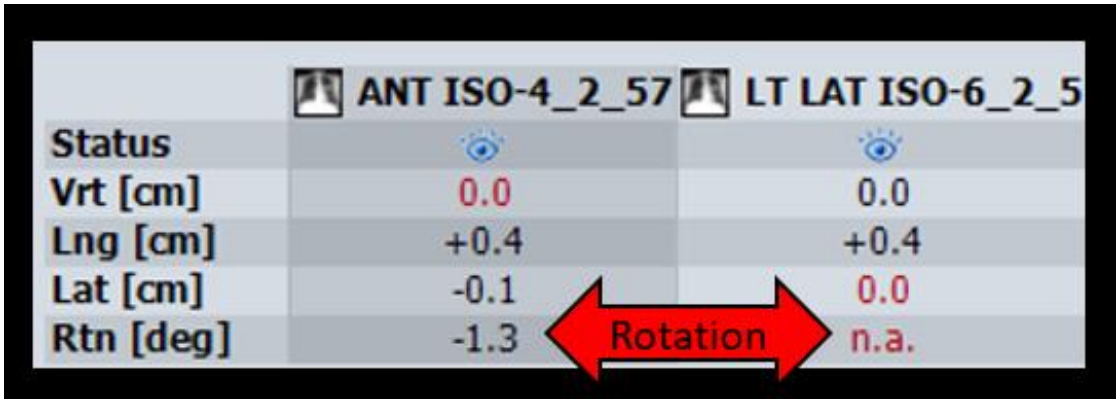

Figure 3.20: Rotational error recorded for the anterior Image, but not for the lateral image (Screenshot from ARIA system)

In this system as applied by the researcher the rotation for the anterior image was recorded with a negative or positive value, depending on the couch's rotational direction needed for adjustment, the measurement is done in degrees (not centimetres). Figure 3.21 indicates the indication of the positive and negative rotational value, and how it was applied to the anatomical site in this study.

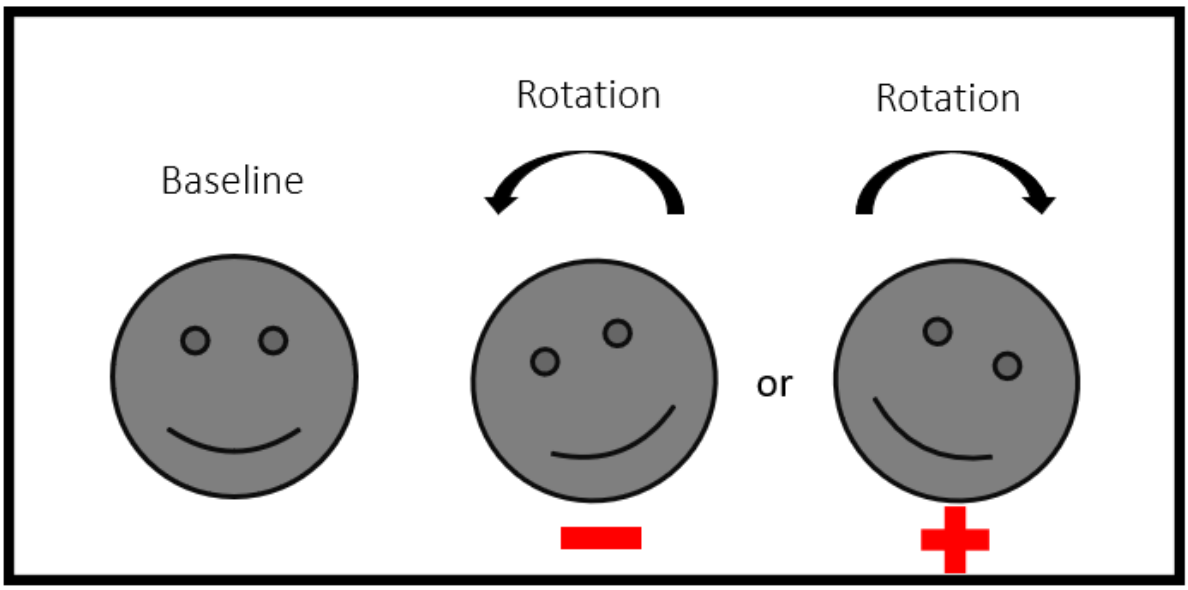

Figure 3.21: Anterior rotation (illustration produced by author)

The lateral rotation of a patient was defined as the flexion or extension of the patient's chin seen on the lateral image. This could lead to an anatomical shift and rotation of the skull and a shift of the cervical vertebrae.

This type of rotation is an anatomical rotation of the patient within the mask, and the couch cannot be tilted in that direction to correct it.

To enable correct image comparison, a rotational offset had to be applied to allow a correct shift of the anatomy. The measurement for this shift was challenging, as there was no digital readout given by this system. The measurement tools of the program had the ability to measure the angle of rotation but had to be measured manually by the researcher. A decision was made to apply a positive rotational reading with flexion of the chin, and a negative reading with extension of the chin, as illustrated n figure 3.22, and figure 3.23, to keep the measured data consistent.

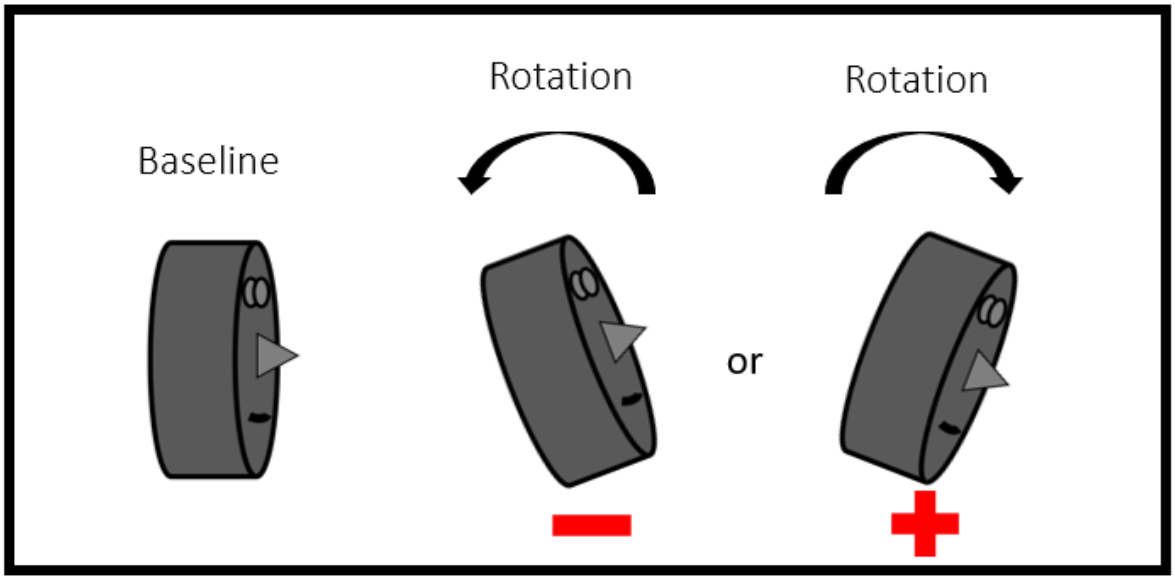

Figure 3.22: Positive and negative angle measurement on lateral image (illustration produced by author)

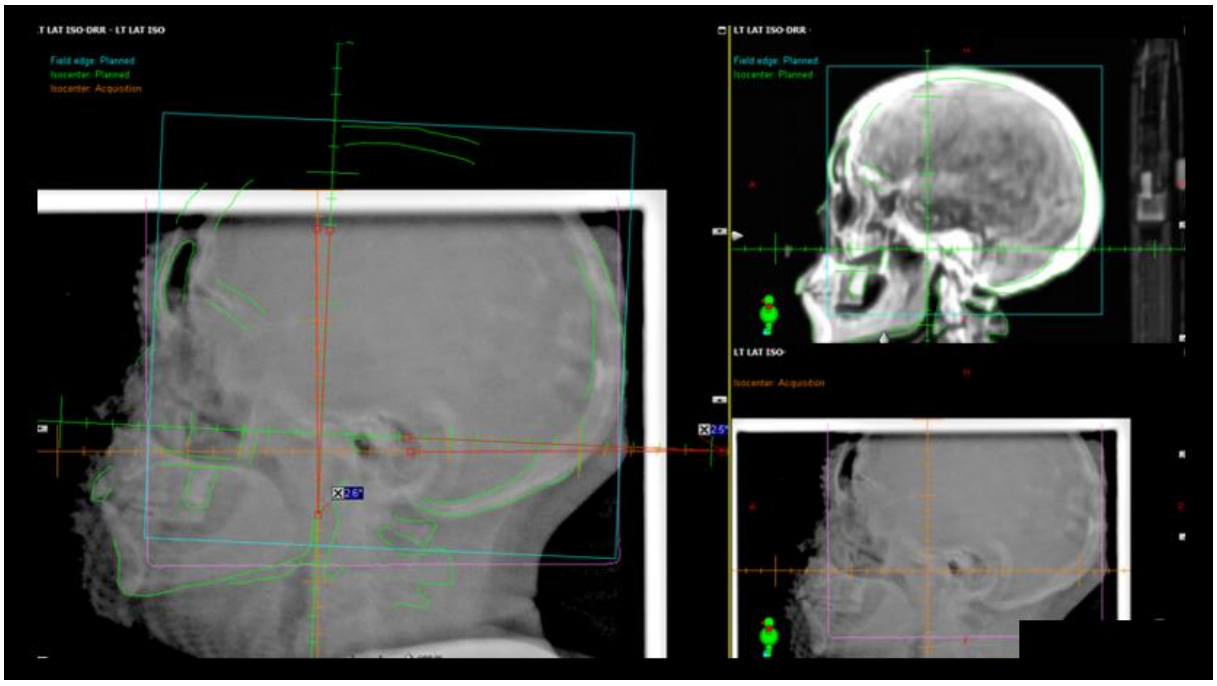

Figure 3.23: Measurement of 2.6 degrees of rotation in a negative direction (illustration produced by author)

3.3.1.6.4 Peer review

All data collection was done by the researcher, followed by multiple peer review comparisons, to verify the reliability and reproducibility of results.

Two experienced radiation therapists (RTTs) were asked to volunteer their time to repeat matching of the patients' data. The RTTs received a list of all the patients' numbers included in the research study. The first RTT started at the first patient and matched every 5^{th} patient. The second RTT started at the 3rd patient and matched every 4th patient in line.

All peer review matching data was found to be within 1mm.

The Head & Neck oncologist, who was the clinical supervisor of this study, reviewed all matching data, and manually re-produced 20% of the matches where the results were found to agree within 1mm.

3.3.1.7 Case study demonstration: Why it is important to apply a rotation in head and neck matching

The following dataset (figure 3.24) was evaluated, and it was observed that the treatment set-up was matched without the use of any contours drawn in on the DRR. These contours in green were drawn in retrospectively by the researcher. A shift of 0.7cm in the longitudinal direction was approved by the original user of this data. The responsible clinical approver of these images focused on the superior orbits, frontal sinus, and the greater wing of the sphenoid. However, in figure 3.24 it is shown with the use of the green contours it can be seen, that the superior skull, is not in agreement.

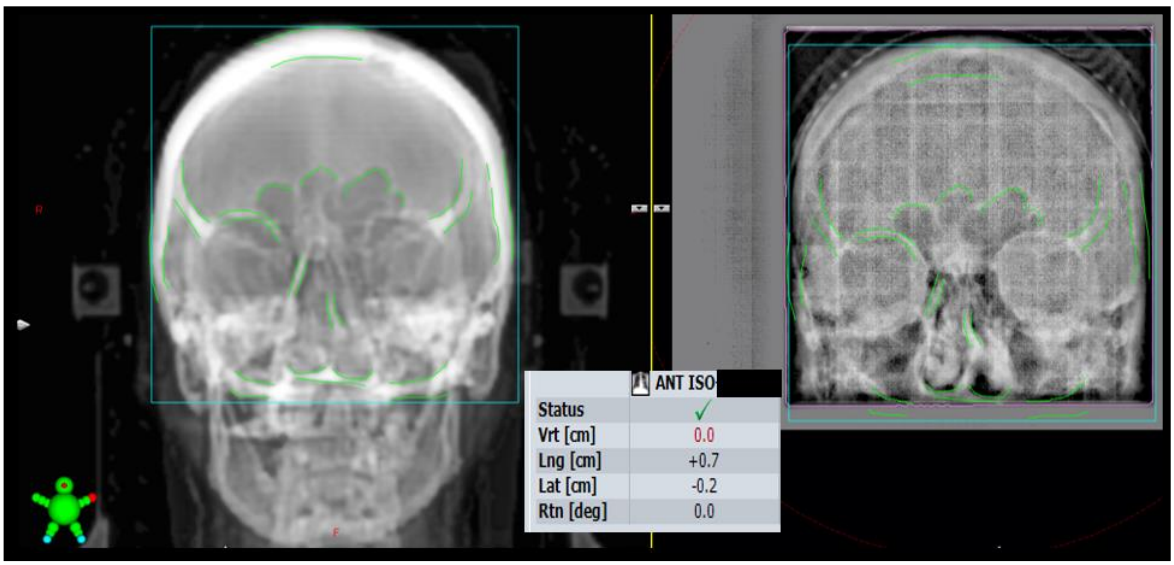

Figure 3.24: Anterior DRR (left) compared to anterior EPID image (right) (illustration produced by author)

A misalignment of anatomical bony structures, as seen on one of the orthogonal images, is an indication that the other image will have a rotational error.

Figure 3.25 shows the result of the lateral image taken on the same day. Image (b) is the image without applying any shift. If the user was still focussing on the orbital plates, he or she will most likely apply the same 0.7 cm longitudinal shift, but when applying the rotation to the image, and therefore correcting for the tilt in the patient's head, it is found that only a 0.3 cm longitudinal shift is needed as seen in image c.

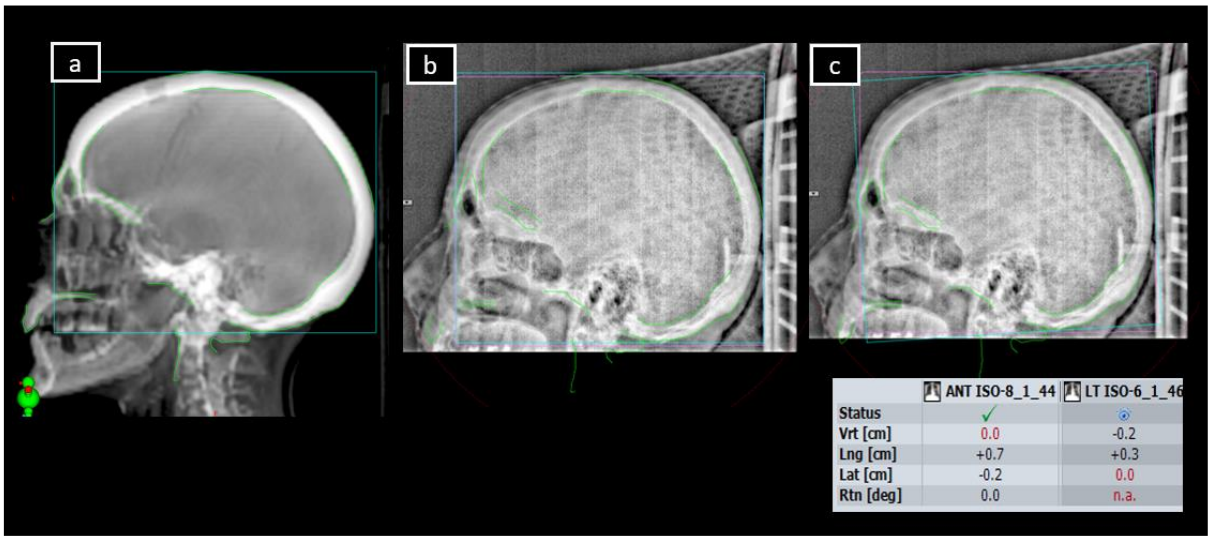

Figure 3.25: **(a) Lateral DRR**
(b) Lateral EPID image without applying any shift
(c) Lateral EPID image applying rotational correction, and a 0.3 cm longitudinal shift
(illustration produced by author)

It must be noted that applying rotational shifts during image matching is a useful tool to help determine the accuracy of the set-up. Simply applying a 2-dimensional shift to a multidimensionally moving object can lead to an incorrect shift. Each RTT or oncologist when performing the manual matching of rotated anatomy may focus on different bony structures, and the result will therefore always be different. For example, the above-mentioned case study could have had one user matching to the skull bone, and the next user focussing on the orbits, and possibly the next user focusing on the mandible. This can prove to be an ineffective use of portal imaging, as the purpose is to correct a possibly incorrect set-up of the patient, or at least to quantify the inaccuracy, and to determine if this value is within departmental acceptable tolerances.

As seen in the figure 3.24, the shift of 0.7 cm could have been outside of this department's accuracy limit of 0.5 cm and could have resulted in a shift being applied for treatment. After

applying the rotation, it is observed that the inaccuracies in all directions are within 0.3 cm, but that a rotational error is present. As this type of rotational error cannot automatically be corrected by a couch shift, the procedure would have been to repeat the set-up, by having the patient's mask re-fitted and the imaging repeated. However, if rotations are never applied during image matching, the user will not know any better than to apply a 2-dimensional couch shift, rather than perform the preferable option of repositioning the patient. W\hen re-doing the clinical set-up the RTT can observe if the patient had shifted or if the mask was ill fitting, or any other clinical scenario that can be corrected.

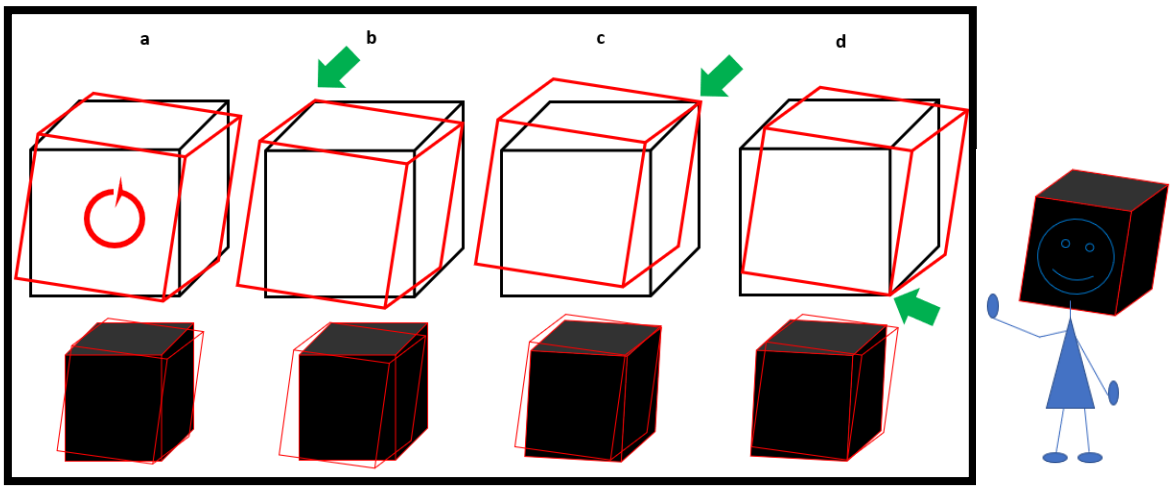

Figure 3.26: Inter-observer error in matching (illustration produced by author)

Figure 3.26 is used to demonstrate a rotational error that is present in a 3-dimensional cube. The black wire-cube represents the patient's head during the initial CT image set, and the resulting DRR that was created. The red wire-cube represents the patient's head being slightly rotated towards the patients left shoulder (a). When the resulting image is then matched from the lateral side, without knowledge of the rotation present in the anterior image, the resulting matching will be performed differently by different observers, as each observer will focus on their specific anatomical area of importance, as illustrated by cube b, c and d. The correct matching result should have zero shifts in any of the x, y and z directions, but rather a corrective rotational measurement.

When shifts in the x, y and z directions are present, but the rotation is corrected, multiple bony landmarks will agree, and a true x, y and z error can be calculated and possibly applied to the patient set-up. Figure 3.27 (b) illustrates this, where all the blue arrows will have the same measurement, and all the green arrows will have the same measurement of dis-agreement to the original image.

In this scenario we are using 2D imaging and we are applying it to a 3D real world scenario. This ability to match not only depends on the rotation but also the actual point of rotation. Unless this point of rotation lies within the 2D plane we are matching, our correction will only be an approximation.

If multiple points of agreement is found as demonstrated in Figure 3.27, it leads to an accurate set-up correction. Larger rotational errors or the presence of consistent miss-agreements even when rotation is applied, must be corrected by repeating the set-up procedure of the patient and repeating the images.

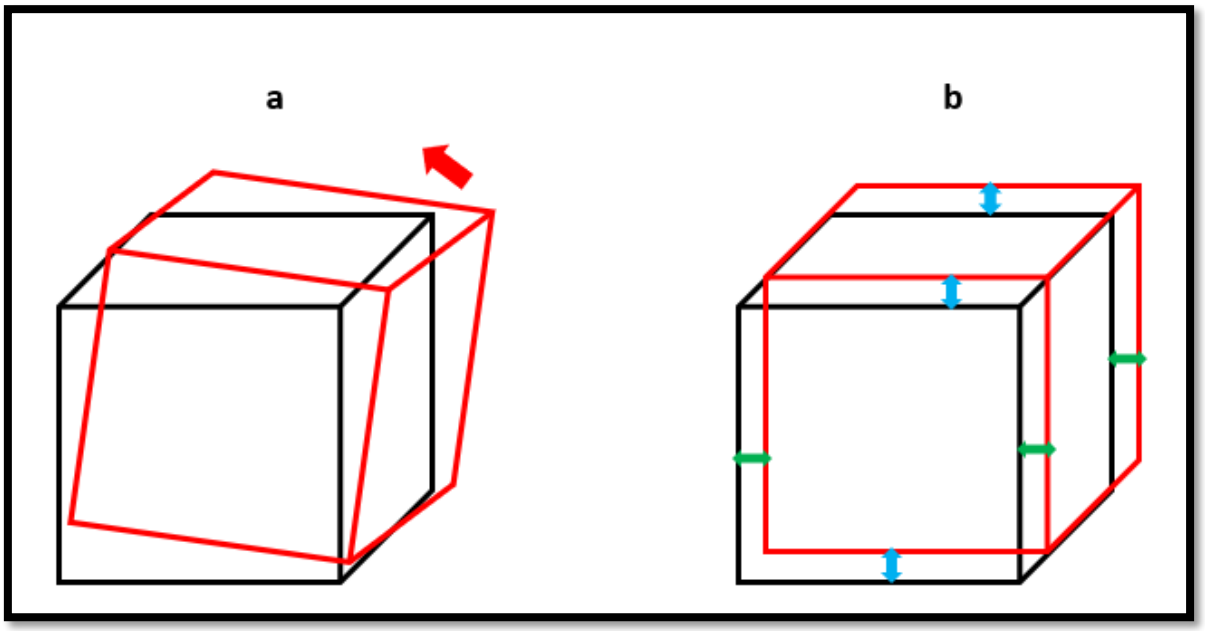

Figure 3.27: When rotations are corrected multiple body landmarks will agree and a true x, y, z offset can be measured (illustration produced by author)

3.3.1.8 Uncertainties during data collection

During data collection it became apparent that a lot of the imaged data were not reviewed at all. Some images had contours drawn on them, but very few anatomical landmarks included. Auto-matching failed due to the complexity of the anatomy in the head and neck region, and comparative contours had to be drawn in manually. During the process of drawing these contours, many uncertainties were identified, and will be listed in the following sub-headings.

3.3.1.8.1 Interpolation

The quality of the DRR is directly related to the slice thickness of the reference CT data. Therefore, an interpolation error increases the complexity of the contouring of the bony landmarks, and the resulting manual matching of the data. Figure 3.28 illustrates the step-like

projections of the bony anatomy seen on the DRR, with the resulting bony contours drawn to replicate this step-like interpolation error. The resulting projection of the contours in image c is shown as registered on the EPID image. Figure 3.29 is an enlarged image of the hard palate and orbital area of the skull to illustrate the complexity of projecting oblique bones in a DRR on to an actual EPID image.

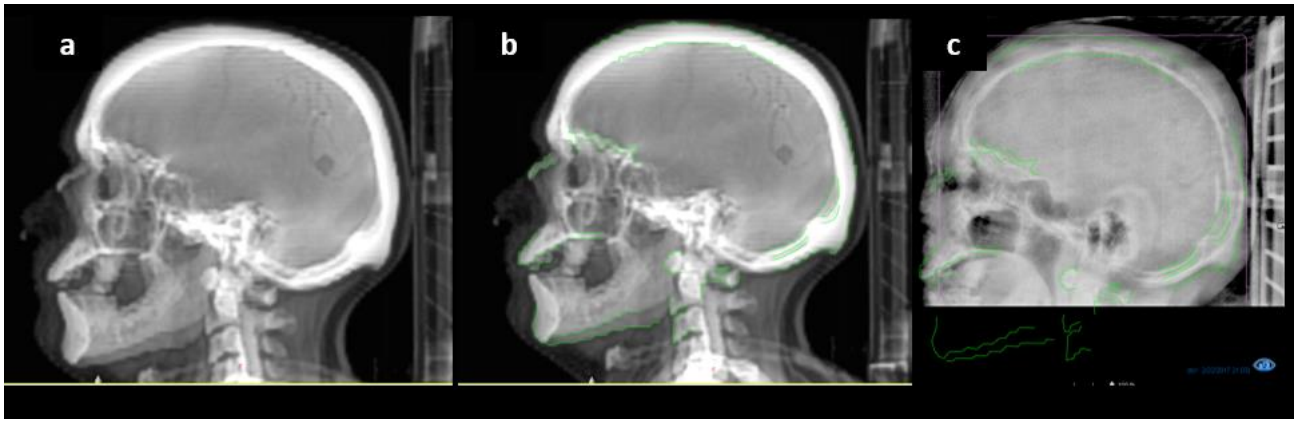

Figure 3.28: Contours done as exact replica of interpolated data.
Image a: Original DRR without contours
Image b: Original DRR with bony landmarks drawn in to replicate interpolation error
Image c: Projection of contours on EPID image
(illustration produced by author)

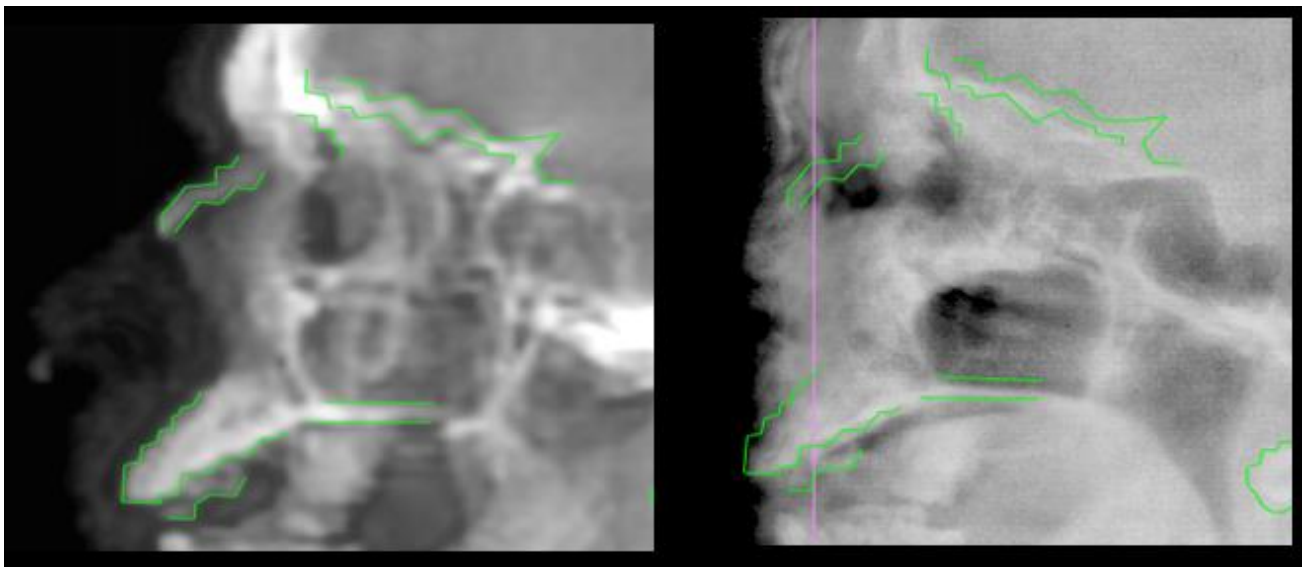

Figure 3.29: Projection of interpolation contours (left) on actual EPID image (right) (illustration produced by author)

In figure 3.30 it is visible that the interpolation of the orbital plates on the DRR appear larger than on the EPID image. The hard palate, although it is a relatively horizontal bone on the DRR, is projected much thicker on the DRR as compared to the EPID image. These types of

interpolation uncertainties are inherent in DRR production. More examples can be seen in Figures 3.31 to 3.33.

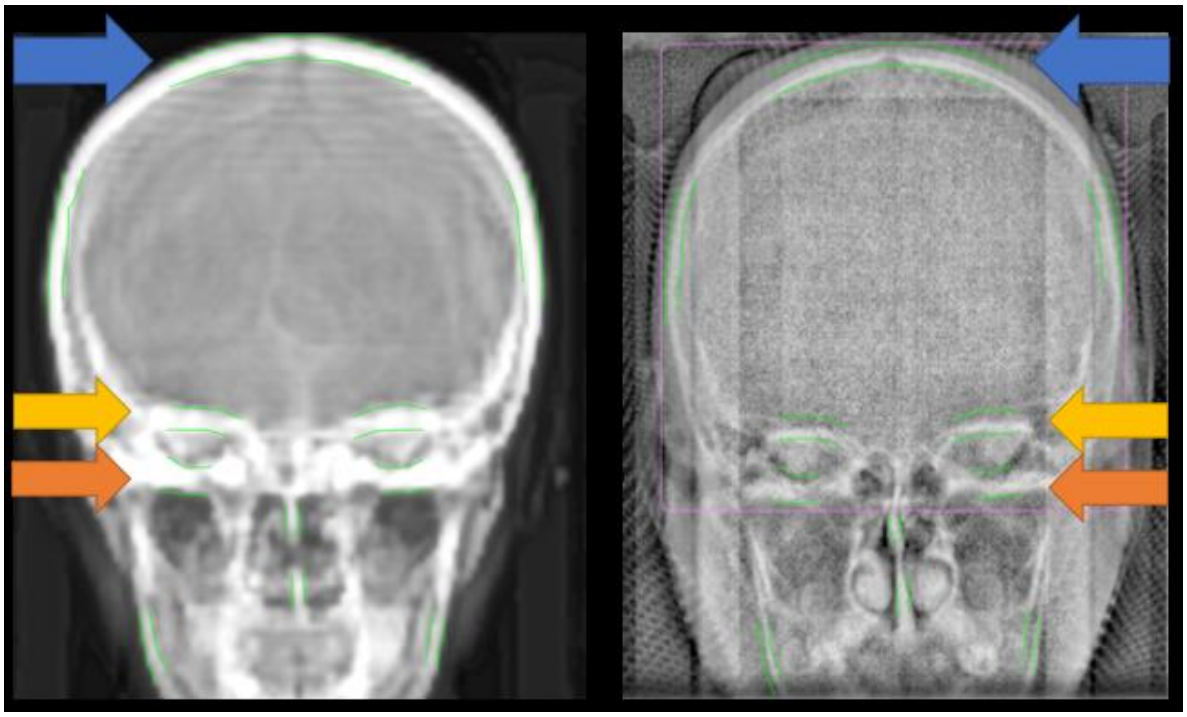

Figure 3.30: Left DRR image, Right EPID image
Blue arrow: Vertex of skull
Yellow arrow: Superior orbital margin
Orange arrow: Oblique and inferior orbital margin
(illustration produced by author)

Figure 3.30 demonstrates the difficulty to contour bony anatomy on a DRR, as the user does not yet have an EPID image available to be assured of the bony anatomy that will be visible on the EPID image. It is further illustrated in this image how important it is to have at least 3 sets of bony landmarks visible on the comparative image in order to enable the superior to inferior set-up error to be calculated correctly. On the right sided image, it is demonstrated that the three contours used to determine the superior to inferior set-up error are uncertain, as not one of the bony landmarks contoured are the exact same size on both image sets.

To quantify the possible bony distortion on the DRR, see figures 3.31 and 3.32, where measurements were made on comparative anterior and lateral image sets. The user has the ability to use multiple image manipulation tools to view these images. In this case, the filter of both the DRR and EPID image was selected, that enabled both images to have a comparable greyscale.

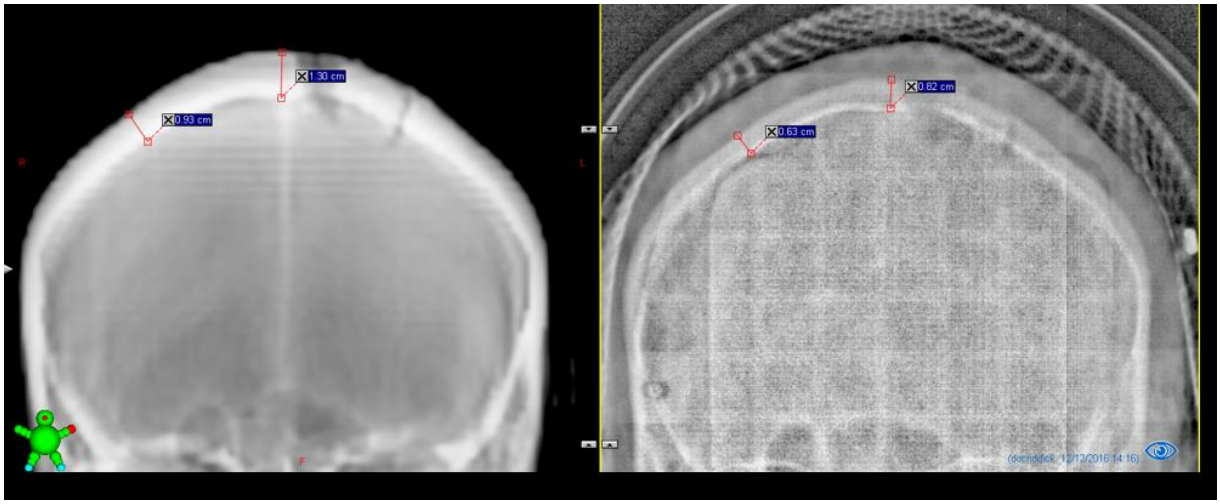

Figure 3.31: Measurements on skull vertex on the DRR (left) and EPID image (right) on an anterior image set (illustration produced by author)

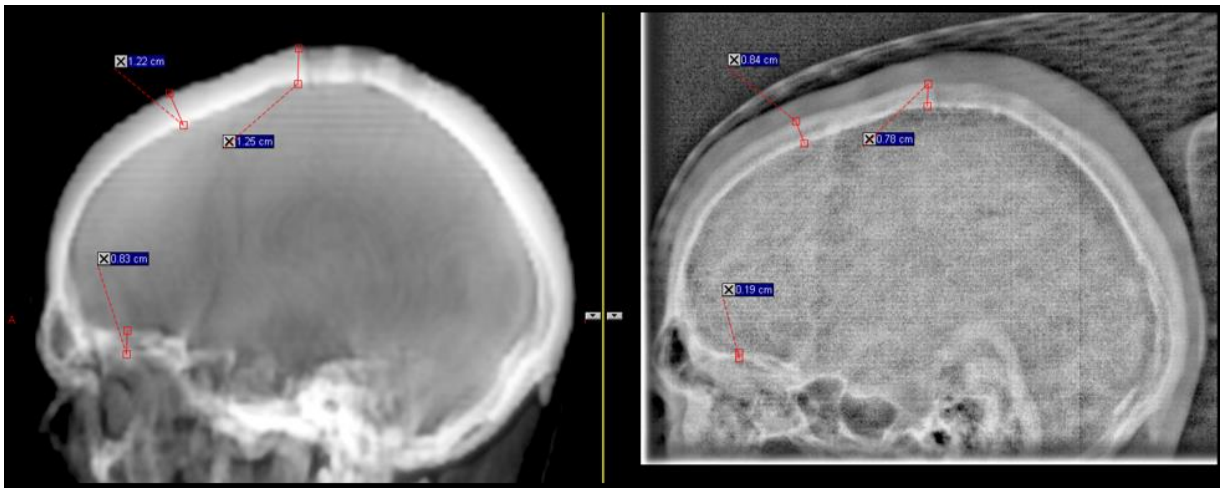

Figure 3.32: Measurements of the skull and orbital plates on a DRR (left) and EPID image (right) of a left lateral image set (illustration produced by author)

Bony anomalies in the skull or post-surgical changes can be of use for comparing DRR and EPID images. However, surgical changes could heal during the time period from acquiring the planning CT and the completion of a course of fully fractionated radiation therapy, which may lead to variability of these bony anomalies. This in turn may mean that they are not clearly visible on EPID images. Figure 3.33 illustrates surgical bone changes to the vertex, as well as the manual measurements of the orbits. This image illustrates that the visibility on the DRR measures the projected visible width to be 0.5cm, compared to the actual bone thickness, on the EPID image, measured at 0.13cm.

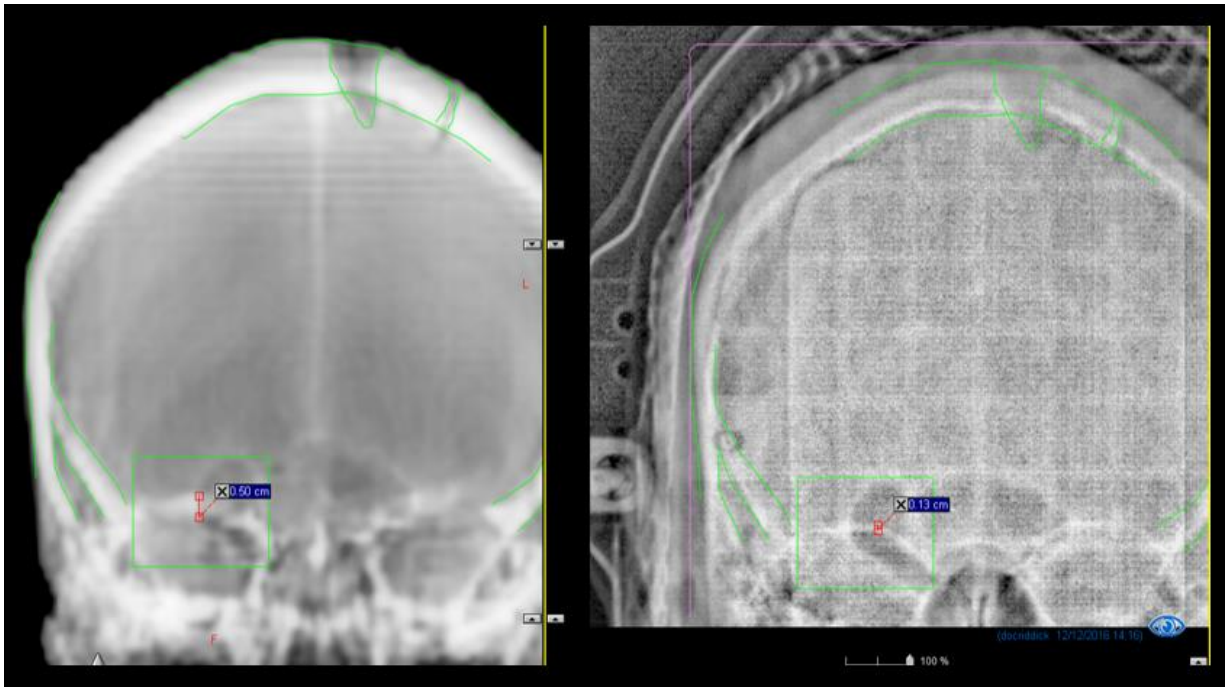

Figure 3.33: Enlarged image of an anterior image set, with measurements of the superior orbital margin on a DRR (left) and an EPID image (right) of an anterior image set (illustration produced by author)

3.3.1.8.2 Verification uncertainty

It is important to have enough anatomy present on the comparing EPID image, to allow any off set to be verified by multiple bony landmarks. Figure 3.34 illustrates the lateral image set of a patient who was receiving radiation therapy to the orbit.

Due to a large rotational mismatch that was measured, multiple bony landmarks had to be used to verify the rotational mismatch. The bony landmarks used to compare this image set, were the nasal bone, orbital bone, orbital plate, and C1. Not only was the vertical change recorded as 0.5 cm, which is outside the acceptable limits, but also a large rotational error was observed. To verify this manual match, it would have been necessary to visualize the posterior and vertex of the skull as well. Unfortunately, the vertex of the skull was not included in the original CT dataset as can be seen on the left side image in figure 3.34.

The practical implication on such an image set would be firstly, to re-image with the whole skull visible; and secondly, when such rotation is still present, to repeat the setup of this patient and to correct the rotational error.

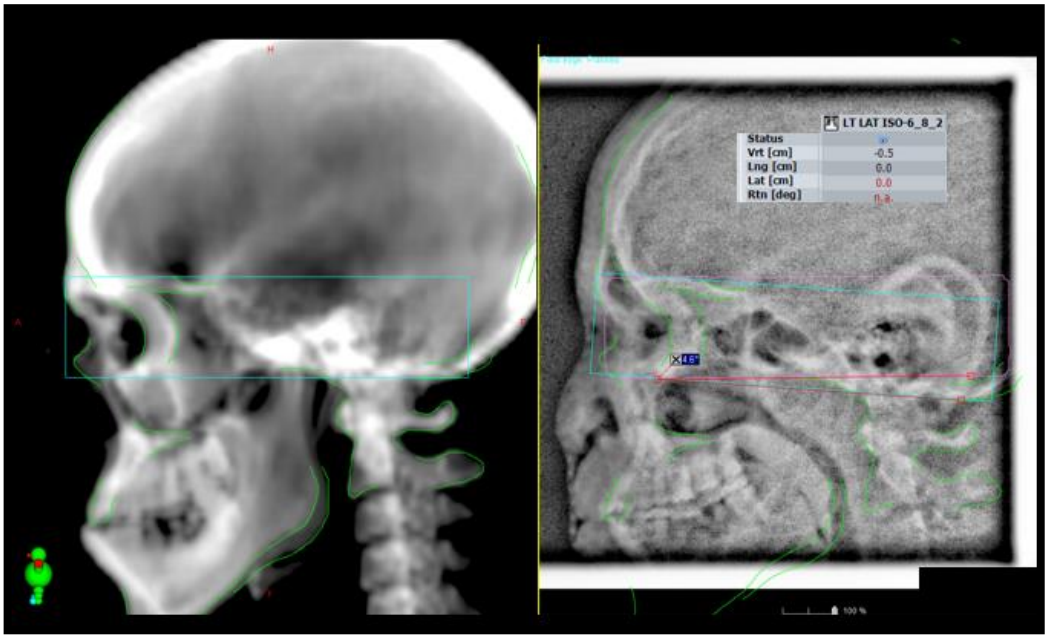

Figure 3.34: Verification uncertainty due to posterior and vertex of skull not being visible on EPID image (right) (illustration produced by author)

3.3.1.8.3 Limited data of anatomical site

In figure 3.35 the matching of a DRR (left image) and EPID image (middle and right sided image) of a patient receiving treatment for nasopharyngeal cancer is shown.

The first stage of image comparison was using the auto match function in the program. The middle image illustrates that this algorithm failed. The second stage of image comparison was manual matching, and this showed a possible rotational error. Unfortunately, with limited skull data present in the images to verify both the rotation and shift, this led to uncertainty in the matching. Not enough anatomy was present to verify the matching results.

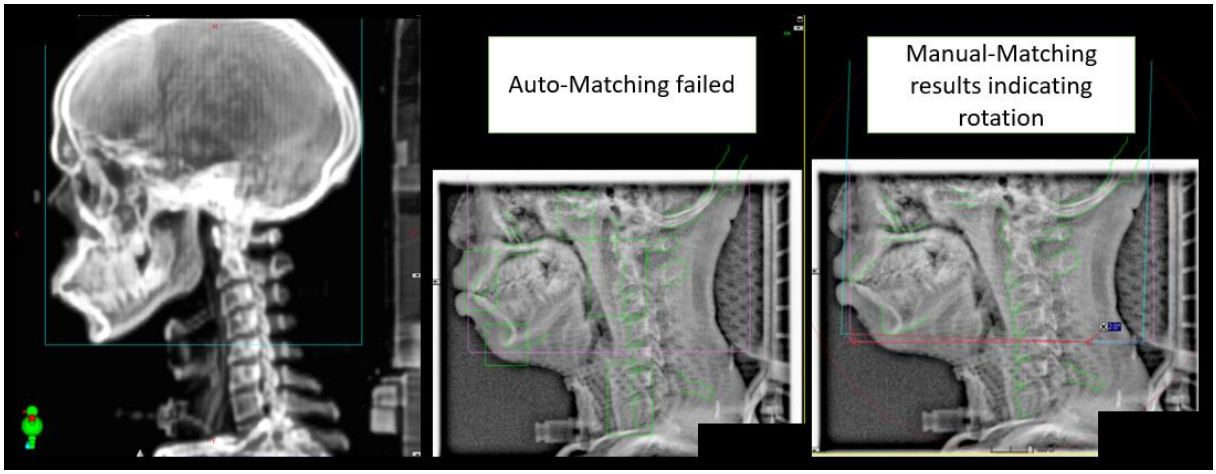

Figure 3.35: Nasopharynx radiation therapy with limited Anatomy of skull (illustration produced by author)

3.3.1.8.3.1 Head and neck radiation therapy example

Figure 3.36 is an example of a head and neck patient who received radiation therapy for oropharynx cancer. In the lateral EPID image the vertebrae are clearly imaged, but in order to verify the head position, the base of skull and hard palate is of great importance. Unfortunately, the shoulders were included in the image, adding no value to the image comparison. On the EPID image a vague mismatch can be seen of the maxilla, but it is very unclear and cannot be verified because of the missing skull anatomy.

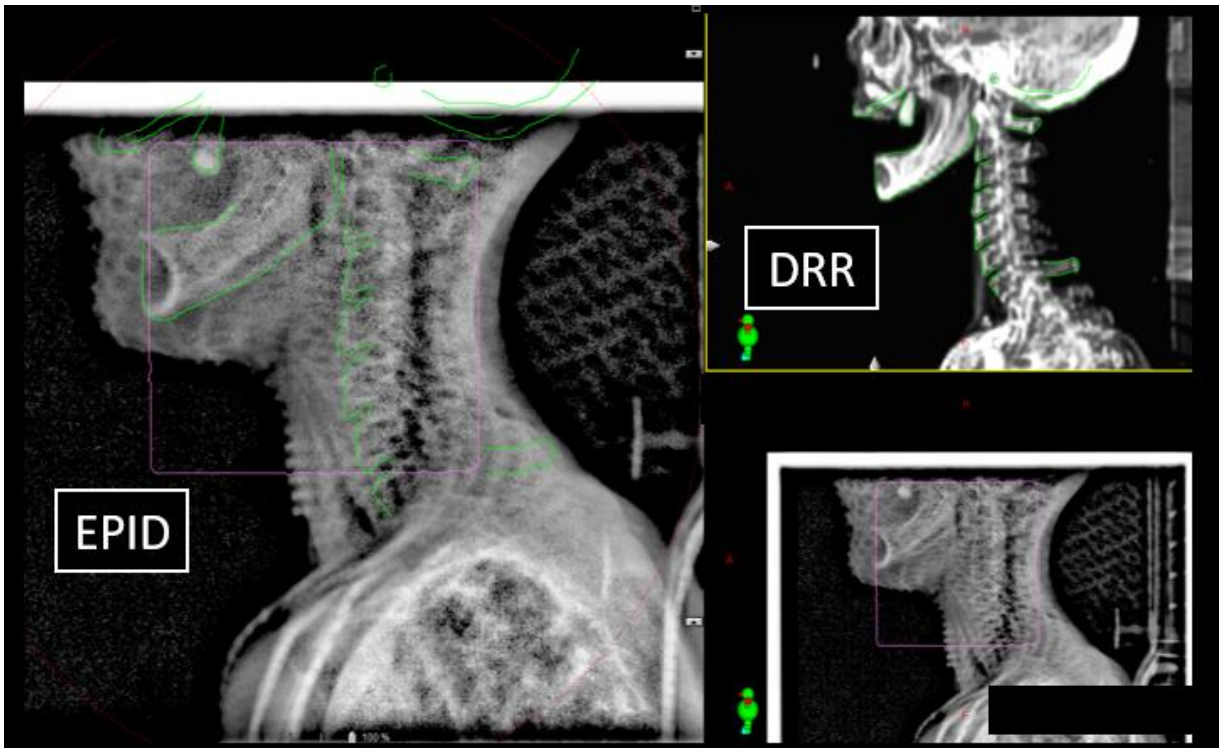

Figure 3.36: No base of skull or maxilla anatomy visible on EPID image to verify head position (illustration produced by author)

Figure 3.37 illustrates how a head and neck patient needed a rotation to be applied to verify the set-up position. Unfortunately, again not enough anatomy was imaged inferiorly and superiorly to verify this rotation, thus leading to uncertainty in the matching results.

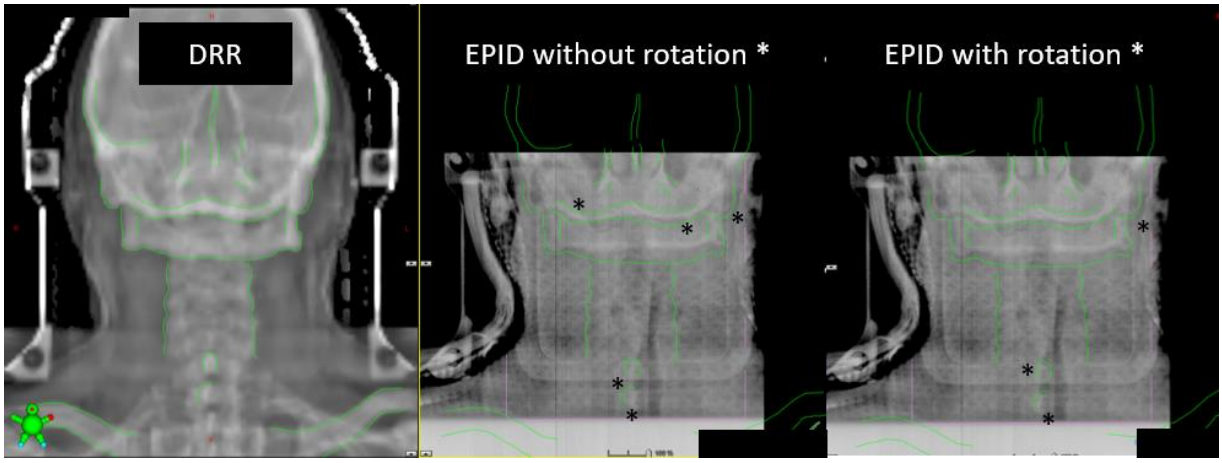

Figure 3.37: Not enough anatomy inferiorly to verify rotation of patient to correct for set-up error (illustration produced by author)

3.3.1.8.3.2 Head only radiation therapy example

Figure 3.38 illustrates the DRR and EPID images of two separate patients, who both received radiation therapy to the head. For any patient receiving RT to the head, the whole skull needs to be imaged, with the C1 and C2 to be included inferiorly. All this anatomical data on the EPID image is needed to ensure an accurate matching result.

Patient **a** did not have the vertex of the skull imaged. The result was that only the orbit could be used for superior to inferior verification of the patient position. Patient **b** had the vertex, orbit, and base of skull clearly visible on the EPID image. As seen on the matched result, where the contours from the DRR are projected onto the EPID image, there is no agreement between the vertex, orbit and base of skull. This is a clear indication that there is a rotational error in the patients positioning. A flexion or extension of the chin is needed, as these three anatomical areas cannot be matched.

The scenario seen in Patient **a**, will lead to less accurate matched results, as there were not enough bony landmarks present on the EPID image to verify the superior to inferior shift. A patient with enough imaged landmarks will have a more accurate matching result.

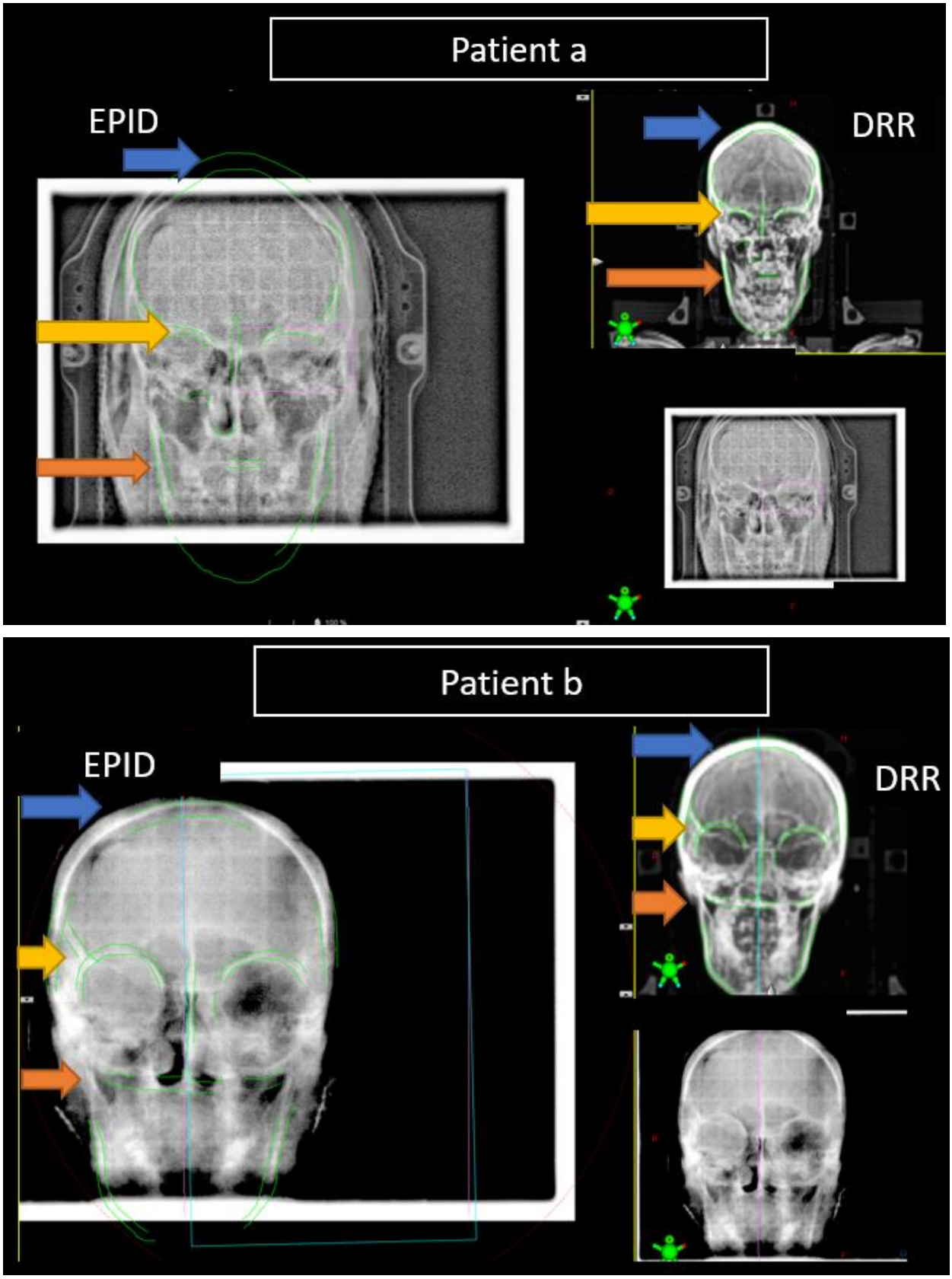

Figure 3.38: Comparison of two EPID images of patients receiving radiation therapy to the head only (illustration produced by author)

3.3.1.8.4 DRR quality

The creation and visualisation of the appropriate anatomy on the DRR is important to complete before the patient starts treatment, as it cannot be changed once an EPID image is linked to it. Figure 3.39 illustrates a DRR of patient **a**, created to visualize only certain bony landmarks, and where the baseplate was also included in the DRR. Comparing this DRR with the EPID image indicates that no facial bones are visible on the DRR.

Patient **b** has the perfect DRR, created for lateral matching of head and neck patients. Both bony landmarks and soft tissue were created as a DRR and can be easily compared to the EPID image.

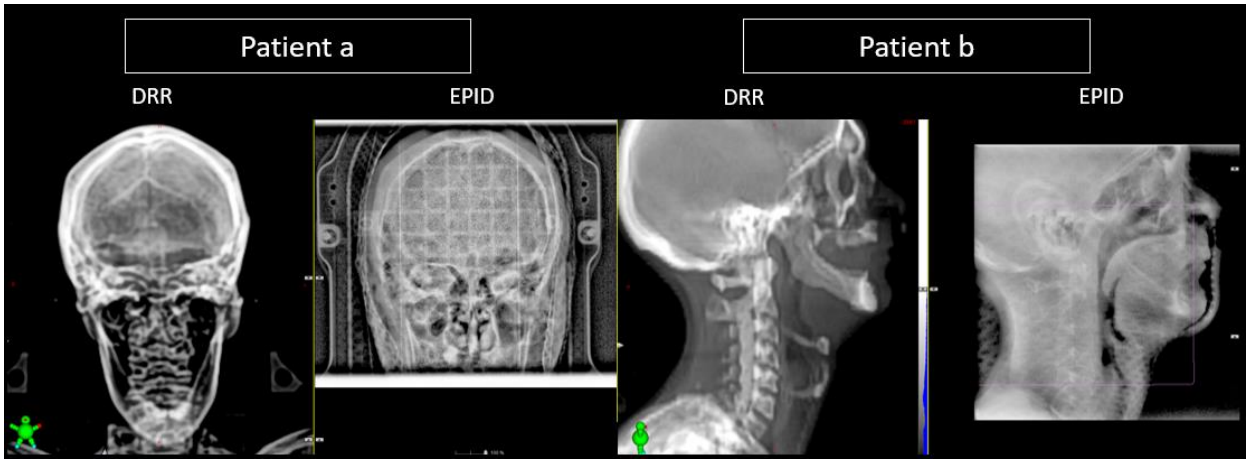

Figure 3.39: Comparison of DRR quality between two patients' data sets. The DRR created for patient a shows no facial anatomy, while the DRR for patient b has very good contrast between soft tissue and bony structures, making it ideal for comparison with EPID image (illustration produced by author)

3.3.1.8.5 Mismatch in treatment area vs verification area

Figure 3.40 illustrates the treatment area for a head and neck patient. This patient was treated to the left side of the head and neck area. On the DRR and EPID image the treatment area is indicated with orange blocks.

It is illustrated that the EPID images did not include the exact anatomy that was receiving radiation therapy.

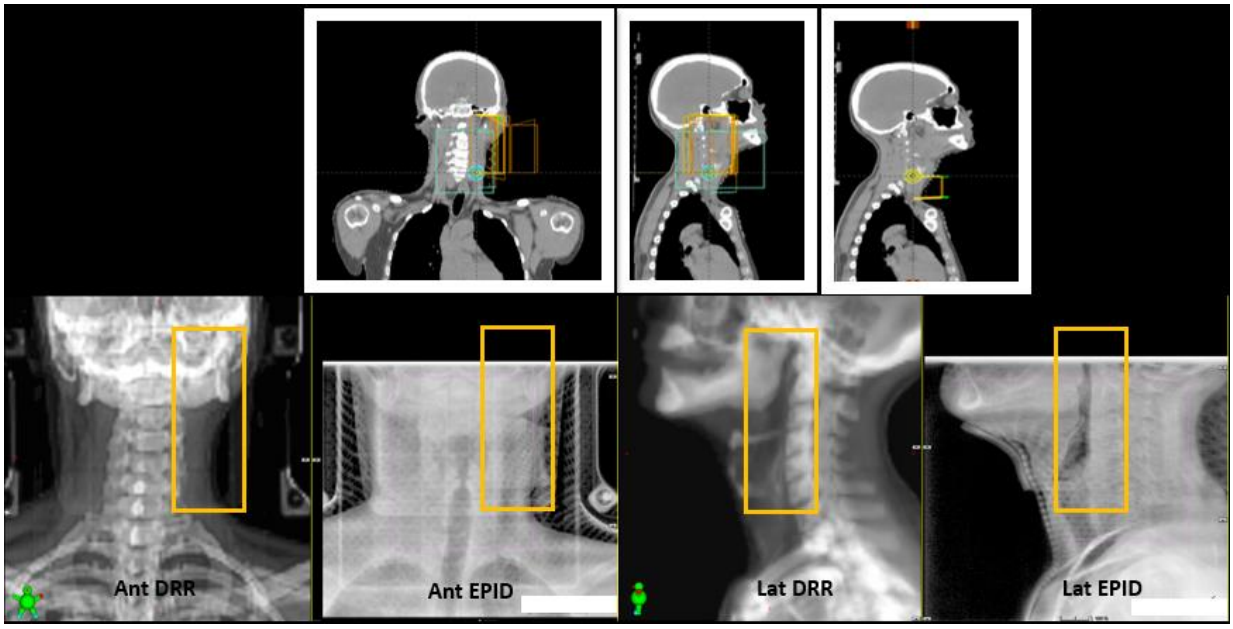

Figure 3.40: Disagreement between anatomy imaged and treatment area (illustration produced by author)

A regular occurrence in radiation therapy is that because of limitations of the field size that can be imaged, the whole treatment area is not always included on the EPID images. However, for these patients shown in the figures produced by the research/author, it could have been included on the EPID images, and less of the shoulder area could have been imaged as it does not add value for EPID image evaluation. The skull structures, together with the cervical vertebrae are important for the head and neck patient. As the base of the skull and hard palate were not included in the EPID images the matching results are shown to be less reliable.

3.3.1.8.6 Auto match failure

The auto match sequence was selected as the initial matching process for multiple patients, but this method failed as illustrated in figure 3.41. This was a disappointing discovery in the clinical research process, as auto matching is mostly used as the first matching option on the linear accelerators, and in theory this would have saved time, as minimal changes would be needed after auto matching has been performed.

It is anticipated that hopefully in the future better algorithms will be available for auto matching. However as shown by the data collection and production methodology, a factor such as the quality of imaging can have a large inter-user variability, and this can potentially result in large manual matching discrepancies.

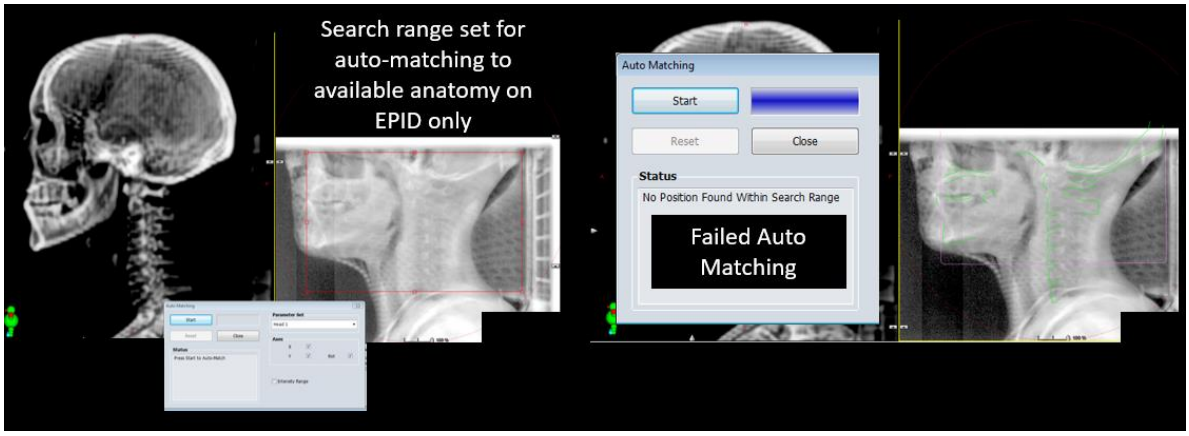

Figure 3.41: Auto matching failing, although search range was limited to a small part of anatomy (illustration produced by author).

3.3.1.8.7 DRR of children

During the matching exercise of three data sets of children, it was repeatedly observed by the researcher/ author that it was essential to image the vertex in order to verify any rotational error. This phenomenon is even more difficult with imaging of children because of the many growth plates and a lower density of developing bones. It would therefore be advantageous to image thinner slices at the planning CT to enable high quality DRRs to be created. Figure 3.42 demonstrates how challenging it is to identify facial and skull structures on a young child.

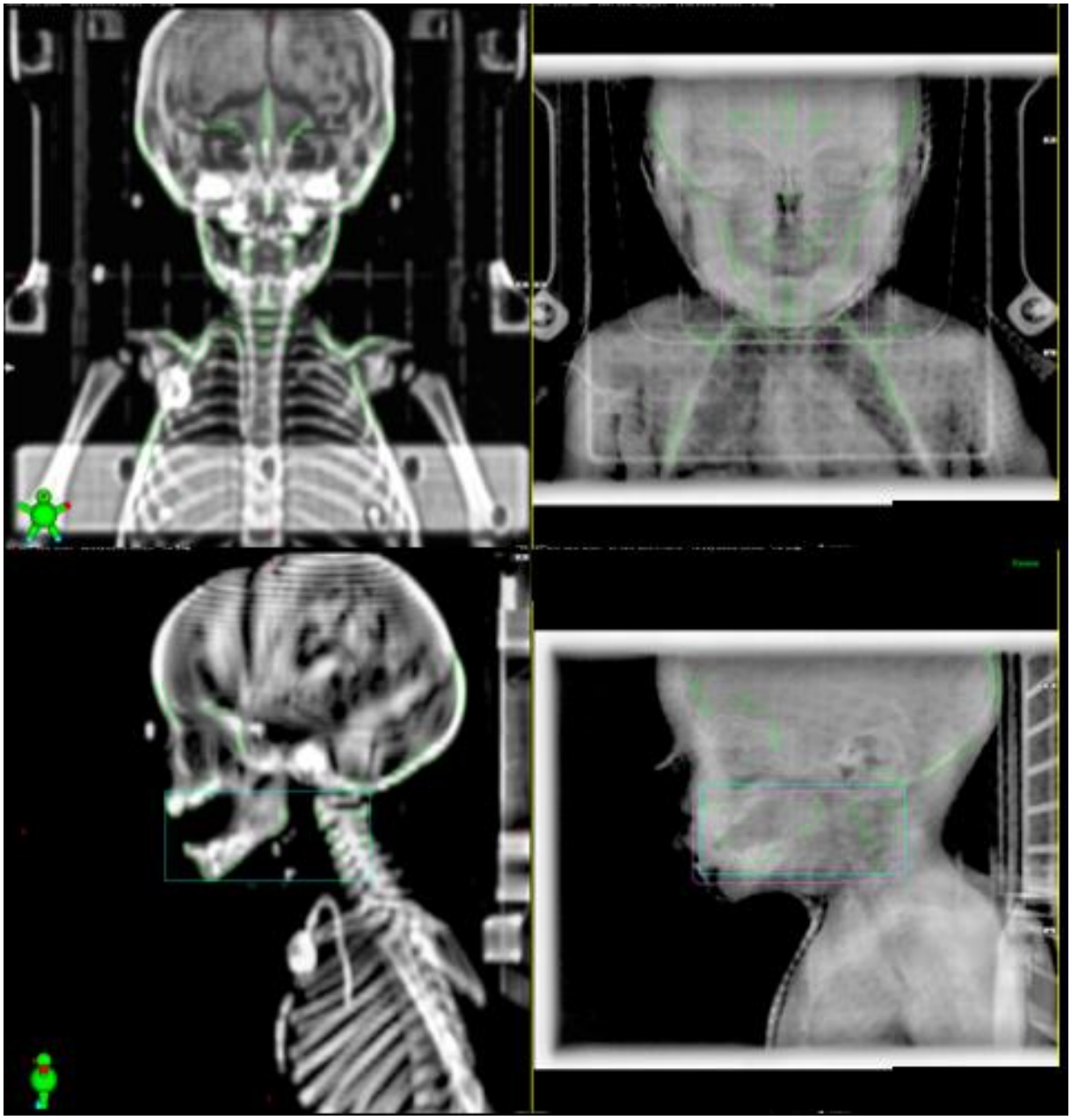

Figure 3.42: DRR quality of young children (illustration produced by author)

3.3.1.8.8 Total anatomical mismatch

To correct rotational errors when doing anatomical matching of the head and neck patient, the rotational shift of the head and the neck must both be in the same direction. If this is not the case, a rotation or anatomical shift cannot be applied. If it is applied, the resulting rotation will correct one half of the anatomy and then create an even larger mismatch in the other half of the anatomy. This is illustrated in figure 3.43 and figure 3.44. When such a shift is needed in the treatment session, the patient must be physically positioned again. It is noted that when viewing such images retrospectively, the matching is based on the anatomical site treated, as well as the organ most at risk, of overdose, for example the spinal cord.

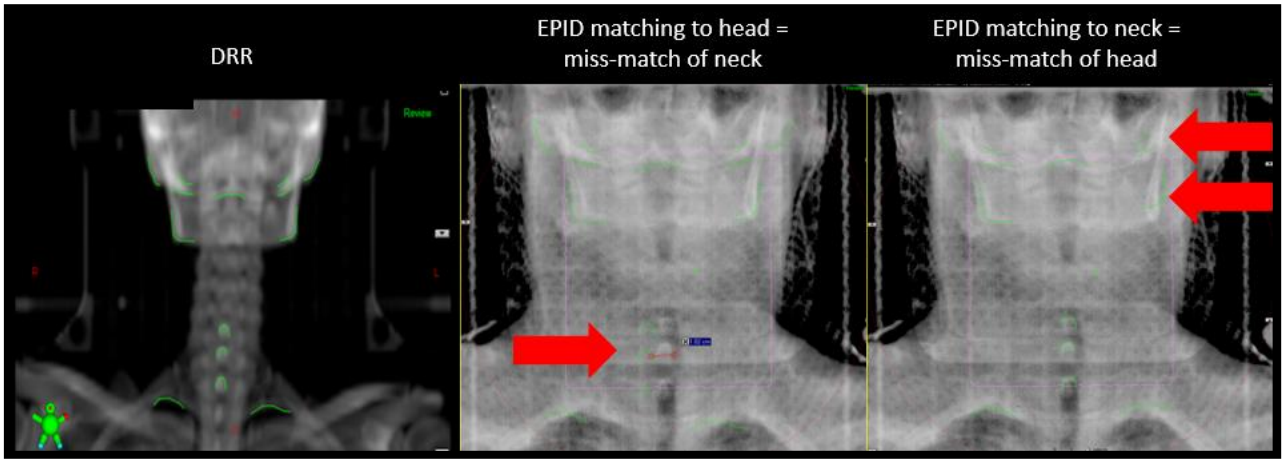

Figure 3.43: Arrows indicating shift of head and spine in opposite directions (illustration produced by author)

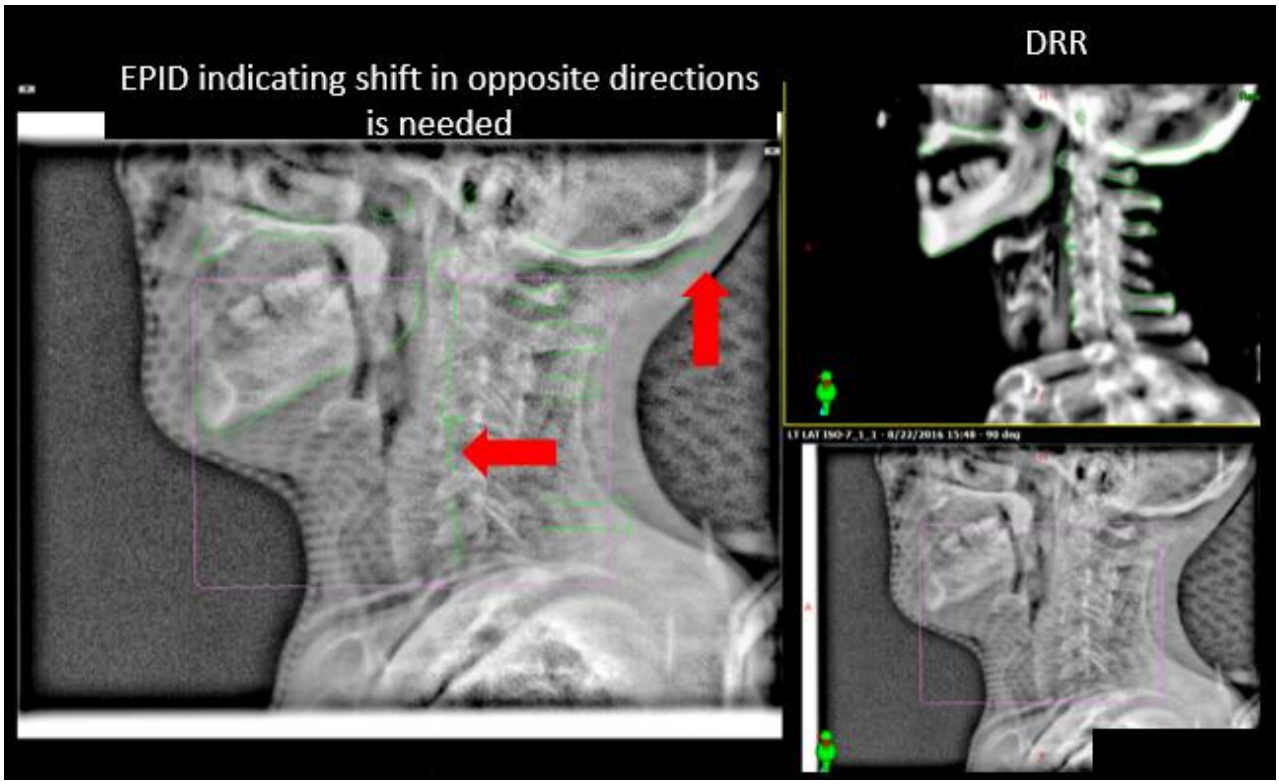

Figure 3.44: Arrows indicating a shift of head and spine in opposite directions (illustration produced by author)

3.3.1.8.9 Immobilisation devices or CT bed included in DRR creation

When creating a DRR in clinical practice, the user could clip any structures out of the data set before the creation of the DRR.

Figure 3.45 indicates the presence of the CT bed reinforcement included in the image creation of the DRR, and it can be seen that it interferes with the anatomical visualisation, as this reinforcement is not present at treatment and not seen on the EPID image.

As illustrated in figure 3.45, some immobilisation devices for example the headrest baseplate, are present on the EPID images and this could be included in the creation of the DRR. Such devices can provide information of anatomical misalignment if the patient is not positioned on top of the immobilisation devices the same way as during the planning CT scan.

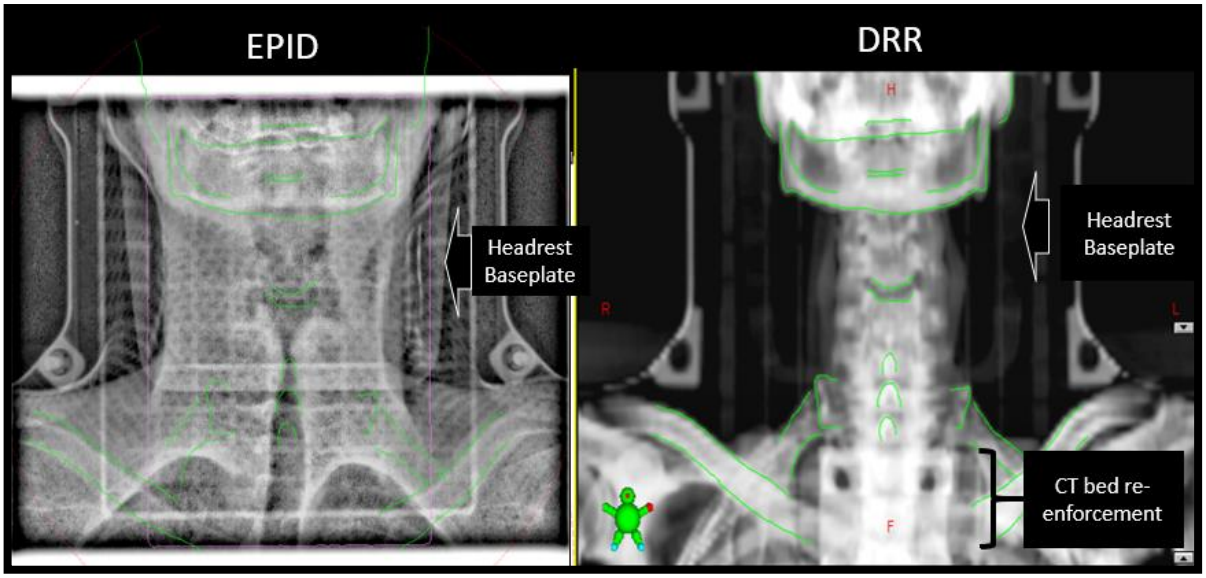

Figure 3.45: Visualisation of CT bed re-enforcement and the Headrest Baseplate on the DRR. The CT bed re-enforcement is not visible on the EPID image (illustration produced by author)

3.3.2 The clinical research process for sub-question 2: What are the critical organ doses for the two planning techniques?

This section details the data collection and production process followed to address sub-question 2, thus identifying the organ doses of VMAT and 3DCRT.

3.3.2.1 Organ at risk creation

In order for dose to be measurable on a radiation therapy plan, each organ at risk (OAR) needs to be manually contoured on the CT images.

Unfortunately, not all the OARs that were needed for this study had been contoured on all patients' data sets and these contours had to be added during the data preparation process. The contouring was done so that all patients included in this study had the same OARs contoured. All contours that were created were checked again by the responsible oncologist supervising the clinical data of this research study.

These contours were: brainstem, right and left cochlear, mandible, oral cavity, right and left parotid, spinal cord and the right and left temporomandibular joints (TMJ).

Although not defined as an OAR, the shoulders were also contoured to enable the dose to be recorded and compared in the final plan analysis.

During the preparation of data, it was found that many anatomical structures were not contoured correctly on the treated, original plans and these had to be corrected. This is demonstrated in figure 3.46 where the right cochlea had been incorrectly drawn on the original anatomical data which is the left image; and this is corrected on the image shown on the right of figure 3.46.

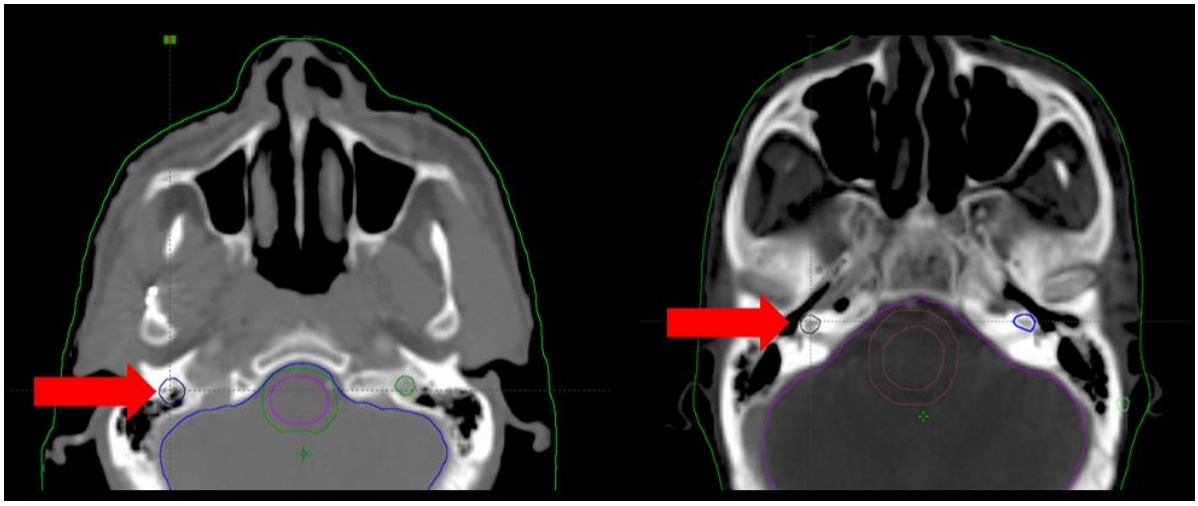

Figure 3.46: Incorrect location of cochlea on left image, and corrected on right image (illustration produced by author)

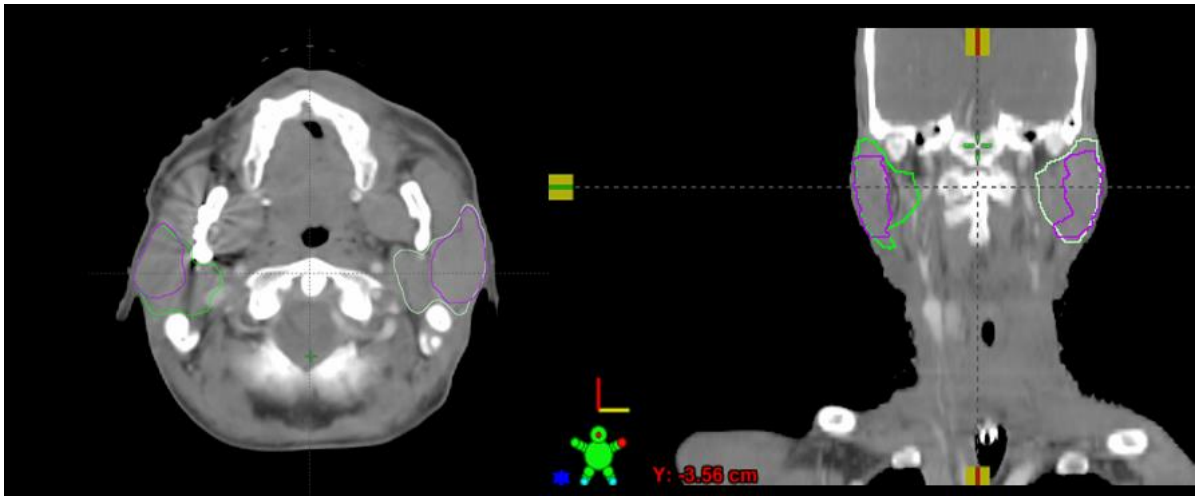

Figure 3.47: Purple parotid contour and corrected green contours on an orthogonal and coronal image (illustration produced by author)

The correction of these anatomical contours indicated that the anatomy that was contoured on the original data set was used for inverse optimisation and subsequent dose reporting. Thus, the doses recorded on the original plan would not necessarily report the dose the actual anatomical structures received. This factor would have led to the incorrect reporting of the dose, as no dose would have been reported for omitted OARs as they would not have been listed on the DVH. In figure 3.47 it is shown that on the original data set the parotids were drawn in purple and were smaller than the corrected green contours.

3.3.2.2 Contouring PRV and “help” contours

According to the ICRU Report 83 (ICRU, 2010), Patient Organ at Risk Volumes (PRV) have to be created for all organs at risk in close proximity to the target volume. As the expansion of the CTV to the PTV is a geometrical concept, and it takes into consideration the net effect of all possible geometric variations in order to ensure that the prescribed dose will be delivered to the CTV, so the OAR has to be expanded to create a PRV.

In this research study it was assumed that a 5 mm margin around the OAR will agree with the CTV to PTV expansion, as this is the current assumption applied at the study site.

It was verified during consultation with the responsible oncologist, that the CTV was not always contoured, but rather it was aimed to contour the PTV with a 5 mm margin around the visible CTV.

During the study period (2016-2017) the set-up error was unknown, and it was the purpose of this research to measure the set-up errors. Thus a starting point had to be defined, and it was agreed that 5mm would be a safe margin from which to create and measure data.

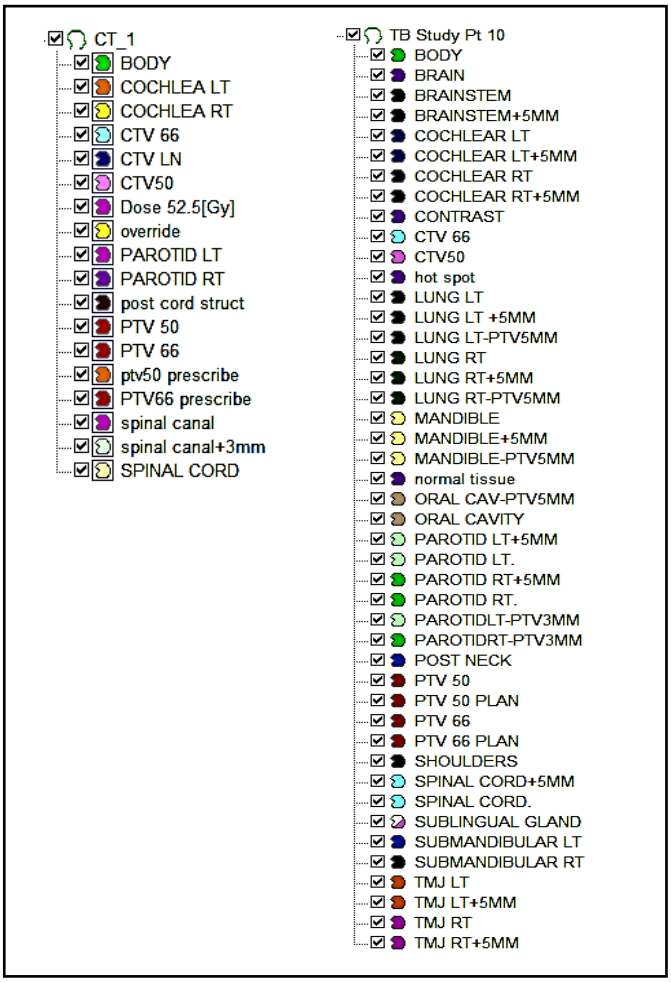

Figure 3.48: List of original patient OARs (left). List of the OARs after anatomical data preparation (right) (illustration produced by author)

Figure 3.48 shows the amount of contouring added to the original data set. This had to be done towards the data production of this study in order to assist with dose constraining and thus, to enable more accurate dose comparisons. Other contours that were created are listed in the four examples below.

Example 1: The baseplate and headrest had to be contoured in order to be included in the dose calculation (figure 3.49).

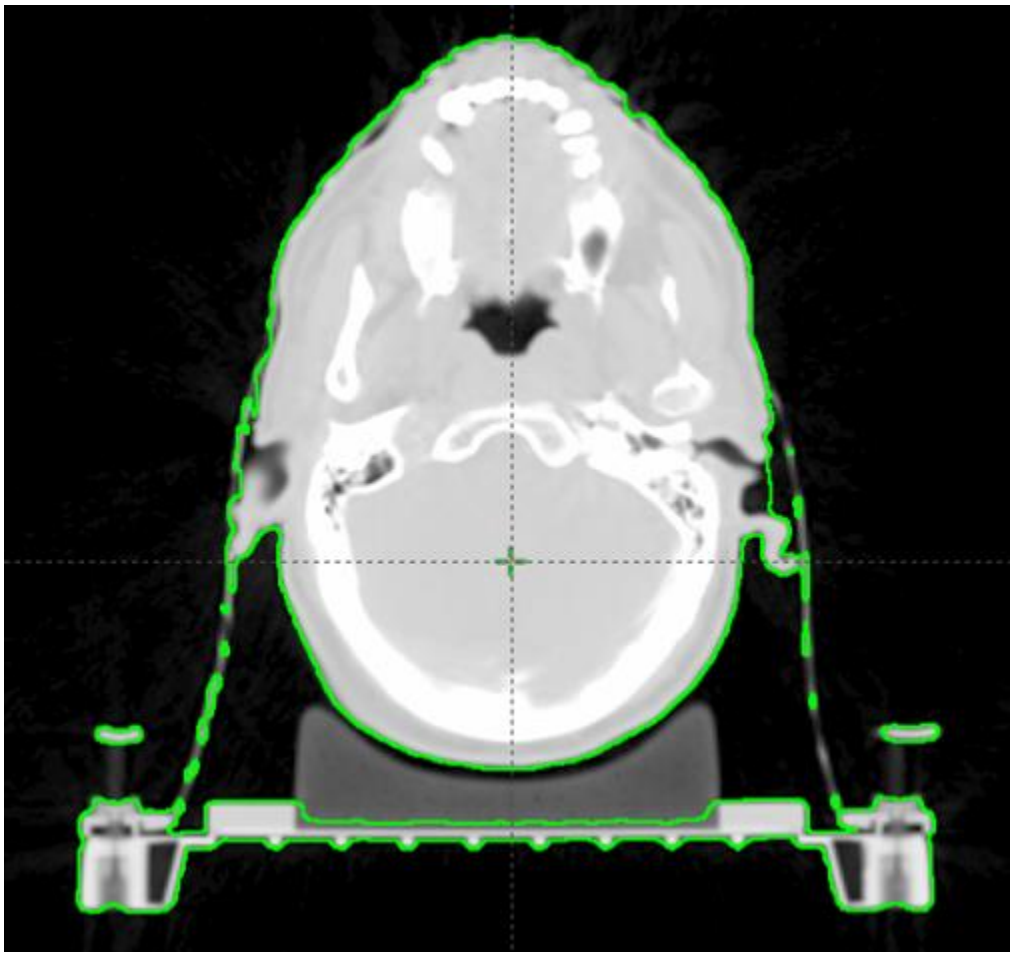

Figure 3.49: Body contour created to include headboard and mask (illustration produced by author)

Example 2: Most patients had contrast administered during the planning CT. This IV contrast imaged as quite dense inside the patient's anatomy but would not have been present during treatment. Therefore, all the contrast had to be contoured and the density corrected to be similar to that of the contralateral structures as illustrated in figure 3.50.

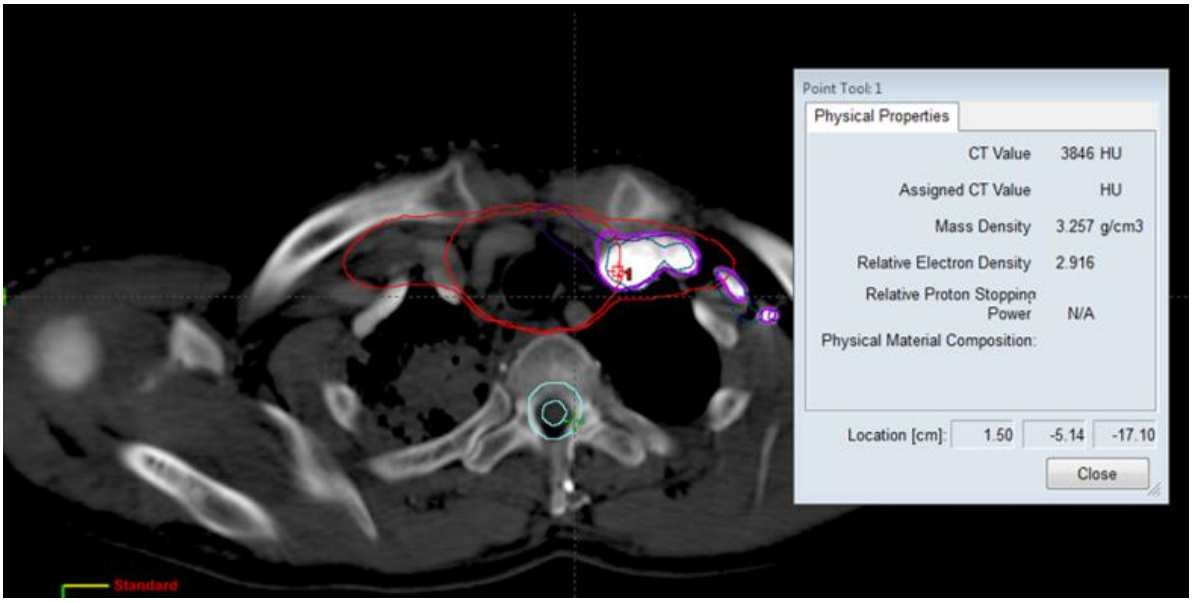

Figure 3.50: Contrast contoured, and density corrected (purple contour) (illustration produced by author)

Example 3: Helper contours: To enable dose manipulation in inverse planning, manual contours had to be drawn to move dose out of certain anatomical sites. These contours are known as "helper" contours. Figure 3.51 illustrates how a structure was placed posteriorly of the spinal canal PRV, to enable the dose to be "pushed out" of the posterior neck region.

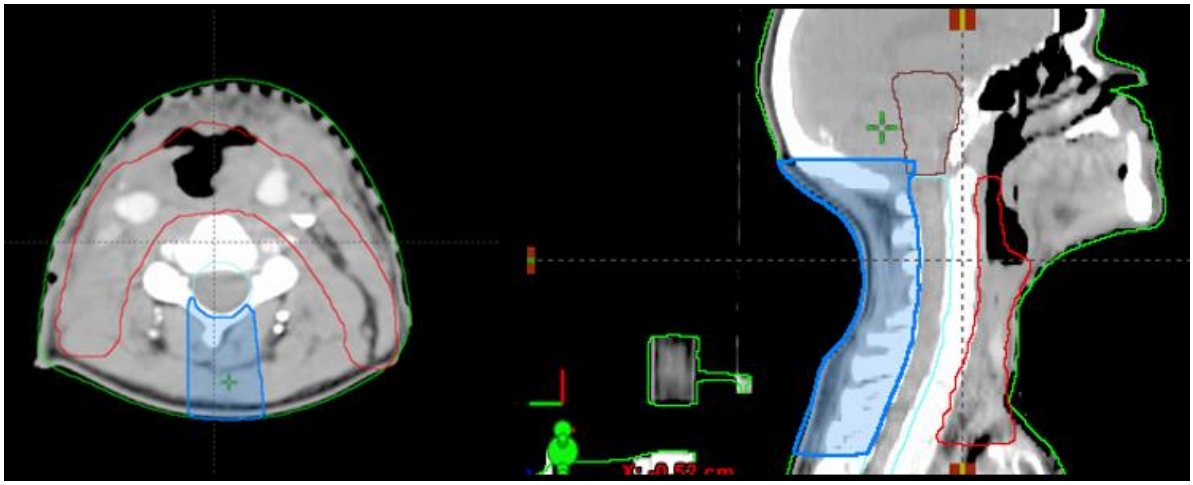

Figure 3.51: Posterior neck helper contour drawn in blue (illustration produced by author)

Example 4: Organs at risk and PRVs often overlap with the PTV. Therefore, overlapping OARs were cropped away from the PTV to enable inverse optimisation instructions not to contradict each other (see figure 3.52).

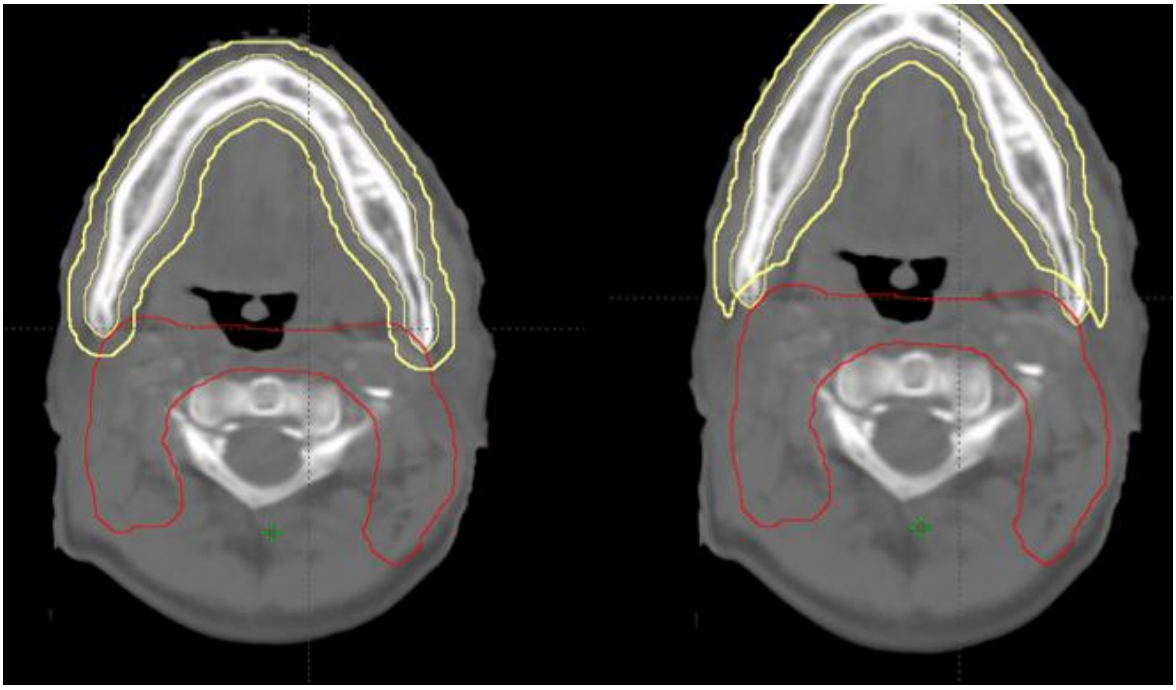

Figure 3.52: (Left) Mandible expanded to create the PRV (yellow) (Right) PRV cropped away from the PTV (illustration produced by author)

Figure 3.51 demonstrate how manual “helper” contours potentially need to be created for dose manipulation and not necessarily only for the organs at risk.

3.3.2.3 Dose recording

After all the treatment plans were completed for approval by the supervising clinical oncologist, the data was retrospectively recorded on a spreadsheet. To enable impartiality, plans were not compared during the planning phase, and not changed after approval by the oncologist.

A variety of data was recorded from the DVH of each plan. This included the doses to the following normal tissue contoured structures:

- Brainstem maximum dose (Dmax)
- Brainstem PRV Dmax
- Mean dose of both cochlea
- Mean dose of combined lungs
- V20 of combined lungs
- Mean dose to mandible and mandible PRV

- Dmax of mandible and mandible PRV
- Dmax and mean dose of oral cavity
- Mean dose and dose to 50% of parotids individually, combined and PRV
- Dmax and mean dose to shoulders
- Dmax of spinal cord and PRV
- Dmax of temporomandibular joint and PRV

Each patient had plans prepared, named 3DCRT, *RA Treat* and *RA Study*. The doses were recorded for each of these plans and transferred from the dose volume histogram into a spreadsheet. These recorded doses are presented in the spreadsheet in Appendix C.

3.3.3 The clinical research process for sub-question 3: Which planning technique offers the best dose coverage and dose homogeneity

This section details the data collection and production process followed to address sub-question 3, focusing on the best dose coverage and dose homogeneity by either VMAT of 3DCRT treatment plans.

3.3.3.1 Diagnosis

The inclusion criteria of patients into this research study was stage 3 and 4 cancer of the larynx.

The age, cell type, staging and TNM classification was recorded for each patient, to verify that they qualified to be included in this research study. It was also recorded if the patient had had surgery before radiation therapy, as well as receiving chemotherapy at any point of their respective treatments. This data is presented in subsection 4.3.1.

3.3.3.2 Creation of the treatment plans

All patients included in this study had been treated with VMAT. Therefore, all patients were re-planned using the 3DCRT technique. In addition, since not all OARs were contoured for the actual treatment and since some were contoured incorrectly (as discussed in section 3.2.1, a new VMAT plan was calculated using the updated contours as well as the additional contours as described in section 3.2.2).

The data production was that each patient had three sets of plans namely:

- The first set of plans being the VMAT plans with which each patient was treated. These were named *RA treat*.
- The second set of plans being the VMAT plan created using the correct and complete set of required contoured structures to optimize the plan. These were named *RA study*.
- The third set of plans was a 3DCRT plan created using the correct and complete set of required contoured structures to optimize the plan. These were named 3DCRT.

A total of 10 patients matching the inclusion criteria treated over a one-year period (2016) were found and all were included in this research study. They can be described as follows: Nine of the patients had two dose levels that were treated, and therefore had a total of 6 plans used for dose comparison. One out of the 10 patients had one dose level and therefore had 3 plans that were used for dose comparison. Example of the dose levels and plans are demonstrated in table 3.1.

Table 3.1: Examples of plans used in the study where patient 4 had two dose levels, and patient 5 only one dose level (table produced by author)

patient 4	3DCRT	50Gy
	RA treat	50Gy
	RA study	50Gy
	3DCRT	16Gy
	RA treat	16Gy
	RA study	16Gy
	3DCRT	50+16Gy
	RA treat	50+16Gy
	RA study	50+16Gy
patient 5	3DCRT	66Gy
	RA treat	66Gy
	RA study	66Gy

3.3.3.3 Data recording

All data was recorded in a spreadsheet and was recorded through volumetric automated measurements and by using the DVH. The purpose of recording these doses was to calculate the dose conformity and dose homogeneity, and to give an indication of the volume of tissue treated.

A variety of endpoints were recorded:

- The volume of the prescribed/ reference isodose (cm^3),
- The volume of the target called the PTV (cm^3),
- D90 (Dose to 90% of the volume) and D10 (Dose to 10% of the volume) (Gy),
- D98 (Dose to 98% of the volume) and D2 (Dose to 2% of the volume) (Gy),
- D95 (Dose to 95% of the volume) and D5 (Dose to 5% of the volume) (Gy),
- Maximum dose (Dmax) inside PTV (Gy),
- Minimum dose (Dmin) inside PTV (Gy) and
- TV_{RI}-The volume inside the target volume receiving the reverence isodose (cm^3)

See Appendix D for all the above measurements recorded on the data collection spreadsheet.

3.4 **Conclusion**

In chapter 3 the clinical research processes to address all three sub-questions was outlined. This included the methodology, analysis process as well as limitations found during data collection. In chapter 4 all the results of this research study will be presented.

CHAPTER 4 Research Results

4.1 Introduction

The data collection and production process described in chapter 3 is followed by reporting the research results from the subsequent analysis of the data in this chapter. The results of sub-question 1 that address the accuracy and reproducibility of the treatment set-up is divided into the accuracy of the patient treated in both the head and neck area (subsection 4.2.1 to 4.2.2) and those only treated in the head area (subsection 4.2.3 and 4.2.4). All data collected and analysed is presented with the proof of statistical significant findings shown along with the inclusion criteria for this patient population.

The results of sub-question 2 regarding the doses to the OARs for the 10 treatment plans, are presented for each OAR individually and then combined into a total planning score, as detailed in subsection 4.3.11.

The results of sub-question 3 regarding the dose to the PTV, is firstly given for each evaluation calculation individually and thereafter combined into a total planning score, as detailed in subsection 4.5 resulting in an overall planning score for each plan type namely *RA Treat, RA Study* and 3DCRT plans.

4.2 Research results for sub-question 1: How accurate and reproducible is the treatment set-up

4.2.1 *Head and neck* patient imaging information.

Thirty-three patients who received treatment in the head and neck area were included in this data group. The purpose of the sample size is to justify the statistical significance of the data produced. The following data was recorded and demonstrated in the figures below:

- The date of the planning CT when the immobilisation mask was made
- The date that treatment started.
- The date the treatment was completed
- The fractionation schedules
- All Electronic Portal Imaging (EPID) days

In Figure 4.1. it is shown that the minimum time between the planning CT and the start of radiation therapy was 7 days and the maximum time 65 calendar days. The average time was 41.2 calendar days.

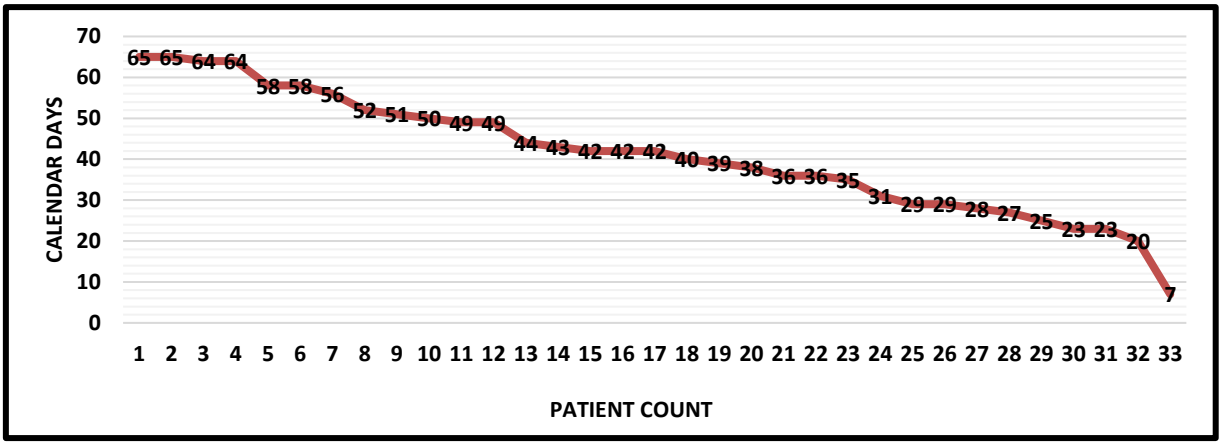

Figure 4.1: Calendar days from planning CT to start of treatment for *Head and Neck* patients

Of the 33 patients included in this study arm, the start and the end date of treatment was recorded for 30 of them. For three patients the start and end dates were not recorded thus they could not be included in figure 4.2. One patient was excluded in this analysis due to not completing the course of treatment. However, these four patients had enough data sets to be included in this study's EPID image analysis. Thus, the final sample shown in figure 4.2 is for 29 patients only.

The average amount of calendar days that these patients were on treatment at this research site was 50.9 days, with a minimum of 29 and a maximum of 62 days as indicated in figure 4.2.

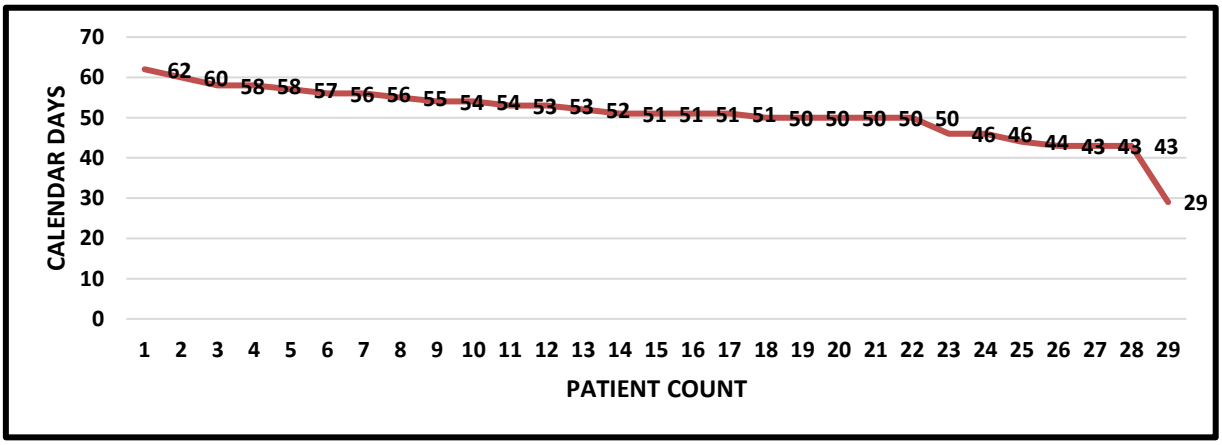

Figure 4.2: Calendar days from start of treatment to end of treatment for *Head and Neck* patients

The fractionation schedules for this patient population ranged from 30 to 35 prescribed fractions, with a minimum of 20 fractions for only one patient, as illustrated in figure 4.3.

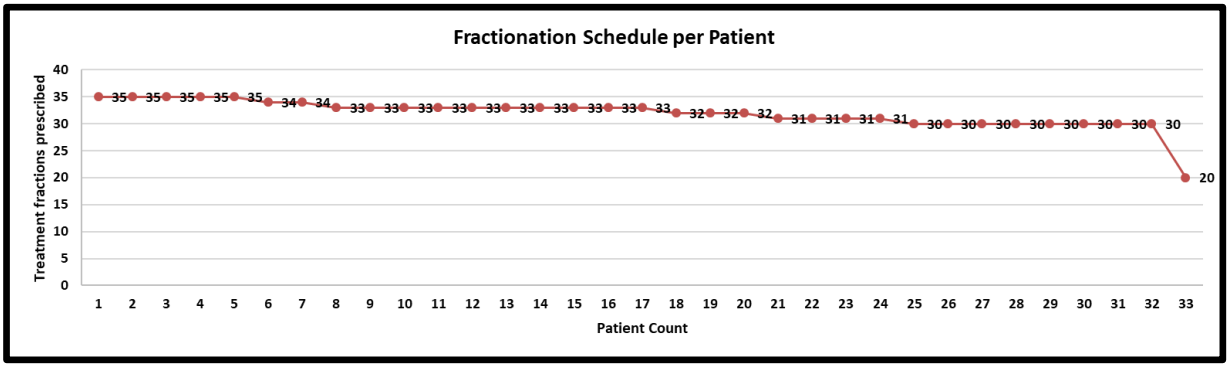

Figure 4.3: Fractionation schedule for *Head and Neck* patients

Figure 4.4 illustrates the imaging days across the whole population. It is observed that all 33 patients had EPID images on day 1 to 3 of treatment and thereafter at regular intervals of approximately 5 treatment days.

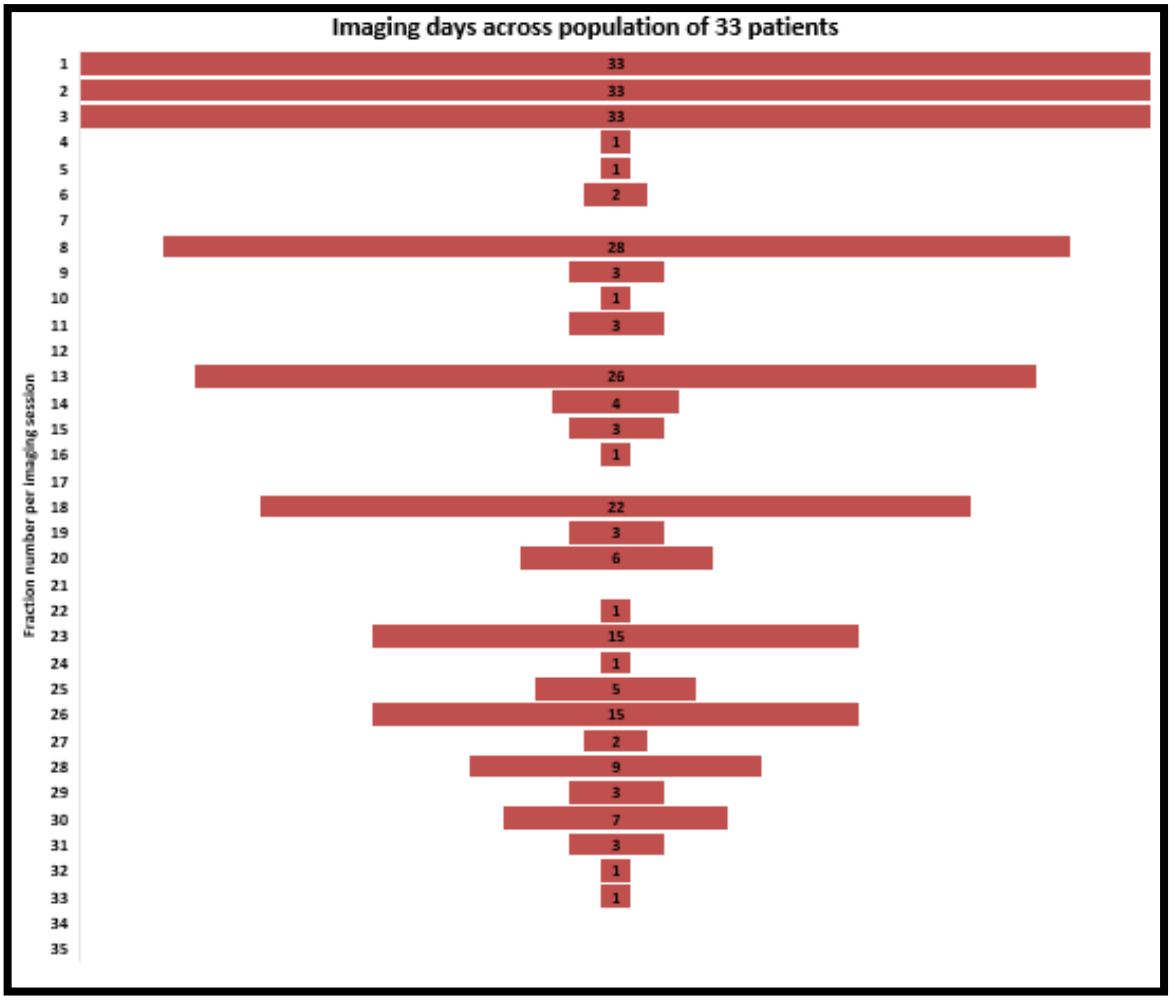

Figure 4.4: Imaging days for patients in the *Head and Neck* group

4.2.2 *Head and neck* imaging results

Across this patient population of 33 patients, the total amount of imaging sets was 272. The minimum number of image sets per patient was 5, and the maximum amount of image sets was 11. This is in line with the sample criteria where a minimum image set of 5 was proposed. This is illustrated in figure 4.5 with an average amount of images of 8.2 per patient.

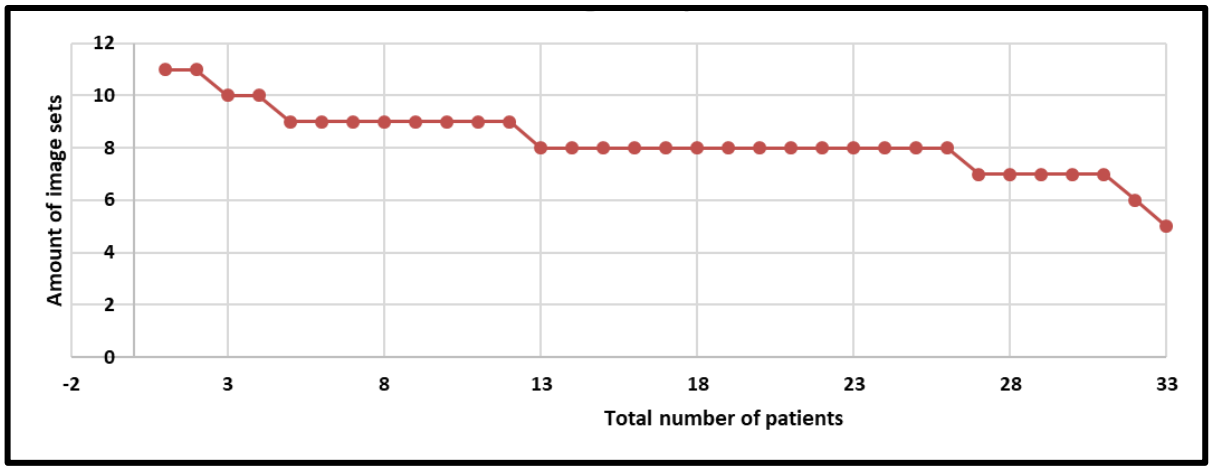

Figure 4.5: Imaging sets per patient for the *Head and Neck* group

The results of each image matching for each patient were recorded in all three directions. The vertical offset represents the anterior to posterior disagreement, the longitudinal offset represents the superior to inferior disagreement, and the lateral offset represents the left to right disagreement. Figure 4.6 shows the distribution of the offsets that were found.

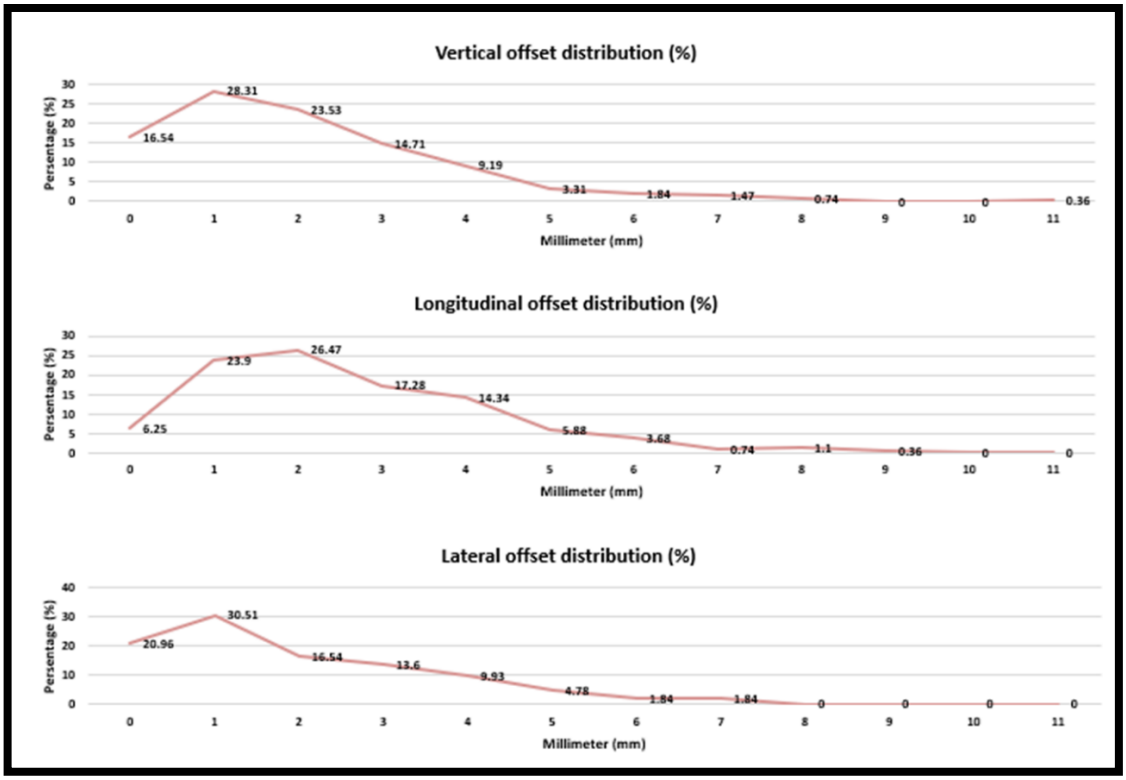

Figure 4.6: Distribution of set-up error

Van Herk's equation was used to obtain the systematic and random errors based on the EPID imaging data sets of the patients (Van Herk, 2004). The mean and standard deviation of all patient shifts were calculated per patient. For the head and neck patients this included the 33 data sets as shown in table 4.1.

The group systematic error is the average of all means which should ideally be close to zero. It can be seen in table 4.1 (mean of mean) that the group systematic error is close to zero except in the vertical direction, which shows an error of -1.1mm. This could potentially point to a subtle imprecision in the equipment or procedure. This calculation, however, does not correspond to the systematic error in van Herk's equation. The standard deviation of the means is an estimator for the standard deviation of the systematic error. This measure was thus used to determine the systematic error which describes how reproducible the treatment preparation is performed. It should be noted that van Herk uses the sample standard deviation in his paper, rather than the population standard deviation (Van Herk, 2004).

Table 4. 1: Mean and Standard Deviation calculated for 33 patients in the head and neck group

Patient	Vert Mean (mm)	Vert Std Dev (mm)	Long Mean (mm)	Long Std Dev (mm)	Lat Mean (mm)	Lat Std Dev (mm)
1	0.71	2.14	-2.00	0.87	-1.43	0.79
2	-3.44	4.19	-1.94	3.50	0.11	2.26
3	2.44	0.88	1.61	0.55	0.89	1.27
4	0.25	1.16	-0.38	0.74	0.38	0.52
5	0.00	1.61	1.27	1.93	1.73	2.87
6	-1.63	1.41	-1.19	1.36	-0.25	0.89
7	1.75	2.43	-0.25	1.93	-2.00	1.77
8	-1.11	2.03	-1.39	0.70	-1.11	1.76
9	-0.22	1.48	2.83	1.85	-1.33	1.73
10	-3.50	0.76	-4.50	0.89	3.88	0.64
11	-3.25	1.49	2.81	1.93	2.06	1.66
12	-1.00	0.89	0.92	1.96	0.00	0.63
13	-3.86	2.54	-0.86	2.64	1.43	0.98
14	-1.63	1.06	0.94	1.47	-5.38	0.92
15	1.00	3.21	1.81	1.22	1.63	0.92
16	0.30	2.63	-1.29	2.22	0.40	1.51
17	-3.13	2.42	3.75	1.10	1.13	1.55
18	-0.50	1.85	1.81	1.77	0.13	0.35
19	-1.00	1.18	-1.36	2.41	1.18	2.14
20	0.50	2.46	-0.60	2.64	1.40	1.51
21	-2.29	2.87	5.50	1.80	-5.57	1.62
22	-3.50	1.31	-0.56	1.45	-2.88	1.64
23	-2.89	1.90	-2.44	3.16	2.22	1.64
24	-1.00	1.41	2.33	3.59	0.00	1.32
25	0.38	2.20	2.94	0.98	-3.75	1.04
26	-4.14	2.19	-1.43	2.76	0.86	1.68
27	-1.29	0.95	-1.43	0.73	-0.14	1.35
28	0.38	2.33	2.69	0.75	-4.13	0.99
29	-0.60	0.89	0.00	1.41	1.20	1.79
30	-1.88	1.36	-2.69	0.80	-0.38	0.92
31	-0.50	1.31	-0.56	1.68	1.00	0.53
32	-1.00	0.87	2.28	1.66	2.33	0.87
33	-0.89	0.78	-2.50	1.79	1.56	1.59
Mean of Mean	-1.11		0.19		-0.09	
Std Dev of Mean	1.68		2.23		2.21	
RMS		1.93		1.89		1.43

The random error is obtained by taking the root mean square of the standard deviations of all patients in each direction. This metric is given by the square root of the sum of squares of all standard deviations, divided by the square root of the number of patients (i.e. $\sqrt{33}$ for the head and neck group)

The results of the van Herk equation is shown in table 4.2. These results show that a non-symmetrical expansion of the CTV should be applied for the expansion to the PTV.

Table 4.2: Results of van Herk's equation (CTV to PTV expansion parameters)

Systematic Error [mm]			Random Error [mm]		
Vertical	Longitudinal	Lateral	Vertical	Longitudinal	Lateral
1.68	2.23	2.21	1.93	1.89	1.43
CTV to PTV margin expansion: 2.5 x systematic error + 0.7 x random error [mm]					
Vertical		Longitudinal		Lateral	
5.6		**6.9**		**6.5**	

The van Herk equation assumes that the minimum dose to the CTV is 95 % for 90 % of the patients. If 95% of the patients be included, the multiplication factor of 2.5 x systematic error gets replaced with 2.79, and for 99% of the patients this becomes 3.36 x systematic error.

If the planning system does not allow for CTV to PTV expansion of different values (mm) in individual directions, it can be useful to calculate a single margin all around:

Margin = $\sqrt{}$ [((5.6x5.6) + (6.9x6.9) + (6.5x6.5)) ÷ 3] = 6.4 mm

All data collected can be seen in Appendix A, which shows the measurements done for each of the image matching and the offsets measured in the 3 directions, as well as the rotational measurements that were not used in the van Herk's equation.

4.2.3 Head patient imaging information.

In this data set there were thirty-six (36) patients who received treatment in the head area only. The purpose of the sample size is to justify the statistical significance of the data produced. The following data was recorded and shown in the figures below:

- The date of the planning CT when the immobilisation mask was made
- The date that treatment started.
- The date the treatment was completed
- The fractionation schedules
- All Electronic Portal Imaging (EPID) days

It is shown in Figure 4.7 that there is a large range of calendar days between the planning CT and the start of treatment. These range from 7 to 70days, with an average of 29.4 days.

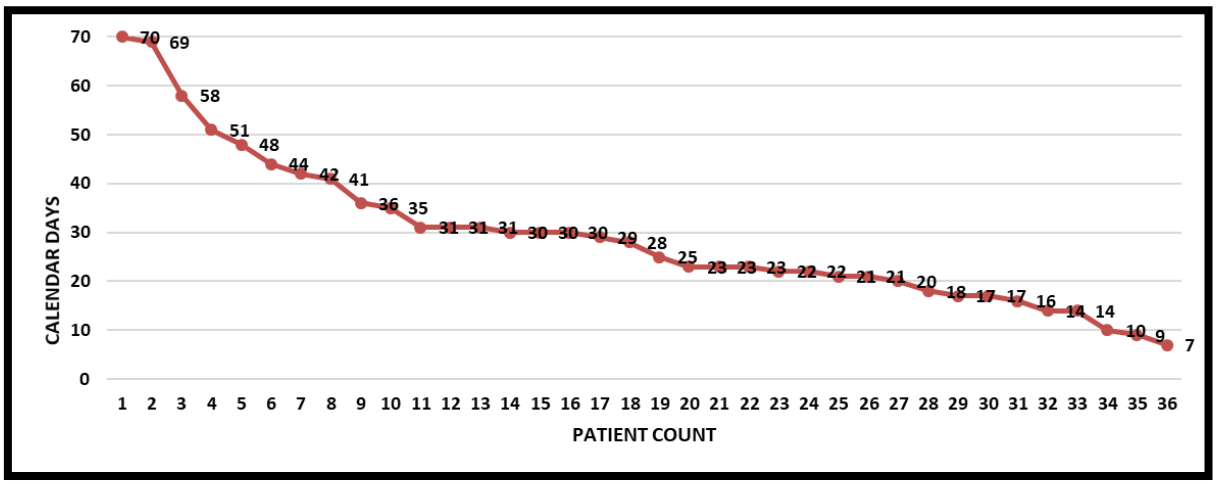

Figure 4.7: Calendar days from Planning CT to Start of Treatment for *Head* patients

The duration of treatment was calculated using the start date and the end date of treatment. One patient did not complete treatment, and another had a treatment duration of 85 days, so these two patients were excluded from figure 4.8. Therefore, only 34 patients are represented in figure 4.8. The maximum duration of treatment was 52 calendar days and the minimum duration 23 calendar days. The average duration of treatment was 43 calendar days as can be seen in figure 4.8.

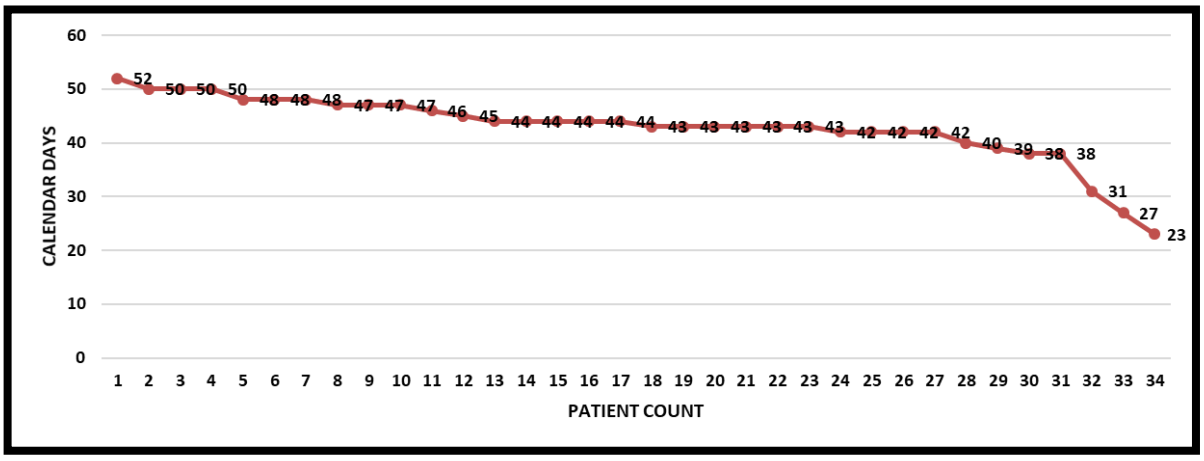

Figure 4.8: Calendar days from Start of treatment to End of Treatment for the *Head* patients

The fractionation schedule for this patient group was between 17 and 35 fractions with an average of 29 fractions as seen in figure 4.9.

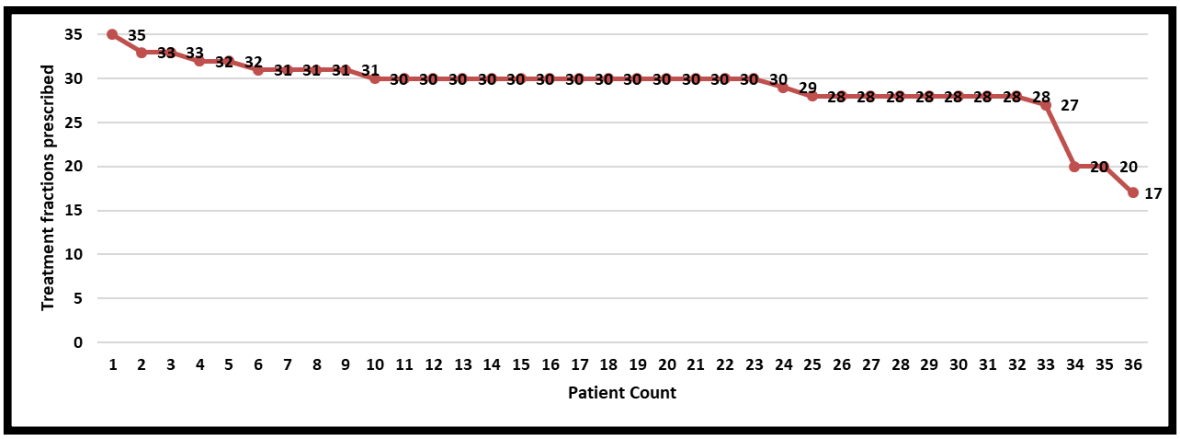

Figure 4.9: Fractionation schedule for *Head* patients

Figure 4.10 illustrates the imaging days. The imaging days of two patients were not recorded, and therefore the imaging days of 34 patients are illustrated. Except for one patient, all patients had imaging done on the first three fractions, and thereafter, on average, every fifth fraction.

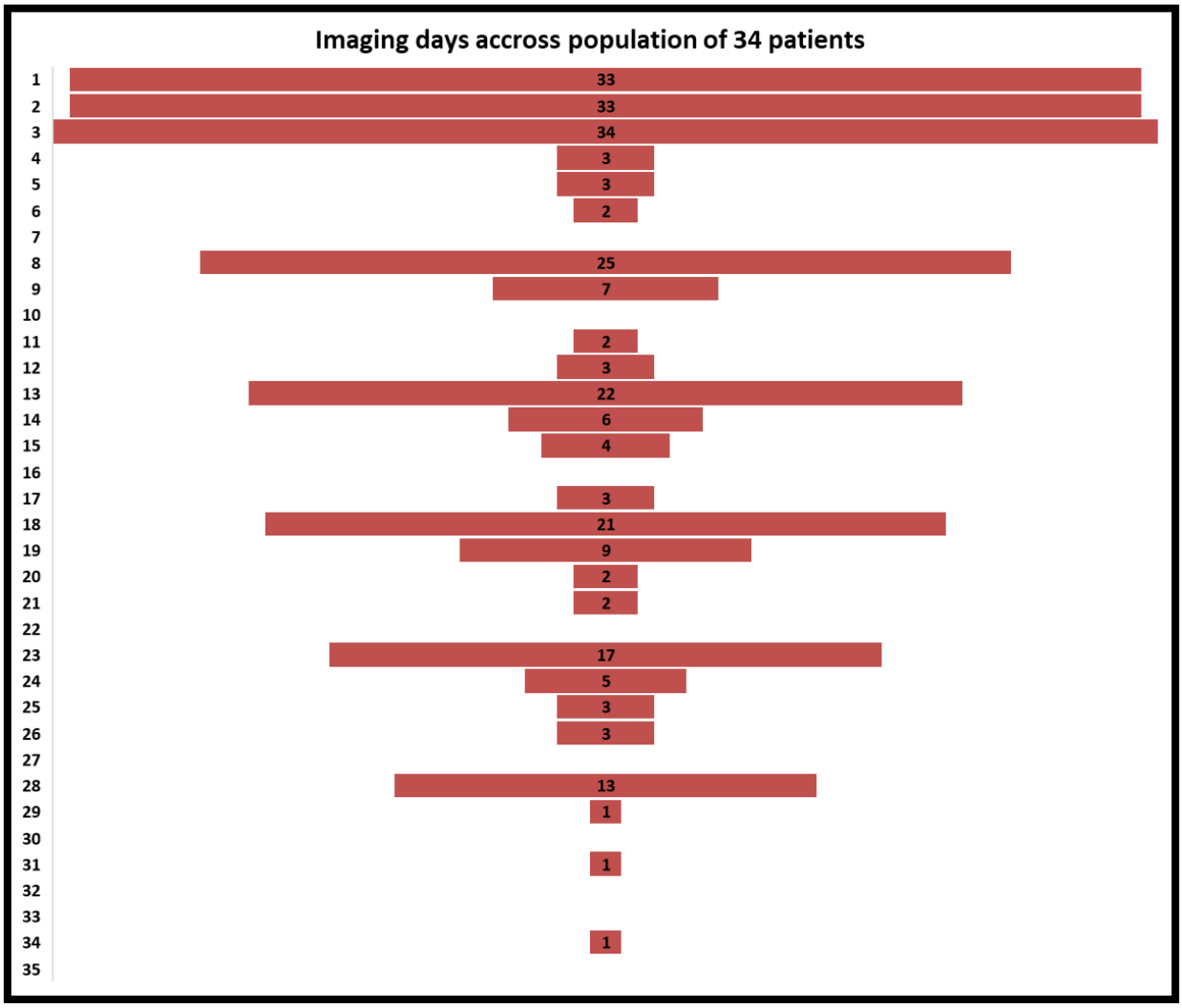

Figure 4.10: Imaging days for patients in the *Head* group

4.2.4 Head imaging results

Within this study sample of 36 patients, 273 images were evaluated. The number of images per patient varied from a minimum of 5 to a maximum of 10, with an average of 7.6 images per patient. This is in line with the imaging criteria where a minimum image set of 5 was proposed.

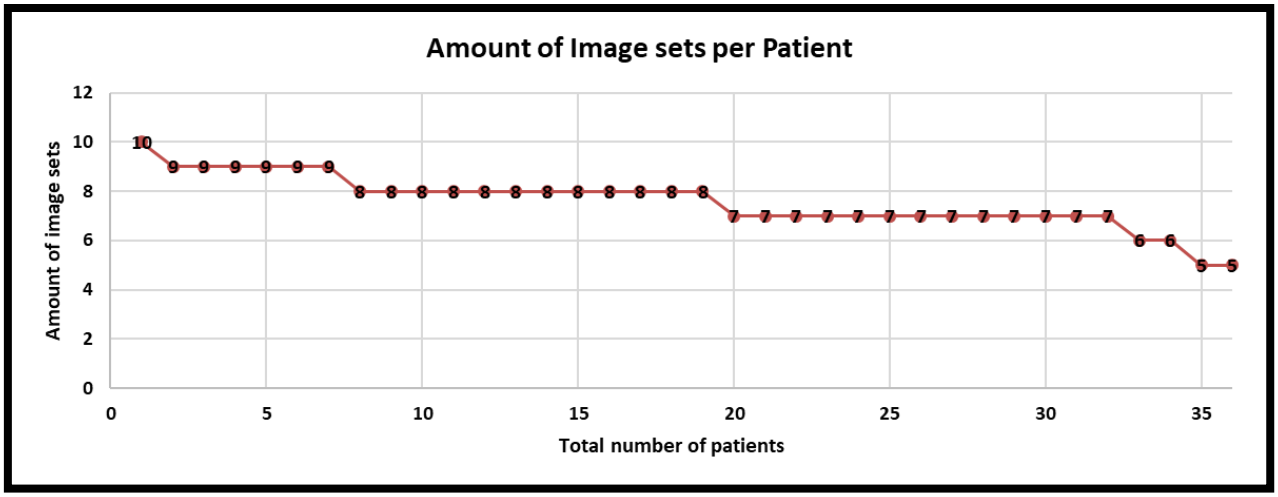

Figure 4.11: Imaging sets per patient for the *Head* group

The distribution of the set-up error across the population is illustrated in figure 4.12. The maximum offset measured was 10mm in the longitudinal direction, with a maximum of 8mm in the vertical and lateral directions.

Most setup errors measured were between 0 and 3 mm, with errors occurring 93.8% in the vertical direction, 77.7% in the longitudinal direction and 93.4% in the lateral direction.

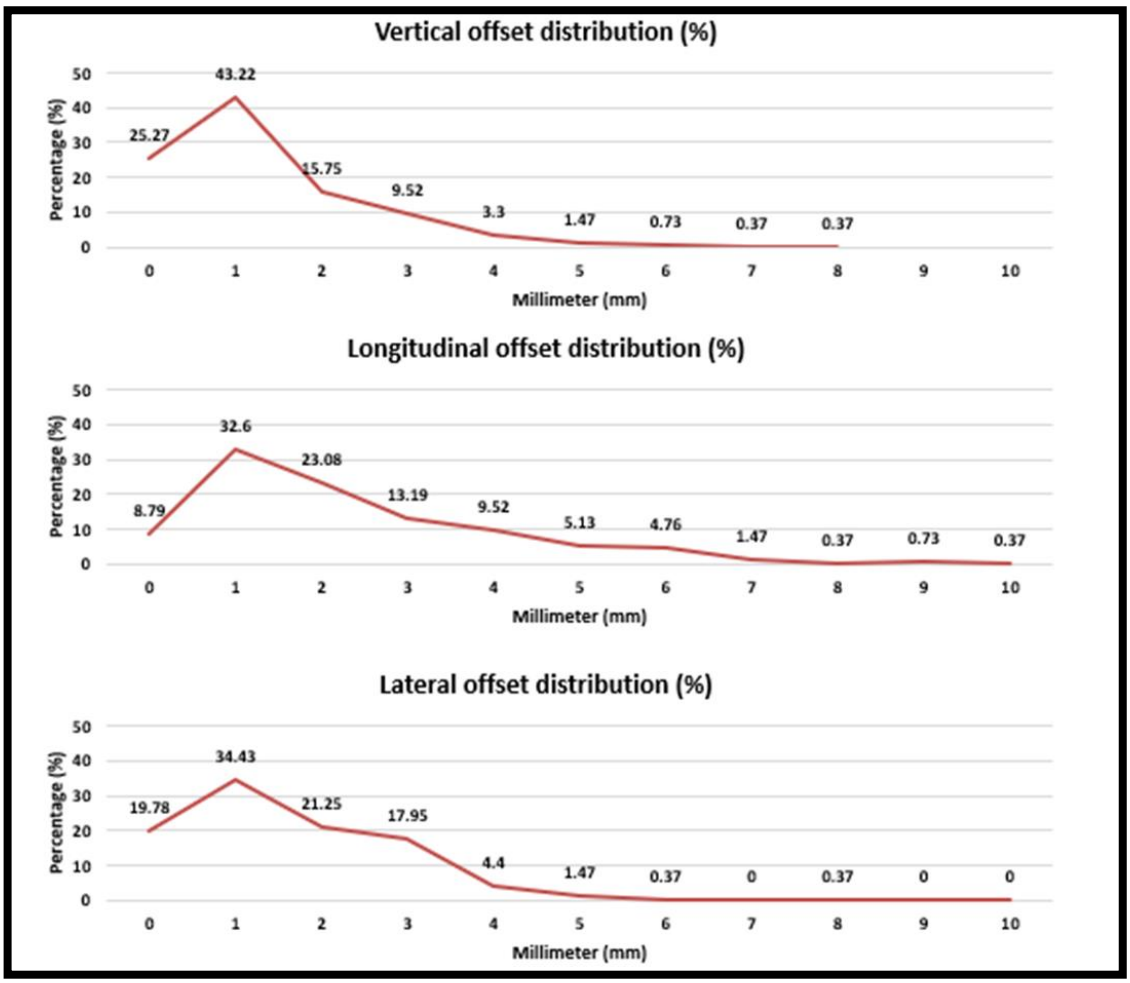

Figure 4.12: Distribution of set-up error across population

Van Herk's equation was used to obtain the systematic and random errors based on the EPID imaging of patients in the head group.

The mean and standard deviation were calculated using all 36 datasets, as demonstrated in table 4.3. The average of all means should be close to zero as this describes how reproducible the treatment preparation is performed. For this group the vertical is -0.13, longitudinal is 0.36, and lateral is -0.26, and therefore very close to zero.

Here it should also be noted that van Herk uses the sample standard deviation in his paper, rather than the population standard deviation (Van Herk, 2004).

Table 4.3: Mean and Standard Deviation calculated for 36 patients in the head group

Patient	Vert Mean (mm)	Vert Std Dev (mm)	Long Mean (mm)	Long Std Dev (mm)	Lat Mean (mm)	Lat Std Dev (mm)
1	-1.00	0.00	0.29	1.52	2.14	0.90
2	-4.40	0.55	2.40	1.78	0.40	0.89
3	-0.50	0.93	1.00	1.22	-0.13	2.17
4	0.57	0.53	1.79	1.82	-1.43	0.79
5	-1.71	1.25	0.00	1.29	0.29	0.76
6	0.38	1.41	-4.19	1.71	-1.88	1.13
7	-0.14	0.38	-0.79	1.07	1.43	1.13
8	-0.71	0.49	1.36	2.84	0.14	0.90
9	-4.33	1.00	-0.61	1.05	1.11	2.62
10	0.86	0.90	-4.07	1.57	2.14	0.69
11	0.33	0.71	-0.17	1.54	0.00	0.87
12	-0.88	1.96	1.13	1.64	-2.75	0.71
13	-0.75	0.46	1.06	1.08	-0.75	3.11
14	0.50	0.53	1.88	0.64	0.13	1.25
15	1.56	1.24	1.39	1.80	1.67	1.22
16	-1.63	1.30	-0.31	1.46	0.63	0.92
17	0.00	1.15	0.50	1.61	3.57	1.40
18	-0.11	1.54	5.06	1.33	-0.33	0.87
19	1.25	1.39	0.81	0.53	-1.75	1.16
20	-2.29	1.11	0.50	1.44	-0.14	1.21
21	0.25	1.04	-0.13	1.77	-2.13	1.25
22	0.22	1.20	1.28	4.51	0.00	1.66
23	2.33	0.82	-0.42	1.93	-0.17	1.17
24	1.33	1.50	-3.72	2.72	-2.67	1.12
25	1.75	0.71	-3.63	0.74	1.25	1.04
26	2.00	0.82	2.79	0.81	-0.71	1.11
27	0.14	0.38	0.29	0.95	-1.00	0.00
28	-0.13	1.25	0.63	1.92	-1.63	2.07
29	-2.00	1.29	0.93	2.05	0.29	1.25
30	-0.75	1.83	0.75	1.91	-2.88	0.35
31	0.50	0.76	0.63	0.95	-1.75	1.16
32	0.00	1.55	0.67	2.32	1.67	1.75
33	1.20	0.84	-1.10	1.24	-2.20	0.84
34	1.57	0.98	4.36	2.27	0.86	0.90
35	0.40	0.97	1.75	4.49	-3.10	1.79
36	-0.43	0.79	-1.00	2.24	0.29	0.76
Mean of Mean	-0.13		0.36		-0.26	
Std Dev of Mean	1.52		2.00		1.60	
RMS		1.92		1.60		1.33

The random error (as explained in subsection 4.2.2) is obtained by taking the root mean square of the standard deviation of all patients in each direction. This metric is given by the square root of the sum of squares of all standard deviations, divided by the square root of the number of patients (i.e. √36 for the head group of patients).

The results of the van Herk equation shown in table 4.4 shows that an asymmetric expansion from the CTV to the PTV should be applied. This margin is slightly smaller than the head and neck group and indicates in practice less variability in positioning or image matching.

Table 4.4: Results of Van Herk's equation (CTV to PTV expansion parameters)

Systematic Error [mm]			Random Error [mm]		
Vertical	Longitudinal	Lateral	Vertical	Longitudinal	Lateral
1.52	2.00	1.60	1.92	1.60	1.33
CTV to PTV margin expansion: 2.5 x systematic error + 0.7 x random error [mm]					
Vertical		Longitudinal		Lateral	
5.1		**6.1**		**4.9**	

Van Herk's equation assumes that the minimum dose to the CTV is 95 % for 90 % of patients. As previously noted, if 95 % of the patients are included, the multiplication factor of 2.5 x systematic error gets replaced with 2.79, and for 99 % of patients this becomes 3.36 x systematic error.

If the planning system does not allow for CTV to PTV expansion of different values (mm) in individual directions, it can be useful to calculate a single margin all around:

Margin = √ [((5.1x5.1) + (6.1x6.1) + (4.9x4.9)) ÷ 3] = 5.4 mm

All data collected can be viewed in Appendix B which shows the measurements done for each of the image matching sets and the offsets measured in the 3 directions as well as the rotational error measured, but that was not included in the van Herk's equation calculation.

4.2.5 In summary

To determine the accuracy and reproducibility of the treatment of patients when using the Klarity Mask system, these two patient data sets, head and neck (33 patients) and the head (36 patients) were used. The measured results were evaluated using the van Herk's equation, which will ensure that the minimum dose to the CTV is 95% for 90% of the patients. From this information the following was concluded:

- The group treated in both the head and neck area, needed to have a CTV to PTV expansion applied asymmetrically, namely: 5.6 mm in the vertical (anterior to posterior)

direction; 6.9 mm in the longitudinal (superior to inferior) direction; and 6.5 mm in the lateral (left to right) direction.

- The group treated in the head area, needs to have a CTV to PTV expansion applied asymmetrically namely: 5.1 mm in the vertical (anterior to posterior) direction; 6.1 mm in the longitudinal (superior to inferior) direction; and 4.9mm in the lateral (left to right) direction.
- The rotational error was recorded but was not used in the calculation of above mentioned expansions.

4.3 **Research results for sub-question 2: What are the critical organ doses for the two planning techniques?**

4.3.1 Patient demographics and plan evaluation score system

Ten patients were included in the study for sub-question 2 and 3. Their age ranged from a minimum of 51 years to a maximum of 64 years. The average age was 57 years.

Of the ten patients, 8 were male, and 2 were female.

All patients had squamous cell carcinoma of the larynx and as can be seen from the staging, presented with large tumours.

The TNM staging of the ten patients were: one patient with T1N3M0, two patients with T2N2Mx, one patient T3N3M0, one patient with T4N0M0, three patients with T4N1M0, and two patients with T4N2M0. Therefore six patients were stage 4A, and four patients were stage 4B.

All patients were post surgery, and 6 out of the 10 patients had had concurrent chemotherapy.

As illustrated in figure 4.13, nine of the patients had two phases of treatment. Phase one of treatment were prescribed to 50Gy for 8 of the patients, and 60Gy for one patient. Phase two were prescriptions that varied between 10Gy and 20 Gy. One patient, only, had one phase of treatment of 66Gy (patient number 5).

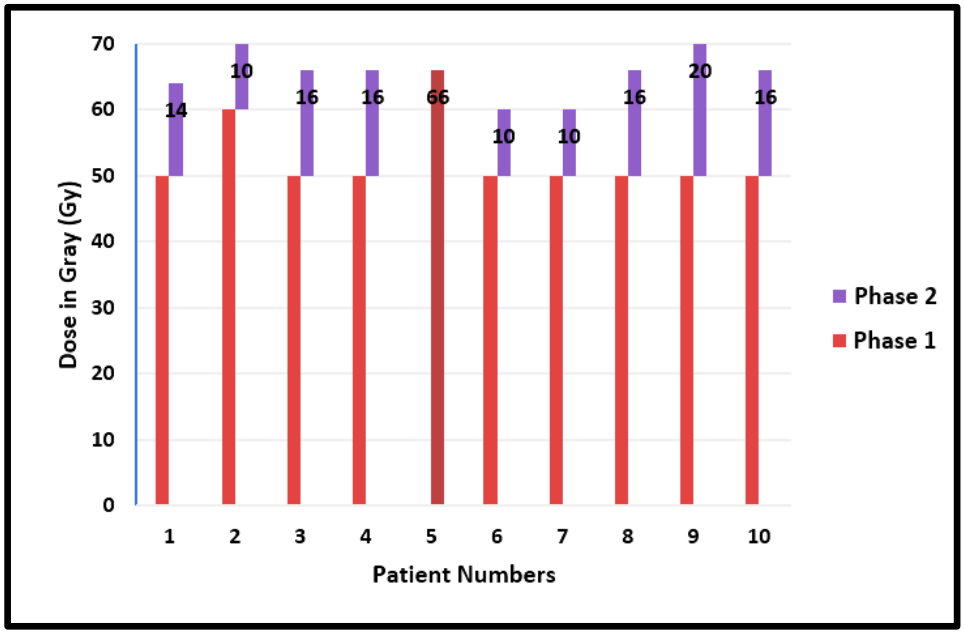

Figure 4.13: Dose prescriptions for planned patients, note that patient 5 had only one phase of treatment

Many OAR doses were evaluated from the combined plan of both phases of treatment. This reflected the total dose the organs received for the total course of treatment. The combined plan doses therefore varied between 60Gy and 70Gy.

For evaluation purposes a scoring system designed by the researcher for this study is shown in figure 4.14.

	Score System								
		Points Allocation		Best Results	Score	Acceptable Results (Gy)	Score	Worst Results (Gy)	Score
PTV	HI: D2/D98	2 points	plan 1	1-1.099	0	1.1-1.2	1	>1.2	2
	HI: D2/D98	2 points	plan 2	1-1.099	0	1.1-1.2	1	>1.2	2
	HI: D5/D95	2 points	plan 1	1-1.099	0	1.1-1.2	1	>1.2	2
	HI: D5/D95	2 points	plan 2	1-1.099	0	1.1-1.2	1	>1.2	2
	HI:D2-D98/Dp	2 points	plan 1	0-0.099	0	0.1-0.2	1	>0.2	2
	HI:D2-D98/Dp	2 points	plan 2	0-0.099	0	0.1-0.2	1	>0.2	2
	HI:D5-D95/Dp	2 points	plan 1	0-0.099	0	0.1-0.2	1	>0.2	2
	HI:D5-D95/Dp	2 points	plan 2	0-0.099	0	0.1-0.2	1	>0.2	2
	CI:V95%/TV	2 points	plan 1	negative 0.95 to 1.05	0	negative 0.85-0.95 and 1.05-1.5	1	<negative 0.85 or >1.5	2
	CI:V95%/TV	2 points	plan 2	negative 0.95 to 1.05	0	negative 0.85-0.95 and 1.05-1.5	1	<negative 0.85 or >1.5	2
	CVF=TV (RI)/TV	2 points	plan 1	0.95-1	0	0.9-0.95	1	<0.9	2
	CVF=TV (RI)/TV	2 points	plan 2	0.95-1	0	0.9-0.95	1	<0.9	2
OAR	Brainstem	6 points	Dmax	<50Gy	0	<53Gy	1	>53Gy	3
	Brainstem PRV		Dmax	<54Gy	0	<54-59Gy	1	>59Gy	3
	Spinal Cord	6 points	Dmax	<45Gy	0	<45Gy-47Gy	1	>47Gy	3
	Spinal Cord PRV		Dmax	<48Gy	0	<48Gy-50Gy	1	>50Gy	3
	Parotid Right	6 points	Mean Dose	<18Gy	0	<18-23Gy	0.5	>23Gy	1
	Parotid Left		Mean Dose	<18Gy	0	<18-23Gy	0.5	>23Gy	1
	Parotid Right PRV		Mean Dose	<20Gy	0	<20-25Gy	0.5	>25Gy	1
	Parotid Left PRV		Mean Dose	<20Gy	0	<20-25Gy	0.5	>25Gy	1
	Parotids Combined		Mean Dose	<23Gy	0	<23-37Gy	0.5	>37Gy	1
	Parotids Combined PRV		Mean Dose	<25Gy	0	<25-39Gy	0.5	>39Gy	1
	Cochlear Right PRV	4 points	Mean Dose	<32Gy	0	<32-45Gy	1	>45Gy	2
	Cochlear Left PRV		Mean Dose	<32Gy	0	<32-45Gy	1	>45Gy	2
	TMJ Right	4 points	Dmax	<60Gy	0	<60-65Gy	0.5	>65Gy	1
	TMJ Left		Dmax	<60Gy	0	<60-65Gy	0.5	>65Gy	1
	TMJ Right PRV		Dmax	<65Gy	0	<65-70Gy	0.5	>70Gy	1
	TMJ Left PRV		Dmax	<65Gy	0	<65-70Gy	0.5	>70Gy	1
	Oral Cavity	2 points	Mean Dose	<40Gy	0	<40-45Gy	1	>45Gy	2
	Mandible	2 points	Dmax	<68Gy	0	<68Gy-70Gy	0.5	>70Gy	1
	Mandible PRV-PTV		Dmax	<70Gy	0	<73Gy	0.5	>73Gy	1

Figure 4.14: Score allocation system developed by the researcher to quantify the results of both the PTV and OAR doses

The scoring system allowed a score range of 0 to 2 to be allocated for each PTV evaluation parameter. The score of 0 was given for the best result, 1 for an acceptable result and 2 for the worst result. Each evaluation parameter is discussed in subsections 4.4.1 to 4.4.5.

The score range for the OAR results varied from 0 to 3 depending on the organ evaluated. As indicated in figure 4.14 the OAR that were most likely to receive dose during radiation therapy to the larynx, had more points allocated than those who were least likely to receive dose. The lowest score indicated the best result and the highest scores indicated worst results. The evaluation of each organ is discussed in subsections 4.3.2 to 4.3.10.

Therefore, the plans that scored the least points were an indicator towards the better plan, thus the lower the points, the better the plan.

4.3.2 Brainstem

The brainstem is a serial organ, therefore the maximum dose recorded to it, is the significant parameter to record. It is observed in figure 4.15 that the maximum dose to the brainstem across the patients shows variability, and may be dependent on the extent of the PTV drawn. Patient 5, with the highest doses for all three planning techniques, was the patient who had been prescribed only one phase of treatment. Therefore, unlike other patients, where the second phase of treatment is done to a much smaller PTV, this patient had one large PTV treated to a high dose.

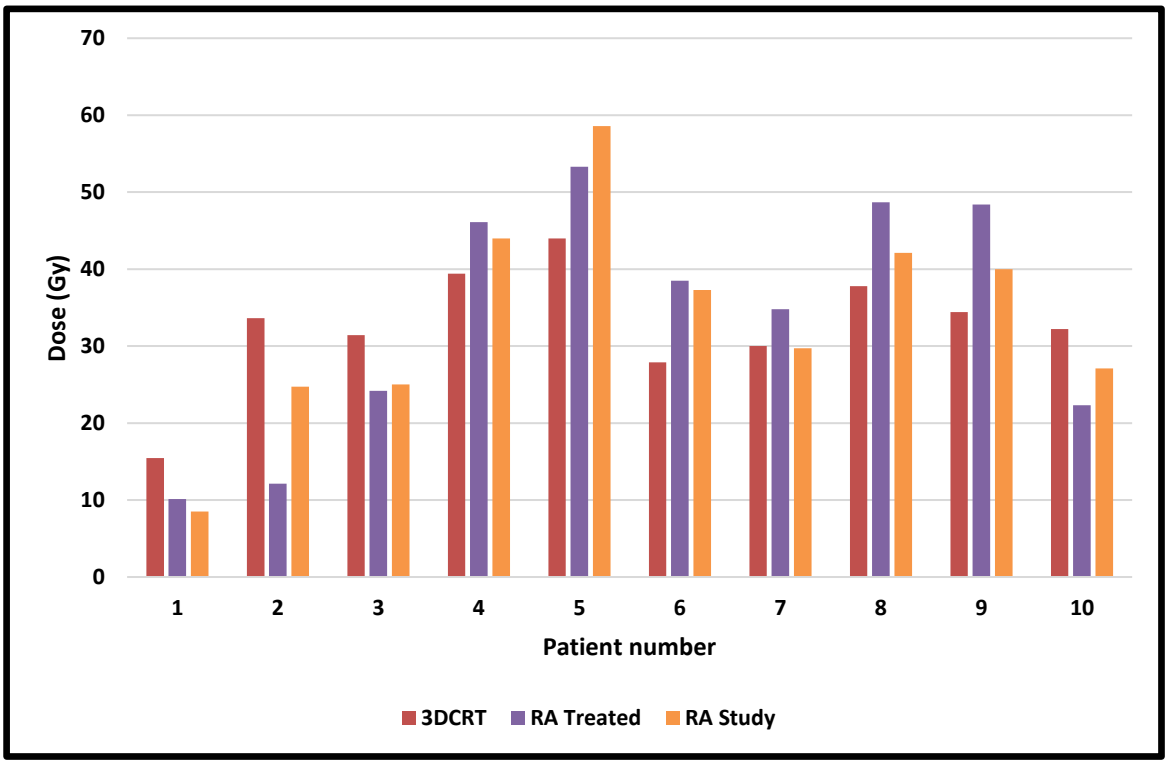

Figure 4.15: Maximum dose for the brainstem recorded per patient

It is interesting that even between the two RA plans per patient, there are different results for each plan, and in some cases, (e.g. patient 2) the difference in dose is as much as 12.6 Gy (12.14Gy vs 24.74Gy)

Figure 4.16 illustrates the maximum doses recorded to the PRV of the brainstem. The expansion of the brainstem to the brainstem PRV was 5 mm. An interesting trend that was observed, was the range of maximum doses that were recorded across the planning techniques. To demonstrate this, figure 4.17 shows the range of Dmax doses received by the brainstem alone when comparing each planning technique.

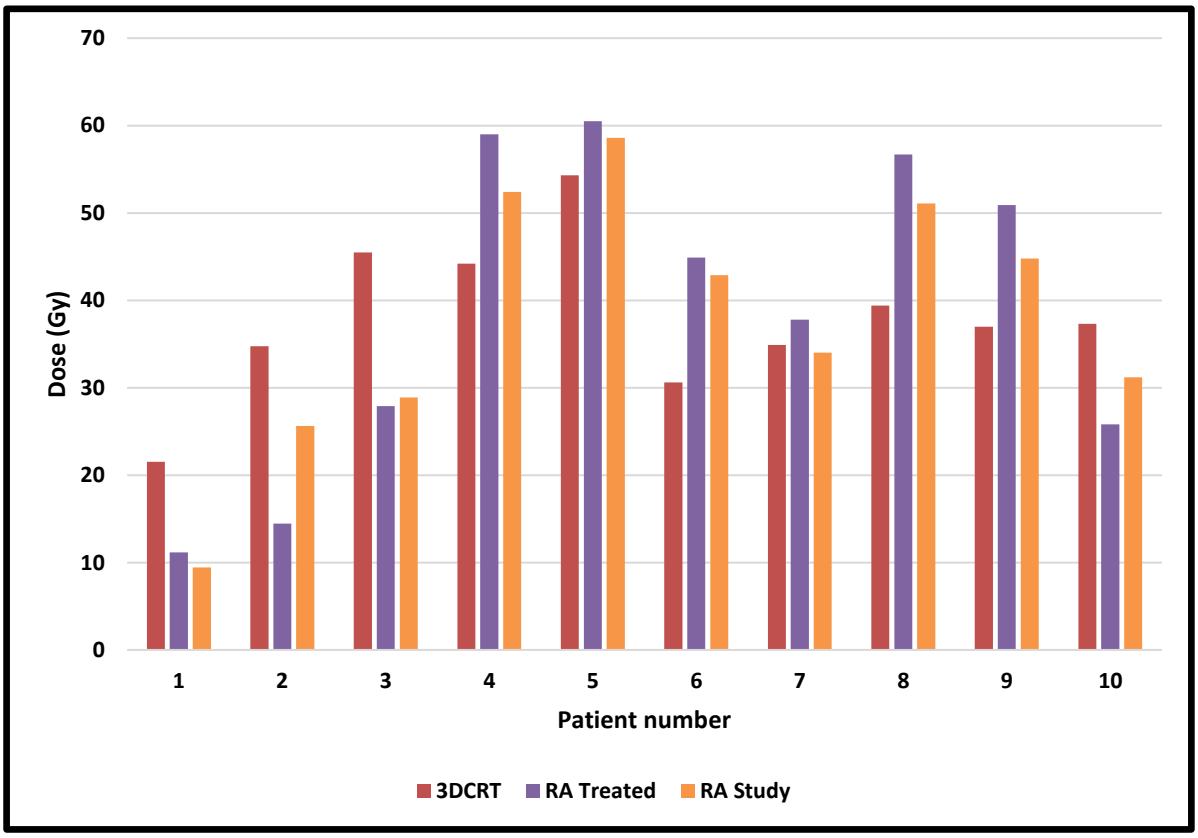

Figure 4.16: Maximum dose for the brainstem PRV per patient

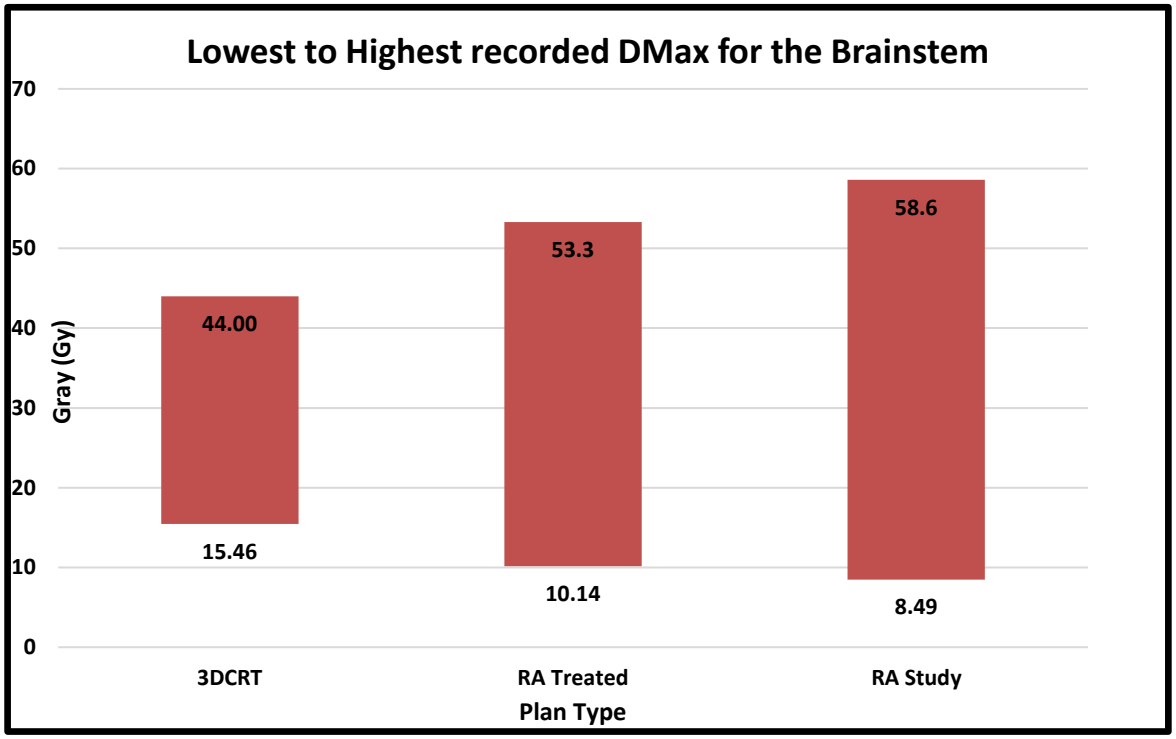

Figure 4.17: Brainstem Dmax dose range per planning technique for all patients

It was observed in figure 4.17, that this dose range is significantly smaller for the 3DCRT plans compared to the *RA Treated*, and *RA Study* groups, namely: 28.54 Gy, 43,16 Gy and 50.11 Gy respectively.

The brainstem was expanded by 5 mm to create the brainstem PRV, and was therefore a exact geometrical expansion in the 3 dimensions. An interesting observation was noted when comparing the dose increase from the brainstem to the brainstem PRV in two planning techniques (figure 4.18 and figure 4.19) The data of 8 patients was used to determine this dose trend. To make a direct comparison of dose increases, all the plans had to be planned to the same endpoint. Eight phase 1 plans were used to compile the data, as they all were planned to 50 Gy. It is observed that the dose increase ranges from 0.95 Gy to 6.7 Gy for the *RA study* plans, and from 1.1 Gy to 9.16 Gy for the 3DCRT plans. Fifty percent of the plans show a dose increase of more than 4.05 Gy for the RA plans and more than 2.8 Gy for the 3DCRT plans.

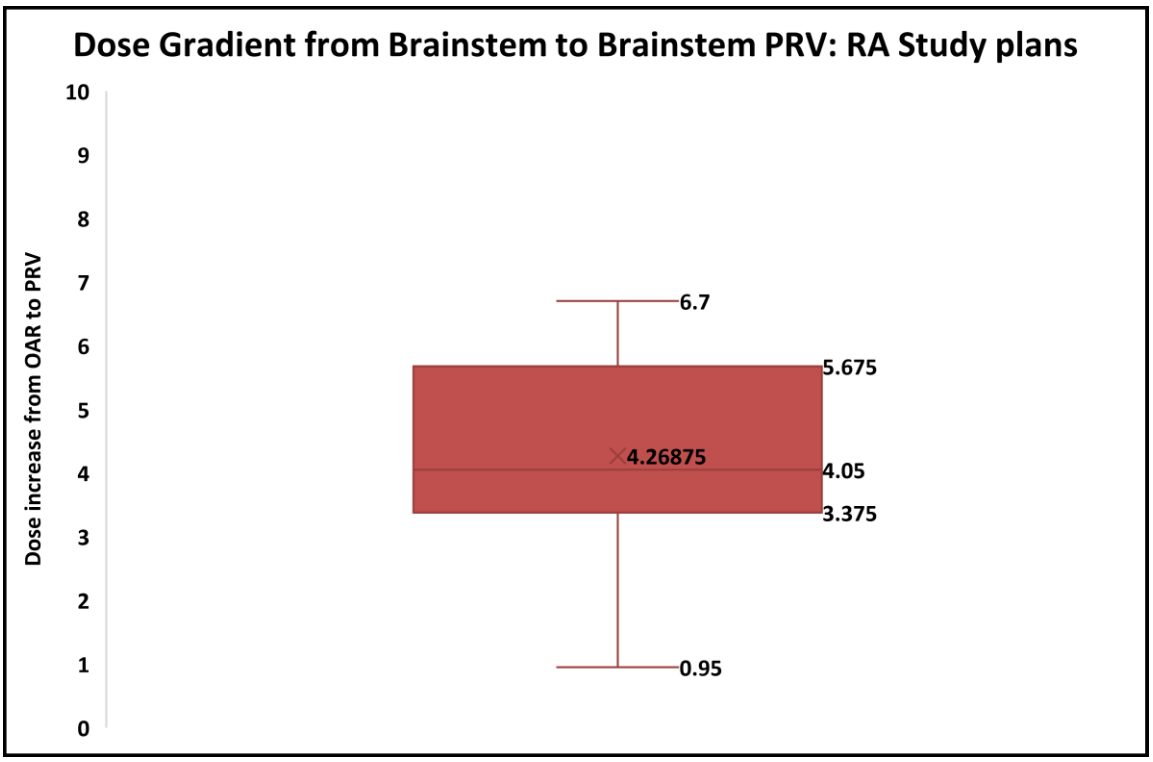

Figure 4.18: Dose increase from brainstem Dmax to brainstem PRV Dmax observed on 50 Gy plans (*RA study* only).

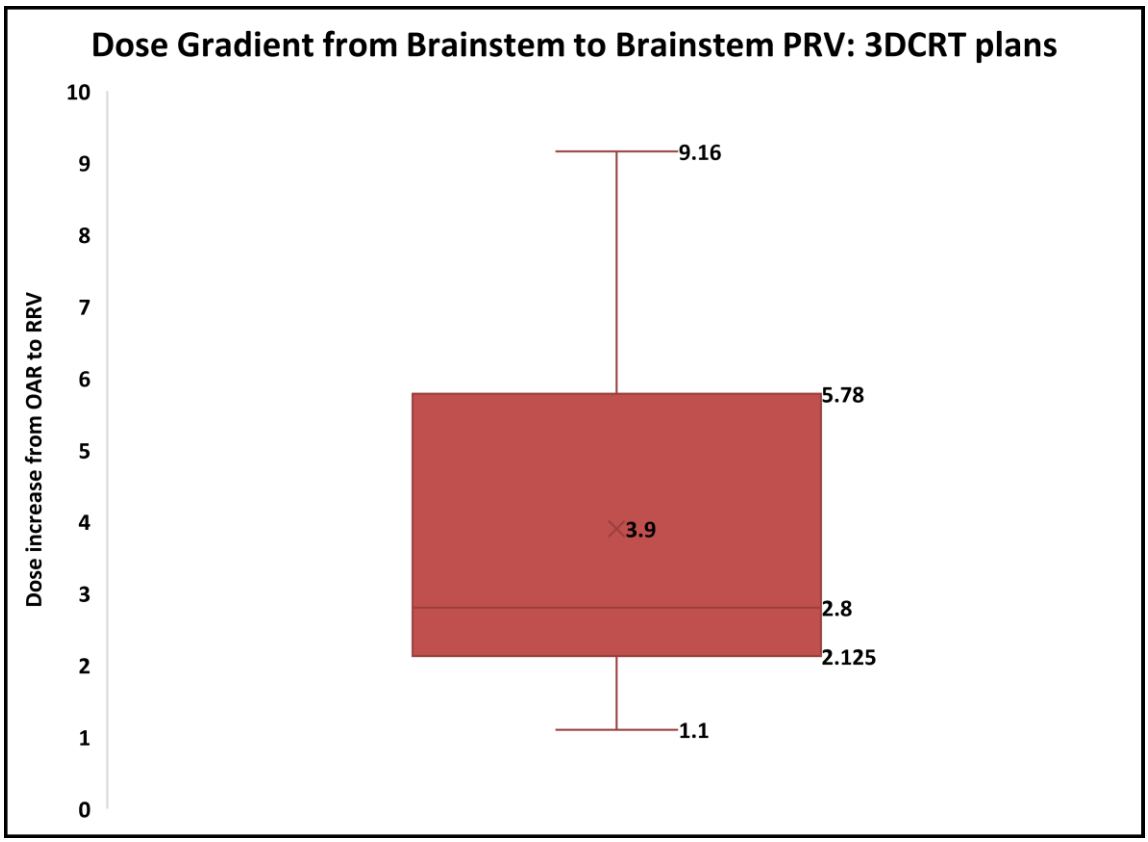

Figure 4.19: Dose increase from brainstem Dmax to brainstem PRV Dmax observed on 50 Gy plans (3DCRT plans only).

The scoring system for the brainstem is illustrated in table 4.5. The tolerance doses are according to the recommendations from Emami, Quantec and Merlotti (Mayo et al., 2010; Emami, 2013; Merlotti et al., 2014). The acceptable doses were applied to the PRV, and a lesser dose level applied to the OAR.

Table 4.5: Plan scoring allocation for the brainstem

			Lowest acceptable Dose (Gy)	Score	Higest acceptable Dose (Gy)	Score	Unacceptable Dose (Gy)	Score
Brainstem	6 points	Dmax	<50Gy	0	<53Gy	1	>53Gy	3
Brainstem PRV		Dmax	<54Gy	0	<54-59Gy	1	>59Gy	3

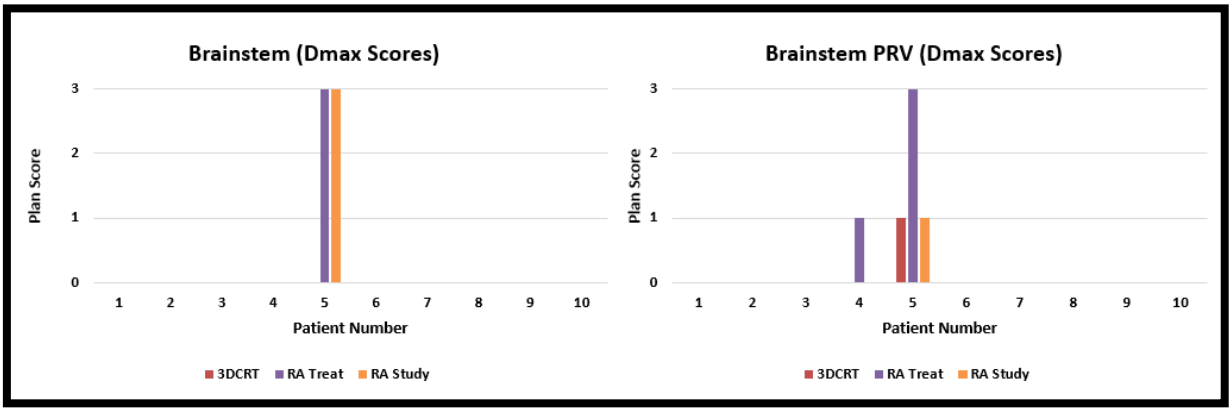

Figure 4.20: Score results of the brainstem and brainstem PRV Dmax per patient

The Independent-Sample Kruskal-Wallis Test is a rank-based nonparametric test that is used to compare outcomes and statistically significant differences between two or more groups of an independent variable (LaMorte, 2017).

The Kruskal-Wallis test applied across the three plan groups, showed no significant difference in doses for both the brainstem (p=0.596) and the brainstem PRV (p=0.715) structure.

It is therefore shown (except for patient 5), that radiation therapy for larynx cancer does not commonly involve the brainstem, and in the majority of cases the brainstem should be well within tolerance for this patient group. If the PTV is in close proximity to the brainstem, it will most likely be for phase one of the treatment and receiving the lower dose level of 46 Gy to 50 Gy. All subsequent higher dose areas will be located further away from the brainstem.

However, it is important to contour the brainstem as an OAR for this patient group, as it will receive dose, and although it will most likely be in tolerance, it is possible that these doses can be higher than expected (e.g. in patient 5).

4.3.3 Spinal cord

The maximum dose given to the spinal cord is the only dose tolerance routinely assessed, as the spinal cord is a class I organ with serial organised tissue, where excess radiation dose will cause severe morbidity (ICRU, 1993).

The aim of RT is to achieve the lowest maximum dose point to this OAR.

The calculation of the biological equivalent dose (EQD2) delivered to an organ is characterised by the use of a specific α/β value. All actual doses recorded for the spinal cord were converted into an isoeffective dose equivalent of 2Gy per fraction (EQD2), using the α/β value of 2 (Sureka & Armpilia, 2017).

Figures 4.21 (spinal cord) and 4.22 (spinal cord PRV) indicate that the lowest Dmax was achieved with the 3DCRT plans, and the highest Dmax for the *RA Treat*ment plans.

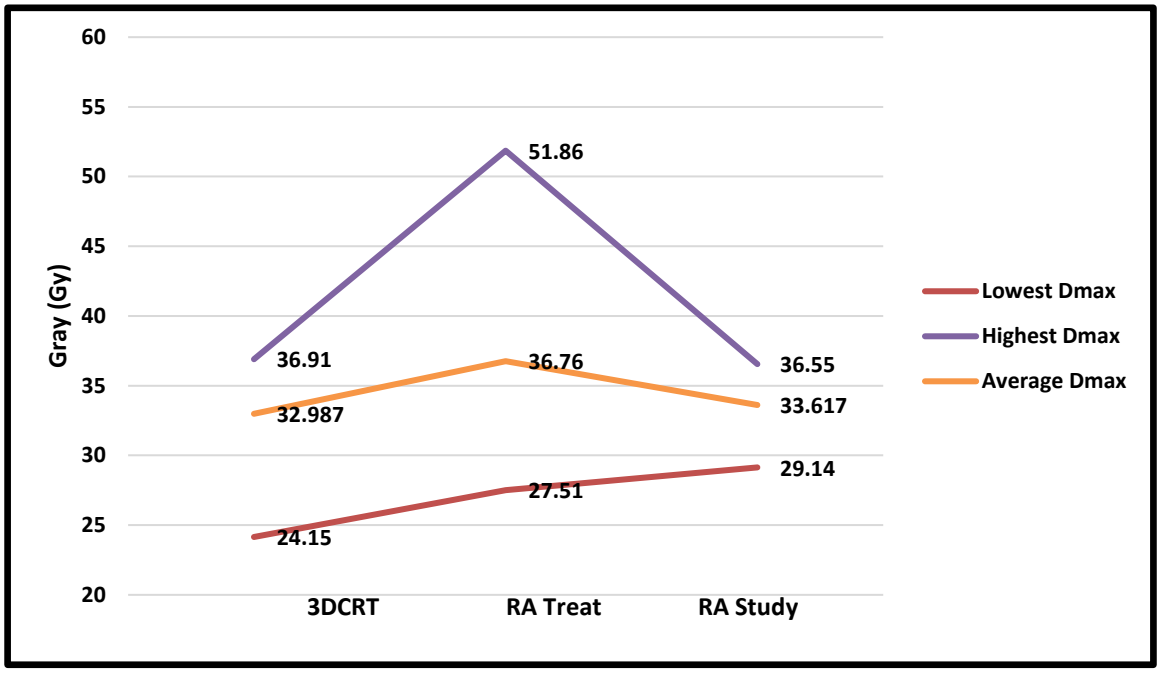

Figure 4.21: Lowest, highest and average Dmax (EQD2) recorded over all 10 plans per planning technique for the spinal cord

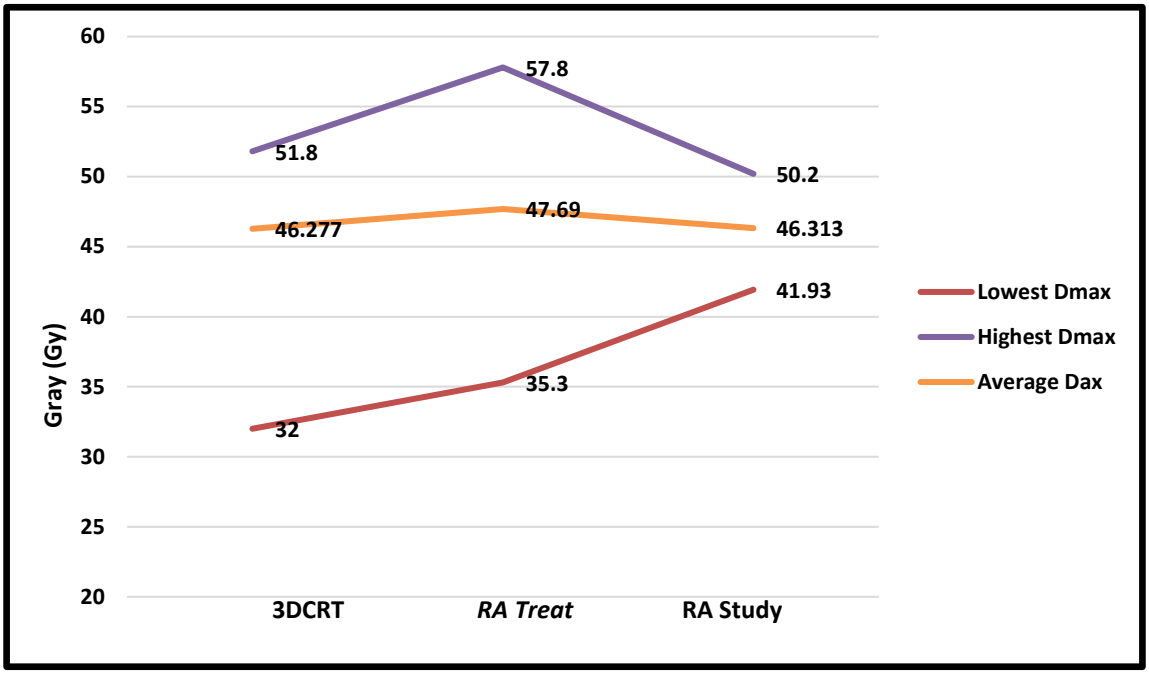

Figure 4.22: Lowest, highest and average Dmax (EQD2) recorded over all 10 plans per planning technique for the spinal cord PRV

The reason for the lower doses recorded for the 3DCRT plan is that the first priority in 3DCRT is to keep the spinal cord dose within tolerance, even if the PTV curative dose is compromised. This is clinical practice due to the limited ability to modulate the dose in 3DCRT and the close proximity of this OAR to the PTV, as well as the resultant high dose gradients needed to achieve the dose to the PTV. The reason for the higher maximum doses for the *RA treat* plans, could be that the optimizer conformed to a smaller PRV, in contrast to the *RA study* plans, where the PRV contour was present and therefore the dose was always instructed to conform around this structure.

Although it is stipulated by Merlotti et al. (2014) that the maximum dose should be set at 46 Gy, local practice tends to keep it to 45 Gy iso effective dose, and therefore in this study 45 Gy was used as the lowest dose threshold. The highest acceptable dose given by Emami (2013) of 50Gy was applied to the PRV structure (see table 4.6).

Table 4.6: Plan scoring allocation for the spinal cord

			Lowest acceptable Dose (Gy)	Score	Higest acceptable Dose (Gy)	Score	Unacceptable Dose (Gy)	Score
Spinal Cord	6 points	Dmax	<45Gy	0	<47Gy	1	>47Gy	3
Spinal Cord PRV		Dmax	<48Gy	0	<50Gy	1	>50Gy	3

A notable score increase is observed as demonstrated in figure 4.23, from the OAR to the OAR PRV. As this OAR is situated in very close proximity to the PTV it is an important critical organ to monitor the dose received.

It can be seen that 3 of the 10 patients in the *RA Treat* group scored 3 points, compared to 1 from the *RA Study* group. This could be due to the larger PRV added for the *RA Study* group as compared to the PRV originally used for the *RA treat* group for optimization.

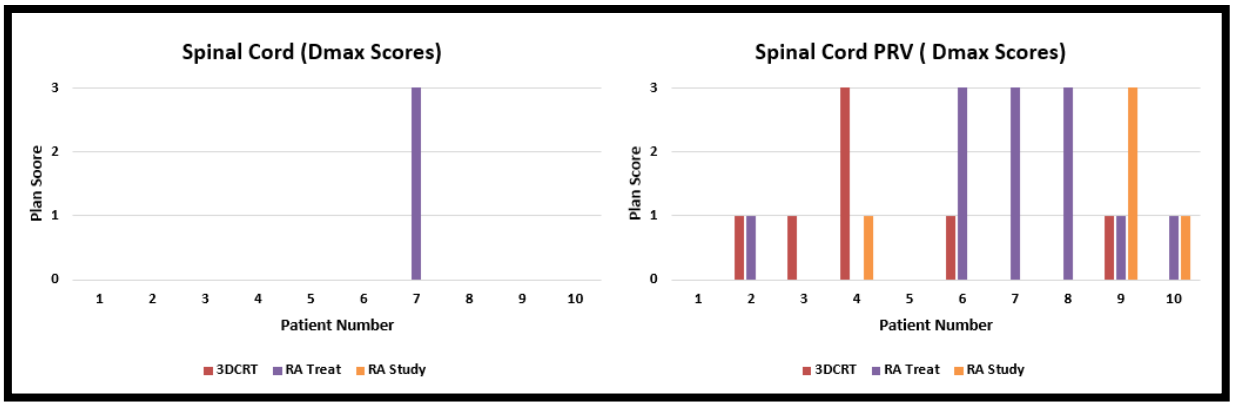

Figure 4.23: Score results of the spinal cord and spinal cord Dmax per patient

The independent-sample Kruskal-Wallis statistical test indicated no statistically significant differences across the scoring for the sample groups (0.368 & 0.351), and therefore multiple comparisons were not performed.

4.3.4 Parotids

It is shown in figures 4.24 and 4.25, that the 3DCRT plans were consistently giving more dose to both the parotids combined, as well as to the parotids combined PRV.

As large parts of the parotids were included in the PTV volume, it was challenging to keep within the lowest dose tolerance threshold of 20Gy for combined parotids.

It is, however, best practice to always keep the dose to the parotids as low as possibly achievable, and therefore it is seen that the VMAT (except for patient 9, RA treat) plans, where the dose can be constrained via modulation, consistently delivered less dose to the parotids.

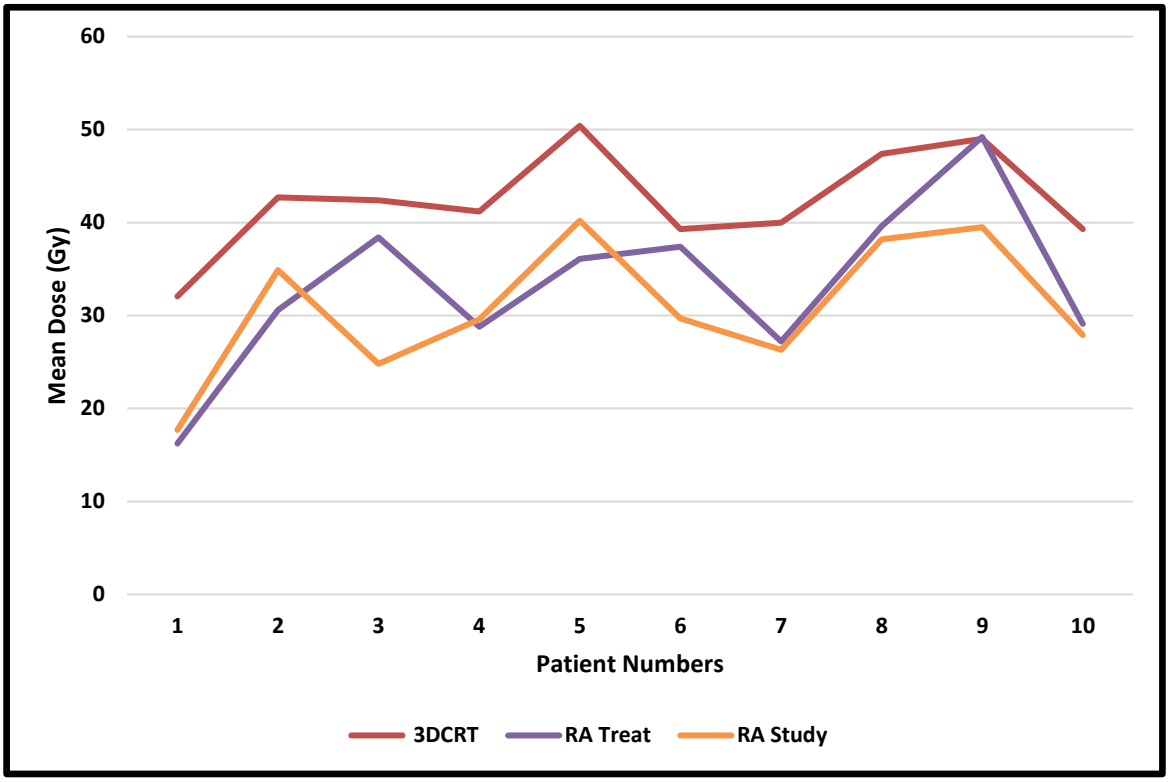

Figure 4.24: Mean dose to parotids Combined

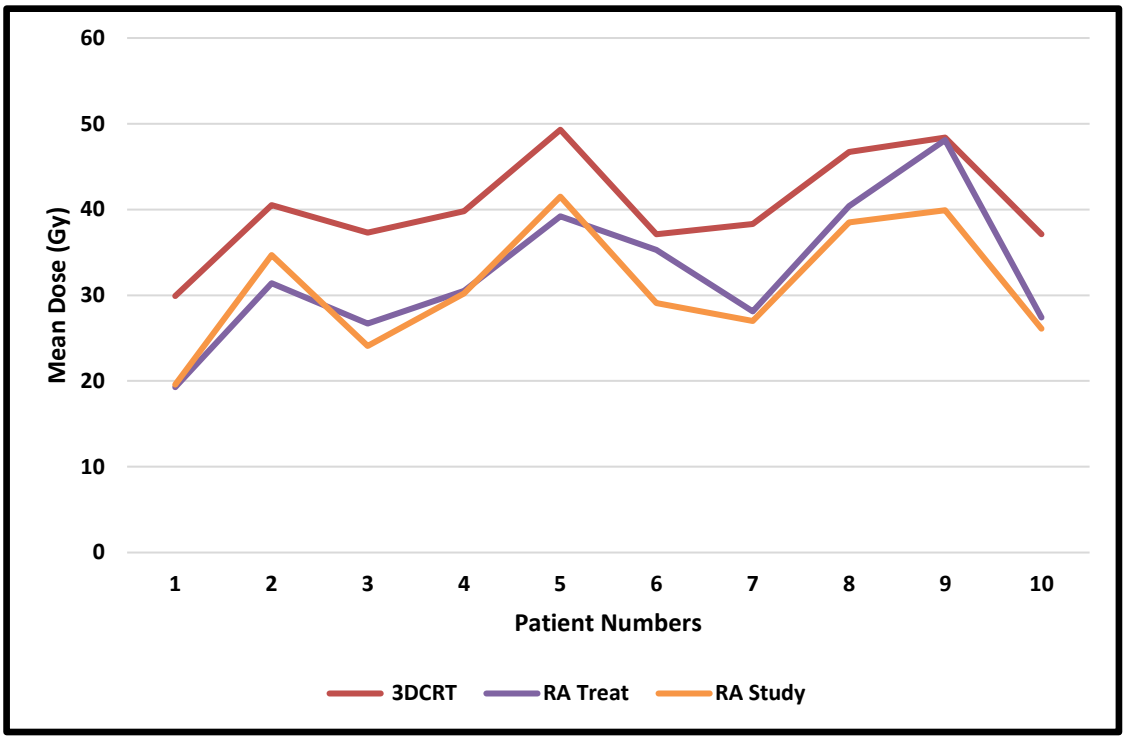

Figure 4.25: Mean dose to parotids combined PRV

The average mean doses achieved for the combined parotid volumes, over the whole population, was 42.38 Gy for 3DCRT, *RA Treat* was 33.26 Gy, and *RA Study* was 33.88 Gy. RA therefore offers superior organ sparing for the parotids.

The scoring system used for the parotids is presented in table 4.7. Quantec summary dose specifications suggest that with a mean dose of 20 Gy to a unilateral parotid, and 25 Gy to bilateral parotids, the salivary function is reduced by 25 % compared to pre-RT limits. These dose limits were therefore applied to the PRVs, and a lesser dose threshold to the OAR (Bentzen et al., 2010).

With a organ tolerance of 39Gy mean dose to the bilateral whole glands, the indicated complication is increased to a 50% rate of zerostomia. This dose level were applied to the parotids combined, and parotids combined PRV as Acceptable and worst results. (Deasy et al., 2010) (see table 4.7)

Table 4.7: Plan scoring allocation for the parotids

Parotid Right	6 points	Mean Dose	<18Gy	0	<18-23Gy	0.5	>23Gy	1
Parotid Left		Mean Dose	<18Gy	0	<18-23Gy	0.5	>23Gy	1
Parotid Right PRV		Mean Dose	<20Gy	0	<20-25Gy	0.5	>25Gy	1
Parotid Left PRV		Mean Dose	<20Gy	0	<20-25Gy	0.5	>25Gy	1
Parotids Combined		Mean Dose	<23Gy	0	<23-37Gy	0.5	>37Gy	1
Parotids Combined PRV		Mean Dose	<25Gy	0	<25-39Gy	0.5	>39Gy	1

Figure 4.26 demonstrates the parotid scoring results according to the planning groups. The lower score indicates the least side effect probability for the patient. It is observed that the minimum points allocated to the 3DCRT plan group were 5 points, out of a possible 6 points (that indicates the worst score and the most predicted side effects to the patient)

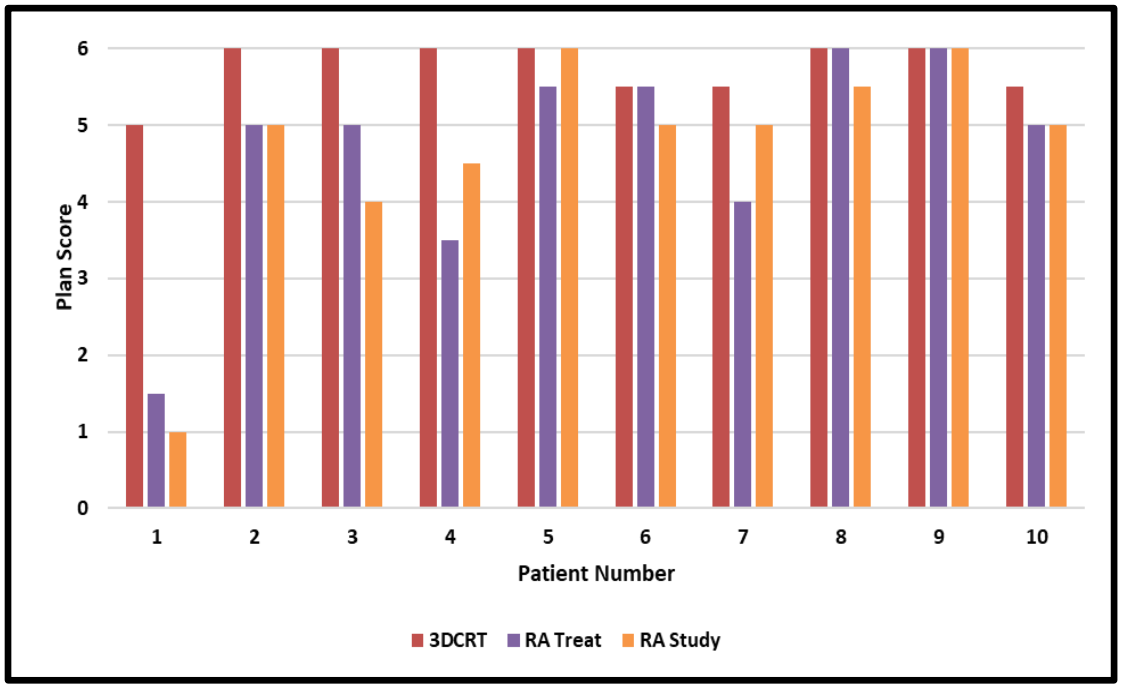

Figure 4.26: Parotids plan scores

Although the Independent-Sample Kruskal-Wallis Test indicated no statistically significant differences across the sample groups (p=0.076), it can be noted that the lowest scores achieved for the RA plans were 1 and 1.5, and in some instances RA plans can significantly decrease the dose to the parotids. No RA plan scored more than the 3DCRT plan. VMAT therefore offers the same or better OAR scores.

4.3.5 Cochlea

As the cochlea is a very small structure, only the cochlea PRV was used for dose comparisons. Ninety percent (90 %) of patients received less than 20.1 Gy mean dose to the cochleas. This means that the cochleas will reeive a lower than tolerance dose. It is, however, seen that one patient in the 3DCRT group received higher doses.

Figure 4.27 demonstrates that a larger percentage of patients in the 3DCRT group received higher doses than the two RA groups.

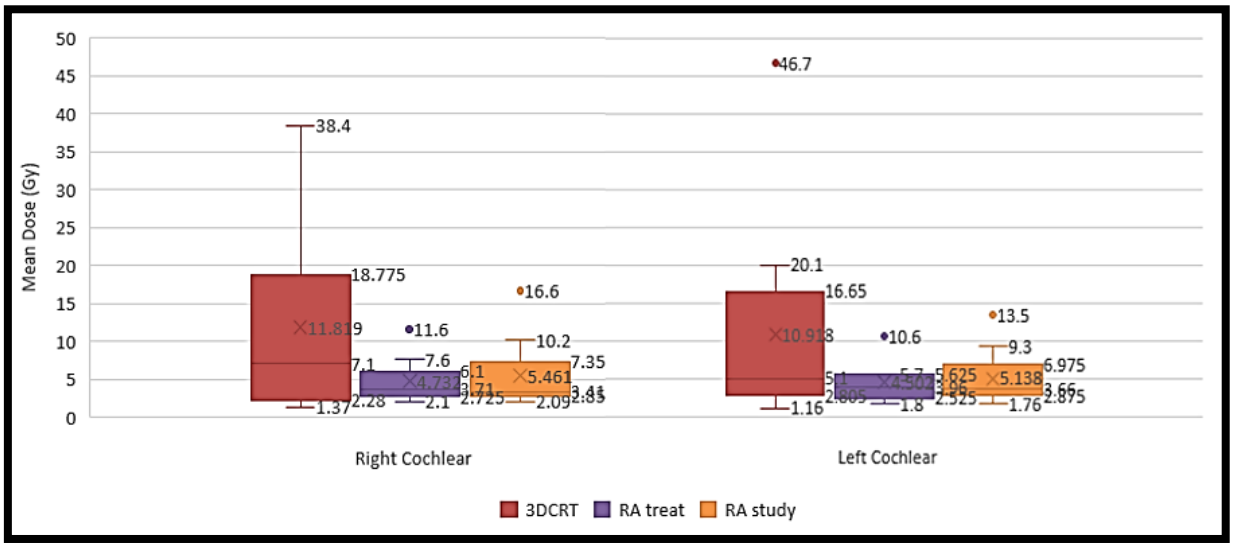

Figure 4.27: Mean dose to the right and left cochlea per planning technique for total population

Guidelines given in the Quantec tolerance tables indicate that with a mean dose of less than 45 Gy, there could be a 30 % chance of sensory neural hearing loss. More recent data indicated that to maintain the toxicity level below 20 %, doses as low as 32 Gy should be maintained, and where radiation therapy is used aong with chemotherapy, doses as low as 22 Gy could limit the side effects of grade 2 tinnitus (Lee et al., 2015).

As indicated in table 4.8, doses of more than 45 Gy were deemed as unacceptable and the highest plan score assigned to it. Doses of less than 32 Gy were set as the lowest acceptable doses, and with a score of 0, it was an indication of the least probability of side effects.

The plan scoring table for the cochleas is demonstrated in table 4.8, and the scoring results in figure 4.28. It is clear that only plan 8 (3DCRT) had a score, and all other plans therefore achieved doses well below dose tolerance. The Independent-Sample Kruskal-Wallis Test revealed no statistical significance for plan scores across all the plan groups for both the right cohlear PRV (0.368) and the left cochlear PRV (0.368) and therefore no multiple comparisons were performed.

Table 4.8: Plan scoring allocation for the cochlea PRV

			Lowest acceptable Dose (Gy)	Score	Higest acceptable Dose (Gy)	Score	Unacceptable Dose (Gy)	Score
Cochlear Right PRV	4 points	Mean Dose	<32Gy	0	<32-45Gy	1	>45Gy	2
Cochlear Left PRV		Mean Dose	<32Gy	0	<32-45Gy	1	>45Gy	2

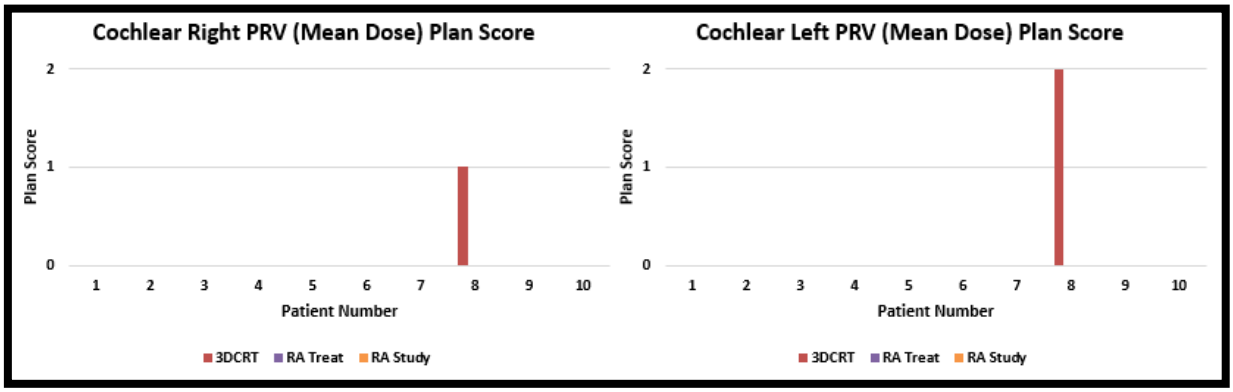

Figure 4.28: Cochlea PRV plan score results

Although no statistical significance was found, it is evident that the 3DCRT group showed increased dose to the cochleas, and this may lead to a significant increase in later hearing difficulties. This is especialy clinically significant when platinum based chemotherapy is administered to these patients, which further contributes to hearing loss.

4.3.6 Lungs

Lung doses are based on the whole lung, which is contoured on using the planning CT data set. Unfortunately none of the patients had the whole lung imaged. Although V20 (Volume of lung receiving 20 Gy) and mean lung doses were recorded for all patients, these doses can not be used for statistical analysis as they do not represent the accurate dose planned for this OAR.

Figure 4.29 indicates that although we can not compare doses on the plans between the patient population, we can clearly see, except for patient 5, that the 3DCRT plans will result in slightly more dose to the lungs, as compared to the two RA plans. The results seen in this figure are however very close in value between the three planning groups. Due to the location of the PTV, we would not expect the lungs to receive doses out of tolerance. The lung doses therefore, were excluded from the plan evaluation criteria, and rightfully so as the whole lungs were not included in the planning CT. In addition, the level 4 lymph nodes and the anatomical position of the larynx are situated superiorly to the lungs, and will therefore probably deliver minimal dose to the lungs, which in turn will allow for repair after the completion of RT.

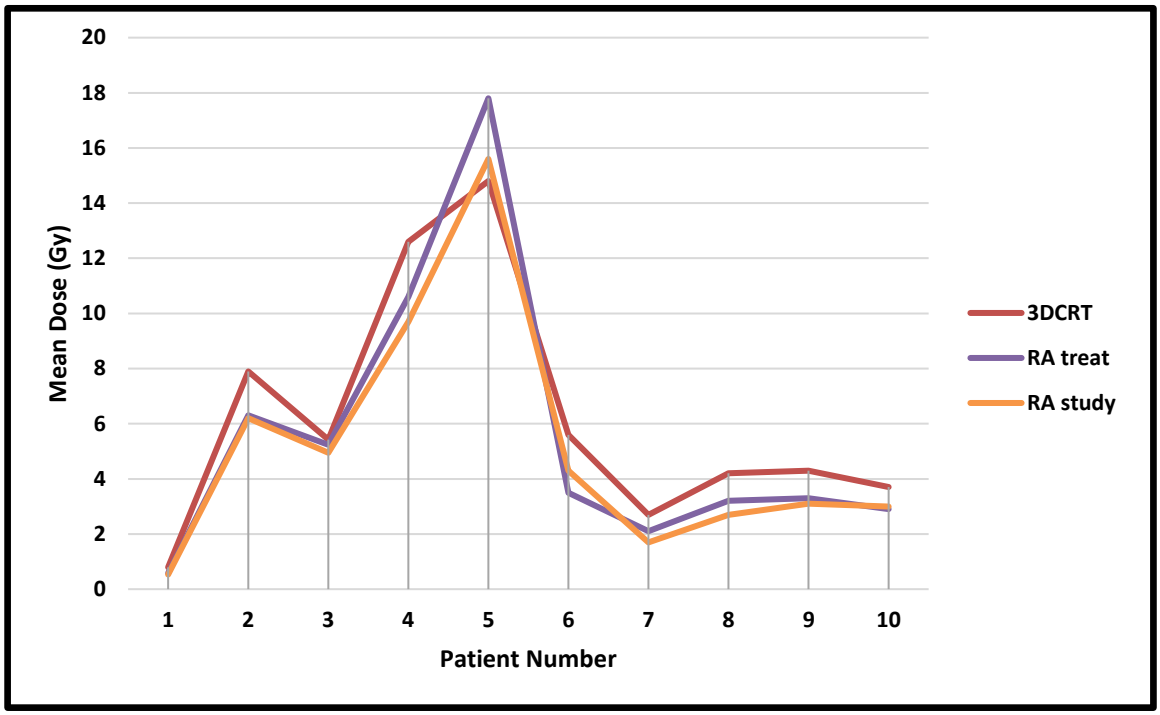

Figure 4.29: Mean lung dose per plan type (note: the whole lungs were not included in the CT data set, but these doses can be used to compare mean lung dose per patient comparing plan types)

4.3.7 Temporomandibular Joints

The Temporomandibular Joints (TMJ) are “generally” situated superiorly to the PTV of the patient with cancer of the larynx, and it is often assumed that these joints will not receive any dose. In certain situations the volume could extend closer to the TMJ, and this is dependent on the immobilised position of the patient and the extent of the disease. The maximum doses to the TMJ PRV is presented in figure 4.30. It is observed that the 3DCRT plan consistently leads to higher doses to both the TMJs, with the exception of patient 9. A possible reason for

this is the use of a non-coplanar lateral beams arangement, which increases the dose to the normal tissue situated superiorly to the PTV.

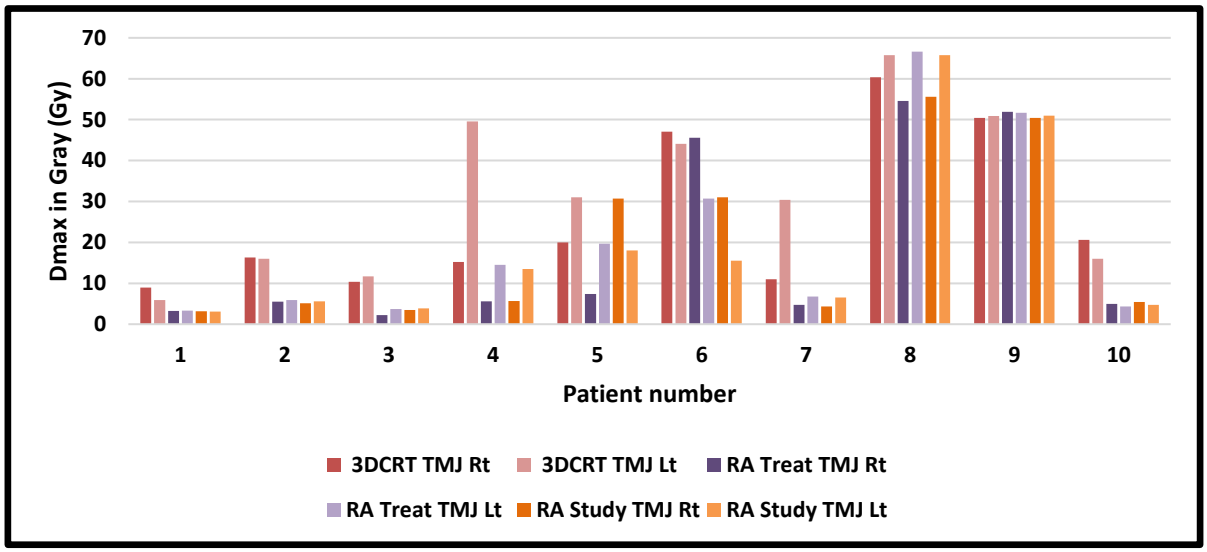

Figure 4.30: Maximum doses to the right and left temporomandibular joints PRV

The dose tolerance for the TMJ and mandible are both defined as a maximum dose point of 70 Gy (Merlotti et al., 2014). This dose threshold was assigned to the PRV as the worse result and the maximum score allocated. Slightly lower doses were assigned to the TMJ.

A maximum amount of points any plan could receive was 4 for the TMJ scoring system. Table 4.9 shows the plan scoring system used. All the plans in this study received doses below this dose threshold.

Table 4.9: Plan scoring allocation for the TMJ

	Points Allowcation		Best Results	Score	Acceptable Results	Score	Worst Results	Score
TMJ Right	4 points	Dmax	<60Gy	0	<60-65Gy	0.5	>65Gy	1
TMJ Left		Dmax	<60Gy	0	<60-65Gy	0.5	>65Gy	1
TMJ Right PRV		Dmax	<65Gy	0	<65-70Gy	0.5	>70Gy	1
TMJ Left PRV		Dmax	<65Gy	0	<65-70Gy	0.5	>70Gy	1

The results of the TMJ scoring are shown in figure 4.31, and indicate that the maximum scores achieved was 0.5 point for one 3DCRT plan. Therefore it can be concluded that the TMJ should receive very little dose for this patient population.

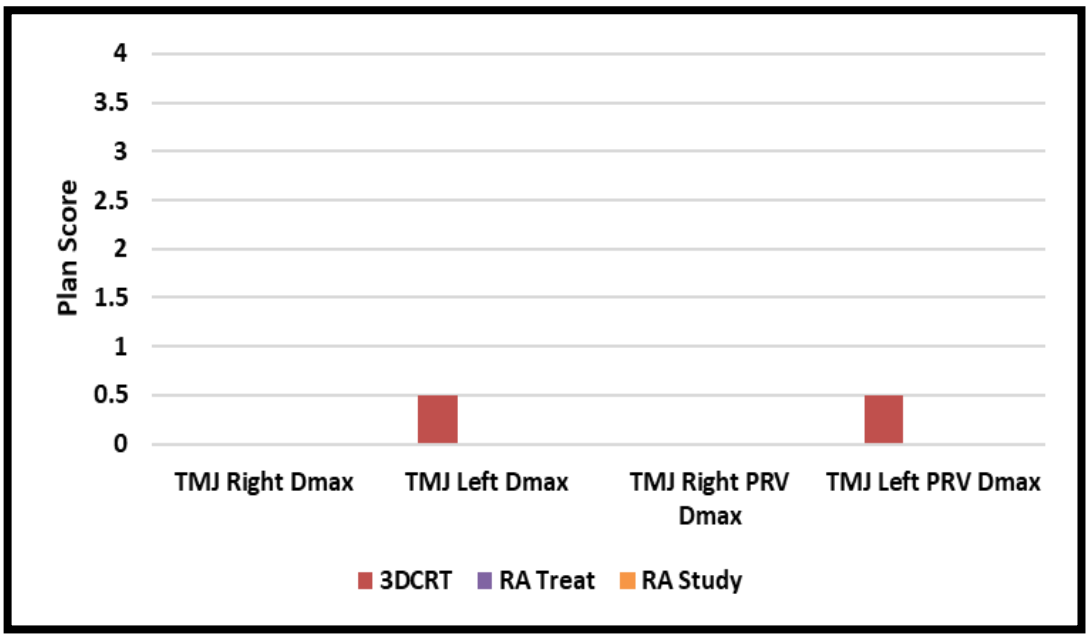

Figure 4.31: Scoring Results for the TMJ

The Independent-Sample Kruskal-Wallis Test resulted in no significance across the plan scores for the 3 plan groups. The results for the TMJ Right ($p = 1.0$), TMJ Left ($p = 0.188$), TMJ Right PRV ($p = 1.0$) TMJ Left PRV ($p = 0.188$), indicated that no further multiple comparisons were needed.

4.3.8 Oral cavity

The maximum dose to the oral cavity, across all the patients, was consistently higher for the 3DCRT plans, as shown in Figure 4.32.

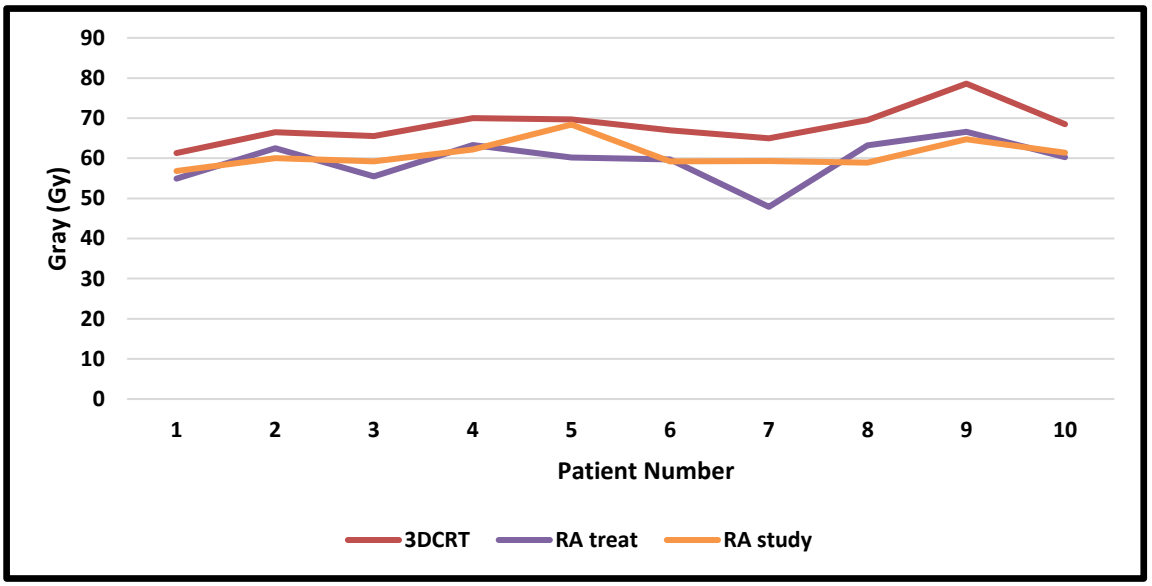

Figure 4.32: Dmax to the Oral Cavity per patient

The average of the maximum doses over the whole population per planning technique, is demonstrated in figure 4.33 and it is clearly seen that 3DCRT consistently achieves a higher Dmax dose to the oral cavity as compared to the two other RA plans.

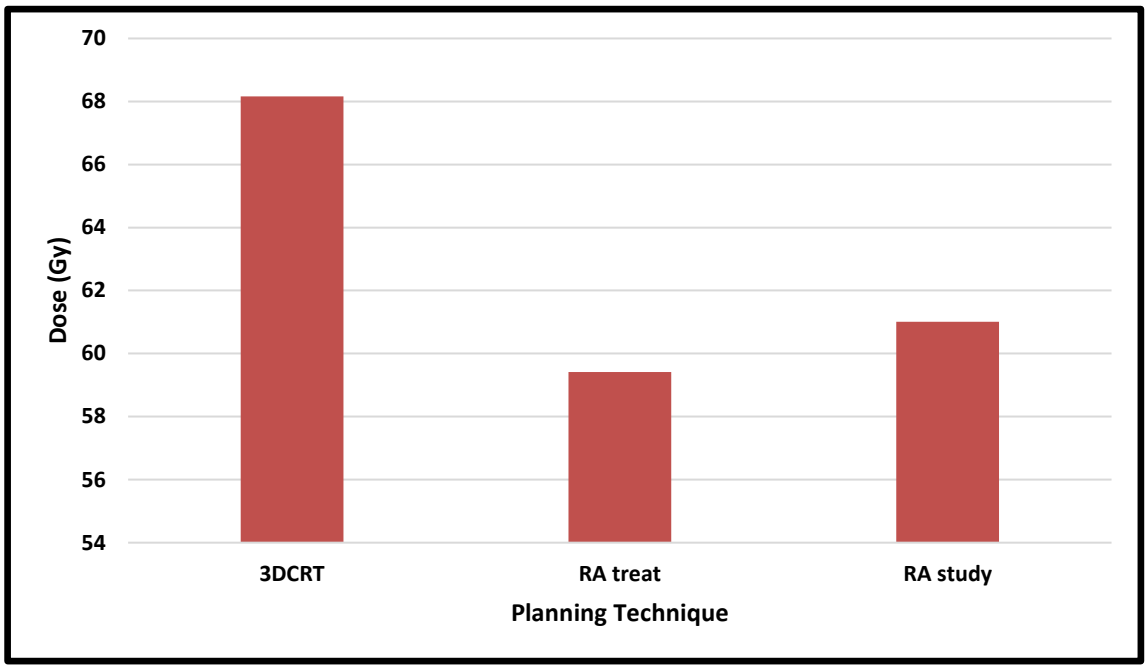

Figure 4.33: Average Dmax over total population per planning technique

The mean dose to the oral cavity does not indicate the same trend, and is demonstrated in figure 4.34, where the *RA treat* plan had higher mean doses than the 3DCRT plans. The *RA study* group had the least mean doses across the population, where the mean doses recorded are between 19.4 Gy and 41.1 Gy. It must be noted that the oral cavity was a OAR that was not contoured for the *RA treat* plans and was therefore not constrained; however as for the *RA study* group this OAR was contoured and could be constrained.

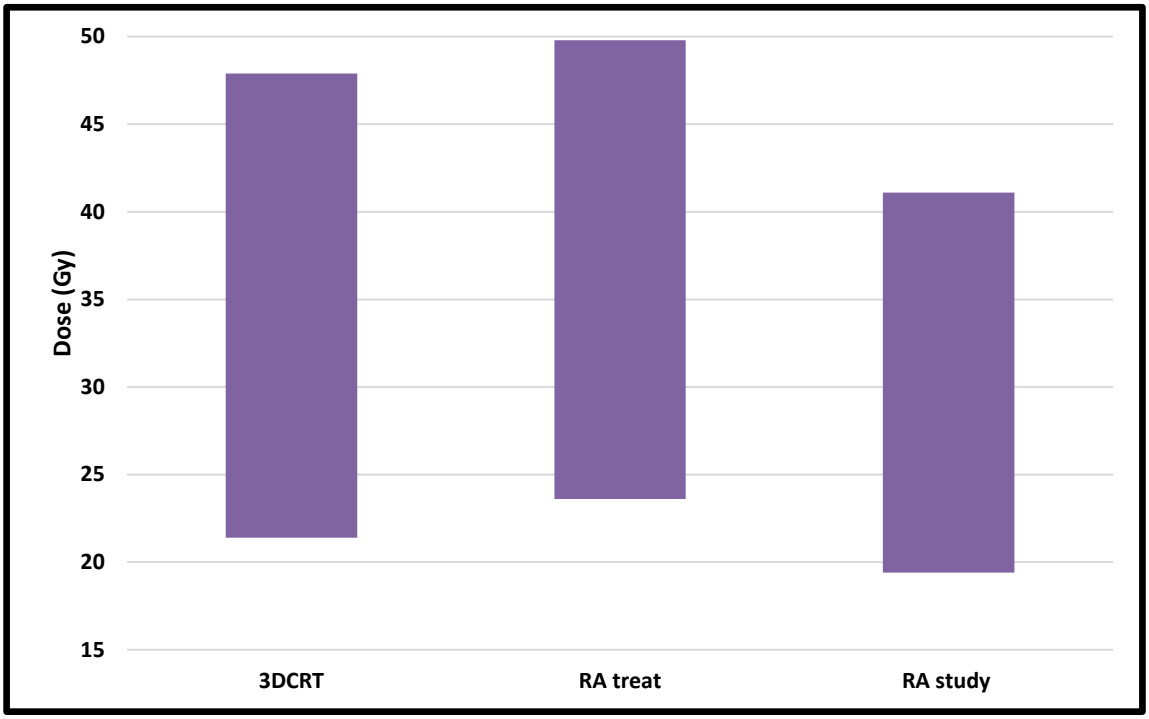

Figure 4.34: Recorded minimum and maximum mean doses to the oral cavity per planning technique

The dose tolerance of the oral cavity that excludes the PTV has been defined as a mean dose less than 40 Gy according to the RTOG 0615 study (Lee et al., 2015). According to Khan and colleagues (2016) the dose is defined as a mean dose of 50 Gy with a planning priority of 3, thus allocating a very low priority (Khan et al., 2016).

As the PTV for this study was posterior to the oral cavity, it was decided to use the lower dose threshold as part of the plan evaluation criteria as seen in table 4.10.

Table 4.10: Plan scoring allocation for the Oral Cavity

			Lowest acceptable Dose (Gy)	Score	Higest acceptable Dose (Gy)	Score	Unacceptable Dose (Gy)	Score
Oral Cavity	2 points	Mean Dose	<40Gy	0	<40-45Gy	1	>45Gy	2

The plan scoring results for the ten patients is shown in figure 4.35, and the Independent-Sample Kruskal-Wallis Test resulted a p-value of 0.690, indicating no statistical significance between the population samples, and no further multiple comparisons were performed.

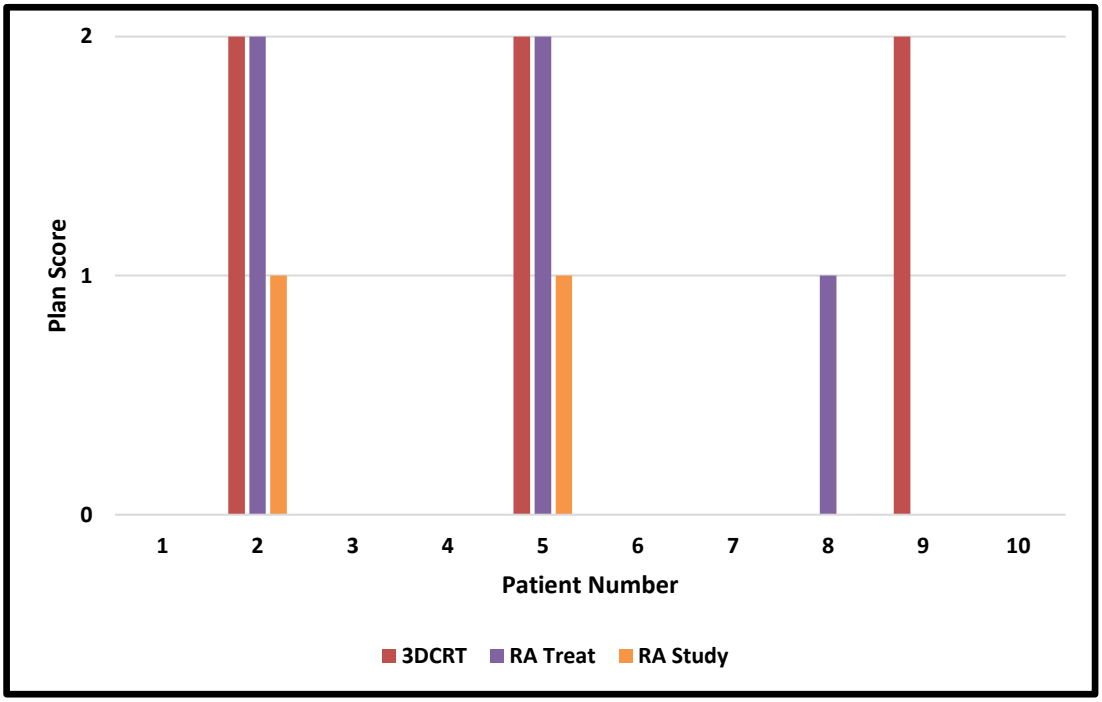

Figure 4.35: Scoring results for the oral cavity

A clinical deduction that can be made, is that the *RA Study* group scored the least points across the population, and this is an indication that contouring this structure does result in less dose to the oral cavity. It would therefore be beneficial to contour it as a standard convention for all RA plans for this patient population.

4.3.9 Mandible

The PTV often extends into the mandible. As a OAR the tolerance dose can not be limited if the dose limit is exceeded by the prescribed dose. In figure 4.36 there is no clear dose difference towards either planning technique, but the trend is towards 3DCRT consistently giving slightly more dose than the RA plans (except patient 7).

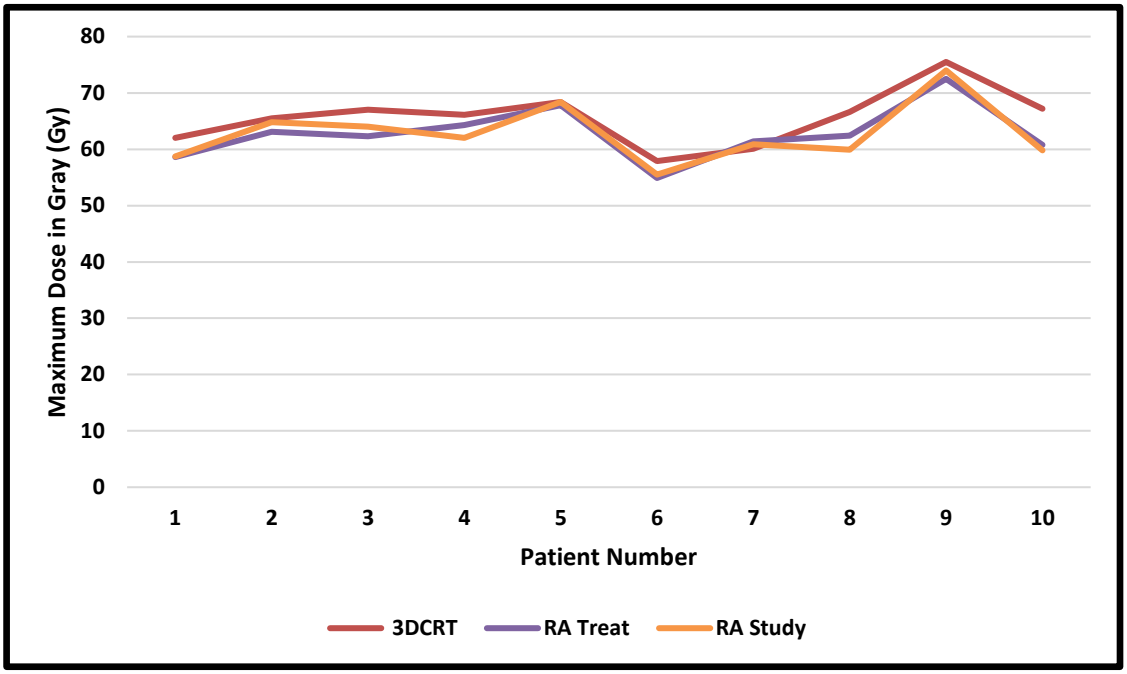

Figure 4.36: Maximum doses to the mandible

The creation ot the mandible PRV and subtracting the overlapping PTV from it, creates for the planner a structure to which the dose can be constrained. Figure 4.37 indicates the maximum doses recorded for this structure. It is observed that the RA plans were consistently able to limit the maximum dose to this structure to less than 70 Gy.

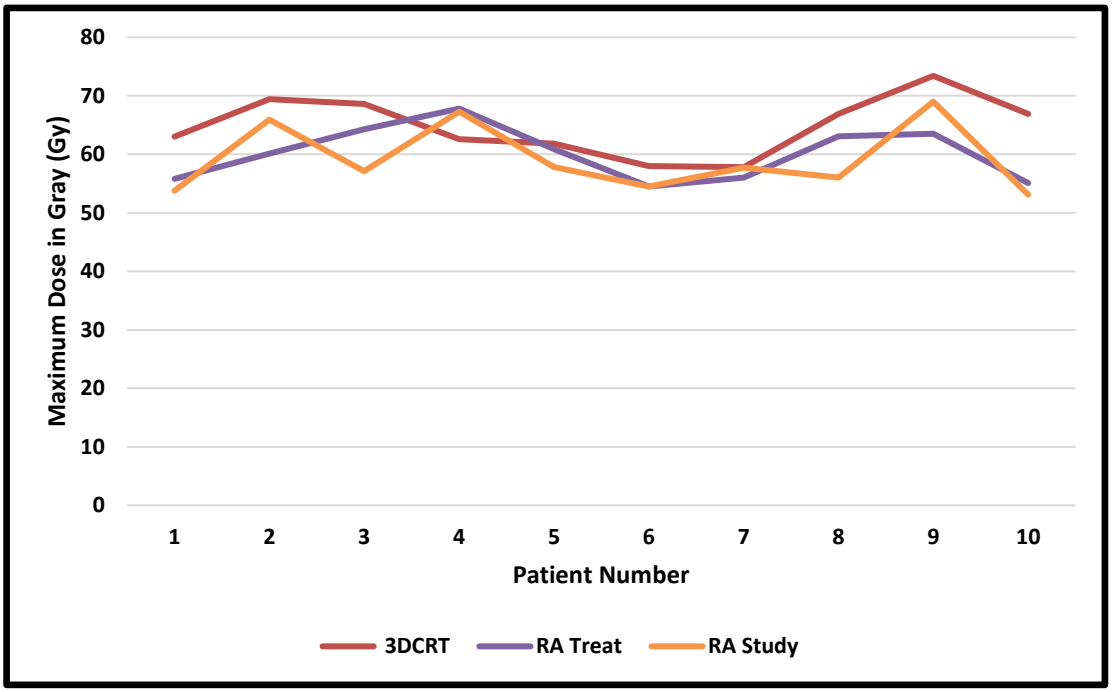

Figure 4.37: Maximum doses to the Mandible PRV cropped from the PTV with a 5mm gap

The maximum dose to the mandible, according to the Emami table, should not exceed a point dose of 70 Gy (Emami, 2013). The view proposed by Khan (2016) increases the dose threshold to 75 Gy. The plan scoring system, as seen in Table 4.11, will use a maximum point of more than 70 Gy to the mandible as unacceptable, and a maximum point exceeding 73Gy to the mandible PRV minus PTV of 73 Gy as unacceptabe. As no treatment prescription exceeded 70 Gy, the lowest acceptable dose was set to less (see table 4.11).

Table 4.11 Plan scoring allocation for the Mandible

			Lowest acceptable Dose (Gy)	Score	Higest acceptable Dose (Gy)	Score	Unacceptable Dose (Gy)	Score
Mandible	2 points	Dmax	<68	0	<70Gy	0.5	>70Gy	1
Mandible PRV-PTV		Dmax	<70	0	<73Gy	0.5	>73Gy	1

As the scores achieved were very low, all scores were summated and presented in figure 4.38.

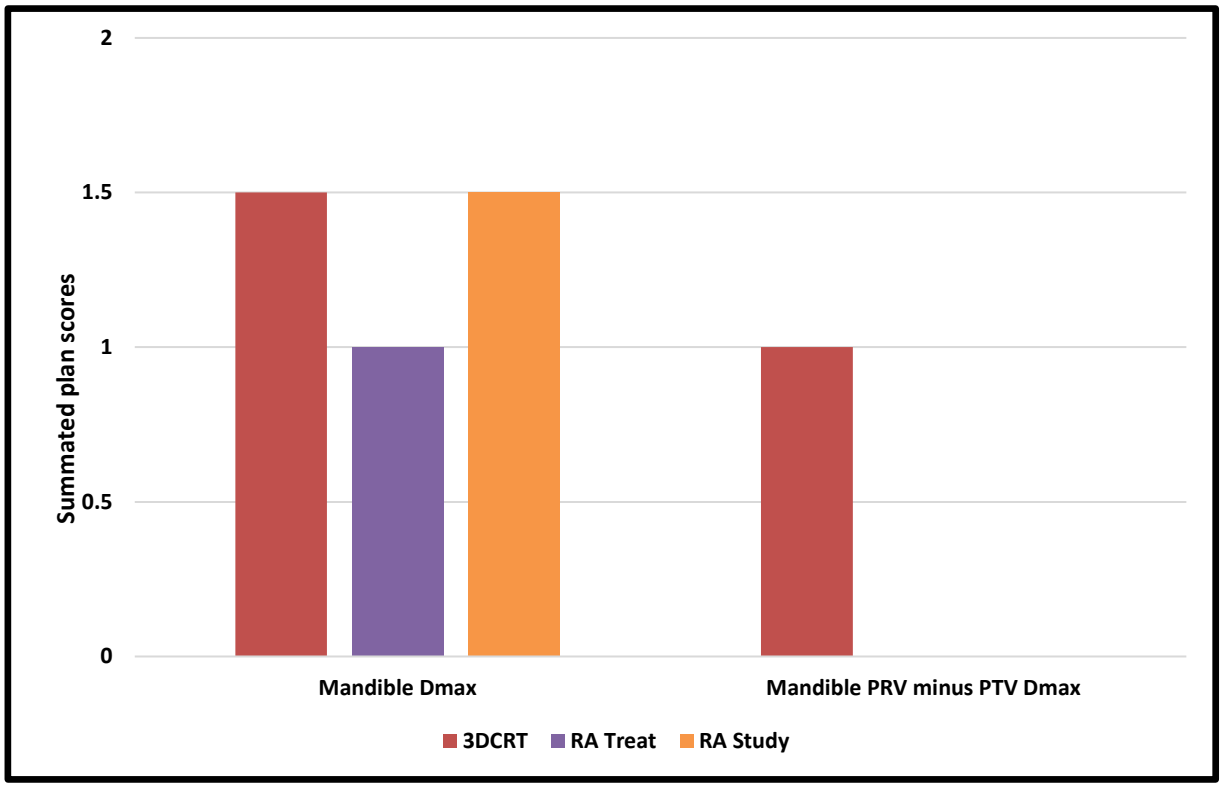

Figure 4.38: Scoring results for the mandible

The 3DCRT plans had slightly higher scores, but the Kruskal-Wallis test indicated no significant differences across the population for both the mandible Dmax scores ($p = 0.830$), and the mandible PRV minus PTV Dmax scores ($p = 0.368$). Due to the non-significance of the scores no further multiple comparisons were performed.

4.3.10 Shoulders

The shoulder contour does not represent an OAR, nor was any dose constrained to it. The purpose of this study was to record the dose that will pass through the shoulders per treatment technique. The contour represents all normal tissue 2 cm lateral to the largest lateral extent of the PTV on both the left and right side of the patient.

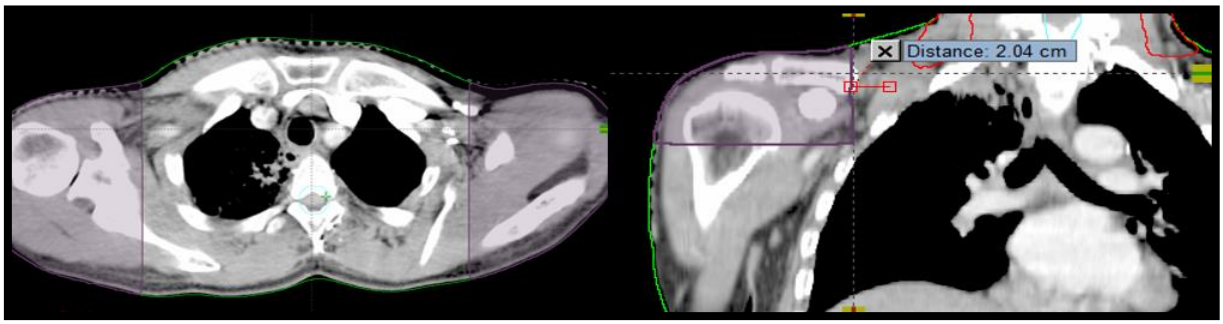

Figure 4.39: Shoulders contour

The dose results were recorded for 9 of the 10 patients included in this study. The results indicated that the mean dose to this structure was well below 9 Gy for all planning techniques, as seen in figure 4.40.

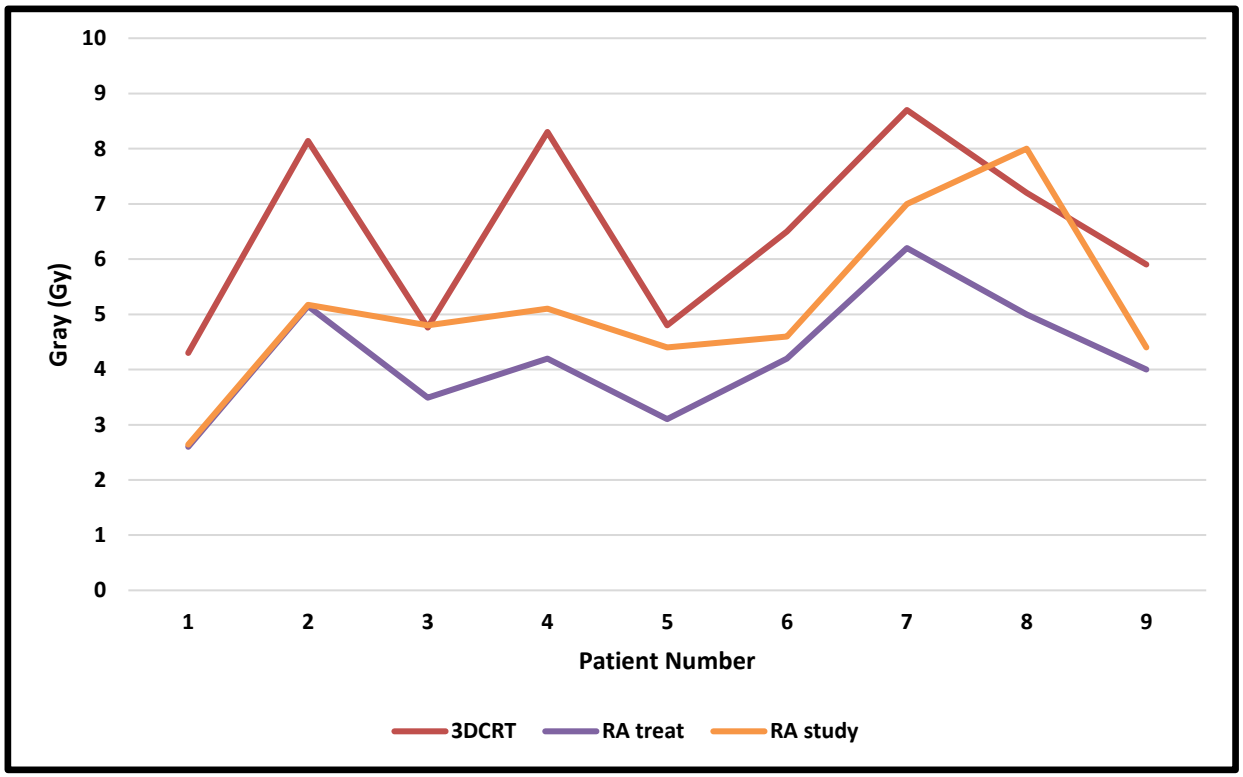

Figure 4.40: Mean doses to the shoulders

The maximum dose recorded is clearly higher for the 3DCRT plans as seen in figure 4.41. The minimum Dmax for the 3DCRT plans exceed the maximum dose recorded for 7 of the 9 patient plans included in the RA plans.

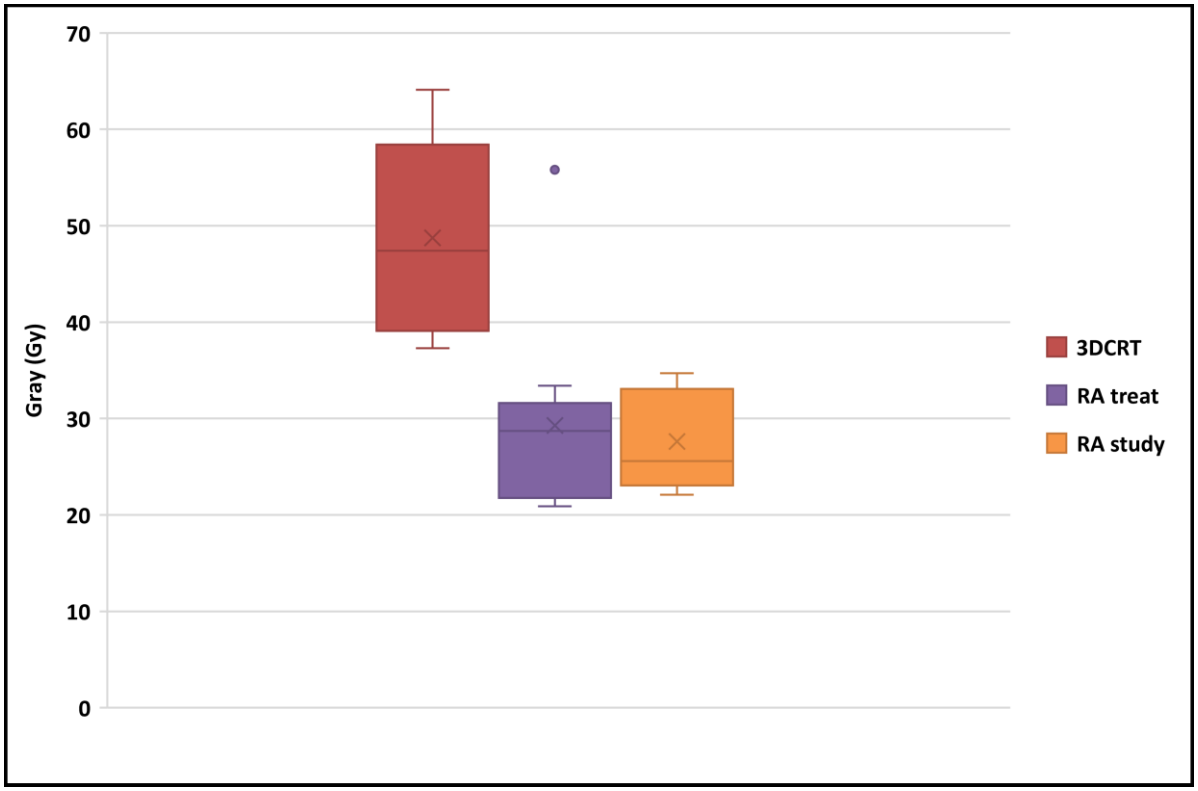

Figure 4.41: Maximum doses recorded for the patient population per planning technique

There is no recorded dose threshold for the shoulders, and this structure is not used in the plan scoring system. It can be noted that the maximum doses recorded in the shoulder are significantly larger in the 3DCRT plan group and could possibly have some side effects to the normal tissue. It also indicates the high dose passing through the shoulders, and therefore the clinical significance of the shoulders being positioned the same for daily treatment, as shoulder misalignment can lead to over or underdosing of the PTV. Therefore, adding this contour to the RT planning process could add value in understanding the importance of set-up reproducibility.

4.3.11 Summary of plan scoring results for all the organs at risk

Table 4.12 shows a compilation of all the criteria used in the plan scoring spreadsheet for OAR specifically, as discussed in sub-sections 4.3.2 to 4.3.10.

Table 4.12: OAR plan score allocation

	Points Allowcation		Best Results	Score	Acceptable Results	Score	Worst Results	Score
Brainstem	6 points	Dmax	<50Gy	0	<53Gy	1	>53Gy	3
Brainstem PRV		Dmax	<54Gy	0	<54-59Gy	1	>59Gy	3
Spinal Cord	6 points	Dmax	<45Gy	0	<45Gy-47Gy	1	>47Gy	3
Spinal Cord PRV		Dmax	<48Gy	0	<48Gy-50Gy	1	>50Gy	3
Parotid Right	6 points	Mean Dose	<18Gy	0	<18-23Gy	0.5	>23Gy	1
Parotid Left		Mean Dose	<18Gy	0	<18-23Gy	0.5	>23Gy	1
Parotid Right PRV		Mean Dose	<20Gy	0	<20-25Gy	0.5	>25Gy	1
Parotid Left PRV		Mean Dose	<20Gy	0	<20-25Gy	0.5	>25Gy	1
Parotids Combined		Mean Dose	<23Gy	0	<23-37Gy	0.5	>37Gy	1
Parotids Combined PRV		Mean Dose	<25Gy	0	<25-39Gy	0.5	>39Gy	1
Cochlear Right PRV	4 points	Mean Dose	<32Gy	0	<32-45Gy	1	>45Gy	2
Cochlear Left PRV		Mean Dose	<32Gy	0	<32-45Gy	1	>45Gy	2
TMJ Right	4 points	Dmax	<60Gy	0	<60-65Gy	0.5	>65Gy	1
TMJ Left		Dmax	<60Gy	0	<60-65Gy	0.5	>65Gy	1
TMJ Right PRV		Dmax	<65Gy	0	<65-70Gy	0.5	>70Gy	1
TMJ Left PRV		Dmax	<65Gy	0	<65-70Gy	0.5	>70Gy	1
Oral Cavity	2 points	Mean Dose	<40Gy	0	<40-45Gy	1	>45Gy	2
Mandible	2 points	Dmax	<68	0	<68Gy-70Gy	0.5	>70Gy	1
Mandible PRV-PTV		Dmax	<70	0	<73Gy	0.5	>73Gy	1

The results of the plan scores for each of the 10 patients per planning technique is given in figure 4.42. Statistical analysis with the Independent-Samples Kruskal-Wallis Test showed no statistical significance across the samples (p = 0.287).

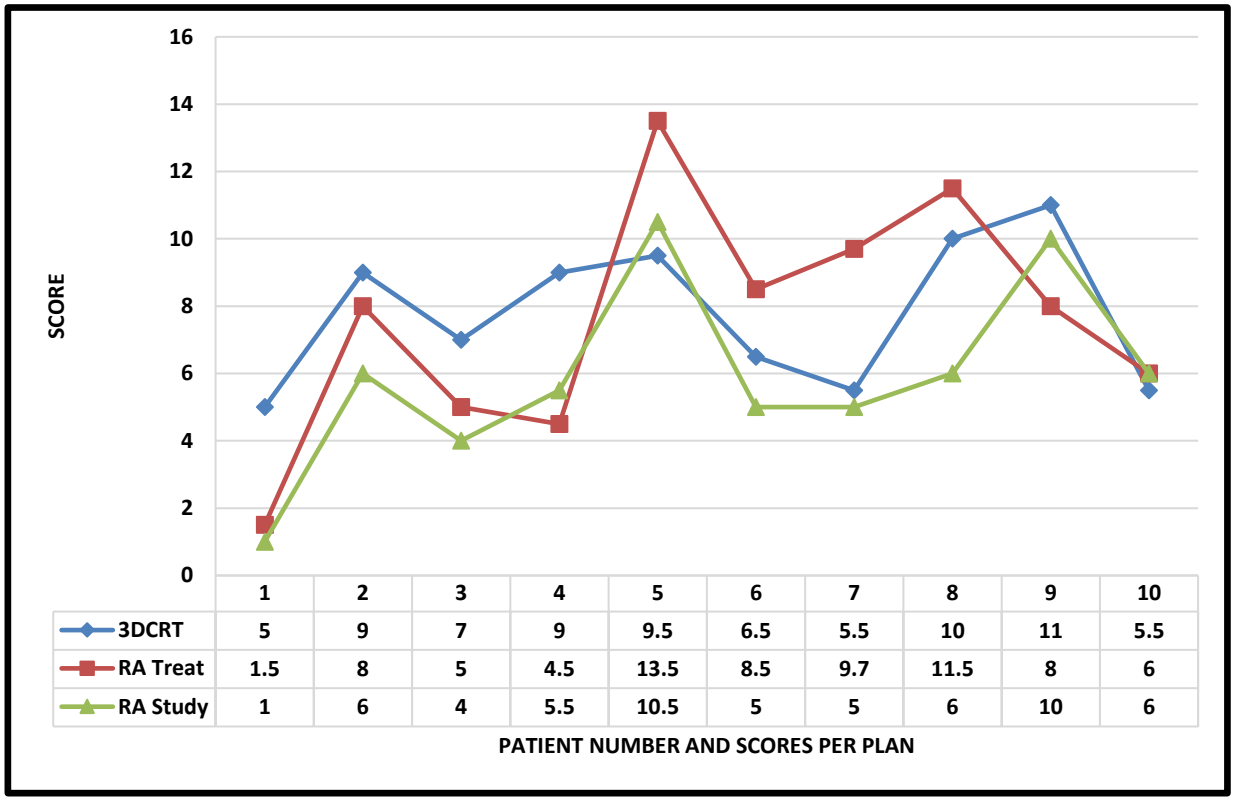

Figure 4.42: OAR plan results

Although no statistical significance was found across the plan types, the clinical impact to the patient could be significant, with less morbidity experienced during and after radiation therapy, if more OAR sparing is achieved.

A lower plan score (figure 4.42) equates to better OAR sparing. When comparing 3DCRT group to the *RA Treat* group, it can be seen that both groups had 5 patients with lower scores. When comparing the 3DCRT group to the *RA Study* group, 8 patients in the *RA Study* group achieved better OAR sparing than the 3DCRT group (2 patients).

In summary of research sub-question 2, the comparison of the *RA Treat* and *RA Study* group, 7 patients achieved a lower score in the *RA study* group, and 1 patient an equal score. This indicates a better score for the *RA study* group. This could be due to the increased number of OARs contoured for the *RA Study* group.

4.4 Research results for sub-question 3: Which planning technique offers the best dose coverage and dose homogeneity of the PTV

4.4.1 Dose coverage

The dose coverage is determined by the equation for conformity, called the conformity index (ICRU, 2010a).

This conformity index (CI) uses the volume of the reference isodose lines (V_{RE}) and divides it by the volume of the target (V_{PTV}). For this study the volume of the 95% isodose line was recorded, as this is the value that is used for curative RT. A conformity index value of 1 equates to the ideal situation, where the volumetric size of the 95 % isodose lines conforms perfectly to the volume of the target. This factor, however, assumes that the target volume and the target dose is in the same area and therefore superimposed onto each other. If this value is larger than 1, it indicates that the area receiving dose is larger than the target volume, and if the value is smaller than 1, that the target is receiving less dose (Feuvret et al., 2006).

Due to the complex shape of the target volume for this patient population, and the limited options in forward planning and designing a 3DCRT plan, it is not guaranteed that the dose and the volume will be congruent with each other, and this reiterates the importance of checking the treatment plan on each CT slice to ensure dose conformity.

Figure 4.43 demonstrates the conformity of the 3DCRT plan as compared to the RA plans. In this figure, the blue line represents the curative dose that should be covering the red PTV contour. The yellow arrows indicate an underdosing of the PTV, as the blue dose line is not

covering the red PTV contour, thud indicating an underdosing of the PTV with dose spillage into the left lateral normal tissue. The blue arrows indicate where the blue line (95 % dose line) provides too wide a dose around the red PTV contour, and therefore placing dose in the normal tissue of the lungs. This CT slice therefore represents a scenario where there is a larger than necessary volume of normal tissue receiving the prescribed dose.

It can therefore be deducted that this disagreement of dose volume to PTV volume can lead to a good conformity index calculated result. However, it is still not an indication of good conformity, as the dose is not conforming to the PTV. There is shown to be underdosing on some CT slices and dose to normal tissue on other CT slices.

The lower two slices in figure 4.43 is an example of a Rapid Arc plan, where the volume of the blue line (95 % isodose line) is more in agreement with the red PTV volume. In this instance, the conformity index can be an indicator of a plan where the dose and the target volume agree.

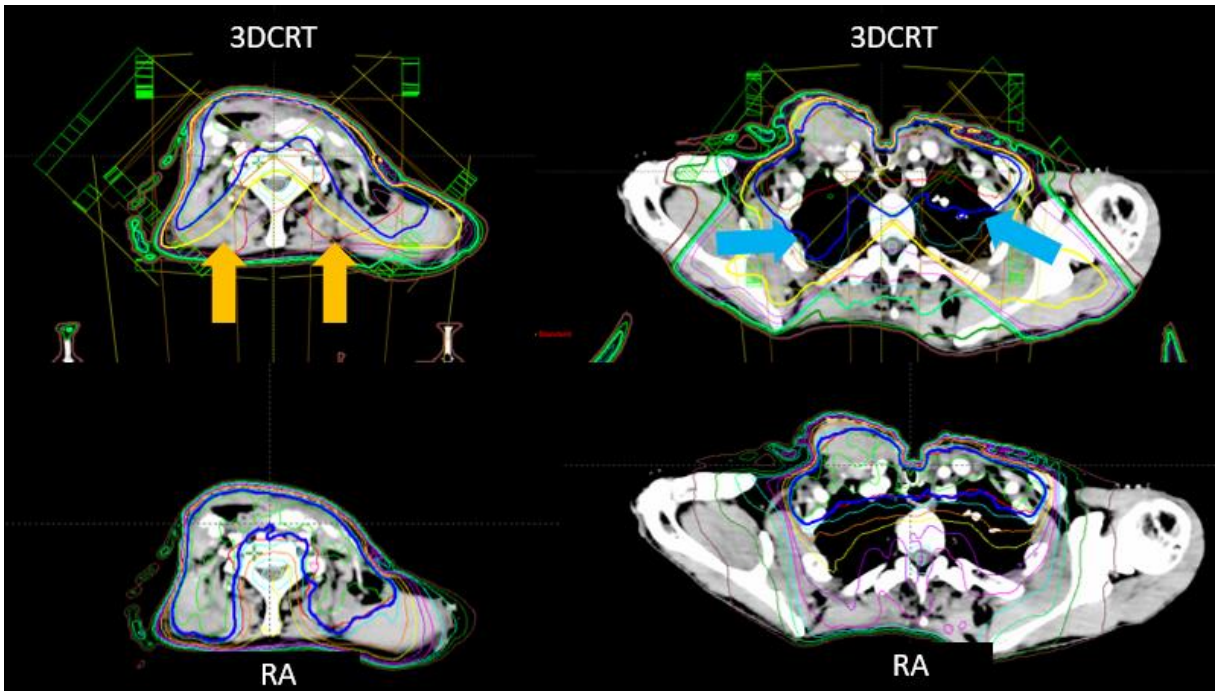

Figure 4.43: Conformity for 3DCRT and RA plans

The use of the conformity index is therefore more relevant for RA plans, than for 3DCRT plans, especially for complex head and neck plans, where the maximum dose that can be given to the PTV is often dependent on the tolerance dose of the spinal cord. The Yellow isodose line in figure 4.43 represents the dose constrained to the spinal cord.

4.4.2 Conformity index scoring system

The conformity index calculation is shown in equation 4.1 (Feuvret et al., 2006).

This calculation was used for each treatment plan. Nine of the ten patients had 2 treatment plans for each planning technique, as these patients had two dose levels to be achieved. Patient number 5 had only one treatment plan per technique.

$$CI = \frac{V95\%}{TV}$$

CI=Conformity Index
V95%=Volume of the 95% Isodose line measured in cm^3
TV=Volume of the Target (PTV) in cm^3

Equation 4.1: Conformity Index equation from Feuvret et al. (2006)

The lowest calculated value over all plans was 0.98 and the highest 2.00. The conformity index scoring system can be seen in table 4.13. A CI result between 0.95 and 1.05 was allocated 0 marks to the plan, as this was the best possible and most conformal plan result that can be achieved. The ideal mathematical result that indicates the most conformal plan will have a result of 1.

A CI result of 0.95 to 0.85 and 1.05 to 1.5 will indicate an acceptable plan and was allocated a score of 1. The least favourable plan conformity index was allocated 2 marks, and that included a score of less than 0.85 or more than 1.5.

Table 4.13: Conformity index score allocation

	Points Allocation		Best Results	Score	Acceptable Results (Gy)	Score	Worst Results (Gy)	Score
CI:V95%/TV	2 points	plan 1	negative 0.95 to 1.05	0	negative 0.85-0.95 and 1.05-1.5	1	<negative 0.85 or >1.5	2
CI:V95%/TV	2 points	plan 2	negative 0.95 to 1.05	0	negative 0.85-0.95 and 1.05-1.5	1	<negative 0.85 or >1.5	2

The CI score allocated a score of 0 for the best CI, 1 for an acceptable result, and 2, indicating the worst CI. The results are shown in figure 4.44.

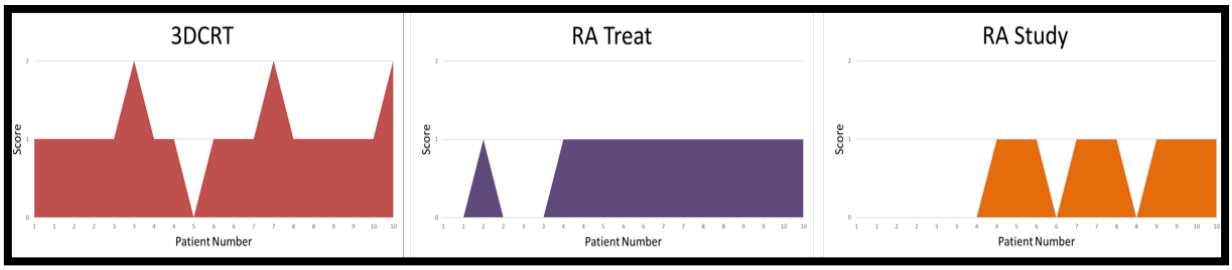

Figure 4.44: Results of conformity index scoring system

The 3DCRT plans had the highest overall scores. Three plans had a score of 2, therefore indicating the worst conformity index. One plan had a score of zero, indicating the best conformity index, and 15 had a score of 1, indicating an acceptable score.

In the RA group, there were no scores of 2, indicating that all the RA plans had an advantageous conformity index. Of all the RA plans, 15 plans had a score of zero, and 23 plans had a score of one.

Statistical analysis with the Kruskal-Wallis test found a statistically significant difference ($p = 0.002$) across the 3 plan groups regarding the CI. The pairwise comparison showed no significance between the two RA plans ($p = 0.293$), or the *RA Treat* and the 3DCRT plan ($p = 0.206$), but that there was a statistical significance between the *RA Study* and the 3DCRT plans CI values ($p = 0.002$).

4.4.3 The lesion coverage factor

The lesion coverage factor (CVF) is the Volume of the Target Volume receiving the Reference Isodose (TV_{RI}) divided by the Volume of the Target Volume (TV). This reference isodose therefore excludes all the dose spilled outside of the PTV, and represents only the dose representing 95 % of the prescription that is on or inside the target volume. (Feuvret et al., 2006)

$$CVF = \frac{TV_{RI}}{TV}$$

CVF=Lesion Coverage Factor
TV_{RI}= Target Volume receiving Reference Isodose in cm³
TV=Volume of the Target (PTV) in cm³

Equation 4.2: The Lesion Coverage Factor equation from Freuyet et al. (2006)

This calculation was applied to all plans, and the results quantified as seen in table 4.14.

A result of 0.95 to 1 indicates that between 95 % and 100% of the target volume is covered by the reference isodose volume, and these criteria were given a score of 0, indicating the best possible result.

A score between 0.9 and 0.95 will indicate that a plan would have achieved 90% to 95% of the target volume to be covered by the reference isodose volume, and these criteria were given a score of 1. A score of less than 0.9 was given a point allocation of 2, as this was the worst plan score, which indicates that less than 90 % of the volume will be covered by the reference isodose volume.

Table 4.14: Lesion coverage factor score allocation

	Points Allowcation		Best Results	Score	Acceptable Results	Score	Worst Results	Score
CVF=TV (RI)/TV	2 points	plan 1	0.95-1	0	0.9-0.95	1	<0.9	2
CVF=TV (RI)/TV	2 points	plan 2	0.95-1	0	0.9-0.95	1	<0.9	2

4.4.4 Lesion coverage results

The results of this scoring system can be seen in figure 4.45. The highest scores (of 2) can be observed for the 3DCRT plans. Twelve (12) of the nineteen (19) 3DCRT plans (63 %) had a score of 2, indicating the worst coverage of dose to the PTV. In contrast, only 5 of the RA plans had a score of 2 (13.1 %). Twenty-two (22) of the RA plans had a score of one (57.9 %), and eleven (11) of all the RA plans had a score of zero (29.0 %).

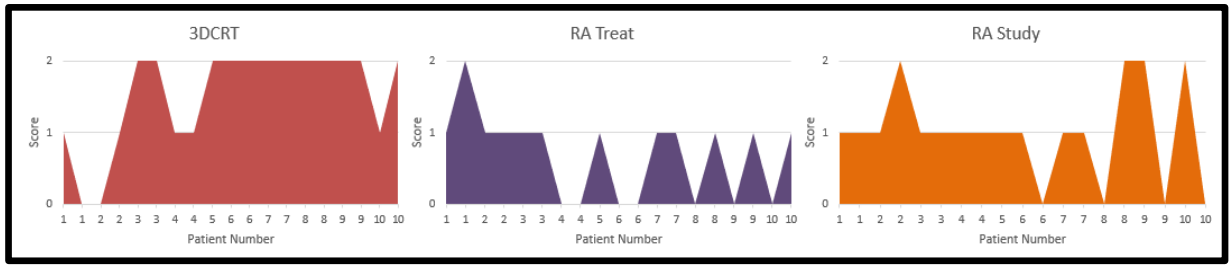

Figure 4.45: Results of Lesion Coverage scoring system

These results indicate that the Rapid Arc plans offer superior lesion coverage as compared to the 3DCRT plans.

The independent-sample Kruskal-Wallis Test showed a statistical significance with a p-value of 0.001, indicating that there is a significant difference between the plan scoring results. The pairwise comparisons of the plans indicated non-significance between the *RA Treat* and *RA Study* plan (0.549) as well as between the *RA Study* and the 3DCRT plan group (0.067). It did, however, indicate a statistically significant result between the *RA Treat* and the 3DCRT plan groups.

Although the statistical tests resulted in no significance between *RA Study* and 3DCRT plan groups, the plan results, seen in Figure 4.45, pose a significant clinical difference. The score of 2 indicates significantly less curative dose being delivered to the tumour. In the 3DCRT group there were 12 plans scoring 2 and in the RA group only 5 plans scoring 2.

4.4.5 Homogeneity index

The homogeneity Index (HI) is a scoring tool to analyse and quantify dose homogeneity in the target volume. It indicates the ratio between the maximum and minimum dose in the target volume, and lower values indicates better homogenous dose distribution within the volume (Helal & Omar, 2015).

The homogeneity index was achieved using 4 calculations (Helal & Omar, 2015).

The scoring system is demonstrated in table 4.15. The best homogeneity index score was awarded 0 points; the acceptable score, 1 point; and the worst results 2 points.

Table 4.15: Homogeneity Index score allocation

	Points Allowcation		Best Results	Score	Acceptable Results	Score	Worst Results	Score
HI: D2/D98	2 points	plan 1	1-1.099	0	1.1-1.2	1	>1.2	2
HI: D2/D98	2 points	plan 2	1-1.099	0	1.1-1.2	1	>1.2	2
HI: D5/D95	2 points	plan 1	1-1.099	0	1.1-1.2	1	>1.2	2
HI: D5/D95	2 points	plan 2	1-1.099	0	1.1-1.2	1	>1.2	2
HI:D2-D98/Dp	2 points	plan 1	0-0.099	0	0.1-0.2	1	>0.2	2
	2 points	plan 2	0-0.099	0	0.1-0.2	1	>0.2	2
HI:D5-D95/Dp	2 points	plan 1	0-0.099	0	0.1-0.2	1	>0.2	2
	2 points	plan 2	0-0.099	0	0.1-0.2	1	>0.2	2

An overview of the homogeneity index results, as seen in figure 4.46, clearly indicates that the 3DCRT group scored the highest amount of 2's, and the least amount of 0's as compared to the RA Test and *RA Study* group.

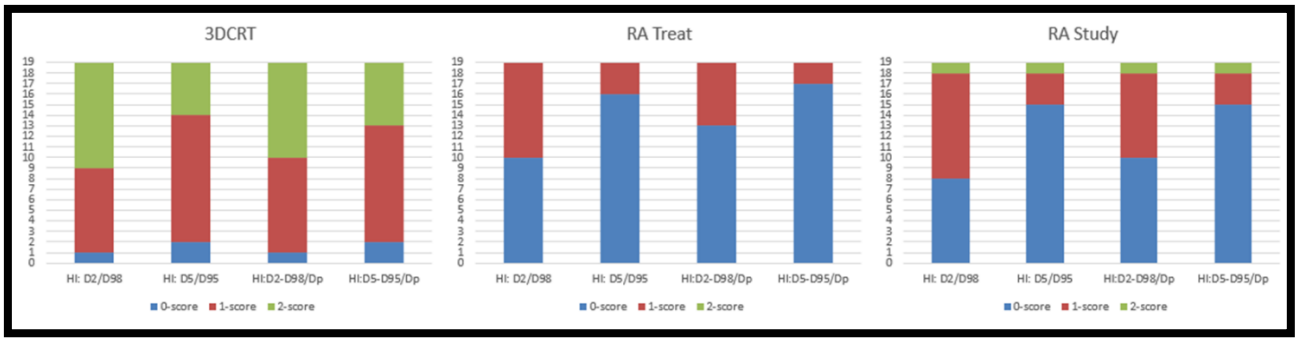

Figure 4.46: Homogeneity Index plan scores comparison for all 19 plans

For 3DCRT plans, across all four the HI calculations, a score of 1 was achieved for between 42 % and 63 % of the plans (figure 4.46 3DCRT-pink colour), and a score of 2 was achieved for between 26 % and 53 % (figure 4.46 3DCRT – green colour). These scores indicate that the 3DCRT planning group offers less homogeneity than the RA plans.

The *RA treat* group had two instances with zero scores, and it is observed that more scores of 0 are achieved for the calculation using D5 and D95 (higher dose received by 5 % of the volume compared with the lower dose achieved by 95 % of the volume) compared to those where D2 and D98 were used (higher dose received by 2 % of the volume compared to the lower dose received by 98 % received by the PTV). This is seen in figure 4.46 where *RA Treat* scores of 0 are indicated in blue.

In this *RA treat* group, the score of 0 (blue colour) was between 53 % and 89 %, and the score of 1 (pink colour) was between 11 % and 47 % of all the calculations.

A score of 2 was achieved for 1 patient in the *RA Study* group as seen in figure 4.46 green colour in the *RA study* group. In this group, the score of 0 was achieved for between 42 % and 79 % (blue colour), and a score of 1 (pink colour) was achieved for between 16 % and 53 % of the calculations.

Comparing the HI results, it is observed that more scores of 1 and less of 0 was observed in the *RA Study* group as compared to the *RA Treat* group.

The Chi-Square test was used as a statistical tool to indicate statistical significance in each study group. A p-value of 0.686 for the 3DCRT plan group and 0.147 for the *RA Study* group indicate no statistical significance. In the *RA treat* group, the p-value of 0.043 indicated a statistically significant difference in this group.

The Kruskal-Wallis test between the planning groups, indicated no significance between the two RA groups (p = 1.0). There was, however, a significant difference between the *RA Treat* and the 3DCRT group (p <0.01) and between the *RA Study* and the 3DCRT (p < 0.01) group. The RA groups therefore offer better homogeneity index results as compared to the 3DCRT group.

The pairwise comparison for each calculation type is indicated in table 4.16. This table also indicates significant differences between the RA and 3DCRT groups, but not between the RA groups.

Table 4.16: Pairwise comparison results for HI calculations

Pairwise Comparison of Plans			
	RA-Treat v RA Study	RA Treat vs 3DCRT	RA Study vs 3DCRT
HI: D2/D98	1	0.000077	0.001
HI: D5/D95	1	0.000011	0.000074
HI:D2-D98/Dp	1	0.000016	0.001
HI:D5-D95/Dp	1	0.000002	0.000057
*Asymptotic significances (2-sided tests) are displayed. The significance level is 0.05			

Statistical analysis and clinical importance are significant between the RA plans and the 3DCRT plans, indicating that the RA plan offers better homogeneity scoring. The use of the HI index was only introduced in the ICRU 83 document for the use of inverse planning techniques (ICRU, 2010). Although it can effectively be used in 3DCRT as well, the complexity of 3DCRT plans in the head and neck area indicate that it is not necessarily a useful tool in this scenario.

The clinical impact of the HI results for all plan types needs to be evaluated along with the dose coverage seen on the CT scan, as using this as the only calculation tool is not adequate as the location of the low and high dose values is unknown when only HI.

4.4.6 Plan scoring results for homogeneity and conformity and coverage of dose to the PTV

Table 4.17 demonstrates the scoring table used for the PTV scoring system, as explained across subsections 4.3.1 to 4.3.5. All the plans were scored, and the results demonstrated in figure 4.46.

Table 4.17: The PTV score allocation table

	Points Allowcation		Best Results	Score	Acceptable Results	Score	Worst Results	Score
HI: D2/D98	2 points	plan 1	1-1.099	0	1.1-1.2	1	>1.2	2
HI: D2/D98	2 points	plan 2	1-1.099	0	1.1-1.2	1	>1.2	2
HI: D5/D95	2 points	plan 1	1-1.099	0	1.1-1.2	1	>1.2	2
HI: D5/D95	2 points	plan 2	1-1.099	0	1.1-1.2	1	>1.2	2
HI:D2-D98/Dp	2 points	plan 1	0-0.99	0	0.1-0.2	1	>0.2	2
	2 points	plan 2	0-0.99	0	0.1-0.2	1	>0.2	2
HI:D5-D95/Dp	2 points	plan 1	0-0.99	0	0.1-0.2	1	>0.2	2
	2 points	plan 2	0-0.99	0	0.1-0.2	1	>0.2	2
CI:V95%/TV	2 points	plan 1	minus 0.95 to 1.05	0	minus 0.95-0.85 and 1.05-1.5	1	<minus0.85 or >1.5	2
CI:V95%/TV	2 points	plan 2	minus 0.95 to 1.05	0	minus 0.95-0.85 and 1.05-1.5	1	<minus0.85 or >1.5	2
CVF=TV (RI)/TV	2 points	plan 1	0.95-1	0	0.9-0.95	1	<0.9	2
CVF=TV (RI)/TV	2 points	plan 2	0.95-1	0	0.9-0.95	1	<0.9	2

The maximum (worst) score possible using this score system, was 24 points.

In figure 4.47 the plan score results for the PTV are presented for each patient. The highest score is observed for a 3DCRT plan with a score of 22. The 3DCRT scores ranged from 7 to 22. It can be seen in figure 4.47, that the highest scores achieved for both the RA and 3DCRT plans was for the same patient (no 9).

The lowest score achieved was 2 in the *RA Treat* group, and the maximum score for a RA plan was 12, in the *RA study* group.

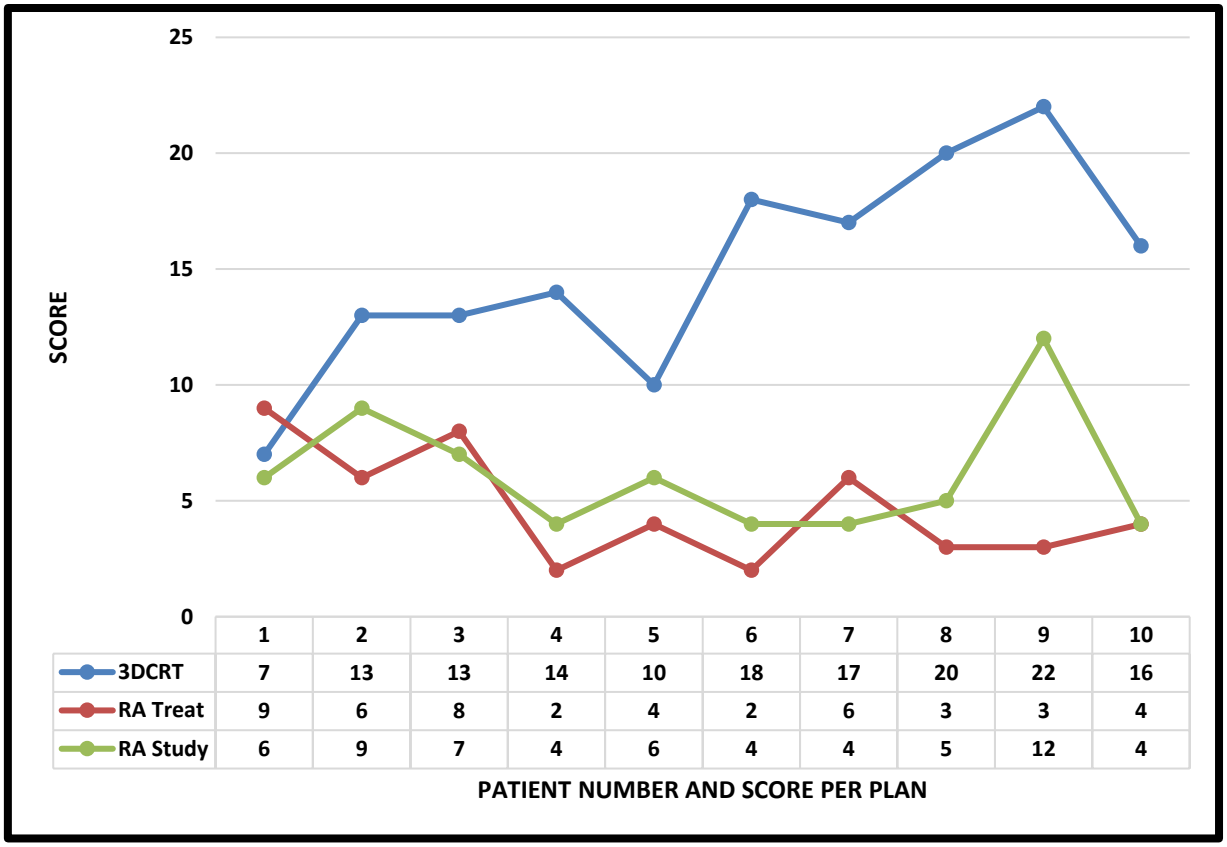

Figure 4.47: Plan score results for the PTV per patient

The independent Sample Kruskal-Wallis Test calculated at p value of 0.00014, indicating a statistical difference between the plan groups. Further analysis with pairwise statistical comparison of the plan groups showed no statistical significance between the two RA plan groups (p=1.00). There was however a statistically significant difference found between the *RA treat* and 3DCRT group (p=0.00013), and the *RA Study* and the 3DCRT group (p=0.005)

4.5 Summation of research results for both sub-question 2 and 3

On evaluation of the OAR score results in figure 4.48, the results are spread out between all 3 plan groups and the 10 patients. Figure 4.49 however shows a significant higher and therefore worse score for the 3DCRT group (with the exception of patient 1).

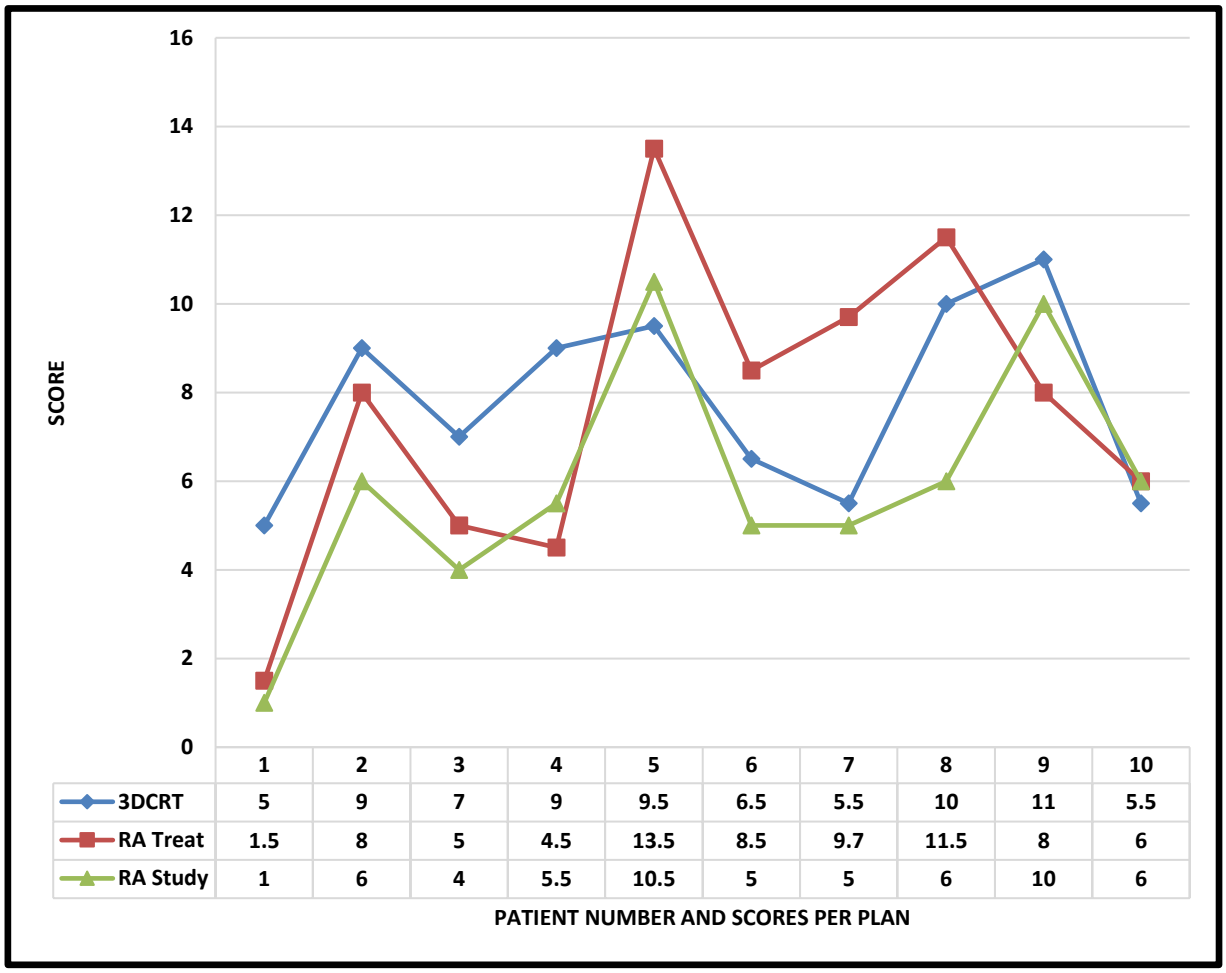

	1	2	3	4	5	6	7	8	9	10
3DCRT	5	9	7	9	9.5	6.5	5.5	10	11	5.5
RA Treat	1.5	8	5	4.5	13.5	8.5	9.7	11.5	8	6
RA Study	1	6	4	5.5	10.5	5	5	6	10	6

Figure 4.48 Plan score results for the OAR per patient

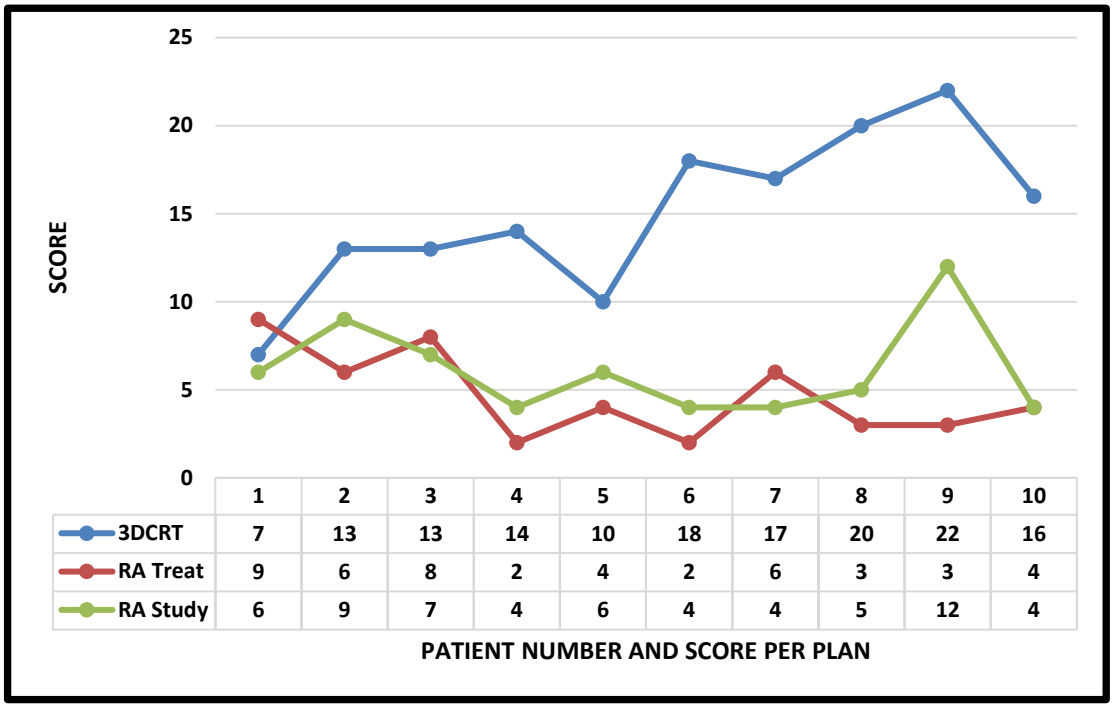

Figure 4.49 Plan score results for the PTV per patient

The summation of the results from the OAR and the PTV study as shown in figure 4.50, resulted in a noticeably higher score for the 3DCRT group, and therefore probable worse plan outcomes as compared to the RA plans.

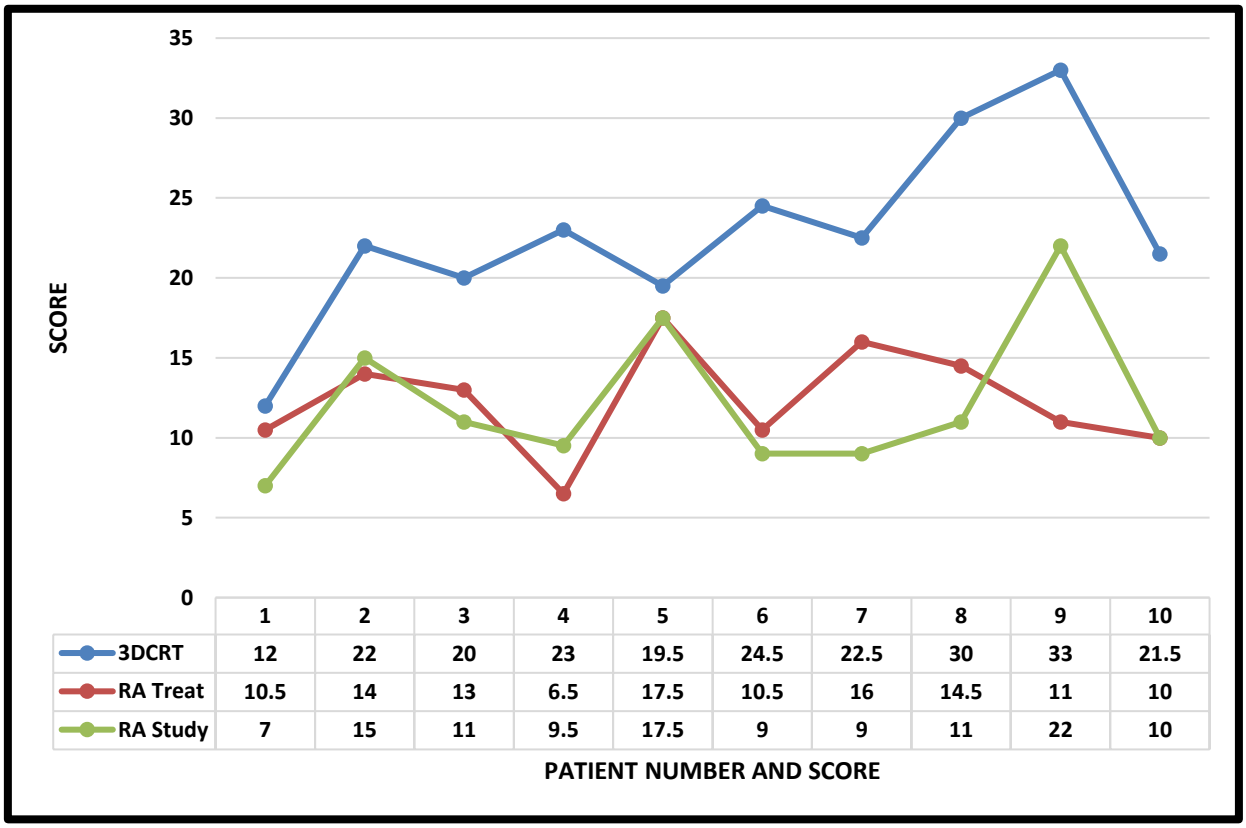

Figure 4.50 Summation of OAR and PTV planning score results per patient

An interesting observation of patient 5, who had only one volume with a high dose prescription, was that similar plan results were achieved for all three plan groups.

4.6 Conclusion

The research results presented in this chapter for sub-question 1, described the set-up error found in patients treated with the Klarity mask system. The results were presented for both those treated in the head and neck area and those treated only in the head area as was summarised in subsection 4.2.5.

Sub-question 2 and 3 where the same 10 patients' data was used to evaluate dose achieved to the OAR and the PTV and was shown for each measured parameter. Thereafter a total combined score was achieved for each planning technique for each patient. These results were summarised in subsection 4.5.

As chapter 4 reported the results of this research study, chapter 5 will focus on how to position this research into standard protocols, as well as further recommendations regarding the results.

CHAPTER 5 Conclusion and Recommendations

5.1 Introduction

Chapter 4 reported all the results that were achieved from this research study. In this chapter these results are used to objectively discuss and conclude this research study. The author's aim to achieve clinical relevance is stated in the conclusion of each sub-question, and further recommendations are given addressing relevant issues that were observed during the research process.

5.2 Conclusion of Sub-question 1: How accurate and reproducible is the treatment set-up

The treatment setup accuracy has been evaluated and was based on a comparison of the planned treatment position using the DRR and the actual treatment position using the MV EPID images created on VARIAN linacs using ARIA version 10 software. Two orthogonal images were compared for each instance. This in theory enables the user to compare the patients position from two-dimensional (2D) directions, that is orthogonal (90 degrees) from each other.

The patient could have setup inaccuracies in other directions that could be detected with 2D-2D matching but this cannot be achieved completely. It has become clear to the researcher the value that can be brought by a 4D couch and the use of linac based CT verification, or by improving the image quality by changing from MV to KV imaging. In everyday clinical practice, no patient will ever be able to be positioned daily for RT in precisely the same position. The safety margin that should be acceptable, is that which has the correct expansion margins in use, to enable the correct consistent treatment. With these known margins, it becomes possible to identify and eliminate any possible random and systematic process that can jeopardize the setup accuracy.

The role of the RTT during the radiation therapy process of the patient is much deeper and more meaningful than just treating the patient. As a RTT one develops a relationship with the patient. You also get familiar with the nature of the patient, anxiety, uncontrollable movements, the inability to lie still, claustrophobia or other personal traits, over and above the dreaded immobilisation mask that the patient must wear during each treatment. This mask, in itself poses challenges, with firstly positioning the patient on the first day of treatment on the headrest in exactly the same way he/she was positioned during the mask-making process, and thereafter fitting the mask. This mask should be not too tight or too loose in any point of contact to the skin, but should be tight enough for the patient to be kept immobile during treatment.

Through personal clinical experience, it has been observed that many patients get used to how the mask should fit, and can position themselves after many days of treatment into the mask system, and then they indicate to the RTT, that in fact the mask is fitting correctly or not. This "recall memory" of the clinical position is useful to the RTT, as the set-up process is easier and reproducible. However, this flashback by the patient, is absent at the start of treatment, and as often the production of the mask and the start of treatment can be days or weeks apart and poses more challenges during the first few treatment days. In this research study, the average calendar days from the day of the production of the mask and planning CT, to the start of treatment was 41 days for the head and neck group, and 29 days for the head group (see figure 4.1 in chapter 4). In the light of this phenomenon it can be concluded that there is the need for further research to link this time delay to reproducible treatment accuracy.

Irrespective of the time delay during planning CT and the treatment starting, a further treatment time for this patient population of 6 to 7 weeks, on average adds up to 13 weeks for the patient in the radiation therapy department. Ang et al (2001) concluded that the overall treatment time and, that to include both surgery and the conclusion of radiation therapy are directly related to the 5-year locoregional control. The authors (Ang et al.,2001) stated that locoregional control for patients with high risk features who have had an overall treatment time of <11 weeks was 76%, for 11-13 weeks 62% and >13 weeks as low as 38%. This therefore indicates that shortening the time from mask production to treatment initiation could not only be advantageous to setup accuracy, but also significantly advantageous to the locoregional recurrence rates. Head and neck squamous cell carcinomas were placed first on the list of tumour types as being most affected by interruptions during RT (Royal College of Radiologists, 2019). It has also been shown that auditing the workflow can dramatically improve the time from planning CT to start of treatment (Vieira et al., 2019). This was done to such good effect that the waiting times at an institution in California, reduced their waiting time from 2 weeks to 1 week (Agazaryan et al., 2020). Any reduction in waiting times for this patient population from surgery to start of radiation therapy, is therefore advantageous.

In the researcher's clinical experience, the relationship that the RTT and patient builds up over time can aid in the improvement in the patient set-up. As this relationship leads to trust between the patient and RTT it can lead to better collaboration by the patient during the treatment session. This relationship could be compromised with the regular staff rotation between treatment units, for example as practiced at the research study unit, that could potentially therefore lead to a larger introduction of random error. In an academic teaching hospital environment, the presence of students in training, could also have an influence on the workflow at the treatment unit, as much supervision needs to be given to the students to ensure they work correctly. In clinical experience, it is possible that a patient is more tense during treatment when the treatment is administered by a student, and therefore this multiplicity of factors may

contribute to a potentially larger setup inaccuracy. This is naturally not intended, but rather a result of a routine that needs to be considered when understanding and calculating set-up accuracies.

Patient specific factors that contribute to setup reproducibility errors are weight loss (Barrett et al., 2009), due to treatment side effects as loss of appetite, pain, and mucositis (Tolentino et al., 2011). Furthermore, changes in the tumour bed and surgical scars can be from swelling or atrophy or even the use of certain medication that can lead to tissue changes.

Irrespective of all external factors that could have an influence on the patient's treatment accuracy, the only determination of accuracy of patient position available is to evaluate the imaged data. All these external or internal factors can only be documented when measured and researched. Furthermore, these factors are always changing. Equipment is replaced, staff members rotate through workplaces, and junior staff need to gain experience. Therefore yearly audits are essential to verify the current treatment margins and the protocols must be evaluated repeatedly and updated (Royal College of Radiologists, 2008).

As junior staff join the staff complement and students visit clinical departments, it is the duty of the more experienced staff to lead and teach. By law in South Africa (Health professions act, 2016), the radiation oncologist is responsible for the prescription and instructions for radiation therapy treatment of the patient. It is however the RTTs, that within their cope of practice, treat the patient daily and should be and effectively are responsible for treatment accuracy and therefore image interpretation, verification and ultimately the correct treatment. This high level of care as well as the shortage of radiation oncologists has led to the development of specialist programs in countries such as Canada. Alimonte et al (2017) found that the role expansion of RTTs has led to the creation of an innovative model to successfully manage an increase of patient complexities. Harnett et al (2018) stated that the advanced practice of radiation therapists has led to autonomy in some aspects of practice, thereby assisting the radiation oncologist in successfully integrating evidence-based medicine and thus establishing a pool of additional knowledge and skills into the field of radiation therapy.

The CTV to PTV expansion results for this research study for the head and neck patient group, resulted in an anterior to posterior margin of 5.6mm, superior to inferior margin of 6.9mm and a lateral margin of 6.5 mm. A similar study in Bosnia and Serbia, showed a 6mm symmetric margin from CTV to PTV (Strbac & Jokic, 2013) which compares well to this research study. Verma et.al. (2017) separated their margin results into results of the head area and results for the neck area. They also used the same mask system as used in this research study but compared both the masks that are reinforced and unreinforced. The CTV to PTV expansion results for the head region comparing the unreinforced mask with the reinforced mask were as

follows: anterior to posterior 0.44 mm and 0.40 mm, superior to inferior 0.46 mm and 0.34 mm, and left to right margin were 0.27 mm and 0.26 mm respectively. The results for the neck area were: anterior to posterior 0.78 mm and 0.48mm, superior to inferior 0.45 mm and 0.33 mm and left to right margin 0.41 mm and 0.33 mm. These measurements are less than what was found in this research study, as this study utilised the reinforced mask system only. However these types of errors are typically departmental, personnel and equipment specific, and when comparing data it is indicative that one department cannot utilize, necessarily, the set-up accuracy from another department, even if the exact immobilisation equipment is used.

Research from the University of Witwatersrand published results for the systematic and random errors for the head and neck patient population. They stated that the overall random error for patients treated with IMRT was 6.1mm, and the systematic error 4.4mm (van Wyk et al., 2017). Compared to this research study, where the random error was calculated as anterior to posterior 1.93mm, superior to inferior 1.89 mm and left to right 1.43 mm and the systematic error calculated was anterior to posterior 1.68 mm, superior to inferior 2.23 mm and left to right 2.21 mm respectively. Therefore, the accuracy levels of this research study are shown to be superior to those of the published data by WITS university.

This research study aim was to determine the expansion margins needed for the patient population treated with the specific Klarity immobilisation mask system, to enable these margins to be known for the research planning population, namely late stage larynx cancer patients that are treated in the head and neck anatomical area. As many uncertainties were identified during the data collection of sub-question 1 (as listed in subsection 3.3.1.8), the data collection was split between those treated in only the head that represents one area of treatment, and those treated in both the head and neck area that represents two treated areas of the body.

The CTV to PTV expansion margins calculated in this research study for the head group was reported in table 4.4 as 5.1 mm vertical (anterior to posterior), 6.1mm longitudinal (superior to inferior) and 4.9mm lateral (left to right). These margins were larger than findings by Kenakavelu & Jebaseelan (2016), who reported their calculation from a single institution in India to be 3.45mm lateral (left to right), 2.98mm longitudinal (superior to inferior) and 1.75mm vertical (anterior to posterior). They did however immobilise with a head only mask, and had improved the imaging frequency of not only the first three fractions, but also twice weekly, as compared to this research study that only imaged the first three fractions and then once per week. A research group in Iran (Molana et al., 2018) also reported smaller errors than this research study. The systematic and random error reported by Molana et al. (2018) compared to this research study are: systematic error vertical 0.61 mm :1.52 mm , longitudinal 0.8 mm :

2.0 mm, lateral 0.93 mm :1.6 mm and random errors vertical 0.5 mm :1.92 mm, longitudinal 0.4 mm : 1.6 mm and lateral 0.72 mm :1.33 mm.

The aim of sub-question 1 was to determine the setup error of the patient population treated in a specific mask system. These results are extremely important to enable accurate expansion margins to be used during treatment planning as well as accurate action protocols for imaging during treatment. These quantified expansion margins are not only useful for the CTV to PTV expansion, but also for expansion of OAR to PRV.

This research study agreed with the contouring of anatomical landmarks on the DRR to enable comparison with the EPID image as defined by Tamponi et al. (2014) and the Royal College of Radiologists (2008). This research study has shown the importance of contouring both sides of bony landmarks where possible to show positional accuracy, however little or no appropriate research in this respect was found in the available literature. This bi-lateral contouring of the bony landmarks will aid in less variabilities being apart in peer review matching and will increase the accuracy due to interpolation error during DRR creation.

5.3 Recommendations relating to sub-question 1: How accurate and reproducible is the treatment set-up.

5.3.1 Introduction

The recommendations for su b-question 1, has been divided into logical work-flow process subsections. These subsections enable the whole process of image creation to be divided into smaller parts. Each step of image creation has an impact on the final evaluation of set-up accuracy to achieve the eventual goal: the smallest measurable setup accuracy. This will enable the smaller CTV to PTV margin to be needed, and in return less normal tissue will be receiving radiation dose.

5.3.2 Including the vertex of skull in the planning CT

The planning CT for both patient groups (those treated in the head only and those treated in the head and neck) must include the vertex of the skull, as it is very important to see its location when determining any rotation in the head. As demonstrated in figure 5.1, all contoured

anatomy is found to be in agreement accept the vertex of the skull, which is an indication of a rotation of the head that could be seen on the lateral image.

This is also important if the brain as an OAR that has to be contoured. This ensures that a partial organ is not contoured.

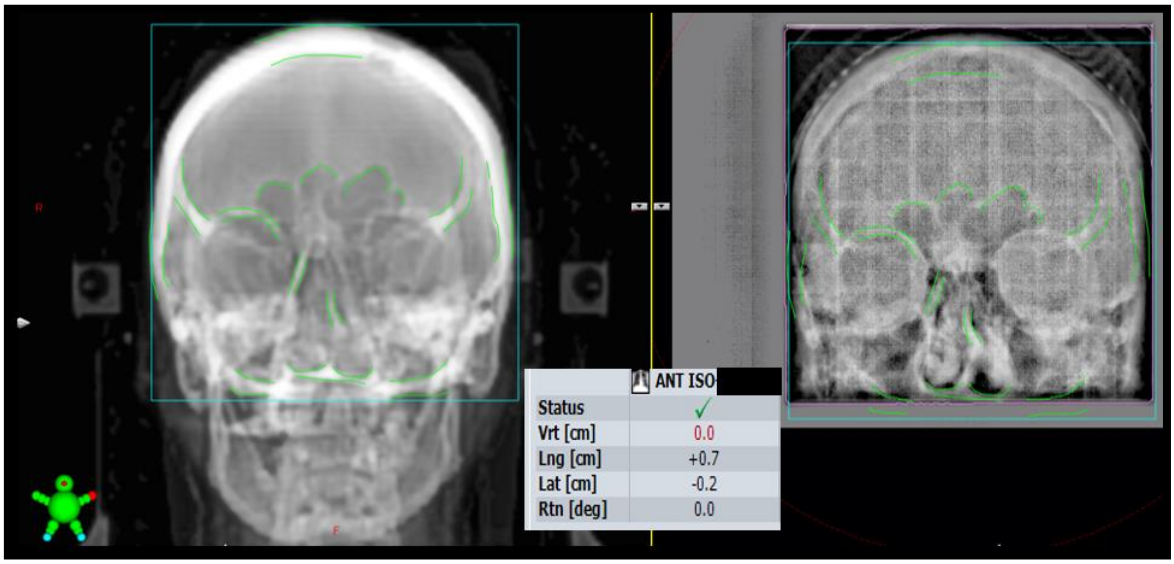

Figure 5.1: Illustration of the vertex skull bone that is not in agreement on the EPID image (right side). This will be an indication that a rotation of the head will be seen on the lateral image (image created by author).

5.3.3 DRR Quality and Creation

5.3.3.1 Thinner CT slice thickness

DRR quality is directly related to the planning CT slice thickness and should be the smallest slice thickness possible. As 3 mm slice thickness was used for all the DRRs created in this research study, it will be advantageous to lower this slice thickness further to 2mm. This is discussed in greater detail in subsection 3.3.1.8, where it was noted how the complex bony structures in the head and neck can be interpolated wrongly, when compared to an actual 2D image.

In subsection 3.3.1.8.7 it is demonstrated how challenging it is to perform image matching on children with DRRs produced from 3mm slice thickness. It is therefore recommended to perform planning CT for children with a 1mm slice thickness.

5.3.3.2 Standardise greyscale selection

DRR creation must be carefully selected to have a similar greyscale and anatomy contrast to the EPID image that is acquired on the linac. This will make it easier to manually compare two

images, and lead to a consistent quality of imaging. This is discussed in detail in subsection 3.3.1.8.

5.3.3.3 Cropping the CT data to exclude the CT bed artefact when creating the DRR

The CT couch artefacts must be cropped away from the patient's anatomy during creation of the DRR. This is a process of indicating to the computer the part of the CT data that must be used for the creation of the DRR. As the CT couch is not present during treatment, the very dense structures inside the CT couch, if included in DRR creation will be overlaid on vital anatomy, and this anatomy is then not visible and useful for image matching. When couch artefacts are included in the DRR creation, it poses a risk of misinterpretation of anatomy, and a risk of error in the image matching process. This is discussed in detail in subsection 3.3.1.8.

5.3.3.4 Standardise anatomical levels for EPID imaging

The correct anatomy must be selected for imaging (thus the acquiring of the EPID image) of each specific patient group. Strict imaging protocols must enforce that the correct anatomical sites are imaged on the linacs. As illustrated in subsection 3.3.1.8.5, the area treated was not included in the images acquired on the linac and this will lead to failure in image matching.

5.3.3.5 Imaging margins for patients receiving RT in both the head and neck area

As illustrated in figure 5.2, for a patient receiving treatment to both the head and the neck area, the anterior image should include as much information of both the head and neck areas, as the imaging field size allows. The lateral image should be cropped to not include the shoulders, where no anatomy can be identified, and more anatomy imaged of the head and cervical spine. Although this adds time to the image acquisition as the RTT must enter the treatment room to move the imaging arm on Varian linacs, this is essential to quality treatment and image interpretation. As the imaging field size can be determined at creation of the DRR, adhering to these field limits (as should be stipulated in imaging protocols), will aid in successful and meaningful imaging acquired at the linac.

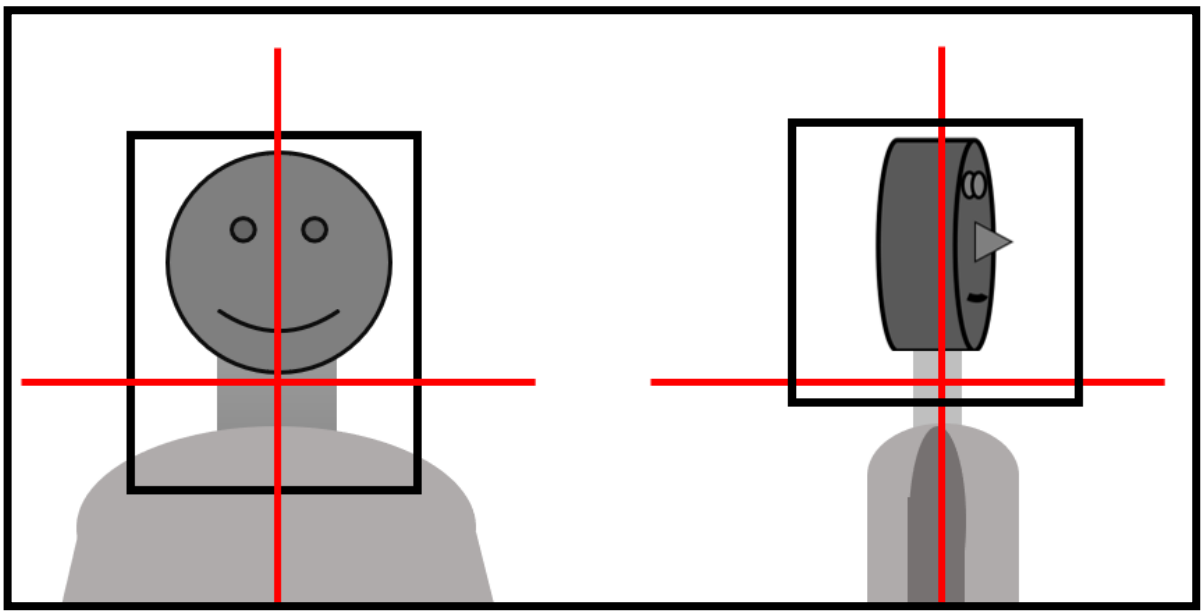

Figure 5.2: Imaging area for the Anterior image (left) and the Lateral image (right) for the patient receiving treatment to both the head and the neck area (illustration produced by author).

5.3.3.6 Imaging margins for patients receiving RT to the head area.

The correct anatomy must be included when creating the imaging field size on the DRR for the patient receiving treatment to the head. Irrespective of the location in the head that will be treated, the whole skull should be included in the reference image field size to enable correct imaging as demonstrated in figure 5.3.

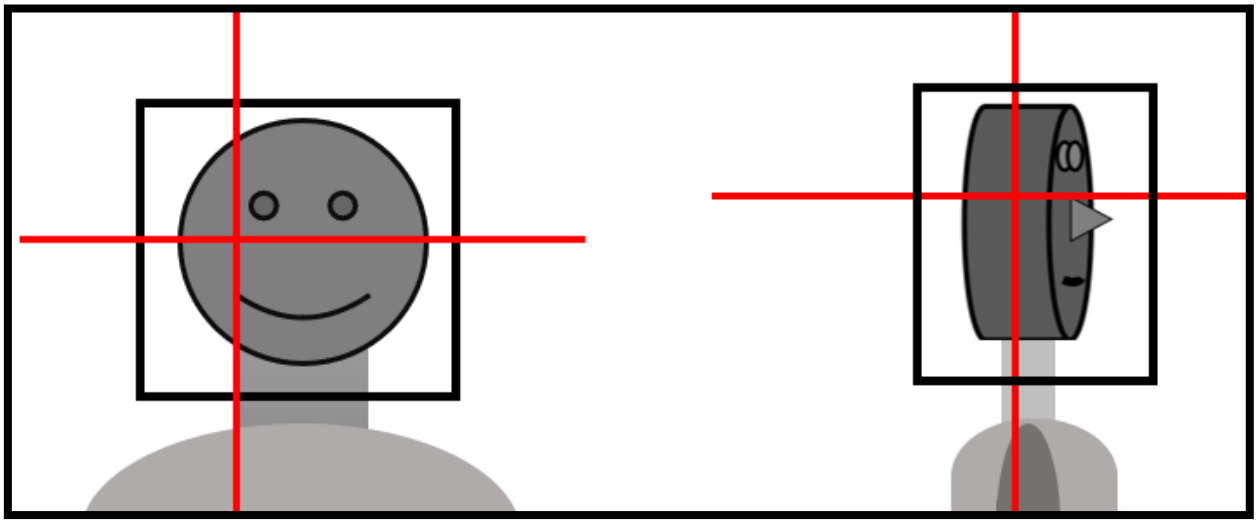

Figure 5.3: Imaging area for Anterior image (left) and the lateral image (right) for patients receiving RT to the head (illustration produced by author).

5.3.4 Contouring on DRR

5.3.4.1 Bi-lateral structure contouring

Reference bony or soft tissue landmarks should be drawn in, on both sides of the structure (as illustrated in figure 5.4) on the DRR due to the interpolation errors that were observed on the EPID images that can lead to errors. This will enable the RTT the opportunity to immediately recognize misalignment and rotational errors when comparing the DRR to the EPID image. This is especially visible when the slice thickness of the CT is large, and interpolation errors occurs. This can lead to incorrect image matching and large inter-observer errors. This observation was discussed in subsection 3.3.1.8.1.

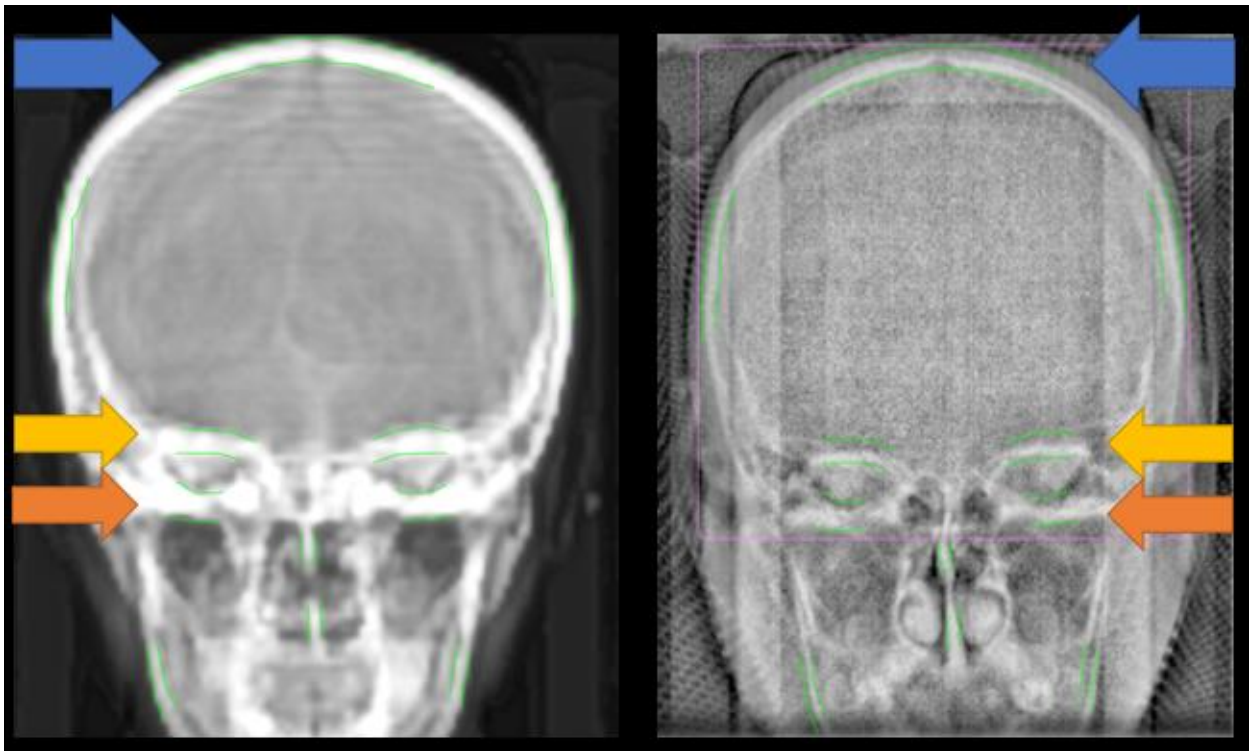

Figure 5.4 Left DRR image, Right EPID image
Blue arrow: Vertex of skull
Yellow arrow: Superior orbital margin
Orange arrow: Oblique and inferior orbital margin
(illustration produced by author)

5.3.4.2 Contouring at least three anatomical structures for each matching direction

At least 3 landmarks must be contoured for each direction such that misalignment can be observed as illustrated in figure 5.5. Therefore, on the anterior image, 3 landmarks will be contoured for the superior to inferior measurement and 3 landmarks for the left to right measurement. On the lateral image, three contours must be contoured for the superior to

inferior measurement and three contours for the anterior to posterior measurement. Some contours can be used for both directional measurements, for example, the orbital bones that are oblique. This finding agrees with the recommendations provided by the Royal College of Radiologists (2008).

There is, however, no limitation on the number of contours that can be drawn. It should however always be considered that contours drawn in on the DRR must be visible on the EPID image as well.

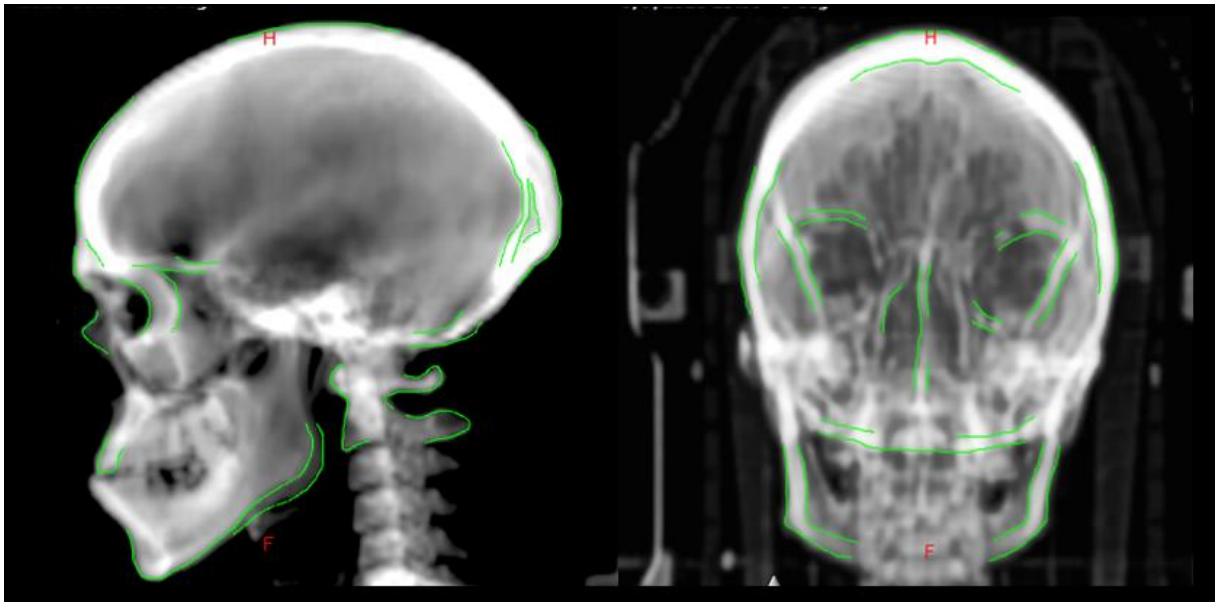

Figure 5.5 Manual contour drawn on the DRR before Portal imaging (illustration produced by author).

5.3.5 EPID image acquisition

5.3.5.1 Double exposure adds little value

The creation of a double exposure adds little value in the complex anatomical site of the head and neck, especially if the planned field size is not completely imaged during portal imaging. Figure 5.6 demonstrates that although a field size has been planned to be imaged, the incorrect positioning of the EPID device leads to the planned area not being imaged. This has a direct impact on the quality of image comparison, as valuable anatomy is not available for image matching. The aim of imaging in the head and neck must always be to have as much anatomy imaged as possible to enable correct image matching. Figure 5.6 demonstrates the shoulders included in the imaging field for a lateral image, where the more superior part of the head would have added more valuable information to the imaging of this patient. Therefore, one large

open field would have provided a valuable overview of the complete area to be matched rather than a double exposure into air.

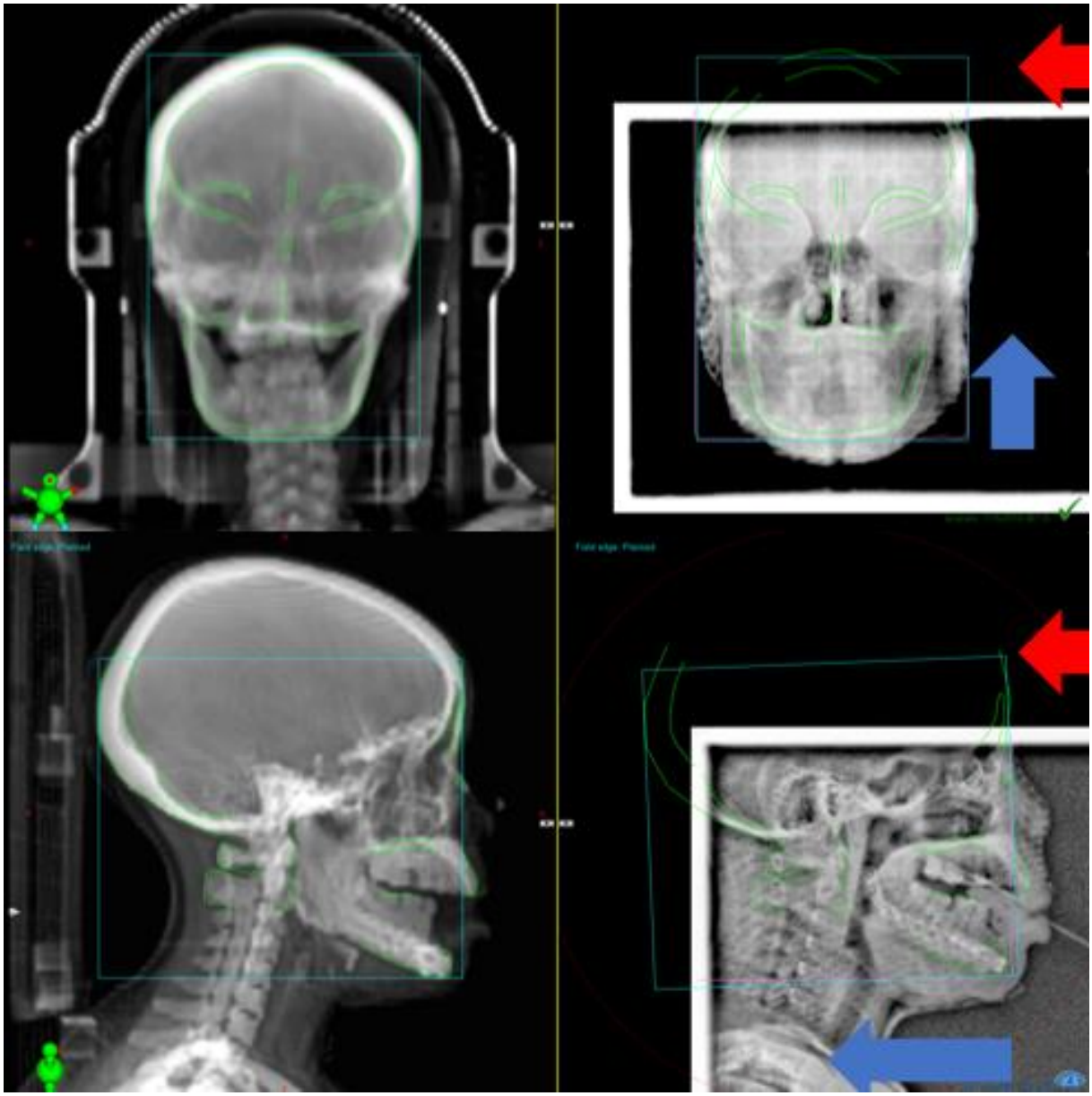

Figure 5.6: Reference DRRs prepared and contoured on the left, and comparable EPID images on the right. The red arrow indicates valuable missing anatomy not imaged and blue arrow indicates imaging information not adding value (illustration produced by author).

5.3.5.2 Include bilateral anatomy on the anterior image

The anterior image acquired on the linac must include total bilateral anatomy of the head of the patient even if the treatment site is unilateral. For patients receiving RT to the head, the whole skull superiorly, as well as the first and second vertebral body and the mandible inferiorly, should be included in the EPID image. If the treatment area involves both the head and the neck, the inferior border must be lengthened inferiorly to the suprasternal notch, and the superior border respectively more inferior than the skull apex. The RTT should strive to

have as much anatomy of the skull included as the imaging field size allows. This was discussed in subsection 3.3.1.8.3. and figures 5.2 and 5.3 illustrate this further.

5.3.5.3 Include anterior, posterior and where possible the vertex on the lateral image

The lateral image acquired must always include all anatomy, both anteriorly and posteriorly. The superior border will be similar to the anterior image, except for the patient receiving RT to both the head and neck area, in which case the inferior imaging field border should be above the shoulder and the superior field border as superior as the field size of the imager allows. This is illustrated in figures 5.2 and 5.3 and discussed in sub-section 3.3.1.8.2.

5.3.5.4 Measure and correct rotation of anatomy

The rotation of the patient's head during image matching can be in a variety of directions. In 2D-2D matching, only 2 types of rotation can be measured. In the presence of any rotation, the risk of inter-observer variability during the matching process is large and this has been observed during data collection. This was discussed in detail in subsection 3.3.1.7. In the absence of a 4D couch, these rotations must be identified and corrected by re-doing the immobilisation of the patient, and re-imaged before continuing with treatment.

5.3.5.5 Standardise and then imaging frequency

As image matching has become easier with the use of DRR contouring, the frequency of imaging on the linac should be increased. This research study used imaging data that was done only once per week, except for the first three fractions, for each patient. Imaging should be increased to enable more accurate treatment set-up verification. As showed by Molana et al. (2018) an increase in imaging frequency and a good correction protocol had a significant reduction in CTV to PTV expansion margins.

It has been noted during data collection that the start of the second phase of treatment, did not have 3 consecutive days of imaging done. Consecutive phases of treatment result in a smaller treatment site, and an increased need to ensure accurate treatment is achieved, as these are the areas of a high tumour burden requiring an increase in radiation dose. As the side-effects of radiation therapy increase over time, when phase 2 of the treatment begins could have an influence on random and systematic error.

5.3.6 Systematic error correction

Systematic errors should be adjusted according to departmental and national protocol. As shown in table 5.1, systematic errors were observed and not adjusted during treatment. Isocentre correction for these patients would have resulted in smaller margins needed for

structure expansions during the planning process. Any adjustments made to the isocentre must as standard protocol be followed by imaging being repeated for another 2 or 3 days in order to verify the reproducibility of the adjusted isocentre.

As the systematic error is multiplied by 2.5 in the van Herk equation, the tolerance for adjustment should be small, and systematic errors of as small as 2mm must be adjusted to adhere to the expansion margins that are used during planning.

Table 5.1: Example of data collected from three patients. Random errors have been greyed, and the systematic errors that should have been adjusted are shown in white areas (Table produced by author)

	Vertical	Longitudinal	Lateral
Patient 1	-0.2	-0.65	-0.2
	0.2	-0.4	-0.1
	0.1	-0.1	-0.2
	0	-0.5	0
	-0.1	-0.6	-0.3
	0	-0.4	-0.1
	0.1	-0.35	-0.3
	0.2	-0.35	-0.3
Patient 2	-0.4	-0.1	0.8
	-0.4	-0.2	0
	-0.4	0	0
	-0.5	-0.1	0.1
	-0.5	0.1	0
	-0.3	-0.1	0
	-0.3	-0.1	0
	-0.6	0.1	0.1
	-0.5	-0.15	0
Patient 3	0.1	-0.2	0.1
	0.1	0	0.5
	0.1	0.1	0.3
	-0.2	0.25	0.4
	0	0.1	0.3
	-0.1	0.2	0.4
	0	-0.1	0.5

5.3.7 Role expansion for RTTs, regular protocol and audit requirements, and further investigations required

5.3.7.1 Current immobilisation devices should be investigated

Large variations were found for patients treated in the head and neck area, and some patients were excluded from this study due to gross mismatch of images. It has been shown in this research study that the immobilisation of this patient population should be investigated, and perhaps an individualised headrest produced for each patient, which could lead to improved immobilisation of the neck and shoulder area. It was suggested by Strbach et.al. (2013) that adding 3-point set-up tattoos onto the body of the patient (inferior of the mask) could be used to improve reproducibility of the neck and shoulder area of patients.

5.3.7.2 Strict imaging protocols should insure that all imaged data are evaluated and approved

During data collection it was found that many images were not matched and when guiding contours were used, it was unclear what they were. Workflow changes such as peer review image matching, might be needed to address this.

5.3.7.3 Imaging protocols should stipulate exact anatomical contours needed on DRR's for each treatment site

Guiding contours to be used should be clearly stated per treatment site in image-matching protocols. This will enable unambiguous and consistent matching decision making. During this study, it was noted that on some patients' DRRs, contours were drawn, but there were very few, and inconsistent. Refer to figure 3.16 for clinical examples found during data collection.

5.3.7.4 RTT role expansion as imaging specialist is needed

Image interpretation for patient positioning verification has become a field of speciality for radiation therapists. The traditional orthogonal imaging has evolved into oblique imaging utilising ExacTrac (Brainlab, 2013) and CT imaging using cone beam CT, that needs to be compared to the original planning data. This complex process lends a high level of responsibility as the interpretation of these verification images has a direct impact on the resultant treatment accuracy and success. Not only is it important to evaluate the images, but also to interpret and understand the adjustments needed to the patient to correct certain errors. As the RTT utilise this technology on a daily basis, they are more accustomed to the use and interpretation thereof than the radiation oncologist that only on occasion has to view linac based imaging.

Especially in teaching institutions, such specialists could assist in teaching of junior RTTs, students and oncology registrars. They will also be able to easily implement correction

strategies to increase treatment accuracy and have a direct impact on the size of the CTV to PTV expansion margins and ensuring improvements in the size of these margins.

This expansion in the scope of practice for the RTT will have a direct impact on the quality of care as the accuracy of the treatment determines the outcome of the intended radiation therapy.

This specialisation of the RTT professional and empowerment of practice can potentially result in significant operational advantages. The shortage of radiation oncologists means that this field of specialisation for RTTs would result in the radiation oncologist having to attend to certain current operation requirements, for example image queries and approvals, less frequently. This would potentially lead to a optimised workflow, and efficient patient care.

5.3.7.5 RTT skills auditing

The skill of RTTs must be audited by a peer review process (Royal College of Radiologists, 2008). This is a tool to ensure a high quality of patient treatment accuracy is consistently applied by all staff. A skills audit also aids in staff education. Skill audits can be managed by RTT imaging specialists.

5.3.7.6 Yearly imaging audits of set-up accuracy

Yearly audits of set-up accuracy should be performed for each treatment unit and it is a good tool to verify that the correct expansion margins are used for this patient population. The whole research process in sub-question 1 detailed in this thesis is an example of how a peer-reviewed yearly audit can be performed to ensure that there is a consistent quality of care to the patient.

This research study has shown the great value of independently matching each data set, and not just recording matching results retrospectively, as it has been found that many images were not accurately matched.

5.3.7.7 Rotational errors should be investigated

Although rotational measurements were not included in the calculations for sub question 1, in this thesis, the amount of rotational errors observed and measured as seen in appendices A and B where all measured offsets are listed, are noted with concern. This needs to be investigated further, as these errors will have a larger further expansion of margins.

However, rotational errors can only be clearly verified and measured if enough anatomy is included in each imaging session. Therefore, it is again recommended to ensure the correct anatomical data in each verification image. When present, it should be corrected by re-set up of the patient.

Further research should include an investigation of both the head and the neck area individually to investigate the quality of the immobilisation devices currently in use.

As was found during this research study the head and the neck area can rotate in different directions, and therefore the placement of tattoos inferior of the mask system, and the production of an individualised head and neck pillow, could aid in less inter-fraction variability of treatment set-up.

5.4 Conclusion of sub-questions 2 and 3

The study aims for sub-question 2 and 3 was to compare two treatment techniques. This was achieved with the use of 10 patient's planning data. Due to the absence of some of the OAR from the *RA treat* plan set with which all patients were treated, it led to the necessity to create another treatment plan set, called *RA study* with all the necessary OAR data contoured.

This research therefore aimed to compare 3DCRT to VMAT, but further evolved to having data of a third RA plan. The original RA treatment plan the patient received was labelled *RA treat*, as compared to the 3DCRT plan created and a further RA plan that included all OAR, labelled *RA study*.

In the overall comparison of the two planning techniques, it was shown that the OAR sparing is well comparable between the 3DCRT and VMAT groups. It must however be noted that the priority during 3DCRT planning for such complex volumes is the sparing of critical OARs, for example the spinal cord and brainstem due to the high morbidity rate that would occur if these OARs were over irradiated. Great care in the 3DCRT planning is therefore needed, but the dose coverage of the PTV may suffer because of the attention to the planned OARs doses. It was therefore shown that the OAR sparing was similar for the two planning techniques, however the PTV scoring indicated much better treatment of the PTV using VMAT as compared to 3DCRT.

No research studies comparing 3DCRT and VMAT for late stage larynx cancer was found at the time of data collection, but when comparing 3DCRT to IMRT, Ismael et.al. (2020) found that the CI and HI scores indicated that IMRT is the better modality to use. The authors (Ismael & Hassan, 2020) only used the parotid gland dose as an OAR to compare the planning techniques and found that IMRT resulted in less dose to the parotids. Although a different technique was used, these findings are similar to that of this research study.

Lambrechts et al. (2013) retrospectively evaluated long term side effects for patients with late stage SCC in the head and neck and found that those treated with IMRT showed significantly less acute side effects than the 3DCRT group. Interestingly it was also reported when comparing IMRT to VMAT plans for late stage head and neck cancers, that there were

significant benefits in the use of VMAT rather than IMRT both for the OAR and PTV (Holt et al., 2013; Fung-Kee-Fung, 2012). It was also noted that using the VMAT technique decreased the treatment time significantly. The use of VMAT has also decreased the amount of treatment time compared to 3DCRT in this research study, as most VMAT plans had 2 arcs or 4 half arcs, whereas the amount of 3DCRT treatment fields varied from 6 to 16. The exact treatment time has not been measured, but in clinical experience, it has been observed that 2 full arcs are treated in 2 to 4 minutes versus 16 fields can take up to 25minutes. As this research study was done retrospectively, the exact treatment times of each technique fell outside the scope of this study.

In the comparison of the two VMAT plans, it was shown that the additional contours of OARs that were present during the *RA study* group, has led to an increased sparing of these OAR as compared to the *RA treat* group where many OARs were not contoured. It is therefore important to contour all relevant OARs when constructing VMAT plans. Even if these OAR are not constrained, the dose received by these OARs is measurable on the DVH, and it is important for the side-effects predictions included in the consent process with the patient.

The ICRU 83 document (2010) stipulates dose reporting to the PTV as well as to the OAR. It also states the value of reporting the doses to the whole organ (where possible) and therefore to contour complete organs, and not partial organs. Therefore, to record dose to the lungs or brain, the total organ must be CT imaged.

As contouring takes time, it is important to know the OAR that are essential for planning for the late stage larynx patient population. Therefore, when working in a resource limited environment the minimum amount of contours is known. This study indicates that contouring of the brainstem, spinal cord, parotids, cochlear, oral cavity, mandible and TMJ is necessary, and that the lungs are not necessary as they receive very little dose in this scenario.

It has been noted that prescribed textbooks (Barrett et al., 2009; Brady et al., 2011) explain in great detail the contouring of the GTV, CTV and PTV, but neglect to indicate that all OARs should be included in the contouring and planning process for each diagnosis. The OAR contoured are often linked to the side effects expected for the treatment site, and for this contouring atlases has been developed (Sun et al., 2014; Merlotti et al., 2014). They are however not specific to each cancer type, but rather a cancer site. This study indicated exactly which OARs are needed for contouring for late stage larynx cancer, and the importance to do so accurately. During the data collection stage of this study, it was noted that some critical OARs were not contoured for patient treatment plans used for treatment.

The ICRU 83 document (2010) further stipulates that dose reporting should include the PRV and not only to the OAR. The OAR is replaced by the PRV as this structure takes into

consideration all possible inaccuracies during the treatment period. More data are needed to finalize dose constraints to the PRV as well as the margins needed to the PRV in larynx cancer treatment. The field of radiation therapy is also desperately in need of prospective side effects data collection and furthered studies, as the use of IMRT and VMAT is radically changing the dose deposition method compared to 3DCRT as explained in subsection 2.4.4, and figures 2.8 and 2.9.

The dose gradients seen around the PTV when comparing 3DCRT and VMAT plans had had a great influence on the importance of measurable treatment set-up accuracy. Displacement of a few millimetres of the patient receiving RT to the Larynx when treated with 3DCRT could have had a result of a dose decrease to the PTV of only 10 or 20%. But in VMAT, the dose gradients especially between the PTV and the PRV are steep, such that a displacement could have a detrimental effect of dose to the PTV, with large underdosing resulting from the steep dose gradients covering the PTV, and equally so, the high dose (i.e. maximum doses, 100% and 95%) placed directly in the PRV. These dose gradients are demonstrated in figure 5.7 with the use of red and blue annotations. Here it can be seen that the 3DCRT plan has larger dose gradients, and the RA study plan the tightest dose gradients.

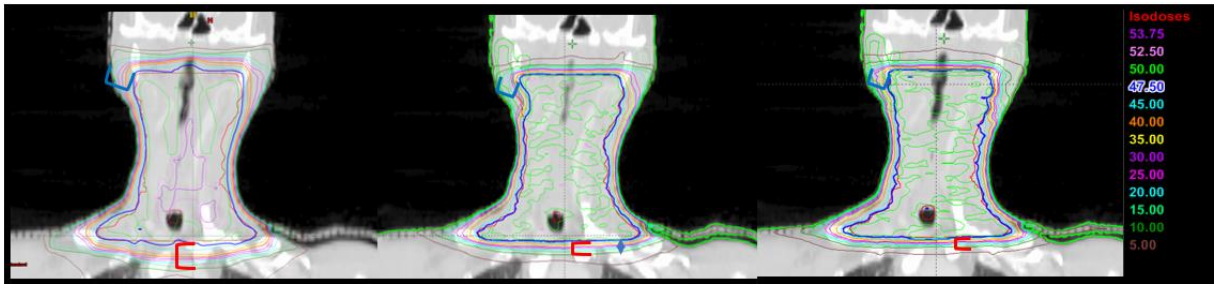

Figure 5.7: The image on the left (3DCRT), middle (RA treat) and right (RA study) indicate different dose gradients (image created by Author)

Many research studies have compared 3DCRT plans with IMRT plans, and IMRT with VMAT, but very few has compared 3DCRT to VMAT. This is quite logical, as historically the clinical use of 3DCRT was followed by IMRT, and IMRT followed by VMAT. There are however many hospitals in Africa, as well as this research institution, where a shift from 3DCRT straight to VMAT has happened, and therefore the need to compare these 2 treatment techniques is valuable for our knowledge base. This is especially so in a complex anatomical area such as the head and neck.

5.5 Recommendations relating to sub-question 2 and 3

5.5.1 Organs at risk

5.5.1.1 Recommended mandatory OAR contours that should be included for advanced stage larynx cancer

This research study has determined that the recommended compulsory OARs to be contoured for the planning of late stage larynx cancers are:

- Brainstem
- Spinal Cord
- Parotids
- Cochlear
- Oral cavity
- Mandible
- Temporomandibular Joint

5.5.1.2 Brainstem and brain contour to be included for one (very high dose) phase of treatment planning

This research study has shown that the brainstem does not standardly receive a dose exceeding the tolerance for patients with multiple dose levels, as the treated volume is reduced as the dose is increased. Consecutive phases of treatment are also mostly to the larynx and adjacent nodal levels that are anatomically located much more inferior to the brainstem.

Where a treatment plan has only one dose level (for example patient 5), when all the dose to the target is delivered in one phase without any reduction in PTV volume, the brainstem dose was significantly elevated. The addition of the brain contour during VMAT planning could also ensure excess dose is not placed in brain tissue adjacent to the brainstem during optimisation.

It is therefore advantageous to minimize dose to the brain and brainstem, by having multiple dose levels for patients with late stage larynx cancer.

5.5.1.3 Lung contours not mandatory for late stage larynx cancer

It has been observed, in this patient population, that the lungs received minimal dose. The research site experiences the challenges of a low to middle income country (LMIC) and under-resourced healthcare system, with time constraints, high patient load and a shortage of skilled staff. It is therefore not essential to include the lung contours for this patient population if external factors prohibit it.

Nevertheless, it would however be thorough to include all tissue receiving dose in the contouring protocol. If dose should be measured to the lungs, the whole extent of both lungs must be present on the planning CT, to ensure correct dose measurements.

5.5.1.4 More prospective research needed for OAR tolerance doses in VMAT planning

There is a great need to prospectively study the patient population at the research site and in South Africa, to verify tolerance dose levels for OARs in the head and neck area. With the high treatment doses utilised in the head and neck area, and the possibilities to achieve this with VMAT planning combined with improvements in immobilisation and imaging, the spread of doses in and around OARs have changed when compared with the spread of dose in 3DCRT.

In VMAT planning, more dose levels need to be investigated for each OAR sparing. For example, it should be investigated if a small part of the parotid glands can tolerate very high doses, that could lead to better PTV dose coverage and a therapeutic gain.

5.5.1.5 Contrast agent administration at CT to be investigated to lesser density of contrast in subclavian vein

The contrast density was demonstrated to be very dense in the treated area especially in the region of the subclavian vein in the same side of the arm where the contrast was injected. The density was much higher than the density tables used in the planning system. It will be advantageous to adjust the contrast timing to enable better contrast distribution throughout the treatment site, that will then have a lesser density and would not need to have timing adjustments. Alternatively, this very dense contrast in the treatment area needs to be accurately contoured and the anatomical density adjusted to the same density as that of the opposing subclavian vain that is contrast free.

5.5.2 Verification of shoulder positioning needs further research

The dose received by the shoulders for both planning techniques emphasize the importance of positioning of the patients' shoulders during treatment. It has been shown in section 4.3.10 that a significant amount of dose will be absorbed in the shoulders. If there is a shift of the shoulders more inferiorly, anteriorly or posteriorly during daily treatment, this will lead to a dose increase in the neck of the patient which in turn will cause an increase of dose to the spinal cord and other OAR's.

Further research is needed regarding the verification of shoulder positioning.

5.5.3 Peer review needed for OAR contouring

During this research study it was found that not all relevant OARs were contoured, or they were contoured incorrectly. Good clinical practice is to ensure that all relevant contours are present for each patient, and a peer review system is in place that can verify the accuracy of the contours. This will add significant value to the quality of the plan and treatment of each patient.

5.5.4 Better OAR sparing demonstrated when they were contoured before planning

It was also demonstrated that the *RA study* group, that was optimised with all OAR contours present achieved more OAR sparing for 7 of the 10 patients as compared to the *RA treat* group. It is therefore important to ensure all OARs are present during the planning phase.

5.5.5 Multiple phases of treatment increase OAR sparing

Although only one of the 10 patients had a single dose level prescribed, the OAR sparing for 3DCRT scored less than both the VMAT plans in this patient, indicating more dose to the OAR for the VMAT plans, but that the PTV coverage was better for the VMAT plan. The total plan score results for this patient were approximately similar across all three plans. This could be an indication that multiple dose levels of RT where the PTV becomes smaller as the dose increases, results in better OAR sparing in VMAT than with 3DCRT.

5.5.6 GTV, CTV and PTV contouring

The RTT is not responsible for the contouring of any tumour volumes. During this research study, only the PTV was contoured for all patients by the radiation oncologist, and the GTV and CTV omitted. This omission makes the planning process extremely difficult for the RTT as it reduces the option of the placement of higher doses in appropriate anatomical areas where the high doses would be advantageous for cancer control.

The meticulous contouring of GTV and CTV, and thereafter an automatic expansion to achieve the PTV, would ensure that the therapeutic margins calculated are applied and the van Herks equation that ensures that 95% of the dose will be achieved in the CTV for 90% of the patients.

5.5.7 3DCRT for late stage larynx cancer

Although the 3DCRT planning technique offers good treatment options in the absence of VMAT, the proximity of the OAR, for example the spinal cord, necessitates the planner to prioritize the limitation of dose to these organs above the dose to the PTV.

It is therefore very important that GTV, CTV and PTV contours are present for 3DCRT planning, as the planner often needs to compromise dose to the PTV to achieve the tolerance doses to the spinal cord and brainstem. Any compromising of the dose to the PTV remains the decision of the combined treatment team and must be discussed in detail between the RTT and radiation oncologist to ensure that the therapeutic aim is achieved.

These plans could offer improved treatment options if more planning phases are used, as the size of the PTV becomes smaller for subsequent plans, allowing the planner more options to limit dose to the OAR. This however greatly depends on the extent of the cancer and is not always possible.

Using the VMAT technique better PTV coverage than 3DCRT can be achieved, and the recommendation is to use VMAT where possible.

5.5.8 Therapeutic indexes are not useful in evaluation of late stage larynx planning

The use of the conformity index and homogeneity index are not useful tools for 3DCRT, but the lesion coverage factor could give the oncologist information regarding the actual volume of the PTV covered by the curative prescribed dose. However, these mathematical calculations cannot replace the actual visualisation of the dose on the axial CT image. The dose on the CT image provides information on the anatomical location of any underdosing of the PTV and the location of the higher doses inside the patient.

Due to the complex shape of the PTV and the proximity of the PTV to the skin in this patient population, the CI and HI seemed not to be a useful tool to evaluate the VMAT plans. All the plans used in this research study were acceptable for patient treatment, but few scored the best results when using these calculation matrixes. These matrixes are very useful for PTV shapes that are found, for example in the abdomen, pelvis and brain, but not for the large volumes and tumour shapes found in certain head and neck cancers and seen in this research study. The flexibility with inverse planning technology can lead to complex trade-offs imbedded in both the algorithm and the physics-based explanation with radiation scatter in the patient related to the dose distribution. The ability to manipulate both the target dose uniformity and

OAR sparing is resulting in a “re-think“ of target dose uniformity and the ability to increase OAR sparing if less emphasis is placed on uniformity of dose inside the PTV (Craft et al., 2016).

Craft et al (2016) stated that in stereotactic radiation therapy and brachytherapy highly non-uniform target doses are acceptable practice. But currently due to historical precedence in the history of 3DCRT dose reporting and the goal for uniformity, these may be compromising our ability to increase OAR sparing.

It is recommended by the researcher to re-think the need for target uniformity, and perhaps place OAR sparing as a higher priority in head and neck planning, due to the excellent target coverage achieved using VMAT.

The lesion coverage factor that uses the actual volume of the target receiving the reference isodose can be much more useful, as this can give a real and direct indication of therapeutic gain.

5.5.9 Plan score results

The discussion in section 4.3 and 4.4 of this score results of the OAR and PTV combined indicated that the VMAT plans are superior to the 3DCRT plans.

It is noted that the unexpected necessity to plan a second VMAT plan where all OARs were present has given an extra interesting comparison of VMAT to VMAT. It is recommended that this could be further explored in future research.

5.6 **Conclusion to this research study**

This research study set out to achieve the comparison of two planning techniques, namely VMAT and 3DCRT at a specific research site. Here the 3DCRT technique was well established and in use for many years, whereas the VMAT technique was introduced as a new planning and treatment technique. This led to this scientific comparison to ensure that the new technique does not do harm, but rather improves treatment protocols and ultimately care to the patient.

With international guidelines for VMAT planning given in the ICRU 83 (2010) documents and the use of the PTV and PRV mandatory, it was also extremely important to know exactly what the expansion margins should be, and therefore sub-question 1, set out to determine what margin should be used.

All the objectives were achieved in this research study, and it is hoped that the results and discussions can contribute to the knowledge base in radiation therapy, and can be used in the improvement of current protocols, in particular for lower to middle income countries who are at the present time introducing 3DCRT protocols and also moving towards VMAT protocols in radiation therapy.

It is recommended that future population-based studies should include the finer analysis of set-up errors and organ doses utilizing daily treatment image matching. Although the size of the CTV to PTV expansion was calculated, the size of the OAR to PRV expansion is still unclear. Currently the same expansion margins are applied to the OARs, but movable structures present in the head and neck region, for example the lenses, larynx, tongue and lungs, could require different expansion margins which can only be determined with the use of 4DCT. The ICRU 83 (2010) document stipulates that the OAR doses must be applied and recorded for the PRV, and therefore set-up accuracy and re-producibility protocols must be improved in order to keep these expansion margins as small as possible to enable a higher conformity of dose to the tumour.

The addition of daily CBCT will enable researchers to accurately record the actual doses to OARs and to prospectively determine the side effect profiles for all the OARs. This will be particularly useful for this specific patient population of head and neck cancers, as most retrospective tolerance tables originate from Europe and America when 3DCRT was most prominently used. There is the need to research these tolerance levels in our specific patient population and in the setting of VMAT with steeper dose gradient. This will greatly enhance the oncology team's ability to predict side effects and knowledge in placing access dose during VMAT planning in the correct anatomical areas to limit long term side-effects.

Dose gradients achieved in VMAT emphasise accuracy in treatment as high doses are conformed around the PTV and high dose gradients constrain high dose levels away from OARs. Both these factors could have significant consequences during set up errors resulting in extremely high doses in the OAR and extremely low dose into the PTV.

List of References

Agazaryan, N., Chow, P., Lamb, J., Cao, M. & Raldow, A. 2020. The Timeliness Initiative: Continuous Process Improvement for Prompt Initiation of Radiation Therapy Treatment. *Advances in Radiation oncologyadiation oncology*, 5: 1014–1021.

AJCC. 2018. *AJCC Cancer Staging Manual, 8th edition*.

AJCC. 2010. *AJCC Cancer Staging Manual 7th Ed*. 7th ed. A. Edge, Stephen.B, April, Fritz, G., Byrd, David, R., Green, Frederick, L., Compton, Carolyn, C., Trotti, ed. Springer.

Ali, I., Tubbs, J., Hibbitts, K., Algan, O., Thompson, S., Herman, T. & Ahmad, S. 2010. Evaluation of the setup accuracy of a stereotactic radiotherapy head immobilization mask system using kV on-board imaging. *journal of applied medical physics*, 11(3): 26–37.

Alimonte, L.D., Holden, L., Turner, A., Erler, D., Sinclair, E., Harnett, N. & Prospero, L. Di. 2017. Advancing Practice , Improving Care the Integration of Advanced Practice Radiation Therapy Roles into a Radiotherapy Department : A Single Institution Experience. *Journal of Medical Imaging and Radiation Sciences*, 48(2): 118–121. http://dx.doi.org/10.1016/j.jmir.2017.02.073.

Ang, K., Trotti, A., Brown, B., Garden, A. & Et.al. 2001. Randomized Trial addressing risk Features of Surgery and Time Factors of Surgery plus Radiotherapy in Advanced Head-and-Neck Cancer. *International Journal of Radiation Oncology, Biology, Physics*, 51(3): 571–578.

Anon. 1948. Varian Medical Systems, Inc.

Augusto, G., Nogueira, S., Lourenc, G.J., Borges, C., Oliveira, M., Augusto, F., Marson, L., Lopes-aguiar, L., Francislaine, E., Costa, D., Regine, T., Lima, P., Liutti, V.T., Leal, F., Castro, V., Santos, A. & Rinck-junior, A. 2015. Association between genetic polymorphisms in DNA mismatch repair-related genes with risk and prognosis of head and neck squamous cell carcinoma. *International Journal of Cancer*, 137: 810–818.

Babic, S., Lee, Y., Ruschin, M., Lochray, F., Lightstone, A., Atenafu, E., Phan, N., Mainprize, T., Tsao, M., Soliman, H. & Sahgal, A. 2018. To frame or not to frame ? Cone-beam CT-based analysis of head immobilization devices specific to linac-based stereotactic radiosurgery and radiotherapy. *Journal of applied clinical medical physics*, 19(2): 111–120.

Bahl, A., Sharma, S.C., Ghosal, S., Kapoor, R. & Bhattacharya, T. 2012. Clinical Implications of Thermoplastic Mask Immobilization on Acute Effects of Radiotherapy in

Head and Neck Cancers. *Journal of Postgraduate Medicine, Education and Research*, 46(4): 187–189.

Barrett, A., Dobbs, J. & Roques, T. 2009. *Practical Radiotherapy Planning Fourth Edition*. http://books.google.com/books?id=kdtGzT62rvQC&pgis=1.

Baskar, R., Lee, K.A., Yeo, R. & Yeoh, K.W. 2012. Cancer and radiation therapy: Current advances and future directions. *International Journal of Medical Sciences*, 9(3): 193–199.

Bentzen, S.., Constine, L.S., Deasy, J.., Eisbruch, A., Jackson, A. & Marks, L.B. 2010. QUANTEC_Summary_2010. *International journal of radiation oncology, biology and physics*, 76(3): Table 1.

Bhattacharyya, K.B. 2016. Godfrey Newbold Hounsfield (1919–2004)_ The man who revolutionized neuroimaging. *Annals of Indian Academy of Neurology*, 19(4): 448–450.

Bhide, S. & Nutting, C. 2010. Recent Advances in Radiotherapy. *BMC Medicine*, 8(25): 1–5. http://www.biomedcentral.com/1741-7015/8/25.

Boffetta, P., Hayes, R.B., Sartori, S., Lee, Y.-C. & Muscat, J. 2016. Mouthwash use and cancer of the head and neck a pooled analysis from the International Head and Neck Cancer Epidemiology Consortium. *Euopean Journal of Cancer Prevention*, 25(4): 344–348.

Boyle, P. & Levin, B. 2008. *World Cancer report 2008*.

Brady, L.., Heilmann, H.., Molls, M. & Nieder, C. 2011. *Decision making in radiation oncology. Volume 1*. 1st ed. M. Brady, L.W., Heilmann, H.P., Molls, ed.

Brainlab. 2013. Exactrac Image-guided radiotherapy ®. : 1–12. https://www.brainlab.com/wp-content/uploads/2014/01/Brochure-ExacTrac.pdf.

Cancer in South Africa 2003-2014 Full Report. 2014. Cancer in South Africa 2003-2014 Full Report. *National Cancer Registry*. http://www.nicd.ac.za/centres/national-cancer-registry/cancer-statistics/ 4 November 2019.

Carol, M., Grant III, W., Pavord, D., Eddy, P., Targovnik, H., Butler, B., Woo, S., Figura, J., Onufrey, V., Grossman, R. & Selkar, R. 1996. Initial Clinical Experience with the Peacock Intensity Modulation of a 3-D Conformal Radiation Therapy System. *Stereotactic Functional Neurosurgery*, 66: 30–34.

Chamberlain, D.D., Yu, J.B. & Decker, R.H. 2017. *Pocket Guide to Radiation Oncology*.

1st ed. Springer Publishing Company.

Cherry, P. & Duxbury, A. 2009. *Practical Radiotherapy Physics and Equipment*. second. Blackwell Publishing Ltd.

Cho, B. 2018a. Intensity-modulated radiation therapy : a review with a physics perspective. *Radiation Oncology Journal*, 36(1): 1–10.

Cho, B. 2018b. Intensity-modulated radiation therapy: A review with a physics perspective. *Radiation Oncology Journal*, 36(1): 1–10.

Cmelak, A.J., Arneson, K., Chau, N.G., Gilbert, R.W. & Haddad, R.I. 2013. Locally advanced head and neck cancer. *American Society of Clinical Oncology educational book 2013*: 237–244. http://www.ncbi.nlm.nih.gov/pubmed/23714512.

Craft, D., Khan, F., Young, M. & Bortfeld, T. 2016. The Price of Target Dose Uniformity. *International Journal of Radiation Oncology Biology Physics*, 96(4): 913–914.

Cronin, B., Mccarthy, A., Claire, K., Starling, P., Deegan, T., Owen, R., Roberts, L. & Mcquitty, S. 2013. Quality Improvement Investigation for Head and Neck Stabilization in Radiotherapy Using Setup Tattoos. *Journal of Medical Imaging and Radiation Sciences*, 44(2): 92–99. http://dx.doi.org/10.1016/j.jmir.2012.11.002.

Dalvie, S. 2013. Radiotherapy Protocol - Locally Advanced Larynx Cancer. : 1–4.

Deasy, J.O., Moiseenko, V., Marks, L., Chao, K.S.C., Nam, J. & Eisbruch, A. 2010. Radiotherapy Dose-Volume Effects on Salivary Gland Function. *International Journal of Radiation Oncology Biology Physics*, 76(3 SUPPL.): 58–63.

Dequanter, D., Geukens, D., Bailly, J., Shahla, M., Paulus, P. & Lothaire, P. 2011. Is Routine Bilateral Neck Dissection Absolutely Necessary in the Management of N0 CT Negative Neck in Patients with T4 Laryngeal Head and Neck Carcinoma ? *Journal of Cancer therapy*, 2(August): 322–324.

Dieterich, S., Ford, E., Pavord, D. & Zeng, J. 2016. *Practical Radiation Oncology Physics*. 1st ed. Philadelphia: Elsevier.Inc.

Elekta. 2008. Elekta Announces First two Clinical sites using VMAT cancer treatment capability. https://www.elekta.com/press/26c6a25e-4cb3-4b5c-8161-b5fafedbf91c/elekta-announces-first-two-clinical-sites-using-vmat-cancer-treatment-capability/.

Emami, B. 2013. Tolerance of normal tissue to therapeutic irradiation. *Reports of Radiotherapy and Oncology*, 1(1): 35–48.

Feuvret, L., Noël, G., Mazeron, J.J. & Bey, P. 2006. Conformity index: A review. *International Journal of Radiation Oncology Biology Physics*, 64(2): 333–342.

Fleming, I. & Cooper, J.S. 1999. *AJCC Cancer Staging Manual*. 5th ed.

Forastiere, A. a., Zhang, Q., Weber, R.S., Maor, M.H., Goepfert, H., Pajak, T.F., Morrison, W., Glisson, B., Trotti, A., Ridge, J. a., Thorstad, W., Wagner, H., Ensley, J.F. & Cooper, J.S. 2013. Long-term results of RTOG 91-11: A comparison of three nonsurgical treatment strategies to preserve the larynx in patients with locally advanced larynx cancer. *Journal of Clinical Oncology*, 31(7): 845–852.

Fung-Kee-Fung, S.D. 2012. A prospective trial of volumetric intensity-modulated arc therapy vs conventional intensity modulated radiation therapy in advanced head and neck cancer . *World Journal of Clinical Oncology*, 3(4): 57.

Gasinska, A., Denekamp, J., Evans, H., Blakely, E., Travis, E.L., Stewart, F., Dutreix, A., West, C., Olive, P., Turesson, I., Jeggo, P. & Szumiel, I. 2015. The contribution of women to radiobiology : Marie Curie and beyond ☪. *Reports of Practical Oncology and Radiotherapy*, 21(3): 250–258. http://dx.doi.org/10.1016/j.rpor.2015.11.006.

Giraldi, L., Panic, N., Cadoni, G., Bocia, S. & Leoncini, E. 2017. Association between Mediterranean diet and head and neck cancer. *Euopean Journal of Cancer Prevention*, 26.

Glide-Hurst, C., Gopan, E. & Hugo, G. 2010. Anatomical and Pathological Variability during Radiation Therapy for a Hybrid Active Breath Hold Gating Technique. *International Journal of Radiation Oncology Biology Physics*, 77(3): 910–917.

Grégoire, V., Ang, K., Budach, W., Grau, C., Hamoir, M., Langendijk, J. a., Lee, A., Le, Q.T., Maingon, P., Nutting, C., O'Sullivan, B., Porceddu, S. V. & Lengele, B. 2014. Delineation of the neck node levels for head and neck tumors: A 2013 update. DAHANCA, EORTC, HKNPCSG, NCIC CTG, NCRI, RTOG, TROG consensus guidelines. *Radiotherapy and Oncology*, 110(1): 172–181.

Gregoire, V., Lefebvre, L. & Licitra, L. 2010. Squamous cell carcinoma of the head and neck: EHNS-ESMO-ESTRO Clinical Practice Guidelines for diagnosis, treatment and follow up. *Annals of Oncology*, 21(Supplement 5): 184–186.

Grégoire, V., Levendag, P., Ang, K.K., Bernier, J., Braaksma, M., Budach, V., Chao, C.,

Coche, E., Cooper, J.S., Cosnard, G., Eisbruch, A., El-Sayed, S., Emami, B., Grau, C., Hamoir, M., Lee, N., Maingon, P., Muller, K. & Reychler, H. 2003. CT-based delineation of lymph node levels and related CTVs in the node-negative neck: DAHANCA, EORTC, GORTEC, NCIC, RTOG consensus guidelines. *Radiotherapy and Oncology*, 69(3): 227–236.

Gregoire, V., Scalliet, P. & Ang, K.K. 2004. Clinal Target Volumes in Conformal and Intensity Modulated Radiation Therapy-A Clinical Guide to Cancer Treatment.

Guckenberger, M., Meyer, J., Vordermark, D., Baier, K., Wilbert, J. & Fentje, M. 2006. Magnitude and Clinical Relevance of Translational and Rotational Patient Setup errors: A cone-beam CT study. *International Journal of Radiation Oncology Biology Physics*, 65(3): 934–42.

Hadley, S.W., Kelly, R. & Lam, K. 2005. Effects of immobilization mask material on surface dose. *Journal of applied clinical medical physics*, 6(1): 1–7.

Harnett, N, Bak, K., Lockhart, E., Harnett, Nicole, Ang, M., Zychla, L., Gutierrez, E. & Warde, P. 2018. The Clinical Specialist Radiation Therapist (CSRT): A case study exploring the effectiveness of a new advanced practice role in Canada. *Journal of Medical Radiation Sciences*, 65: 86–96.

Health professions act, 1978 (Act no.56). 2016. Health Professions Act: Regulations: Defining scope of profession of radiography. *Government Gazette*, 0001(970): 23–29.

Helal, A. & Omar, A. 2015. Homogeneity Index : Effective tool for evaluation of 3DCRT. *Pan Arab Journal of Oncology*, 8(2): 20–23.

Henderson, D., Tree, A., Harrington, K. & van As, N. 2018. Dosimetric Implications of Computerised Tomography-Only versus Magnetic Resonance-Fusion Contouring in Stereotactic Body Radiotherapy for Prostate Cancer. *Medicines*, 5(2): 32.

Van Herk, M. 2004. Errors and Margins in Radiotherapy. *Seminars in Radiation Oncology*, 14(1): 52–64.

Van Herk, M., Remeijer, P., Rasch, C. & Lebesque, J. V. 2000. The probability of correct target dosage: Dose-population histograms for deriving treatment margins in radiotherapy. *International Journal of Radiation Oncology Biology Physics*.

Herrassi, M.Y., Bentayeb, F. & Malisan, M.R. 2013. Comparative study of four advanced ed-conformal radiation therapy treatment planning techniques for head and neck cancer. *Journal of Medical Physics*, 38(2): 98–105.

Holt, A., Van Gestel, D., Arends, M.P., Korevaar, E.W., Schuring, D., Kunze-Busch, M.C., Louwe, R.J.W. & van Vliet-Vroegindeweij, C. 2013. Multi-institutional comparison of volumetric modulated arc therapy vs. intensity-modulated radiation therapy for head-and-neck cancer: A planning study. *Radiation Oncology*, 8(1): 1–11.

Hong, T., Ritter, M., Tome', W. & Harari, P. 2005. Intensity-modulated radiation therapy : emerging cancer treatment technology. *British Journal of Cancer*, 92: 1819–1824.

IAEA. 2016. *Accuracy Requirements and Uncertainties in Radiothearpy*. Austria: IAEA.

IAEA. 2019. *Introduction of Image Guided Radiotherapy into Clinical Practice*. International Atomic Energy Agency.

ICRU. 1993a. ICRU report 50: Prescribing, recording and reporting photon beam therapy (ICRU report 50). *Journal of ICRU*: 357–360.

ICRU. 1999. *ICRU Report 62: Prescribing , Recording and Reporting Photon Beam Therapy (Supplement to ICRU Report 50)*. 7910 Woodmont Avenue Bethesda, Maryland 20814, U.S.A.

ICRU. 2010a. ICRU Report 83 Prescribing, Recording and Reporting Photon-Beam Intensity-Modulated Radiation Therapy (IMRT). *Journal of the ICRU*, 10(1): 1–35.

ICRU. 2010b. *Prescribing, Recording and Reporting Photon-Beam Intensity Modulated Radiation Therapy (IMRT) (ICRU Report 83)*.

ICRU. 1993b. *Prescribing, Recording and Reporting Photon Beam Therapy*. 7910 Woodmont Avenue Bethesda, Maryland 20814, U.S.A.

Ismael, D.K. & Hassan, F.F. 2020. 3D-Conformal Radiation Therapy and IntensityModulated Radiation Therapy Techniques for Laryngeal Cancer Taking Parotid Glands as Organ at Risk. *Hospital Practices and Research*, 5(1): 10–16. https://doi.org/10.34172/hpr.2020.03.

Izmirli, M., Çakır, T., Avcu, S. & Nart, M. 2016. Impact of contrast agents on dose algorıthms of planning systems. *International journal of Radiation Research*, 14(1): 25–30.

Kanakavelu, N. & Jebaseelan, J. 2016. Determination of patient set-up error and optimal treatment margin for intensity modulated radiotherapy using image guidance system. , 21(2): 505–511.

Kang, H., Lovelock, D.M., Yorke, E.D., Kriminiski, S., Lee, N. & Amola, H. 2011. Accurate positioning for head and neck cancer patients using 2D and 3D image guidance. *Journal of Applied Clinical Medical Physics*, 12(1): 3270.

Khan, F.., Gibbons, J.. & Sperduto, Paul, W. 2016. *Khan's Treatment planning in Radiation Oncology 4th ed.*

Kirkpatrick, J.P., Van der Kogel, A.J. & Schulth Eiss, T.E. 2010. Radiation dose-volume effects in the spinal cord. *International journal of radiation oncology, biology, physics*, 76(3 Suppl): S42-9. http://www.ncbi.nlm.nih.gov/pubmed/20171517.

KlarityMedical. 2013. Klarity product Guide. : 1–32.

Klippel, N., Schmücking, M., Terribilini, D., Geretschläger, A., Aebersold, D.M. & Manser, P. 2015. Improved VMAT planning for head and neck tumors with an advanced optimization algorithm. *Zeitschrift für Medizinische Physik*, 5(2): 1–8. http://linkinghub.elsevier.com/retrieve/pii/S0939388915000574.

Krishnan, J., Rao, S., Hegde, S. & Shetty, J. 2015. A Dosimetric Comparison of Double Arc Volumetric Modulated Arc Therapy with Large Field Intensity Modulated Radiation Therapy for Head and Neck Cancer. *International journal of medical physics, Clinical Engineering and Radiaition Oncology*, 4(November): 353–363.

Kung, J.S., Tran, W.T., Poon, I., Atenafu, E.G., Courneyea, L., Higgins, K., Enepekides, D., Sahgal, A., Chin, L. & Karam, I. 2019. Evaluation of the Efficacy of Rotational Corrections for Standard-Fractionation Head and Neck Image-Guided Radiotherapy. *Technology in cancer research & treatment*, 18: 1–7.

Lambrecht, M., Nevens, D. & Nuyts, S. 2013. Intensity-modulated radiotherapy vs. parotid-sparing 3D conformal radiotherapy. *Strahlentherapie und Onkologie*, 189(3): 223–229. https://doi.org/10.1007/s00066-012-0289-7.

LaMorte, W. 2017. Nonparametric Tests. *Boston University School of Public Health*. https://sphweb.bumc.bu.edu/otlt/mph-modules/bs/bs704_nonparametric/BS704_Nonparametric7.html.

Lee, S., Cao, Y. & Kim, C. 2015. *Physical and Radiobiological Evaluation of Radiotherapy Treatment Plan*. Chapter 5: http://dx.doi.org/10.5772/60846.

Lee, T.F., Yeh, S.A., Chao, P.J., Chang, L., Chiu, C.L., Ting, H.M., Wang, H.Y. & Huang, Y.J. 2015. Normal tissue complication probability modeling for cochlea constraints to avoid causing tinnitus after head-and-neck intensity-modulated radiation therapy.

Radiation Oncology, 10(1): 1–8. http://dx.doi.org/10.1186/s13014-015-0501-x.

Leech, M., Coffey, M., Mast, M., Moura, F., Osztavics, A. & Pasini, D. 2017. ESTRO ACROP guidelines for positioning , immobilisation and position verification of head and neck patients for radiation therapists. *Technical Innovations & patients support in Radiation Oncology*, 1: 1–7.

Lu, H., Lin, H., Feng, G., Chen, J., Shu, L., Pang, Q., Cheng, J., Peng, L., Wu, D., Liao, C. & Mo, Y. 2012. Interfractional and intrafractional errors assessed by daily cone-beam computed tomography in nasopharyngeal carcinoma treated with intensity-modulated radiation therapy: A prospective study. *Journal of Radiation Research*, 53(6): 954–960.

Mackie, T.R. 2006. History of tomotherapy. *Physics in Medicine and Biology*, 51(13): 427–453.

Magram, M., Kommana, H., Mahmoud, F. & Ashlock, R. 2008. The role of PET/CT in the management of laryngeal cancer. *The Journal of Nuclear Medicine*, 49(1): 179.

Maier, H. & Tisch, M. 1997. Epidemiology of laryngeal cancer: results of the Heidelberg control study. *Acta Oto-Laryngologica*, 117: 527.

Mans, A., Wendling, M., McDermott, L.N., Sonke, J.J., Tielenburg, R., Vijlbrief, R., Mijnheer, B., Van Herk, M. & Stroom, J.C. 2010. Catching errors with in vivo EPID dosimetry. *Medical Physics*, 37(6): 2638–2644.

Markou, K., Christoforidou, A., Karasmanis, I., Tsiropoulos, G., Triaridis, S., Constantinidis, I., Vital, V. & Nikolaou, A. 2013. Laryngeal cancer : epidemiological data from Northern Greece and review of the literature. *HIPPOKRATIA*, 17(4): 313–318.

Matsuo, K. & Palmer, B. 2009. Coordination of mastication, swallowing and breathing. *Japanese Association for Dental Science*, 45: 31–40.

Mayo, C., Yorke, E. & Merchant, T.E. 2010. Radiation Associated Brainstem Injury. *International Journal of Radiation Oncology Biology Physics*, 76(3 SUPPL.): 36–41.

Merlotti, A., Alterio, D., Vigna-Taglianti, R., Muraglia, A., Lastrucci, L., Manzo, R., Gambaro, G., Caspiani, O., Miccichè, F., Deodato, F., Pergolizzi, S., Franco, P., Corvò, R., Russi, E.G. & Sanguineti, G. 2014. Technical guidelines for head and neck cancer IMRT on behalf of the Italian association of radiation oncology - head and neck working group. *Radiation Oncology*, 9(1): 1–32.

Molana, S., Arbabi, F., Sanei, M. & Hashemi, E. 2018. Evaluation of Patient setup

Accuracy and Determination of Optimal Setup Margin for External Beam Radiation therapy using Electronic Portal Imaging Device. *Cancer therapy & Oncology International Journal*, 11(2).

Nakata, A., Tateoka, K., Fujimoto, K., Saito, Y., Nakazawa, T., Abe, T., Yano, M. & Sakata, K. 2013. The Reproducibility of Patient Setup for Head and Neck Cancers Treated with Image-Guided and Intensity-Modulated Radiation Therapies Using Thermoplastic Immobilization Device. *International Journal of Medical Physics, Clinical Engineering and Radiation Oncology*, 02(04): 117–124.

NICE. 2018. AlignRT for intracracranial stereotactic radiosurgery. : 1–12.

Nihan, S.T. 2020. Karl Pearsons chi-square tests. *Educational Research and Reviews*, 15(9): 575–580.

Nuyts, S. 2007. Defining the target for radiotherapy of head and neck cancer. *Cancer Imaging*, 7(SPEC. ISS. A): 50–55.

Pelc, N.J. 2015. Recent and Future Directions in CT imaging. *Annals of Biomedical Engineering*, 42(2): 260–268.

Peng, G., Masood, K., Gantz, O. & Sinha, U. 2016. Neuromuscular Electrial Stimulation Improves Radiation-Induced Fibrosis Throuh Tgf-B1/MyoD Homeostasis in Head and Neck Cancer. *Journal of Surgical Oncology*, 114(1): 1–5.

Pfister, D.G., Ang, K.-K., Brizel, D.M., Burtness, B.A. & Busse, P.M. 2012. Head and Neck Cancers. *NCCN Clinical Practical Guidelines in Oncology*, (1.2012): 1–35. http://dx.doi.org/.

Psyrri, A., Seiwert, T.Y. & Jimeno, A. 2013. *Molecular Pathways in Head and Neck Cancer : EGFR , PI3K , and More*. asco.org/edbook.

Richards, M. 2012. National Radiotherapy Implementation Group Report: Image Guided Radiotherapy (IGRT).

Riegel, A.C., Antone, J.G., Zhang, H., Jain, P., Raince, J., Rea, A., Bergamo, A.M., Kapur, A. & Potters, L. 2016. Deformable image registration and interobserver variation in contour propagation for radiation therapy planning. *Journal of Applied Clinical Medical Physics*, 17(3): 347–357.

Royal College of Radiologists. 2008. On target : ensuring geometric accuracy in radiotherapy. : 1–76. http://www.rcr.ac.uk/docs/oncology/pdf/BFCO(08)5_On_target.pdf.

Royal College of Radiologists. 2019. *The timely delivery of radical radiotherapy : guidelines for the management of unscheduled treatment interruptions Fourth edition*. 4th ed.

Sahgal, A., Lo, S.., Ma, L. & Sheehan, J.. eds. 2016. *Image-Guided Hypofractionated Stereotactic Radiosurgery*. CRC Press, Taylor&Francis Group.

Salter, B., Fuss, M., Vollmer, D., Sadeghi, A. & Bogaev, C. 2001. The TALON removable head frame system for stereotactic radiosurgery/radiotherapy: measurement of the repositioning accuracy. *International journal in Radiation onclogy biology physics*, 51(2): 555–62.

Shang, Q., Shen, Z.L., Ward, M.C., Joshi, N.P., Koyfman, S.A. & Xia, P. 2015. Evolution of treatment planning techniques in external-beam radiation therapy for head and neck cancer. *Applied Radiation Oncology*, (September).

Sjogren, E.V., Langeveld, T.P.M. & Baatenburg de Jong, R.J. 2008. CLINICAL OUTCOME OF T1 GLOTTIC CARCINOMA SINCE THE INTRODUCTION OF ENDOSCOPIC CO 2. *Wiley InterScience*, (September): 1167–1174.

Smith, G.L. & Smith, B.D. 2020. Sea Change: A Decade of Intensity-Modulated Radiation Therapy for Treatment of Breast Cancer. *Journal of the National Cancer Institute*, 112(3): 221–223.

Snider, J.W., Kalavagunta, C., Xu, H., Schrum, A., Vadnais, P., Marter, K., Lin, M.H. & Suntharalingam, M. 2015. Bolus Effect of Immobilization Masks in Head and Neck Radiation Therapy Mitigated by Mask Alteration and Dosimetric Optimization for Skin Avoidance. *International Journal of Radiation Oncology,Biology,Physics*, 93(3S): E627–E628.

Storer, D. & Teljeur, E. 2006. A report for National Treasury. : 2–46.

Strbac, B. & Jokic, V.S. 2013. Evaluation of set-up errors in head and neck radiotherapy using electronic portalimaging. *Physica Medica*, 29(5): 531–536. http://dx.doi.org/10.1016/j.ejmp.2012.12.001.

Sun, Y., Yu, X.L., Luo, W., Lee, A.W.M., Wee, J.T.S., Lee, N., Zhou, G.Q., Tang, L.L., Tao, C.J., Guo, R., Mao, Y.P., Zhang, R., Guo, Y. & Ma, J. 2014. Recommendation for a contouring method and atlas of organs at risk in nasopharyngeal carcinoma patients receiving intensity-modulated radiotherapy. *Radiotherapy and Oncology*, 110(3): 390–397. http://dx.doi.org/10.1016/j.radonc.2013.10.035.

Sureka, C.S. & Armpilia, C. 2017. *Radiation Biology for Medical Physicists*.

Tamponi, M., Poggiu, A., Dedola, M.F., Madeddu, R., Carnevale, A., Manca, G., Tola, R., Bona, R., Carai, A., Fundoni, C., Naitana, A., Giordani, N., Aresu, L., Soddu, S., Squintu, S., Marini, P., Conti, M. & Meloni, G.B. 2014. Random and systematic set-up errors in three-dimensional conformal radiotherapy - Impact on planning target volume margins: The experience of the Radiation Oncology Centre of Sassari. *Journal of Radiotherapy in Practice*, 13(2): 166–179.

Teoh, M., Clark, C.H., Wood, K. & Whitaker, S. 2011. Volumetric modulated arc therapy : a review of current literature and clinical use in practice. *The British journal of Radiology*, 84(November): 967–996.

Tolentino, E. de S., Centurion, B.S., Ferreira, L.H.C., Souza, A.P. de, Damante, J.H. & Rubira-Bullen, I.R.F. 2011. Oral adverse effects of head and neck radiotherapy: literature review and suggestion of a clinical oral care guideline for irradiated patients. *Journal of Applied Oral Science*, 19(5): 448–454. http://www.scielo.br/scielo.php?script=sci_arttext&pid=S1678-77572011000500003&lng=en&nrm=iso&tlng=pt 17 July 2015.

Tryggestad, E., Christian, M., Ford, E. & Kut, C. 2010. Inter- and Intrafraction Patient Positioning Uncertainties for Intracranial Radiotherapy: A Study of Four Frameless, Thermoplastic immobilization Strategies Using Daily Cone-Beam CT. *International journal of radiation oncology, biology, physics*, 80(1): 281–290.

UICC. 2014. *Head and Neck Cancer-2014 Revies of Cancer Medicines on the WHO list of Essential Medicines*.

Vaculik, M.F., MacKay, C.A., Taylor, S.M., Trites, J.R.B., Hart, R.D. & Rigby, M.H. 2019. Systematic review and meta-analysis of T1 glottic cancer outcomes comparing CO2 transoral laser microsurgery and radiotherapy. *Journal of Otolaryngology - Head & Neck Surgery*, 48(1): 1–11.

Varian. 2008. Varian Announces Global Clinical Council to Develop RapidArc TM Cancer Treatments. *Oncology*. https://www.varian.com/about-varian/newsroom/press-releases/varian-announces-global-clinical-council-develop-rapidarc.

Varian. Varian Web Page. www.varian.com 21 October 2020.

Verma, M., Sait, A., Senthil Kumar, S., Maria Das, K., Lal, P. & Kumar, S. 2016. An Audit of Setup Reproducibility in Radiotherapy of Head and Neck Cancers. *Journal of Radiation*

and Cancer Research, 7(3): 85.

Videtic, G.M.M. & Woody, N.M. 2015. *Handbook of Treatment Planning in Radiation Oncology*. Second. G. M. M. Videtic & N. M. Wood, eds. Demos Medical Publishing.

Vieira, B., Demirtas, D., Kamer, J.B. Van De, Hans, E.W. & Harten, W. Van. 2019. Improving workflow control in radiotherapy using discrete-event simulation. *DMC Medical Informatics and Decision Making*, 19: 1–13.

Vinod, S.K., Jameson, M.G., Min, M. & Holloway, L.C. 2016. Uncertainties in volume delineation in radiation oncology: A systematic review and recommendations for future studies. *Radiotherapy and Oncology*, 121(2): 169–179. http://dx.doi.org/10.1016/j.radonc.2016.09.009.

Wang, L., Cmelak, A.J. & Ding, G.X. 2018. A simple technique to improve calculated skin dose accuracy in a commercial treatment planning system. , (July 2017): 191–197.

Wild, C., Weiderpass, E. & Stewart, B. 2020. *World Cancer Report 2020*. Lyon.

Wild, C.P. & Steward, B.W. 2014. World Cancer Report 2014. *World Health Organization*.

van Wyk, B., Dumela, K. & Vand der Merwe, D. 2017. Analysis of Set-up Parameters in Head and Neck Patients at the Charlotte Maxeke Johannesburg Academic Hospital (A Review of Current Clinical Practice). *Journal of Integrative Oncology*, 6(1): 1–8.

Yamada, S., Ueguchi, T., Ogata, T., Mizuno, H., Ogihara, R. & Koizumi, M. 2014. Radiotherapy treatment planning with contrast-enhanced computed tomography : feasibility of dual-energy virtual unenhanced imaging for improved dose calculations. *Radiation Oncology*, 9: 1–7.

Zhao, B., Maquilan, G., Jiang, S. & Schwartz, D.L. 2018. Minimal mask immobilization with optical surface guidance for head and neck radiotherapy. *Radiation Oncology Physics*, 19(1): 17–24.

Appendix A: Data collected for Head and Neck image matching

Patient Number	Amount of image sets	Vertical offset (cm)	Longitudinal offset (cm)	Lateral offset (cm)	Anterior Rotation (degrees)	Lateral Rotation (degrees)
1	1	-0.2	-0.25	0	-0.3	0
1	2	-0.1	-0.2	-0.1	0	0
1	3	-0.1	-0.2	-0.1	0	0
1	4	0.2	-0.35	-0.2	0.6	0
1	5	0.2	-0.1	-0.2	-1.8	2.6
1	6	0.4	-0.1	-0.2	-0.7	2.2
1	7	0.1	-0.2	-0.2	-0.7	1.4
2	1	-0.2	0.25	0.1	-1.7	0
2	2	0	0.1	0.1	-2.9	0
2	3	-0.2	-0.1	0.1	-1.1	0
2	4	-0.2	0	-0.1	-1.6	0
2	5	0	-0.1	0.3	-0.1	1.2
2	6	0.1	-0.3	-0.3	-3.2	3.8
2	7	-0.7	-0.7	0.3	-0.6	9
2	8	-1.1	-0.8	-0.3	-5.4	7
2	9	-0.8	-0.1	-0.1	-2.8	1.4
3	1	0.2	0.15	0.2	-0.9	0
3	2	0.2	0.2	0.3	-0.9	0
3	3	0.3	0.1	0	0	0
3	4	0.3	0.2	-0.1	-2.5	0
3	5	0.3	0.2	0.1	-1.1	-2.1
3	6	0.1	0.1	0	-1.3	0
3	7	0.4	0.25	0.1	-0.5	1
3	8	0.2	0.15	0.2	0	0
3	9	0.2	0.1	0	0	0
4	1	0	0	0	0	0
4	2	-0.1	-0.1	0	0	0
4	3	-0.1	0	0	0	0
4	4	-0.1	0.1	0	0	0
4	5	0.1	0	0.1	0	0
4	6	0.1	-0.1	0	-1.5	0
4	7	0.1	-0.1	0.1	0.6	0
4	8	0.2	-0.1	0.1	-0.7	-0.8
5	1	-0.1	0	0.7	0	0
5	2	-0.3	0.15	0.4	-0.9	0
5	3	-0.1	0.1	0.5	0	0
5	4	-0.1	0	-0.2	-1.5	0
5	5	0	-0.1	0.1	-1.1	0
5	6	0.2	0.2	-0.1	-0.6	1.2
5	7	0.2	0.15	-0.2	-0.8	0
5	8	-0.1	-0.1	0.1	0	0
5	9	0.2	0.1	0.2	0	0
5	10	0.1	0.55	0.3	0.7	0.6
5	11	0	0.35	0.1	0	0

Patient Number	Amount of image sets	Vertical offset (cm)	Longitudinal offset (cm)	Lateral offset (cm)	Anterior Rotation (degrees)	Lateral Rotation (degrees)
6	1	-0.1	-0.15	-0.2	-0.8	-1.1
6	2	0	0	-0.1	-0.3	0
6	3	-0.1	-0.3	0	0	-1.9
6	4	0	-0.2	0	0	-2.9
6	5	-0.2	-0.2	0	-0.4	-1.6
6	6	-0.2	0	0.1	-0.2	-1.2
6	7	-0.3	0.1	0	-0.4	-1.5
6	8	-0.4	-0.2	0	-0.8	-1.4
7	1	0.7	0	-0.5	-0.8	1.4
7	2	0.3	0.2	-0.2	0	1.6
7	3	0.1	0.2	-0.1	-1.1	0
7	4	0.2	-0.3	0	0.1	1
7	5	0.1	-0.15	-0.2	0	0
7	6	0.1	-0.2	-0.2	-0.1	0
7	7	-0.1	-0.1	-0.4	-2.1	-1.3
7	8	0	0.15	0	0	0
8	1	-0.2	-0.2	-0.1	0	0
8	2	-0.3	-0.1	0	0	-0.7
8	3	0.2	0	0	-1.2	1.2
8	4	0	-0.2	-0.1	-0.3	0.6
8	5	-0.3	-0.2	0.1	-0.4	-0.9
8	6	-0.2	-0.2	-0.2	-1.4	0
8	7	-0.3	-0.1	-0.2	0.2	0
8	8	0.2	-0.15	-0.5	-0.8	2
8	9	-0.1	-0.1	0	0	0
9	1	0.1	0.3	0.1	-0.8	0
9	2	-0.2	0.4	-0.4	-3.3	-1.3
9	3	0.3	-0.2	-0.3	-3	-0.8
9	4	0	0.35	-0.1	-0.9	0
9	5	-0.1	0.35	0.1	-0.4	-1.3
9	6	-0.1	0.3	-0.2	-0.7	0
9	7	0	0.3	-0.2	-1.4	0
9	8	-0.1	0.4	-0.2	-2.4	-0.9
9	9	-0.1	0.35	0	-0.9	-1
10	1	-0.4	-0.35	0.4	0	-2.6
10	2	-0.3	-0.55	0.4	0	-3
10	3	-0.2	-0.35	0.4	0	-1.9
10	4	-0.4	-0.45	0.5	0	-3.2
10	5	-0.3	-0.4	0.3	-0.4	-2.9
10	6	-0.4	-0.4	0.3	-1.4	-2.8
10	7	-0.4	-0.55	0.4	-0.8	-3.9
10	8	-0.4	-0.55	0.4	-0.5	-3.2

Patient Number	Amount of image sets	Vertical offset (cm)	Longitudinal offset (cm)	Lateral offset (cm)	Anterior Rotation (degrees)	Lateral Rotation (degrees)
11	1	-0.5	0.2	0.35	1.3	0
11	2	-0.3	0.2	0.3	1.4	0
11	3	-0.4	0.3	0.2	0	1.3
11	4	-0.3	0.1	0.4	0	0
11	5	-0.4	0.2	0.1	0	0
11	6	-0.3	0.15	0.3	0	0
11	7	0	0.7	0.1	0	-0.5
11	8	-0.4	0.4	-0.1	0	0
12	1	-0.1	0	-0.1	0.5	0
12	2	0	0.1	0.1	0.6	0
12	3	0	0.4	0	0.6	0
12	4	-0.1	0.1	0	0.5	0
12	5	-0.2	-0.2	0	-1.1	0
12	6	-0.2	0.15	0	0.4	0
13	1	-0.5	-0.35	0.3	0	2.7
13	2	-0.5	0.25	0.1	0	2.8
13	3	-0.7	-0.2	0.2	0	3
13	4	-0.3	-0.15	0.1	1.1	-0.4
13	5	-0.3	0.3	0	0	0
13	6	-0.5	-0.1	0.2	0	0
13	7	0.1	-0.35	0.1	-0.7	1.8
14	1	-0.2	0.25	-0.5	1	0.8
14	2	-0.3	0.1	-0.7	-1.3	0.5
14	3	-0.2	-0.25	-0.4	2.5	0.9
14	4	-0.3	0.1	-0.6	0.7	0.5
14	5	-0.1	0.15	-0.5	1.5	0.6
14	6	-0.1	0.1	-0.5	0.9	0.5
14	7	-0.1	0.15	-0.5	0.7	0.4
14	8	0	0.15	-0.6	0.2	0.6
15	1	0.4	0.1	0.1	-1	-2.1
15	2	0.5	0.2	0.1	-1.4	-2.8
15	3	0.5	0.2	0.2	-1.5	-3
15	4	-0.1	0	0.2	0.2	0.3
15	5	-0.2	0.35	0.3	0.9	2.3
15	6	-0.3	0.35	0	-0.9	2.9
15	7	0	0.15	0.2	1.1	1
15	8	0	0.1	0.2	0	0

Patient Number	Amount of image sets	Vertical offset (cm)	Longitudinal offset (cm)	Lateral offset (cm)	Anterior Rotation (degrees)	Lateral Rotation (degrees)
16	1	-0.3	-0.3	0.4	0	-0.7
16	2	0.1	0.25	0	-0.9	-1.4
16	3	0	0.2	0	-1.6	-1.1
16	4	-0.4	-0.25	0.1	-1.5	-1.2
16	5	-0.2	-0.25	0.1	-1.8	-0.9
16	6	0.2	0.1	0.1	0	-1.8
16	7	0.4	-0.2	-0.1	0.4	-2.3
16	8	0	-0.25	-0.1	0	0
16	9	0.2	-0.34	0	-0.5	-1.5
16	10	0.3	-0.25	-0.1	0	-1.6
17	1	-0.3	0.4	0.2	0.9	-1.2
17	2	-0.1	0.6	-0.2	-0.5	-1.7
17	3	0	0.25	0.3	2.1	1.1
17	4	-0.2	0.4	0.2	1.6	-0.9
17	5	-0.4	0.4	0	0.8	-1.1
17	6	-0.3	0.25	0.1	1.7	-0.5
17	7	-0.4	0.35	0.2	1.3	-0.6
17	8	-0.8	0.35	0.1	1.4	-2.2
18	1	0	0.2	0	-1.1	0
18	2	-0.3	0.3	0	-1.1	0.6
18	3	-0.2	0.2	0	-0.7	1.7
18	4	0	0	0.1	1	0.5
18	5	0	-0.1	0	0	0.4
18	6	-0.2	0.1	0	-0.3	1.3
18	7	0.3	0.45	0	-0.5	1
18	8	0	0.3	0	0.9	1.1
19	1	0	0.35	0.3	1.3	0
19	2	-0.1	0.2	0.3	1.7	-1.5
19	3	-0.1	-0.2	0.4	1.3	-1.8
19	4	0	-0.1	0.3	1.4	-1.7
19	5	-0.1	-0.1	-0.1	-1	-0.29
19	6	0	-0.1	0.3	2.5	0
19	7	-0.1	-0.45	-0.1	-0.7	0
19	8	-0.1	-0.4	-0.1	0	0
19	9	0	-0.1	0.2	3.3	0
19	10	-0.4	-0.3	-0.1	0	2.5
19	11	-0.2	-0.3	-0.1	0.4	2

Patient Number	Amount of image sets	Vertical offset (cm)	Longitudinal offset (cm)	Lateral offset (cm)	Anterior Rotation (degrees)	Lateral Rotation (degrees)
20	1	-0.3	-0.1	0.2	0.8	1.8
20	2	-0.2	-0.1	0.1	0	1.2
20	3	-0.3	0.1	0	-0.1	2.1
20	4	0.1	0.15	0	0.5	1.8
20	5	0	0.45	-0.1	0	3.3
20	6	0.2	-0.4	0.1	-1.1	0
20	7	0.4	-0.4	0.2	-0.1	0
20	8	0.3	-0.2	0.4	2	-1.4
20	9	0.2	0.1	0.2	0	0.5
20	10	0.1	-0.2	0.3	0	0.8
21	1	-0.2	0.4	-0.4	-2.1	-1
21	2	-0.1	0.3	-0.6	-2.7	0
21	3	0.2	0.75	-0.7	-1	-1.9
21	4	-0.5	0.5	-0.7	-1.8	2.1
21	5	-0.4	0.6	-0.7	-2.2	0
21	6	-0.6	0.8	-0.5	-0.7	2
21	7	0	0.5	-0.3	0	-2
22	1	-0.3	-0.1	-0.2	-0.7	0
22	2	-0.2	0	-0.3	-1.1	0.4
22	3	-0.3	0.1	-0.6	-2.8	0
22	4	-0.2	-0.1	-0.4	-0.9	0
22	5	-0.4	-0.15	-0.3	-1.3	-2.1
22	6	-0.4	-0.2	-0.3	0	-1.8
22	7	-0.6	-0.2	-0.1	0	-3.4
22	8	-0.4	0.2	-0.1	-1	-1.6
23	1	-0.1	-0.4	0.2	-0.1	0
23	2	-0.2	-0.4	0.4	0	0
23	3	-0.2	-0.4	0.4	0	0
23	4	-0.2	-0.1	0.4	0	0
23	5	-0.6	0.15	0	-1.1	-2.7
23	6	-0.1	0.1	0	-1.8	-0.7
23	7	-0.3	0	0.1	-0.8	-1.4
23	8	-0.6	-0.3	0.2	0.5	-3
23	9	-0.3	-0.85	0.3	0.6	-1.5
24	1	0	0.6	-0.1	0	0
24	2	0	0.45	-0.1	0	0
24	3	-0.1	0.45	0	0.9	0
24	4	-0.1	0.3	0.3	1.8	-0.6
24	5	0.1	0.25	-0.1	-0.3	0.8
24	6	-0.1	0.5	0.1	2.4	0.8
24	7	-0.1	-0.2	-0.1	1.3	-1.3
24	8	-0.2	-0.5	0	0.7	-1.1
24	9	-0.4	0.25	0	0.9	-1.5

Patient Number	Amount of image sets	Vertical offset (cm)	Longitudinal offset (cm)	Lateral offset (cm)	Anterior Rotation (degrees)	Lateral Rotation (degrees)
25	1	0.3	0.3	-0.3	-1.1	1.5
25	2	0	0.45	-0.4	0	-1.2
25	3	0.1	0.2	-0.3	1	0
25	4	-0.1	0.4	-0.4	0.7	-1.1
25	5	0	0.25	-0.4	-0.2	0
25	6	0.4	0.15	-0.2	0.6	0.8
25	7	-0.2	0.3	-0.5	-0.1	0
25	8	-0.2	0.3	-0.5	-0.8	-1.5
26	1	-0.6	-0.1	0	0	-1.9
26	2	-0.5	-0.1	-0.1	-0.6	0
26	3	-0.3	-0.3	0.1	1.5	0.8
26	4	-0.1	-0.5	-0.1	-0.6	0
26	5	-0.5	-0.2	0.3	2.3	-1.9
26	6	-0.2	-0.2	0.3	2	0
26	7	-0.7	0.4	0.1	0	-2.1
27	1	-0.2	-0.15	-0.2	-1.7	-1.5
27	2	-0.2	-0.1	0	0.2	0
27	3	0	-0.1	0.1	-0.4	0
27	4	-0.1	-0.1	0.2	0	-0.9
27	5	0	-0.1	-0.1	-0.6	0
27	6	-0.2	-0.3	-0.1	-1.9	0
27	7	-0.2	-0.15	0	-1.9	0
28	1	0.3	0.3	-0.4	-1	-1.7
28	2	-0.1	0.25	-0.4	0	-1.2
28	3	0.2	0.2	-0.3	1	0
28	4	-0.1	0.4	-0.4	0.7	-1
28	5	0	0.25	-0.4	-0.2	0
28	6	0.4	0.15	-0.3	0.8	-1.2
28	7	-0.2	0.3	-0.5	-0.1	-0.8
28	8	-0.2	0.3	-0.6	-0.8	-1.2
29	1	-0.1	0.1	0	0	0.6
29	2	0.1	-0.1	0	0.6	0
29	3	-0.1	0.1	0	0	0.5
29	4	-0.1	0.1	0.4	2.3	0
29	5	-0.1	-0.2	0.2	1.4	0
30	1	-0.3	-0.2	-0.2	-1.4	-1.5
30	2	-0.1	-0.2	-0.1	-1.1	0.8
30	3	-0.3	-0.35	0	-0.4	-1.3
30	4	-0.2	-0.35	0	-0.9	-0.9
30	5	0.1	-0.35	0	-1.6	0.6
30	6	-0.3	-0.15	-0.1	-2.3	-1.2
30	7	-0.2	-0.3	0	-0.9	-0.9
30	8	-0.2	-0.25	0.1	-1	1.1

Patient Number	Amount of image sets	Vertical offset (cm)	Longitudinal offset (cm)	Lateral offset (cm)	Anterior Rotation (degrees)	Lateral Rotation (degrees)
31	1	-0.3	-0.15	0	0	-1.9
31	2	-0.1	-0.35	0.1	0.8	-1
31	3	0	-0.1	0.1	0	-0.6
31	4	0	-0.15	0.1	0.9	-1.3
31	5	0.1	0.15	0.1	1.7	0.9
31	6	0.1	0	0.1	0.6	0
31	7	-0.1	0	0.1	1.2	-1.1
31	8	-0.1	0.15	0.2	0.8	1.1
32	1	-0.2	0.25	0.3	0.1	-1
32	2	-0.1	0.4	0.3	-0.8	0
32	3	-0.2	0.1	0.2	-0.5	-1.1
32	4	0	0.3	0.3	-0.5	0
32	5	0	0.35	0.1	-0.3	-0.6
32	6	-0.2	0.25	0.1	-0.4	-0.4
32	7	-0.1	0.4	0.3	0	0
32	8	0	0.1	0.2	0	0
32	9	-0.1	-0.1	0.3	0	0
33	1	0	-0.3	0.1	0	-0.9
33	2	-0.2	-0.15	0	1	0
33	3	-0.2	-0.45	0.1	0	-1
33	4	-0.1	-0.15	0.2	0.5	0
33	5	-0.1	-0.2	0.5	1.6	-0.5
33	6	-0.1	-0.5	0.3	0	-0.6
33	7	0	-0.3	0.1	0	0
33	8	-0.1	0.1	0.1	-0.8	-0.7
33	9	0	-0.3	0	-0.7	-1.8

Appendix B: Data Collected for Head image matching

Patient Number	Amount of image sets	Vertical offset (cm)	Longitudinal offset (cm)	Lateral offset (cm	Anterior Rotation (degrees)	Lateral Rotation (degrees)
1	1	-0.1	0.2	0.2	1.2	1.8
1	2	-0.1	-0.1	0.4	1	-1.6
1	3	-0.1	-0.15	0.2	1	-1.8
1	4	-0.1	0.2	0.2	0	-2.2
1	5	-0.1	0	0.2	0	-2
1	6	-0.1	0.15	0.1	0.9	-1.5
1	7	-0.1	-0.1	0.2	0.5	-0.8
2	1	-0.5	0	0.1	0	-2.4
2	2	-0.4	0.35	0	-0.5	-2.2
2	3	-0.5	0.4	0.1	0	-1.6
2	4	-0.4	0.1	-0.1	0	-2.8
2	5	-0.4	0.35	0.1	0	-1.9
3	1	0	0.3	0.2	0	-5.4
3	2	-0.2	0.05	-0.1	0.5	-2.3
3	3	-0.1	0.2	0	-0.2	0
3	4	0	-0.1	-0.2	0.6	-2
3	5	0	0.15	-0.2	1.4	-4.1
3	6	-0.1	0.1	-0.2	-1.3	-1
3	7	0.1	0	0.4	0.4	0
3	8	-0.1	0.1	0	1.5	0
4	1	0.1	0.45	-0.1	-1	0.9
4	2	0.1	0.15	-0.2	-1.4	0
4	3	0	0.2	-0.1	-2	0
4	4	0	0.25	0	0	1.5
4	5	0.1	-0.15	-0.2	-1.2	0
4	6	0.1	0.1	-0.2	-2	-1.3
4	7	0	0.25	-0.2	-2.9	-1
5	1	-0.2	-0.2	-0.1	0	1
5	2	0	0.1	0.1	-0.8	-1.3
5	3	-0.2	0.1	0	0	-2.6
5	4	-0.2	-0.1	0	-1.6	0
5	5	-0.3	0.1	0.1	-0.3	0
5	6	-0.3	0.1	0.1	0.7	0
5	7	0	-0.1	0	0	0

Patient Number	Amount of image sets	Vertical offset (cm)	Longitudinal offset (cm)	Lateral offset (cm	Anterior Rotation (degrees)	Lateral Rotation (degrees)
6	1	-0.2	-0.65	-0.2	0	0
6	2	0.2	-0.4	-0.1	0	0
6	3	0.1	-0.1	-0.2	0	1.6
6	4	0	-0.5	0	-0.7	1.6
6	5	-0.1	-0.6	-0.3	0	1.4
6	6	0	-0.4	-0.1	0	1.2
6	7	0.1	-0.35	-0.3	0	0
6	8	0.2	-0.35	-0.3	-0.3	0
7	1	-0.1	0	0	0	0
7	2	0	0	0.2	0	0.6
7	3	0	-0.2	0.3	0	0.7
7	4	0	-0.1	0.1	0	0.4
7	5	0	0	0.2	0	0
7	6	0	-0.25	0.2	0	0
7	7	0	0	0	0.6	-1.1
8	1	-0.1	-0.1	0.1	-0.9	-0.9
8	2	0	0.4	0.1	-1.3	2.9
8	3	-0.1	0.2	0	-1.4	1.4
8	4	-0.1	0.3	0.1	-1.5	4.5
8	5	-0.1	-0.4	-0.1	-2	4.8
8	6	0	0.3	-0.1	-2	1.9
8	7	-0.1	0.25	0	-1.5	1.2
9	1	-0.4	-0.1	0.8	0.7	-3.5
9	2	-0.4	-0.2	0	0.7	-4.1
9	3	-0.4	0	0	0	-2.4
9	4	-0.5	-0.1	0.1	0	-2.3
9	5	-0.5	0.1	0	0	-4.4
9	6	-0.3	-0.1	0	0.8	-4.8
9	7	-0.3	-0.1	0	1.1	-4
9	8	-0.6	0.1	0.1	0.2	-4.6
9	9	-0.5	-0.15	0	0.8	-3.7
10	1	0.1	-0.7	0.3	0.3	-2.6
10	2	0.1	-0.3	0.1	-1.5	0.9
10	3	-0.1	-0.25	0.3	0	-1.3
10	4	0.1	-0.3	0.2	-1.9	-1.4
10	5	0.1	-0.35	0.2	0	-1.4
10	6	0.2	-5.5	0.2	-0.7	-1.3
10	7	0.1	-0.45	0.2	-0.7	-1.1

Patient Number	Amount of image sets	Vertical offset (cm)	Longitudinal offset (cm)	Lateral offset (cm	Anterior Rotation (degrees)	Lateral Rotation (degrees)
11	1	0	-0.1	0.1	0	1.4
11	2	0.1	0	-0.1	-0.8	0
11	3	-0.1	0.3	0	0	2.4
11	4	0	-0.2	0	-0.9	0
11	5	0	-0.1	-0.1	-1.4	0
11	6	0	0	0.1	0	1
11	7	0.1	0.15	0.1	0	-0.8
11	8	0.1	-0.1	0	-0.7	0
11	9	0.1	-0.1	-0.1	0	-0.9
12	1	0	0.4	-0.1	0	0
12	2	0.3	0	-0.3	0	-1.1
12	3	0	0.1	-0.3	0	0
12	4	-0.3	0.1	-0.3	0	1.6
12	5	-0.1	-0.1	-0.3	-0.6	1.5
12	6	-0.3	0	-0.3	-1.3	2
12	7	-0.1	0.1	-0.3	0	0
12	8	-0.2	0.3	-0.3	0	0
13	1	-0.1	0.2	0.3	0	0
13	2	-0.1	0.1	0.3	0	-2.1
13	3	0	0.2	0.3	-1.4	0.9
13	4	0	0	-0.3	-1.7	-1.2
13	5	-0.1	0.1	-0.3	-2.6	0.9
13	6	-0.1	0.2	-0.3	-1.3	2
13	7	-0.1	-0.1	-0.3	0	0
13	8	-0.1	0.15	-0.3	-0.8	0
14	1	0	0.15	0.1	0	0
14	2	0	0.25	0.2	0.7	0
14	3	0.1	0.1	0	-1.5	0
14	4	0.1	0.2	0.1	-0.3	0
14	5	0	0.15	0	0	0
14	6	0.1	0.2	-0.1	-1.6	0
14	7	0.1	0.15	-0.2	-1.4	0
14	8	0	0.3	0	-1	1.7
15	1	0	-0.1	0.2	0	0
15	2	0.1	0.4	0.4	0	0
15	3	0.2	0.2	0.3	0	1.2
15	4	0.1	0.35	0.2	0	0
15	5	0.3	0	0.1	-1	0.5
15	6	0	-0.1	0.1	0	0
15	7	0.3	0.2	0.1	0	0.5
15	8	0.1	0.2	0.1	0.2	0
15	9	0.3	0.1	0	0	1.3

Patient Number	Amount of image sets	Vertical offset (cm)	Longitudinal offset (cm)	Lateral offset (cm	Anterior Rotation (degrees)	Lateral Rotation (degrees)
16	1	-0.1	0.1	-0.1	-0.8	-1.3
16	2	-0.1	-0.25	0.2	0	0
16	3	0	0.1	0	-1	0
16	4	-0.1	-0.15	0.1	0	-0.9
16	5	-0.2	-0.1	0.1	-1.3	-1
16	6	-0.1	0.1	0.1	-0.6	-1
16	7	-0.3	0.1	0	-0.7	-1.9
16	8	-0.4	-0.15	0.1	-0.3	-2.5
17	1	0.1	-0.2	0.1	-1.5	0
17	2	0.1	0	0.5	-2.8	0
17	3	0.1	0.1	0.3	-2.3	0
17	4	-0.2	0.25	0.4	-2.7	0.8
17	5	0	0.1	0.3	-2.5	0
17	6	-0.1	0.2	0.4	-2.6	
17	7	0	-0.1	0.5	-3	0
18	1	0.2	0.35	0	0	0
18	2	0.1	0.6	0	0	0.7
18	3	0	0.55	0	0	1.1
18	4	-0.3	0.45	0.1	0	0.9
18	5	0	0.6	0	0	1
18	6	0.1	0.65	-0.1	0	0.6
18	7	0	0.25	0	-0.5	1.6
18	8	0	0.6	-0.1	0	1.7
18	9	-0.2	0.5	-0.2	0	1.1
19	1	0.1	0.1	-0.1	0	0
19	2	0.4	0	0	0	0
19	3	0.1	0.1	-0.3	0	0
19	4	-0.1	0.1	-0.3	0	1.7
19	5	0.2	0.1	-0.1	0	0
19	6	0.1	0.15	-0.2	0	0
19	7	0.1	0.1	-0.3	0	0
19	8	0.1	0	-0.1	0	0
20	1	-0.2	0.2	0	-0.6	1.8
20	2	-0.1	0.15	0	-0.5	1.3
20	3	-0.3	-0.1	0.2	-0.5	-1.6
20	4	-0.4	-0.1	-0.1	-1	-0.3
20	5	-0.3	-0.1	-0.2	-0.4	0.7
20	6	-0.1	0.1	0	-0.3	0.3
20	7	-0.2	0.2	0	0	1.2

Patient Number	Amount of image sets	Vertical offset (cm)	Longitudinal offset (cm)	Lateral offset (cm	Anterior Rotation (degrees)	Lateral Rotation (degrees)
21	1	0.2	0.25	-0.1	0	-2.3
21	2	-0.1	-0.2	-0.1	0.4	1.2
21	3	0	-0.1	-0.2	-1.1	0
21	4	0.1	-0.2	-0.2	0	-1.7
21	5	0	-0.15	-0.2	0	-0.7
21	6	-0.1	0.15	-0.2	-0.5	-0.9
21	7	0.1	0	-0.5	-0.2	-0.5
21	8	0	0.15	-0.2	-1.1	-1.3
22	1	-0.2	0.45	-0.1	0	2.8
22	2	0	0.45	-0.1	0	2
22	3	-0.1	0.55	-0.1	0	2.8
22	4	0	0.5	-0.2	0	1.5
22	5	0.1	0.55	0.1	-0.9	0.6
22	6	0	-0.45	-0.1	0	1.2
22	7	0.2	-0.3	0.3	-3	-0.5
22	8	0.1	-0.45	0	-1.9	1.1
22	9	0.1	-0.15	0.2	-2.1	0
23	1	0.2	-0.2	0.1	-2.5	-1.7
23	2	0.1	0.15	0	0	2
23	3	0.3	0.25	0.1	0	-0.4
23	4	0.2	-0.2	-0.2	-2.1	0
23	5	0.3	-0.1	0	0	-1
23	6	0.3	-0.15	-0.1	-1.8	-1.9
24	1	0.4	-0.5	-0.3	0	3.9
24	2	0.3	-0.2	-0.1	0	1.9
24	3	-0.1	-0.1	-0.3	0	0
24	4	0.2	-0.85	-0.3	0	0.8
24	5	0.1	-0.1	-0.4	-0.3	1.9
24	6	0.1	-0.25	-0.3	0	1.6
24	7	0	-0.6	-0.2	-0.9	1.6
24	8	0.1	-0.15	-0.1	-0.5	1.7
24	9	0.1	-0.6	-0.4	-0.1	1.9
25	1	0.1	-0.25	0.2	-0.8	1.8
25	2	0.3	-0.4	0.1	-2.1	1.8
25	3	0.2	-0.35	0	-1	1.2
25	4	0.2	-0.4	0	-1	1.4
25	5	0.2	-0.4	0.1	-1.1	2.1
25	6	0.2	-0.45	0.3	-2.3	2.2
25	7	0.1	-0.4	0.2	-2	2.6
25	8	0.1	-0.25	0.1	-0.9	3.3

Patient Number	Amount of image sets	Vertical offset (cm)	Longitudinal offset (cm)	Lateral offset (cm	Anterior Rotation (degrees)	Lateral Rotation (degrees)
26	1	0.1	0.2	0	0	0
26	2	0.1	0.3	-0.1	0	-1.1
26	3	0.2	0.2	-0.2	1.1	-1.2
26	4	0.2	0.4	-0.1	-1.6	-0.8
26	5	0.2	0.3	0	0	0
26	6	0.3	0.2	0.1	0	-0.9
26	7	0.3	0.35	-0.2	-1.5	-1.5
27	1	0	0.1	-0.1	-1.6	0
27	2	0	0	-0.1	-1.8	-0.9
27	3	0	0.1	-0.1	-1.3	1.2
27	4	0	0.1	-0.1	-1.6	-1
27	5	0	-0.1	-0.1	-3.4	-0.9
27	6	0.1	0.1	-0.1	-1.5	1
27	7	0	-0.1	-0.1	-2.3	-1.1
28	1	0	0.3	-0.2	-2	2.8
28	2	-0.2	-0.2	0.3	0	-2.5
28	3	0.2	0.2	-0.3	0.8	1.6
28	4	0.1	-0.1	-0.2	0	0.7
28	5	0	-0.1	-0.4	-1.2	0
28	6	0	0.1	-0.2	-2.3	0
28	7	-0.1	0	-0.2	-0.8	2.5
28	8	-0.1	0.3	-0.1	-1.2	0
29	2	-0.1	0.3	0.2	0.5	-1.6
29	3	-0.1	0.15	0	-0.5	-0.9
29	4	-0.3	-0.1	0.2	-0.5	1.3
29	5	-0.4	-0.1	-0.1	-1	0.7
29	6	-0.3	-0.1	-0.1	-0.4	0.8
29	7	-0.1	0.1	0	0	0
29	8	-0.1	0.4	0	0	2
30	1	0	0.4	-0.2	-0.4	0
30	2	0.3	-0.1	-0.3	-1	-0.9
30	3	0	0.1	-0.3	0	0
30	4	-0.2	-0.1	-0.3	-0.6	1.3
30	5	-0.1	-0.1	-0.3	-0.6	1.2
30	6	-0.3	0	-0.3	-1.3	2
30	7	-0.1	0.1	-0.3	0	0
30	8	-0.2	0.3	-0.3	0	0

y

Patient Number	Amount of image sets	Vertical offset (cm)	Longitudinal offset (cm)	Lateral offset (cm	Anterior Rotation (degrees)	Lateral Rotation (degrees)
31	1	0.1	0.1	-0.1	0	0
31	2	0.1	-0.15	0	0	0.8
31	3	0	0.1	-0.3	0	0.6
31	4	-0.1	0.1	-0.3	0	1.4
31	5	0	0.1	-0.1	0	1.2
31	6	0.1	0.15	-0.2	0	0
31	7	0.1	0.1	-0.3	0.5	0
31	8	0.1	0	-0.1	0	0
32	1	-0.1	0	0.1	0	-0.8
32	2	0.2	0.1	0.1	0	2.3
32	3	0.2	0.3	0.2	-1.7	2.9
32	4	-0.1	0.1	0.3	0	1.5
32	5	-0.1	0.25	0.4	-2.3	0
32	6	-0.1	-0.35	-0.1	-1.2	1.5
33	1	0.2	-0.15	-0.2	1.4	0
33	2	0	-0.1	-0.1	-0.9	0
33	3	0.2	-0.2	-0.2	-0.8	-1.6
33	4	0.1	0.1	-0.3	0	0
33	5	0.1	-0.2	-0.3	0	0
34	1	0.2	0.6	0.2	-1.1	-2.1
34	2	0.2	0.55	0.2	-1.6	-2.9
34	3	0.1	0.6	0	-1	-1.6
34	4	0.2	0.4	0	-0.6	0
34	5	0	0.1	0.1	-1.3	0
34	6	0.3	0.65	0	-0.8	-2
34	7	0.1	0.15	0.1	-2.8	-1
35	1	0.2	1	-0.2	0	-2.9
35	2	0	0.6	-0.1	2.1	-2.3
35	3	0	0.4	-0.4	1.3	0
35	4	0	-0.25	-0.3	0	-0.7
35	5	0	0.35	-0.4	0	-2.1
35	6	-0.1	0.1	-0.4	-0.1	-1.2
35	7	0.2	0.15	-0.1	-1.4	-1.8
35	8	0	-0.5	-0.5	1.2	0
35	9	0	0.2	-0.6	0	-1.6
35	10	0.1	-0.3	-0.1	0.5	-1.9
36	1	0	0.1	0.1	3.8	-1.4
36	2	0.1	0	0	3.4	-1
36	3	0	-0.15	0.1	2	-2.8
36	4	-0.1	0.25	-0.1	4	-0.4
36	5	-0.1	-0.35	0	3.3	0
36	6	-0.1	-0.3	0.1	4	0.4
36	7	-0.1	-0.25	0	1.6	1.2

Appendix C: Dose recorded to OAR

			Brainstem	
Patient Number	Plan Type	Plan Dose prescription	Brainstem Dmax (Gy)	Brainstem+5mm Dmax (Gy)
1	3DCRT	50Gy	15.26	21.3
1	RA Treat	50Gy	9.9	10.9
1	RA Study	50Gy	8.1	9.05
1	3DCRT	14Gy	0.2	0.21
1	RA Treat	14Gy	0.24	0.25
1	RA Study	14Gy	0.39	0.4
2	3DCRT	60Gy	33.6	34.7
2	RA Treat	60Gy	12.1	14.4
2	RA Study	60Gy	24.7	25.6
2	3DCRT	10Gy	0.04	0.04
2	RA Treat	10Gy	0.04	0.04
2	RA Study	10Gy	0.04	0.04
3	3DCRT	50Gy	30.04	39.2
3	RA Treat	50Gy	20.8	23.9
3	RA Study	50Gy	22	25.2
3	3DCRT	16Gy	1.4	6.3
3	RA Treat	16Gy	3.4	4
3	RA Study	16Gy	3	3.7
4	3DCRT	50Gy	29.8	32
4	RA Treat	50Gy	36	44.4
4	RA Study	50Gy	35.6	41.3
4	3DCRT	16Gy	9.6	12.2
4	RA Treat	16Gy	10.1	14.6
4	RA Study	16Gy	8.4	11.1
5	3DCRT	66Gy	44	54.3
5	RA Treat	66Gy	53.3	60.5
5	RA Study	66Gy	51	58.6
6	3DCRT	50Gy	27.8	30.4
6	RA Treat	50Gy	38.3	44.7
6	RA Study	50Gy	37.1	42.7
6	3DCRT	10Gy	0.1	0.2
6	RA Treat	10Gy	0.2	0.2
6	RA Study	10Gy	0.2	0.2
7	3DCRT	50Gy	26.9	29.9
7	RA Treat	50Gy	30.1	32.3
7	RA Study	50Gy	25.9	29.8
7	3DCRT	10Gy	3.1	5
7	RA Treat	10Gy	4.7	5.5
7	RA Study	10Gy	3.8	4.2
8	3DCRT	50Gy	28.7	29.8
8	RA Treat	50Gy	39.2	45.1
8	RA Study	50Gy	33.2	39.9
8	3DCRT	16Gy	9.1	9.6
8	RA Treat	16Gy	9.5	11.6
8	RA Study	16Gy	8.9	11.2
9	3DCRT	50Gy	30.4	32.5
9	RA Treat	50Gy	45.3	47.3
9	RA Study	50Gy	34.4	38.5
9	3DCRT	20Gy	4	4.5
9	RA Treat	20Gy	3.1	3.6
9	RA Study	20Gy	5.6	6.3
10	3DCRT	50Gy	32	37
10	RA Treat	50Gy	22	25.4
10	RA Study	50Gy	26.8	30.8
10	3DCRT	16Gy	0.2	0.3
10	RA Treat	16Gy	0.3	0.4
10	RA Study	16Gy	0.3	0.4

aa

			Cochlea	
Patient Number	Plan Type	Plan Dose prescription	Cochlear Rt-Mean Dose(Gy)	Cochlear Lt-Mean Dose (Gy)
1	3DCRT	50Gy	1.3	1.1
1	RA Treat	50Gy	2.1	1.8
1	RA Study	50Gy	2	1.68
1	3DCRT	14Gy	0.07	0.06
1	RA Treat	14Gy	0	0
1	RA Study	14Gy	0.09	0.08
2	3DCRT	60Gy	2.2	2.2
2	RA Treat	60Gy	3.9	4.1
2	RA Study	60Gy	3.6	3.7
2	3DCRT	10Gy	0.02	0.02
2	RA Treat	10Gy	0.02	0.02
2	RA Study	10Gy	0.02	0.02
3	3DCRT	50Gy	3.8	6.6
3	RA Treat	50Gy	2.3	2.4
3	RA Study	50Gy	2.4	2.7
3	3DCRT	16Gy	0.2	0.3
3	RA Treat	16Gy	0.2	0.2
3	RA Study	16Gy	0.3	0.4
4	3DCRT	50Gy	3.4	5.6
4	RA Treat	50Gy	3.4	3.9
4	RA Study	50Gy	3.1	3.9
4	3DCRT	16Gy	0.7	1.2
4	RA Treat	16Gy	0.9	1.1
4	RA Study	16Gy	0.9	1
5	3DCRT	66Gy	15.1	15.5
5	RA Treat	66Gy	5.6	5.6
5	RA Study	66Gy	6.4	6.2
6	3DCRT	50Gy	10.7	3.3
6	RA Treat	50Gy	3.4	3.7
6	RA Study	50Gy	2.8	3
6	3DCRT	10Gy	0.1	0.1
6	RA Treat	10Gy	0.1	0.1
6	RA Study	10Gy	0.1	0.1
7	3DCRT	50Gy	2	2.8
7	RA Treat	50Gy	3	3.2
7	RA Study	50Gy	2.8	3.3
7	3DCRT	10Gy	0.3	0.2
7	RA Treat	10Gy	0.4	0.3
7	RA Study	10Gy	0.4	0.3
8	3DCRT	50Gy	36.9	39.2
8	RA Treat	50Gy	10.7	8.6
8	RA Study	50Gy	15.8	12.1
8	3DCRT	16Gy	1.5	7.5
8	RA Treat	16Gy	0.9	2
8	RA Study	16Gy	0.8	1.4
9	3DCRT	50Gy	29.5	19.8
9	RA Treat	50Gy	6.9	5
9	RA Study	50Gy	9.7	8.7
9	3DCRT	20Gy	0.3	0.3
9	RA Treat	20Gy	0.7	0.7
9	RA Study	20Gy	0.5	0.6
10	3DCRT	50Gy	10	3.3
10	RA Treat	50Gy	2.7	2.2
10	RA Study	50Gy	2.8	2.1
10	3DCRT	16Gy	0.1	0.1
10	RA Treat	16Gy	0.1	0.1
10	RA Study	16Gy	0.1	0.1

			Lungs	
Patient Number	Plan Type	Plan Dose prescription	Lungs Combined-Mean Dose (Gy)	Lungs Combined-V20 (
1	3DCRT	50Gy	0.77	0.3
1	RA Treat	50Gy	0.582	0
1	RA Study	50Gy	0.49	0
1	3DCRT	14Gy	0.025	0
1	RA Treat	14Gy	0	0
1	RA Study	14Gy	0.04	0
2	3DCRT	60Gy	7.5	12.6
2	RA Treat	60Gy	6	9.5
2	RA Study	60Gy	5.9	10.4
2	3DCRT	10Gy	0.4	0
2	RA Treat	10Gy	0.3	0
2	RA Study	10Gy	0.3	0
3	3DCRT	50Gy	5.4	12.3
3	RA Treat	50Gy	5.2	9.2
3	RA Study	50Gy	4.9	8.5
3	3DCRT	16Gy	0.02	0
3	RA Treat	16Gy	0.04	0
3	RA Study	16Gy	0.05	0
4	3DCRT	50Gy	12.4	21.6
4	RA Treat	50Gy	10.3	15.8
4	RA Study	50Gy	9.5	16.6
4	3DCRT	16Gy	0.2	0
4	RA Treat	16Gy	0.3	0
4	RA Study	16Gy	0.2	0
5	3DCRT	66Gy	14.8	21.1
5	RA Treat	66Gy	13	21.6
5	RA Study	66Gy	12.7	21.3
6	3DCRT	50Gy	4.8	6.8
6	RA Treat	50Gy	2.9	2.6
6	RA Study	50Gy	3.7	4
6	3DCRT	10Gy	0.8	0
6	RA Treat	10Gy	0.6	0
6	RA Study	10Gy	0.6	0
7	3DCRT	50Gy	2.4	2.8
7	RA Treat	50Gy	1.9	1.8
7	RA Study	50Gy	1.5	1.5
7	3DCRT	10Gy	0.3	0
7	RA Treat	10Gy	0.2	0
7	RA Study	10Gy	0.2	0
8	3DCRT	50Gy	3.3	5.5
8	RA Treat	50Gy	2.6	3.1
8	RA Study	50Gy	2.1	2.7
8	3DCRT	16Gy	0.9	0
8	RA Treat	16Gy	0.6	0
8	RA Study	16Gy	0.6	0
9	3DCRT	50Gy	4.2	7.3
9	RA Treat	50Gy	3.2	4.8
9	RA Study	50Gy	3	4.8
9	3DCRT	20Gy	0.1	0
9	RA Treat	20Gy	0.1	0
9	RA Study	20Gy	0.1	0
10	3DCRT	50Gy	3.1	3.3
10	RA Treat	50Gy	2.4	4.9
10	RA Study	50Gy	2.5	4
10	3DCRT	16Gy	0.6	0
10	RA Treat	16Gy	0.5	0
10	RA Study	16Gy	0.5	0

			Mandible			
Patient Number	Plan Type	Plan Dose prescription	Mandible-Mean Dose (Gy)	Mandible-Dmax (Gy)	Mandible+5 mm-PTV-5mm- Mean Dose (Gy)	Mandible+5 mm-PTV-5mm -Dmax (Gy)
1	3DCRT	50Gy	17.4	50.4	14.5	51.1
1	RA Treat	50Gy	22	52.4	17.5	49.5
1	RA Study	50Gy	19	52.59	14.77	46.7
1	3DCRT	14Gy	0.9	11.65	1.08	11.9
1	RA Treat	14Gy	0.86	6.2	0.9	6.3
1	RA Study	14Gy	1.17	6.16	1.16	7.1
2	3DCRT	60Gy	40.6	64.2	37.1	65.7
2	RA Treat	60Gy	44	62.8	37.5	59.4
2	RA Study	60Gy	37.8	64.5	35.4	65.2
2	3DCRT	10Gy	0.1	1.3	0.1	3.7
2	RA Treat	10Gy	0.1	0.3	0.1	0.7
2	RA Study	10Gy	0.1	0.3	0.09	0.7
3	3DCRT	50Gy	25.7	51.3	25.2	52.6
3	RA Treat	50Gy	30.1	52.4	27.5	53.2
3	RA Study	50Gy	27.3	52	21	44.7
3	3DCRT	16Gy	6.3	15.7	6	16
3	RA Treat	16Gy	5.4	9.9	4.4	11.1
3	RA Study	16Gy	5.3	12	4.4	12.4
4	3DCRT	50Gy	17.6	49.9	16.7	47.5
4	RA Treat	50Gy	29.3	48.8	26.9	52.6
4	RA Study	50Gy	26.6	47.8	24.3	52.8
4	3DCRT	16Gy	5.5	16.2	5.1	15.1
4	RA Treat	16Gy	7.9	15.5	7.1	15.2
4	RA Study	16Gy	7.3	14.2	6.5	14.5
5	3DCRT	66Gy	29.3	68.4	27.3	61.8
5	RA Treat	66Gy	43.9	67.8	43.2	60.9
5	RA Study	66Gy	34	68.4	32.7	57.8
6	3DCRT	50Gy	20.7	48.9	19.3	48
6	RA Treat	50Gy	27	50.9	24	48.2
6	RA Study	50Gy	26.3	50.5	23.1	48.8
6	3DCRT	10Gy	1.5	9	1.4	10
6	RA Treat	10Gy	0.7	4	0.8	6.3
6	RA Study	10Gy	1	5	1.1	5.7
7	3DCRT	50Gy	17	50.4	15.1	49
7	RA Treat	50Gy	20.1	51.5	16.3	45.1
7	RA Study	50Gy	21.6	51	17.2	47.1
7	3DCRT	10Gy	2.3	9.7	2	8.8
7	RA Treat	10Gy	2.6	9.9	2.3	10.9
7	RA Study	10Gy	2	9.9	1.8	10.6
8	3DCRT	50Gy	20.6	50.8	21.8	51.6
8	RA Treat	50Gy	28.3	49.4	27.4	51.6
8	RA Study	50Gy	22.8	48.9	20.7	44.2
8	3DCRT	16Gy	5.1	15.8	5	15.3
8	RA Treat	16Gy	5.3	13	5.2	11.5
8	RA Study	16Gy	4.7	11	4.6	11.8
9	3DCRT	50Gy	31.9	54.7	25.9	53
9	RA Treat	50Gy	34.7	51.8	29.1	47.8
9	RA Study	50Gy	31.8	52.9	25.4	50.7
9	3DCRT	20Gy	9.5	20.8	6.8	20.4
9	RA Treat	20Gy	8.7	20.7	6.3	15.7
9	RA Study	20Gy	9.5	21.1	7.2	18.3
10	3DCRT	50Gy	18	51.4	16.4	51
10	RA Treat	50Gy	23.1	53.4	20.2	46.6
10	RA Study	50Gy	18.4	51.8	16.1	44.1
10	3DCRT	16Gy	1.5	15.8	1.5	15.9
10	RA Treat	16Gy	2.2	7.4	2	8.5
10	RA Study	16Gy	2.1	8	1.9	9

dd

			Parotids				
Patient Number	**Plan Type**	**Plan Dose prescription**	**Parotid Rt-Mean Dose (Gy)**	**Parotid Rt - dose to 50% (Gy)**	**Parotid Lt - Mean Dose (Gy)**	**Parotid Lt - dose to 50% (Gy)**	**Parotid R+L Combined-Mean Dose (Gy)**
1	3DCRT	50Gy	30.92	31.84	31.2Gy	33.88	31.06
1	RA Treat	50Gy	13.2	6.8	18.58	14.34	15.81
1	RA Study	50Gy	18.28	11	16.1	9.9	17.2
1	3DCRT	14Gy	1.066	0.2	0.931	0.2	1.003
1	RA Treat	14Gy	0.46	0.24	0.4	0.21	0.42
1	RA Study	14Gy	0.56	0.38	0.46	0.35	0.5
2	3DCRT	60Gy	45	54.6	39.5	33.7	42.6
2	RA Treat	60Gy	33.8	28.8	26.4	18.7	30.5
2	RA Study	60Gy	36.5	35	32.6	33	34.8
2	3DCRT	10Gy	0.1	0.1	0.1	0.1	0.1
2	RA Treat	10Gy	0.1	0.1	0.1	0.1	0.1
2	RA Study	10Gy	0.1	0.1	0.1	0.1	0.1
3	3DCRT	50Gy	34.2	41	36.5	43.5	35.5
3	RA Treat	50Gy	23.6	23	28.4	32.4	36.3
3	RA Study	50Gy	22.6	18.9	23.6	24.3	23.1
3	3DCRT	16Gy	4.8	3.1	8.5	10.3	6.9
3	RA Treat	16Gy	1.9	1.3	6.9	2.4	2.1
3	RA Study	16Gy	1.5	1.1	4.9	1.6	1.7
4	3DCRT	50Gy	32.8	29.3	30.2	25.5	31.6
4	RA Treat	50Gy	27.5	24.3	16.9	10.5	22.4
4	RA Study	50Gy	24.6	21.3	20.5	17.7	22.6
4	3DCRT	16Gy	10.2	9.5	9	8.2	9.6
4	RA Treat	16Gy	7.9	6.5	4.8	3.5	6.4
4	RA Study	16Gy	8.4	8.2	5.4	4.7	7
5	3DCRT	66Gy	50.8	56.9	50	56.6	50.4
5	RA Treat	66Gy	42.5	41.3	30	17.6	36.1
5	RA Study	66Gy	39.9	39.1	40.5	43.2	40.2
6	3DCRT	50Gy	38.7	42.8	38.5	44.1	38.6
6	RA Treat	50Gy	35.6	38.2	38.4	44.5	36.9
6	RA Study	50Gy	28.6	26.8	30	28.8	29.2
6	3DCRT	10Gy	0.4	0.2	1	0.2	0.7
6	RA Treat	10Gy	0.3	0.2	0.8	0.3	0.5
6	RA Study	10Gy	0.3	0.2	0.7	0.3	0.5
7	3DCRT	50Gy	34	39.5	39	44.3	36.6
7	RA Treat	50Gy	16	14.4	33.3	37.6	25
7	RA Study	50Gy	23.4	20.5	23.3	18.4	23.4
7	3DCRT	10Gy	5.9	5.8	1	0.6	3.4
7	RA Treat	10Gy	3.1	1.6	1.2	1.1	2.2
7	RA Study	10Gy	4.8	5.5	1	0.9	2.9
8	3DCRT	50Gy	40	43.4	40.4	46.7	40.1
8	RA Treat	50Gy	29.5	26.9	37.2	37	33.6
8	RA Study	50Gy	33.6	33.6	33.1	33.6	33.3
8	3DCRT	16Gy	2.9	2.6	11.3	10.9	7.3
8	RA Treat	16Gy	1.3	1.1	10.2	9.4	6
8	RA Study	16Gy	1.1	1	8.3	6.8	4.9
9	3DCRT	50Gy	42.2	49.8	40.5	47.8	41.5
9	RA Treat	50Gy	42.6	46.6	41.5	46	42.1
9	RA Study	50Gy	36.2	42.6	34.3	36.7	35.5
9	3DCRT	20Gy	5	3.7	11.5	12.3	7.5
9	RA Treat	20Gy	6.3	5.4	8.3	8	7.1
9	RA Study	20Gy	1.9	1.9	7.4	6.8	4
10	3DCRT	50Gy	39.6	29.7	37.3	30.6	38.4
10	RA Treat	50Gy	28.7	44.1	28.6	41.7	28.7
10	RA Study	50Gy	27.1	26	27.8	30	27.4
10	3DCRT	16Gy	0.7	0.3	1.1	0.3	0.9
10	RA Treat	16Gy	0.4	0.3	0.5	0.3	0.4
10	RA Study	16Gy	0.3	0.3	0.4	0.3	0.5

		Parotid+5mm expanded				
Plan Type	**Plan Dose prescription**	**Parotid Rt+5mm Mean Dose (Gy)**	**Parotid Rt+5mm- dose to 50% (Gy)**	**Parotid Lt+5mm Mean Dose (Gy)**	**Parotid Lt+5mm- dose to 50% (Gy)**	**Parotid R+L+5mm Combined-Mean Dose (Gy)**
3DCRT	50Gy	28.97	29.3	28.73	29.67	28.86
RA Treat	50Gy	19.69	10Gy	19.69Gy	13.85Gy	18.64
RA Study	50Gy	19.8	12	17.9	10.2	18.9
3DCRT	14Gy	1.5	0.23	1.5	0.2	1.05
RA Treat	14Gy	0.7	0.26	0.58	0.22	0.64
RA Study	14Gy	0.76	0.38	0.6	0.35	0.68
3DCRT	60Gy	43	52	37.2	31.7	40.4
RA Treat	60Gy	34.4	32.5	27.5	19.3	31.3
RA Study	60Gy	35.6	35.2	33.7	30	33.7
3DCRT	10Gy	0.3	0.1	0.1	0.1	0.1
RA Treat	10Gy	0.3	0.1	0.1	0.1	0.1
RA Study	10Gy	0.3	0.1	0.1	0.1	1
3DCRT	50Gy	29.6	32.2	32.7	39	31.3
RA Treat	50Gy	21.8	17.7	26.8	28.4	24.5
RA Study	50Gy	21	14.2	23.4	22	22.3
3DCRT	16Gy	4.4	2.1	7.3	7.7	6
RA Treat	16Gy	1.9	1.1	2.4	2.3	2.2
RA Study	16Gy	1.6	1	2	1.6	1.8
3DCRT	50Gy	32	29	29.4	25.1	30.8
RA Treat	50Gy	27.3	24	19.7	12.5	23.7
RA Study	50Gy	25.1	21.8	21.1	17	23.3
3DCRT	16Gy	9.6	9.1	8.5	7.6	9
RA Treat	16Gy	9	6.5	5.4	4	6.8
RA Study	16Gy	8.2	7.6	5.5	4.6	6.9
3DCRT	66Gy	50.5	57.5	48.1	55.6	49.3
RA Treat	66Gy	43.3	47	35	26.8	39.2
RA Study	66Gy	41.9	45.3	41.2	44.3	41.5
3DCRT	50Gy	36.6	40	35.8	41.2	36.2
RA Treat	50Gy	33.7	36.2	35.4	41.5	34.5
RA Study	50Gy	28.1	26.8	28.6	27	28.4
3DCRT	10Gy	0.5	0.2	1.3	0.2	0.9
RA Treat	10Gy	0.5	0.2	1.1	0.2	0.8
RA Study	10Gy	0.4	0.2	1	0.3	0.7
3DCRT	50Gy	32.5	37.5	37.3	42.6	34.8
RA Treat	50Gy	19.7	17.2	31.4	35.2	25.5
RA Study	50Gy	24	22.8	24	19.1	24
3DCRT	10Gy	5.8	5.7	1.1	0.6	3.5
RA Treat	10Gy	3.9	2	1.3	1.2	2.6
RA Study	10Gy	4.9	5.3	1.1	1	3
3DCRT	50Gy	39.3	45	39.4	46.4	39.3
RA Treat	50Gy	32.1	32.2	36.5	36.9	34.4
RA Study	50Gy	33.8	35.3	33.1	44.4	33.5
3DCRT	16Gy	3.4	2.7	11.1	11.5	7.4
RA Treat	16Gy	1.7	1.3	10	9.4	6
RA Study	16Gy	1.3	1.2	8.5	7.1	5
3DCRT	50Gy	41.7	49.5	39.5	47.5	40.8
RA Treat	50Gy	41.9	47.4	39.9	46	41.1
RA Study	50Gy	36.4	44.1	34.3	38.7	35.6
3DCRT	20Gy	5.6	4	10.6	11.1	7.6
RA Treat	20Gy	6.3	4.7	8.2	6.6	7
RA Study	20Gy	2.1	2	7.6	5.9	4.3
3DCRT	50Gy	37.3	42.6	34.5	37	35.9
RA Treat	50Gy	27.7	28	26.2	26.1	26.9
RA Study	50Gy	25.8	23.8	25.5	26.4	25.6
3DCRT	16Gy	0.7	0.3	1	0.3	1.2
RA Treat	16Gy	0.5	0.3	0.5	0.3	0.5
RA Study	16Gy	0.3	0.3	0.4	0.3	0.5

			Shoulders	
Patient Number	Plan Type	Plan Dose prescription	Shoulders-Mean Dose (Gy)	Shoulders-Dmax (Gy)
1	3DCRT	50Gy	4.2	42.3
1	RA Treat	50Gy	2.5	30.8
1	RA Study	50Gy	2.5	30.9
1	3DCRT	14Gy	0.1	5.5
1	RA Treat	14Gy	0.1	2.6
1	RA Study	14Gy	0.14	1.85
2	3DCRT	60Gy		
2	RA Treat	60Gy		
2	RA Study	60Gy		
2	3DCRT	10Gy		
2	RA Treat	10Gy		
2	RA Study	10Gy		
3	3DCRT	50Gy	8.1	44.3
3	RA Treat	50Gy	5.1	19.7
3	RA Study	50Gy	5.1	20.4
3	3DCRT	16Gy	0.04	3.1
3	RA Treat	16Gy	0.05	1.2
3	RA Study	16Gy	0.07	1.8
4	3DCRT	50Gy	4.6	34.8
4	RA Treat	50Gy	3.3	21.1
4	RA Study	50Gy	4.7	19.8
4	3DCRT	16Gy	0.16	12.1
4	RA Treat	16Gy	0.19	1.4
4	RA Study	16Gy	0.1	2.3
5	3DCRT	66Gy	8.3	64.1
5	RA Treat	66Gy	4.2	28.7
5	RA Study	66Gy	5.1	29.4
6	3DCRT	50Gy	4.1	33
6	RA Treat	50Gy	2.5	51.5
6	RA Study	50Gy	3.9	20.4
6	3DCRT	10Gy	0.7	6.9
6	RA Treat	10Gy	0.6	4.3
6	RA Study	10Gy	0.5	3.5
7	3DCRT	50Gy	6	30.5
7	RA Treat	50Gy	3.7	17.9
7	RA Study	50Gy	4.1	23.1
7	3DCRT	10Gy	0.5	6.8
7	RA Treat	10Gy	0.5	3.1
7	RA Study	10Gy	0.5	2.5
8	3DCRT	50Gy	7.6	49.3
8	RA Treat	50Gy	4.7	21.9
8	RA Study	50Gy	5.7	26.4
8	3DCRT	16Gy	1.1	12.5
8	RA Treat	16Gy	1.5	7.1
8	RA Study	16Gy	1.3	7
9	3DCRT	50Gy	7	43.7
9	RA Treat	50Gy	4.8	25.1
9	RA Study	50Gy	7.8	29.8
9	3DCRT	20Gy	0.2	11.3
9	RA Treat	20Gy	0.2	4.7
9	RA Study	20Gy	0.2	4.9
10	3DCRT	50Gy	4.6	28.6
10	RA Treat	50Gy	3.2	19.1
10	RA Study	50Gy	3.6	20.5
10	3DCRT	16Gy	1.3	9.7
10	RA Treat	16Gy	0.8	3.4
10	RA Study	16Gy	0.8	4.1

			Spinal Cord	
Patient Number	Plan Type	Plan Dose prescription	Spinal Cord-Dmax (Gy)	Spinal Cord+5mm-Dmax (Gy)
1	3DCRT	50Gy	35.6	39.27
1	RA Treat	50Gy	30.16	34.9
1	RA Study	50Gy	29.05	33.03
1	3DCRT	14Gy	3.5	8.2
1	RA Treat	14Gy	7	9
1	RA Study	14Gy	7.9	8.9
2	3DCRT	60Gy	39.1	43.8
2	RA Treat	60Gy	38.9	45
2	RA Study	60Gy	36.7	39.5
2	3DCRT	10Gy	3.3	5.8
2	RA Treat	10Gy	3.5	4
2	RA Study	10Gy	5	5.6
3	3DCRT	50Gy	33.3	42
3	RA Treat	50Gy	33.8	36.5
3	RA Study	50Gy	30	33.4
3	3DCRT	16Gy	2.9	6.1
3	RA Treat	16Gy	9	10.8
3	RA Study	16Gy	9.2	10.7
4	3DCRT	50Gy	33.7	38.4
4	RA Treat	50Gy	27.1	27.7
4	RA Study	50Gy	33.56	39.1
4	3DCRT	16Gy	10.5	13.4
4	RA Treat	16Gy	10.3	11.8
4	RA Study	16Gy	6.9	9.2
5	3DCRT	66Gy	32.4	32
5	RA Treat	66Gy	35.7	35.3
5	RA Study	66Gy	43.9	47.3
6	3DCRT	50Gy	32.9	39.1
6	RA Treat	50Gy	36	45.2
6	RA Study	50Gy	35.2	39.4
6	3DCRT	10Gy	7.5	8.9
6	RA Treat	10Gy	4	5.6
6	RA Study	10Gy	5.3	6.7
7	3DCRT	50Gy	30.8	35.8
7	RA Treat	50Gy	45.4	48.4
7	RA Study	50Gy	35.5	38.3
7	3DCRT	10Gy	7.4	8.1
7	RA Treat	10Gy	9	9.4
7	RA Study	10Gy	5.3	6.2
8	3DCRT	50Gy	31.5	35
8	RA Treat	50Gy	39.3	43.8
8	RA Study	50Gy	33.6	37.2
8	3DCRT	16Gy	10.7	12.2
8	RA Treat	16Gy	9.1	11.9
8	RA Study	16Gy	8.4	10.6
9	3DCRT	50Gy	30.4	34.7
9	RA Treat	50Gy	40.7	42.9
9	RA Study	50Gy	33.5	38.3
9	3DCRT	20Gy	13.5	13.9
9	RA Treat	20Gy	3.7	6.4
9	RA Study	20Gy	9.8	11.9
10	3DCRT	50Gy	37.8	42.1
10	RA Treat	50Gy	36.4	38.3
10	RA Study	50Gy	35	39.5
10	3DCRT	16Gy	1	4
10	RA Treat	16Gy	8.1	10
10	RA Study	16Gy	7.2	8.3

hh

			TM Joint			
Patient Number	Plan Type	Plan Dose prescription	TMJ Right Dmax (Gy)	TMJ Right+5mm Dmax (Gy)	TMJ Left Dmax (Gy)	TMJ Left+5mm Dmax (Gy)
1	3DCRT	50Gy	1.9	8.8	2.1	5.8
1	RA Treat	50Gy	2.6	3.1	2.5	3.2
1	RA Study	50Gy	2.5	3.1	2.4	3
1	3DCRT	14Gy	0.1	0.13	0.1	0.13
1	RA Treat	14Gy	0.1	0.12	0.1	0.12
1	RA Study	14Gy	0.15	0.1	0.15	0.1
2	3DCRT	60Gy	4.67	16.3	4.2	16
2	RA Treat	60Gy	4.7	5.5	5	5.9
2	RA Study	60Gy	4.3	5.1	4.5	5.3
2	3DCRT	10Gy	0.02	0.03	0.2	0.02
2	RA Treat	10Gy	0.02	0.02	0.03	0.03
2	RA Study	10Gy	0.02	0.03	0.03	0.3
3	3DCRT	50Gy	8.8	9.6	8.9	10.3
3	RA Treat	50Gy	2	2	2.6	3.5
3	RA Study	50Gy	2.5	3.2	2.8	3.6
3	3DCRT	16Gy	0.4	0.8	0.6	1.4
3	RA Treat	16Gy	0.2	0.2	0.2	0.2
3	RA Study	16Gy	0.3	0.3	0.3	0.3
4	3DCRT	50Gy	11.1	12.9	15	41.4
4	RA Treat	50Gy	3.6	4.4	4.7	12.1
4	RA Study	50Gy	3.3	4.5	5.5	11.2
4	3DCRT	16Gy	0.8	2.3	2.8	8.2
4	RA Treat	16Gy	1	1.2	1.3	2.4
4	RA Study	16Gy	0.9	1.2	1.2	2.3
5	3DCRT	66Gy	22.8	20	17.5	31
5	RA Treat	66Gy	8.7	7.4	8.7	19.7
5	RA Study	66Gy	11.6	30.7	7.4	18
6	3DCRT	50Gy	32.3	47	18.6	44
6	RA Treat	50Gy	11.9	45.5	7	30.6
6	RA Study	50Gy	8	30.9	7.4	15.4
6	3DCRT	10Gy	0.1	0.1	0.1	0.1
6	RA Treat	10Gy	0.1	0.1	0.1	0.1
6	RA Study	10Gy	0.1	0.1	0.1	0.1
7	3DCRT	50Gy	2.8	10.4	13.9	30.1
7	RA Treat	50Gy	4	4.4	5.9	6.3
7	RA Study	50Gy	3.1	4	3.9	6.3
7	3DCRT	10Gy	0.3	0.6	0.2	0.3
7	RA Treat	10Gy	0.3	0.3	0.5	0.5
7	RA Study	10Gy	0.3	0.3	0.2	0.2
8	3DCRT	50Gy	48.4	50.4	47.5	49.8
8	RA Treat	50Gy	44.7	52.2	32.3	51.3
8	RA Study	50Gy	42	53.6	22.5	51.8
8	3DCRT	16Gy	8.1	10	15	16
8	RA Treat	16Gy	1.6	2.4	6.2	15.3
8	RA Study	16Gy	1.5	2	3.5	14
9	3DCRT	50Gy	48	49.7	48.3	49.4
9	RA Treat	50Gy	34.8	50.4	35.3	50.2
9	RA Study	50Gy	32.5	49.3	34.5	49.6
9	3DCRT	20Gy	0.6	0.7	0.8	1.5
9	RA Treat	20Gy	1	1.5	1.2	1.5
9	RA Study	20Gy	0.8	1.1	1.1	1.4
10	3DCRT	50Gy	13.2	20.4	13	15.8
10	RA Treat	50Gy	3.3	4.8	3	4.1
10	RA Study	50Gy	3.4	5.2	3.1	4.5
10	3DCRT	16Gy	0.2	0.2	0.2	0.2
10	RA Treat	16Gy	0.2	0.2	0.2	0.2
10	RA Study	16Gy	0.2	0.2	0.1	0.2

Appendix D: Dose recorded for Plan comparison

				Conformity Index			Lesion coverage Factor	
	Plan name	Prescription	Prescription in Gy	V95%=Prescription Isodose surface Volume=95% (cm3)	TV=PTV volume (cm3)	Conformity index RTOG: = V95%/TV 1= ideal conformality	CVF=TV_{RI}/TV	TV_{RI}=Volume of Target Volume receiving 95%
patient 1	3DCRT	50Gy	50	543.6	402.7	1.349888254	0.936925751	377.3
	RA treat	50Gy	50	417	411.7	1.012873452	0.91863007	378.2
	RA study	50Gy	50	409.6	402.7	1.017134343	0.926992799	373.3
	3DCRT	14Gy	14	99.5	75.2	1.323138298	0.962765957	72.4
	RA treat	14Gy	14	77	77.2	0.997409326	0.897668394	69.3
	RA study	14Gy	14	77	75.2	1.02393617	0.910904255	68.5
patient 2	3DCRT	60Gy	60	1074.7	788.2	1.363486425	0.955975641	753.5
	RA treat	60Gy	60	886.7	843.6	1.051090564	0.944404931	796.7
	RA study	60Gy	60	794.7	788.2	1.008246638	0.908018269	715.7
	3DCRT	10Gy	10	172.5	146	1.181506849	0.911643836	133.1
	RA treat	10Gy	10	143.7	146	0.984246575	0.901369863	131.6
	RA study	10Gy	10	131.4	132.8	0.989457831	0.894578313	118.8
patient 3	3DCRT	50Gy	50	490.5	442.7	1.107973797	0.880280099	389.7
	RA treat	50Gy	50	465.1	462.7	1.005186946	0.936459909	433.3
	RA study	50Gy	50	434.7	442.7	0.981929072	0.91551841	405.3
	3DCRT	16Gy	16	125.3	70.5	1.777304965	0.707801418	49.9
	RA treat	16Gy	16	74.8	71.8	1.04178273	0.938718663	67.4
	RA study	16Gy	16	71.5	70.5	1.014184397	0.910638298	64.2
patient 4	3DCRT	50Gy	50	985.6	812.4	1.21319547	0.927498769	753.5
	RA treat	50Gy	50	882.6	812.4	1.086410635	0.951132447	772.7
	RA study	50Gy	50	830.3	812.4	1.022033481	0.923929099	750.6
	3DCRT	16Gy	16	509.2	403.7	1.261332673	0.932623235	376.5
	RA treat	16Gy	16	465	403.7	1.15184543	0.964082239	389.2
	RA study	16Gy	16	434.7	403.1	1.078392458	0.944430662	380.7
patient 5	3DCRT	66Gy	66	998.8	965.5	1.034489902	0.734230968	708.9
	RA treat	66Gy	66	1026.8	965.5	1.063490419	0.917141378	885.5
	RA study	66Gy	66	1041.2	965.5	1.078404972	0.909580528	878.2
patient 6	3DCRT	50Gy	50	803.5	735	1.093197279	0.807619048	593.6
	RA treat	50Gy	50	879.2	713.1	1.232926658	0.984293928	701.9
	RA study	50Gy	50	797.1	735	1.084489796	0.938367347	689.7
	3DCRT	10Gy	10	398.1	315.2	1.263007614	0.88642132	279.4
	RA treat	10Gy	10	349	315.2	1.107233503	0.953680203	300.6
	RA study	10Gy	10	338.9	306.8	1.104628422	0.961538462	295
patient 7	3DCRT	50Gy	50	688.5	490	1.405102041	0.874897959	428.7
	RA treat	50Gy	50	615.7	490	1.256530612	0.948367347	464.7
	RA study	50Gy	50	597.5	490	1.219387755	0.948571429	464.8
	3DCRT	10Gy	10	381.8	234.9	1.625372499	0.892294593	209.6
	RA treat	10Gy	10	296.1	234.9	1.260536398	0.949340145	223
	RA study	10Gy	10	288.3	234.9	1.227330779	0.948488719	222.8
patient 8	3DCRT	50Gy	50	899.2	733	1.226739427	0.858117326	629
	RA treat	50Gy	50	821.5	733	1.120736698	0.957435198	701.8
	RA study	50Gy	50	795.9	733	1.085811733	0.951296044	697.3
	3DCRT	16Gy	16	467.6	363.4	1.286736379	0.779856907	283.4
	RA treat	16Gy	16	394.7	363.4	1.086130985	0.91992295	334.3
	RA study	16Gy	16	380.7	363.4	1.047605944	0.894606494	325.1
patient 9	3DCRT	50Gy	50	1523.3	1229.3	1.239160498	0.872366387	1072.4
	RA treat	50Gy	50	1275.9	1138	1.121177504	0.968365554	1102
	RA study	50Gy	50	1523.3	1229.3	1.239160498	0.872366387	1072.4
	3DCRT	20Gy	20	431.5	370.6	1.164328117	0.855639504	317.1
	RA treat	20Gy	20	412.2	391.8	1.052067381	0.942827973	369.4
	RA study	20Gy	20	421.3	370.6	1.136805181	0.978413384	362.6
patient 10	3DCRT	50Gy	50	663.7	531	1.249905838	0.916007533	486.4
	RA treat	50Gy	50	576.4	531	1.085499058	0.953672316	506.4
	RA study	50Gy	50	581.1	531	1.094350282	0.821092279	436
	3DCRT	16Gy	16	301.1	150.4	2.001994681	0.895611702	134.7
	RA treat	16Gy	16	140.1	132.6	1.056561086	0.931372549	123.5
	RA study	16Gy	16	150.5	132.6	1.134992459	0.963800905	127.8

			Homogeneity Index							
	Plan name	Prescription in Gy	D90 (Gy)	D10 (Gy)	D2 (Gy)	D98 (Gy)	D5 (Gy)	D95 (Gy)	Dmax (Gy)	Dmin (Gy
patient 1	3DCRT	50	48.57	53.5	54.13	46.04	53.84	47.51	54.838Gy	35.218
	RA treat	50	48.08	51.9	52.72	46.83	52.33	47.53	55.45Gy	18.664Gy
	RA study	50	48.03	51.93	52.75	47.1	52.34	47.62	56.232Gy	41.275Gy
	3DCRT	14	13.61	14.33	14.59	13.3	14.4	13.45	14.882Gy	12.42Gy
	RA treat	14	13.47	14.5	14.68	12.97	14.6	13.27	14.921Gy	11.415Gy
	RA study	14	13.49	14.52	14.73	13.2	14.63	13.36	15.14	12.39
patient 2	3DCRT	60	58.3	65.6	68.3	56.3	67	57.4	70.6	31.8
	RA treat	60	58	62	62.7	56.8	62.4	57.5	65.1	34.3
	RA study	60	57.5	62.7	63.9	56.2	63.3	56.9	66.8	47.5
	3DCRT	10	9.6	10.2	10.4	9	10.4	9.4	10.607	3.953
	RA treat	10	9.7	10.3	10.3	9.3	10.3	9.5	10.456	4.759
	RA study	10	9.6	10.3	10.4	9.4	10.4	9.5	10.7	8
patient 3	3DCRT	50	47.5	52.5	53.3	45.2	52.9	46.6	54.9	32.8
	RA treat	50	48.3	52	53	47.1	53.5	47.8	54.8	2.9
	RA study	50	48.2	52.1	52.7	46.6	52.4	47.5	55.1	38.6
	3DCRT	16	15.7	16.7	17	15.2	16.8	15.4	17.7	13.8
	RA treat	16	14.5	16.6	16.9	15.2	16.8	15.3	17.2	14.1
	RA study	16	15.4	16.5	16.8	15.1	16.7	15.3	17.3	14
patient 4	3DCRT	50	48.3	53.5	55.4	45.4	54.4	47.3	58.2	39.5
	RA treat	50	48.5	51.3	51.8	47.5	51.5	48	54.4	38.2
	RA study	50	48.3	51.4	51.9	47.1	51.7	47.7	54	39.9
	3DCRT	16	15.5	16.9	17.2	15	17.1	15.3	17.9	1.4
	RA treat	16	15.6	16.3	16.5	15.4	16.4	15.5	17.3	1.3
	RA study	16	15.6	16.4	16.6	15.3	16.5	15.4	17.5	12.8
patient 5	3DCRT	66	45.9	70.1	71.5	41.4	70.9	43.2	74.2	36
	RA treat	66	63.5	67.8	68.5	61.5	68.2	62.7	70.9	20
	RA study	66	63.4	68.8	70	61.8	69.4	62.7	72.9	28.6
patient 6	3DCRT	50	42.5	55.9	57.4	32.9	56.8	35	58.7	15.5
	RA treat	50	49.1	51.2	52	48.5	51.6	48.9	54	26.8
	RA study	50	48.7	51.3	52	46.7	51.7	48	55.1	18.2
	3DCRT	10	9.5	10.4	10.6	9	10.5	9.3	10.8	3.8
	RA treat	10	9.7	10.3	10.5	9.6	10.5	9.7	10.9	4.4
	RA study	10	9.8	10.3	10.4	9.6	10.3	9.7	10.7	9
patient 7	3DCRT	50	47.5	52.7	54.2	35.4	53.7	45.2	55.2	29.3
	RA treat	50	48.7	51.7	52.6	46.9	52.1	48.1	54.1	18.7
	RA study	50	48.7	51.2	51.8	47.5	51.5	48.2	54.3	36.3
	3DCRT	10	9.6	10.4	10.7	9.2	10.5	9.4	11.3	7.7
	RA treat	10	9.7	10.4	10.5	9.6	10.5	9.7	11	7.5
	RA study	10	9.8	10.2	10.3	9.6	10.3	9.7	10.7	8.6
patient 8	3DCRT	50	47	52.9	54.9	42.7	53.8	45.5	57	27.5
	RA treat	50	48.4	51.5	52.1	47.5	51.8	48	54.4	32.2
	RA study	50	48.7	51.2	51.6	47.4	51.4	48.2	53.6	40.6
	3DCRT	16	14.9	17.5	18	13.6	17.8	14.4	18.5	9.3
	RA treat	16	15.6	16.5	16.7	15.3	16.6	15.5	17.4	12.4
	RA study	16	15.5	16.5	16.7	15.1	16.6	15.3	17.5	13.1
patient 9	3DCRT	50	47.2	55.1	57.1	39.2	56.2	44.4	61.3	1.2
	RA treat	50	48.8	51.2	52.3	47.6	51.7	48.3	54.7	42.1
	RA study	50	47.1	55.1	57.1	39.3	56.2	44.4	61.3	1.2
	3DCRT	20	18.8	22.7	23.3	17.5	23	18.3	23.7	13.7
	RA treat	20	19.4	20.6	20.7	18.9	20.6	19.2	21.8	4.7
	RA study	20	19.7	20.3	20.5	19.4	20.4	19.6	21.3	16.3
patient 10	3DCRT	50	48	52.2	53.2	45.2	52.7	47.2	54.6	32.7
	RA treat	50	48.4	51.6	52.5	47.6	52	48.1	54.6	41.1
	RA study	50	48.7	51.2	51.8	47.3	51.5	48.2	53.8	38.6
	3DCRT	16	15.3	16.7	16.9	13.1	16.8	14.7	17.1	4.6
	RA treat	16	15.5	16.4	16.5	15.2	16.4	15.4	17	14.4
	RA study	16	15.7	15.3	16.4	15.5	16.3	15.6	16.9	14.6

kk

			Homogeneity Index Calculations					
	Plan name	Prescription in Gy	D2/D98=1	D5/D95=1	D10/D90=1	D5-D95/Dp=0	D2-D98/Dp=0	D10-D90/Dp=0
patient 1	3DCRT	50	1.175716768	1.133235108	1.101502985	0.1266	0.1618	0.0986
	RA treat	50	1.125774076	1.100988849	1.079450915	0.096	0.1178	0.0764
	RA study	50	1.119957537	1.099118018	1.08119925	0.0944	0.113	0.078
	3DCRT	14	1.096992481	1.07063197	1.052902278	0.067857143	0.092142857	0.051428571
	RA treat	14	1.131842714	1.100226074	1.076466221	0.095	0.122142857	0.073571429
	RA study	14	1.115909091	1.09505988	1.076352854	0.090714286	0.109285714	0.073571429
patient 2	3DCRT	60	1.213143872	1.167247387	1.125214408	0.16	0.2	0.121666667
	RA treat	60	1.103873239	1.085217391	1.068965517	0.081666667	0.098333333	0.066666667
	RA study	60	1.137010676	1.112478032	1.090434783	0.106666667	0.128333333	0.086666667
	3DCRT	10	1.155555556	1.106382979	1.0625	0.1	0.14	0.06
	RA treat	10	1.107526882	1.084210526	1.06185567	0.08	0.1	0.06
	RA study	10	1.106382979	1.094736842	1.072916667	0.09	0.1	0.07
patient 3	3DCRT	50	1.17920354	1.135193133	1.105263158	0.126	0.162	0.1
	RA treat	50	1.125265393	1.119246862	1.076604555	0.114	0.118	0.074
	RA study	50	1.130901288	1.103157895	1.080912863	0.098	0.122	0.078
	3DCRT	16	1.118421053	1.090909091	1.063694268	0.0875	0.1125	0.0625
	RA treat	16	1.111842105	1.098039216	1.144827586	0.09375	0.10625	0.13125
	RA study	16	1.112582781	1.091503268	1.071428571	0.0875	0.10625	0.06875
patient 4	3DCRT	50	1.220264317	1.150105708	1.107660455	0.142	0.2	0.104
	RA treat	50	1.090526316	1.072916667	1.057731959	0.07	0.086	0.056
	RA study	50	1.101910828	1.083857442	1.064182195	0.08	0.096	0.062
	3DCRT	16	1.146666667	1.117647059	1.090322581	0.1125	0.1375	0.0875
	RA treat	16	1.071428571	1.058064516	1.044871795	0.05625	0.06875	0.04375
	RA study	16	1.08496732	1.071428571	1.051282051	0.06875	0.08125	0.05
patient 5	3DCRT	66	1.72705314	1.641203704	1.527233115	0.41969697	0.456060606	0.366666667
	RA treat	66	1.113821138	1.087719298	1.067716535	0.083333333	0.106060606	0.065151515
	RA study	66	1.113821138	1.106858054	1.085173502	0.101515152	0.124242424	0.081818182
patient 6	3DCRT	50	1.744680851	1.622857143	1.315294118	0.436	0.49	0.268
	RA treat	50	1.072164948	1.055214724	1.042769857	0.054	0.07	0.042
	RA study	50	1.113490364	1.077083333	1.05338809	0.074	0.106	0.052
	3DCRT	10	1.177777778	1.129032258	1.094736842	0.12	0.16	0.09
	RA treat	10	1.09375	1.082474227	1.06185567	0.08	0.09	0.06
	RA study	10	1.083333333	1.06185567	1.051020408	0.06	0.08	0.05
patient 7	3DCRT	50	1.531073446	1.188053097	1.109473684	0.17	0.376	0.104
	RA treat	50	1.121535181	1.083160083	1.061601643	0.08	0.114	0.06
	RA study	50	1.090526316	1.06846473	1.051334702	0.066	0.086	0.05
	3DCRT	10	1.163043478	1.117021277	1.083333333	0.11	0.15	0.08
	RA treat	10	1.09375	1.082474227	1.072164948	0.08	0.09	0.07
	RA study	10	1.072916667	1.06185567	1.040816327	0.06	0.07	0.04
patient 8	3DCRT	50	1.285714286	1.182417582	1.125531915	0.166	0.244	0.118
	RA treat	50	1.096842105	1.079166667	1.064049587	0.076	0.092	0.062
	RA study	50	1.088607595	1.066390041	1.051334702	0.064	0.084	0.05
	3DCRT	16	1.323529412	1.236111111	1.174496644	0.2125	0.275	0.1625
	RA treat	16	1.091503268	1.070967742	1.057692308	0.06875	0.0875	0.05625
	RA study	16	1.105960265	1.08496732	1.064516129	0.08125	0.1	0.0625
patient 9	3DCRT	50	1.456632653	1.265765766	1.167372881	0.236	0.358	0.158
	RA treat	50	1.098739496	1.070393375	1.049180328	0.068	0.094	0.048
	RA study	50	1.452926209	1.265765766	1.16985138	0.236	0.356	0.16
	3DCRT	20	1.331428571	1.256830601	1.207446809	0.235	0.29	0.195
	RA treat	20	1.095238095	1.072916667	1.06185567	0.07	0.09	0.06
	RA study	20	1.056701031	1.040816327	1.030456853	0.04	0.055	0.03
patient 10	3DCRT	50	1.17699115	1.116525424	1.0875	0.11	0.16	0.084
	RA treat	50	1.102941176	1.081081081	1.066115702	0.078	0.098	0.064
	RA study	50	1.095137421	1.06846473	1.051334702	0.066	0.09	0.05
	3DCRT	16	1.290076336	1.142857143	1.091503268	0.13125	0.2375	0.0875
	RA treat	16	1.085526316	1.064935065	1.058064516	0.0625	0.08125	0.05625
	RA study	16	1.058064516	1.044871795	0.974522293	0.04375	0.05625	-0.025

Score System

		Points Allowcation		Best Results (Gy)	Score	Acceptable Results (Gy)	Score	Worst Results (Gy)	Score
PTV	HI: D2/D98	2 points	plan 1	1-1.099	0	1.1-1.2	1	>1.2	2
	HI: D2/D98	2 points	plan 2	1-1.099	0	1.1-1.2	1	>1.2	2
	HI: D5/D95	2 points	plan 1	1-1.099	0	1.1-1.2	1	>1.2	2
	HI: D5/D95	2 points	plan 2	1-1.099	0	1.1-1.2	1	>1.2	2
	HI:D2-D98/Dp	2 points	plan 1	0-0.099	0	0.1-0.2	1	>0.2	2
	HI:D2-D98/Dp	2 points	plan 2	0-0.099	0	0.1-0.2	1	>0.2	2
	HI:D5-D95/Dp	2 points	plan 1	0-0.099	0	0.1-0.2	1	>0.2	2
	HI:D5-D95/Dp	2 points	plan 2	0-0.099	0	0.1-0.2	1	>0.2	2
	CI:V95%/TV	2 points	plan 1	minus 0.95 to 1.05	0	minus 0.95-0.85 and 1.05-1.5	1	<minus0.85 or >1.5	2
	CI:V95%/TV	2 points	plan 2	minus 0.95 to 1.05	0	minus 0.95-0.85 and 1.05-1.5	1	<minus0.85 or >1.5	2
	CVF=TV (RI)/TV	2 points	plan 1	0.95-1	0	0.9-0.95	1	<0.9	2
	CVF=TV (RI)/TV	2 points	plan 2	0.95-1	0	0.9-0.95	1	<0.9	2
OAR	Brainstem	6 points	Dmax	<50Gy	0	<53Gy	1	>53Gy	3
	Brainstem PRV		Dmax	<54Gy	0	<54-59Gy	1	>59Gy	3
	Spinal Cord	6 points	Dmax	<45Gy	0	<45Gy-47Gy	1	>47Gy	3
	Spinal Cord PRV		Dmax	<48Gy	0	<48Gy-50Gy	1	>50Gy	3
	Parotid Right	6 points	Mean Dose	<18Gy	0	<18-23Gy	0.5	>23Gy	1
	Parotid Left		Mean Dose	<18Gy	0	<18-23Gy	0.5	>23Gy	1
	Parotid Right PRV		Mean Dose	<20Gy	0	<20-25Gy	0.5	>25Gy	1
	Parotid Left PRV		Mean Dose	<20Gy	0	<20-25Gy	0.5	>25Gy	1
	Parotids Combined		Mean Dose	<23Gy	0	<23-37Gy	0.5	>37Gy	1
	Parotids Combined PRV		Mean Dose	<25Gy	0	<25-39Gy	0.5	>39Gy	1
	Cochlear Right PRV	4 points	Mean Dose	<32Gy	0	<32-45Gy	1	>45Gy	2
	Cochlear Left PRV		Mean Dose	<32Gy	0	<32-45Gy	1	>45Gy	2
	TMJ Right	4 points	Dmax	<60Gy	0	<60-65Gy	0.5	>65Gy	1
	TMJ Left		Dmax	<60Gy	0	<60-65Gy	0.5	>65Gy	1
	TMJ Right PRV		Dmax	<65Gy	0	<65-70Gy	0.5	>70Gy	1
	TMJ Left PRV		Dmax	<65Gy	0	<65-70Gy	0.5	>70Gy	1
	Oral Cavity	2 points	Mean Dose	<40Gy	0	<40-45Gy	1	>45Gy	2
	Mandible	2 points	Dmax	<68	0	<68Gy-70Gy	0.5	>70Gy	1
	Mandible PRV-PTV		Dmax	<70	0	<73Gy	0.5	>73Gy	1
	TOTAL PTV SCORE				0		12		24
	TOTAL OAR SCORE				0		13		30
	TOTAL PTV+ OAR SCORE				0		25		54

mm

Appendix E: The Plan Scoring system and Result

Patient 1					
3DCRT	*RA Treat*	*RA Study*	3DCRT	*RA Treat*	*RA Study*
Dose			**Score**		
1.175717	1.125774	1.119958	1	1	1
1.096992	1.131843	1.115909	0	1	1
1.133235	1.100989	1.099118	1	1	0
1.070632	1.100226	1.09506	0	1	0
0.1618	0.1178	0.113	1	1	1
0.092143	0.122143	0.109286	0	1	1
0.1266	0.096	0.0944	1	0	0
0.067857	0.095	0.090714	0	0	0
1.349888	1.012873	1.017134	1	0	0
1.323138	0.997409	1.023936	1	0	0
0.936926	0.91863	0.926993	1	1	1
0.962766	0.897668	0.910904	0	2	1
15.46	10.14	8.49	0	0	0
21.51	11.15	9.45	0	0	0
32.66	29.43	29.14	0	0	0
47.47	43.9	41.93	0	0	0
31.986	13.66	18.84	1	0	0.5
32.131	18.98	16.56	1	0.5	0
30.47	20.39	20.56	1	0.5	0.5
30.23	20.27	18.5	1	0.5	0
32.063	16.23	17.7	0.5	0	0
29.91	19.28	19.58	0.5	0	0
1.37	2.1	2.09	0	0	0
1.16	1.8	1.76	0	0	0
2	2.7	2.65	0	0	0
2.2	2.6	2.55	0	0	0
8.93	3.22	3.2	0	0	0
5.93	3.32	3.1	0	0	0
26.553	23.6	19.4	0	0	0
62.05	58.6	58.75	0	0	0
63	55.8	53.8	0	0	0
			7	9	6
			5	1.5	1
			12	10.5	7

nn

Patient 2					
3DCRT	*RA Treat*	*RA Study*	3DCRT	*RA Treat*	*RA Study*
Dose			**Score**		
1.213144	1.103873	1.137011	2	1	1
1.155556	1.107527	1.106383	1	1	1
1.167247	1.085217	1.112478	1	0	1
1.106383	1.084211	1.094737	1	0	0
0.16	0.081667	0.106667	1	0	1
0.1	0.08	0.09	1	0	0
0.2	0.098333	0.128333	2	0	1
0.14	0.1	0.1	1	1	1
1.363486	1.051091	1.008247	1	1	0
1.181507	0.984247	0.989458	1	0	0
0.955976	0.944405	0.908018	0	1	1
0.911644	0.90137	0.894578	1	1	2
33.64	12.14	24.74	0	0	0
34.74	14.44	25.64	0	0	0
34.48	34.42	33.32	0	0	0
49.6	49	45.1	1	1	0
45.1	33.9	36.6	1	1	1
39.6	26.5	32.7	1	1	1
43.3	34.7	35.9	1	1	1
37.3	27.6	33.8	1	1	1
42.7	30.6	34.9	1	0.5	0.5
40.5	31.4	34.7	1	0.5	0.5
2.22	3.92	3.62	0	0	0
2.22	4.12	3.72	0	0	0
4.69	4.72	4.32	0	0	0
4.4	5.03	4.53	0	0	0
16.33	5.52	5.13	0	0	0
16.02	5.93	5.6	0	0	0
45.2	49.6	39	2	2	1
65.5	63.1	64.8	0	0	0
69.4	60.1	65.9	0	0	0
			13	6	9
			9	8	6
			22	14	15

Patient 3					
3DCRT	*RA Treat*	*RA Study*	3DCRT	*RA Treat*	*RA Study*
Dose			**Score**		
1.179204	1.125265	1.130901	1	1	1
1.118421	1.111842	1.112583	1	1	1
1.135193	1.119247	1.103158	1	1	1
1.090909	1.098039	1.091503	0	0	0
0.162	0.118	0.122	1	1	1
0.1125	0.10625	0.10625	1	1	1
0.126	0.114	0.098	1	1	0
0.0875	0.09375	0.0875	0	0	0
1.107974	1.005187	0.981929	1	0	0
1.777305	1.041783	1.014184	2	0	0
0.88028	0.93646	0.915518	2	1	1
0.707801	0.938719	0.910638	2	1	1
31.44	24.2	25	0	0	0
45.5	27.9	28.9	0	0	0
29.45	42.38	31.24	0	0	0
48.1	47.3	44.1	1	0	0
39	25.5	24.1	1	1	1
45	35.3	28.5	1	1	1
34	23.7	22.6	1	0.5	0.5
40	29.2	25.4	1	1	1
42.4	38.4	24.8	1	1	0.5
37.3	26.7	24.1	1	0.5	0
4	2.5	2.7	0	0	0
6.9	2.6	3.1	0	0	0
9.2	2.2	2.8	0	0	0
9.5	2.8	3.1	0	0	0
10.4	2.2	3.5	0	0	0
11.7	3.7	3.9	0	0	0
21.4	33.3	32.1	0	0	0
67	62.3	64	0	0	0
68.6	64.3	57.1	0	0	0
			13	8	7
			7	5	4
			20	13	11

pp

Patient 4					
3DCRT	*RA Treat*	*RA Study*	3DCRT	*RA Treat*	*RA Study*
Dose			**Score**		
1.220264	1.090526	1.101911	2	0	1
1.146667	1.071429	1.084967	1	0	0
1.150106	1.072917	1.083857	1	0	0
1.117647	1.058065	1.071429	1	0	0
0.2	0.086	0.096	2	0	0
0.1375	0.06875	0.08125	1	0	0
0.142	0.07	0.08	1	0	0
0.1125	0.05625	0.06875	1	0	0
1.213195	1.086411	1.022033	1	1	0
1.261333	1.151845	1.078392	1	1	1
0.927499	0.951132	0.923929	1	0	1
0.932623	0.964082	0.944431	1	0	1
39.4	46.1	44	0	0	0
44.2	59	52.4	0	1	0
36.91	29.36	32.98	0	0	0
51.8	39.5	48.3	3	0	1
43	35.4	33	1	1	1
39.2	21.7	25.9	1	0.5	1
41.6	36.3	33.3	1	1	1
32.7	16.5	21.6	1	0	0.5
41.2	28.8	29.6	1	0.5	0.5
39.8	30.5	30.2	1	0.5	0.5
4.1	4.3	4	0	0	0
6.8	5	4.9	0	0	0
11.9	4.6	4.2	0	0	0
17.8	6	6.7	0	0	0
15.2	5.6	5.7	0	0	0
49.6	14.5	13.5	0	0	0
33.9	45	34.9	0	0	0
66.1	64.3	62	0	0	0
62.6	67.8	67.3	0	0	0
			14	2	4
			9	4.5	5.5
			23	6.5	9.5

Patient 5					
3DCRT	*RA Treat*	*RA Study*	3DCRT	*RA Treat*	*RA Study*
Dose			**Score**		
1.727053	1.113821	1.113821	2	1	1
1.641204	1.087719	1.106858	2	0	1
0.456061	0.106061	0.124242	2	1	1
0.419697	0.083333	0.101515	2	0	1
1.03449	1.06349	1.078405	0	1	1
0.734231	0.917141	0.909581	2	1	1
44	53.3	58.6	0	3	3
54.3	60.5	58.6	1	3	1
24.15	27.51	36.55	0	0	0
32	35.3	47.3	0	0	0
50.8	42.5	39.9	1	1	1
50	30	40.5	1	1	1
50.5	43.3	41.9	1	1	1
37.1	34.2	28.5	1	1	1
50.4	36.1	40.2	1	0.5	1
49.3	39.2	41.5	1	1	1
15.1	5.6	6.4	0	0	0
15.5	5.6	6.2	0	0	0
22.8	8.7	11.6	0	0	0
17.5	8.7	7.4	0	0	0
20	7.4	30.7	0	0	0
31	19.7	18	0	0	0
45.9	49.8	41.1	2	2	1
68.4	67.8	68.4	0.5	0	0.5
61.8	60.9	57.8	0	0	0
			10	4	6
			9.5	13.5	11.5
			19.5	17.5	17.5

Patient 6					
3DCRT	*RA Treat*	*RA Study*	3DCRT	*RA Treat*	*RA Study*
Dose			**Score**		
1.744681	1.072165	1.11349	2	0	1
1.177778	1.09375	1.083333	1	0	0
1.622857	1.055215	1.077083	2	0	0
1.129032	1.082474	1.061856	1	0	0
0.49	0.07	0.106	2	0	1
0.16	0.09	0.08	1	0	0
0.436	0.054	0.074	2	0	0
0.12	0.08	0.06	1	0	0
1.093197	1.232927	1.08449	1	1	1
1.263008	1.107234	1.104628	1	1	0
0.807619	0.984294	0.938367	2	0	1
0.886421	0.95368	0.961538	2	0	0
27.9	38.5	37.3	0	0	0
30.6	44.9	42.9	0	0	0
33.83	33.76	33.8	0	0	0
48	50.8	46.1	1	3	0
39.1	35.9	28.9	1	1	1
39.5	39.2	30.7	1	1	1
55.6	26.8	44.3	1	1	1
37.1	36.5	29.6	1	1	1
39.3	37.4	29.7	1	1	0.5
37.1	35.3	29.1	0.5	0.5	0.5
10.8	3.5	2.9	0	0	0
3.4	3.8	3.1	0	0	0
32.4	12	8.1	0	0	0
18.7	7.1	7.5	0	0	0
47.1	45.6	31	0	0	0
44.1	30.7	15.5	0	0	0
34.6	35	32.1	0	0	0
57.9	54.9	55.5	0	0	0
58	54.5	54.5	0	0	0
			18	2	4
			6.5	8.5	5
			24.5	10.5	9

Patient 7					
3DCRT	*RA Treat*	*RA Study*	3DCRT	*RA Treat*	*RA Study*
Dose			**Score**		
1.531073	1.121535	1.090526	2	1	0
1.163043	1.09375	1.072917	1	0	0
1.188053	1.08316	1.068465	1	0	0
1.117021	1.082474	1.061856	1	0	0
0.376	0.114	0.086	2	1	0
0.15	0.09	0.07	1	0	0
0.17	0.08	0.066	1	0	0
0.11	0.08	0.06	1	0	0
1.405102	1.256531	1.219388	1	1	1
1.625372	1.260536	1.227331	2	1	1
0.874898	0.948367	0.948571	2	1	1
0.892295	0.94934	0.948489	2	1	1
30	34.8	29.7	0	0	0
34.9	37.8	34	0	0	0
34.33	51.86	34.4	0	3	0
43.9	57.8	44.5	0	3	0
39.9	19.1	28.2	1	0.5	1
40	34.5	24.3	1	1	1
38.3	23.6	28.9	1	0.5	1
38.4	32.7	25.1	1	1	1
40	27.2	26.3	1	0.5	0.5
38.3	28.1	27	0.5	0.5	0.5
2.3	3.4	3.2	0	0	0
3	3.5	3.6	0	0	0
3.1	4.3	3.4	0	0	0
14.1	6.4	4.1	0	0	0
11	4.7	4.3	0	0	0
30.4	6.8	6.5	0	0	0
31.9	27.3	25.4	0	0	0
60.1	61.4	60.9	0	0	0
57.8	56	57.7	0	0	0
			17	6	4
			5.5	10	5
			22.5	16	9

Patient 8					
3DCRT	*RA Treat*	*RA Study*	3DCRT	*RA Treat*	*RA Study*
Dose			**Score**		
1.285714	1.096842	1.088608	2	0	0
1.323529	1.091503	1.10596	2	0	1
1.182418	1.079167	1.06639	1	0	0
1.236111	1.070968	1.084967	2	0	0
0.244	0.092	0.084	2	0	0
0.275	0.0875	0.1	2	0	1
0.166	0.076	0.064	1	0	0
0.2125	0.06875	0.08125	2	0	0
1.226739	1.120737	1.085812	1	1	1
1.286736	1.086131	1.047606	1	1	0
0.858117	0.957435	0.951296	2	0	0
0.779857	0.919923	0.894606	2	1	2
37.8	48.7	42.1	0	0	0
39.4	56.7	51.1	0	1	0
34.6	42.23	34.5	0	0	0
47.2	55.7	47.8	0	3	0
42.9	30.8	34.7	1	1	1
51.7	47.4	41.4	1	1	1
42.7	33.8	35.1	1	1	1
50.5	46.5	41.6	1	1	1
47.4	39.6	38.2	1	1	1
46.7	40.4	38.5	1	1	0.5
38.4	11.6	16.6	1	0	0
46.7	10.6	13.5	2	0	0
56.5	46.3	43.5	0	0	0
62.5	38.5	26	0.5	0	0
60.4	54.6	55.6	0	0	0
65.8	66.6	65.8	0.5	0.5	0.5
39	40.9	30.3	0	1	0
66.6	62.4	59.9	0	0	0
66.9	63.1	56	0	0	0
			20	3	5
			10	11.5	6
			30	14.5	11

uu

Patient 9					
3DCRT	*RA Treat*	*RA Study*	3DCRT	*RA Treat*	*RA Study*
Dose			**Score**		
1.456633	1.098739	1.452926	2	0	2
1.331429	1.095238	1.056701	2	0	0
1.265766	1.070393	1.265766	2	0	2
1.256831	1.072917	1.040816	2	0	0
0.358	0.094	0.356	2	0	2
0.29	0.09	0.055	2	0	0
0.236	0.068	0.236	2	0	2
0.235	0.07	0.04	2	0	0
1.23916	1.121178	1.23916	1	1	1
1.164328	1.052067	1.136805	1	1	1
0.872366	0.968366	0.872366	2	0	2
0.85564	0.942828	0.978413	2	1	0
34.4	48.4	40	0	0	0
37	50.9	44.8	0	0	0
35.74	39.1	35.27	0	0	0
48.6	49.3	50.2	1	1	3
47.2	48.9	38.1	1	1	1
52	49.8	41.7	1	1	1
47.3	48.2	38.5	1	1	1
50.1	48.1	41.9	1	1	1
49	49.2	39.5	1	1	1
48.4	48.1	39.9	1	1	1
29.8	7.6	10.2	0	0	0
20.1	5.7	9.3	0	0	0
48.6	35.8	33.3	0	0	0
49.1	36.5	35.6	0	0	0
50.4	51.9	50.4	0	0	0
50.9	51.7	51	0	0	0
47.9	39.7	32.4	2	0	0
75.5	72.5	74	1	1	1
73.4	63.5	69	1	0	0
			22	3	12
			11	8	10
			33	11	22

Patient 10					
3DCRT	*RA Treat*	*RA Study*	3DCRT	*RA Treat*	*RA Study*
Dose			**Score**		
1.176991	1.102941	1.095137	1	1	0
1.290076	1.085526	1.058065	2	0	0
1.116525	1.081081	1.068465	1	0	0
1.142857	1.064935	1.044872	1	0	0
0.16	0.098	0.09	1	0	0
0.2375	0.08125	0.05625	2	0	0
0.11	0.078	0.066	1	0	0
0.13125	0.0625	0.04375	1	0	0
1.249906	1.085499	1.09435	1	1	1
2.001995	1.056561	1.134992	2	1	1
0.916008	0.953672	0.821092	1	0	2
0.895612	0.931373	0.963801	2	1	0
32.2	22.3	27.1	0	0	0
37.3	25.8	31.2	0	0	0
33.72	37.55	34.97	0	0	0
46.1	48.3	47.8	0	1	1
40.3	29.1	27.4	1	1	1
38.4	29.1	28.2	1	1	1
38	28.2	26.1	1	1	1
35.5	26.7	25.9	1	1	1
39.3	29.1	27.9	1	0.5	0.5
37.1	27.4	26.1	0.5	0.5	0.5
10.1	2.8	2.9	0	0	0
3.4	2.3	2.2	0	0	0
13.4	3.5	3.6	0	0	0
13.2	3.2	3.2	0	0	0
20.6	5	5.4	0	0	0
16	4.3	4.7	0	0	0
28.3	26.7	19.9	0	0	0
67.2	60.8	59.8	0	0	0
66.9	55.1	53.1	0	0	0
			16	4	4
			5.5	6	6
			21.5	10	10

ww

Appendix F: Ethics approval

Cape Peninsula
University of Technology

HEALTH AND WELLNESS SCIENCES RESEARCH ETHICS COMMITTEE (HW-REC)
Registration Number NHREC: REC- 230408-014

P.O. Box 1906 • Bellville 7535 South Africa
Symphony Road Bellville 7535
Tel: +27 21 959 6917
Email: sethn@cput.ac.za

17 September 2015
REC Approval Reference No:
CPUT/HW-REC 2015/H22

Faculty of Health and Wellness Sciences – Biomedical Sciences Department

Dear Theresa Binz

Re: YOUR APPLICATION TO THE HW-REC FOR ETHICS APPROVAL

Approval was granted by the Health and Wellness Sciences-REC to Ms Theresa Binz for ethical clearance. This approval is for research activities related to staff research in the Department of Radiography Sciences at this Institution.

TITLE: A comparison between volumetric modulated arc therapy and 3D conformal radiotherapy of stage 3 and 4 carcinoma of the larynx.

Supervisor: **Ms Bridget Wyrley-Birch**

Comment:
Approval will not extend beyond 18 September 2016. An extension should be applied for 6 weeks before this expiry date should data collection and use/analysis of data, information and/or samples for this study continue beyond this date.

The investigator(s) should understand the ethical conditions under which they are authorized to carry out this study and they should be compliant to these conditions. It is required that the investigator(s) complete an **annual progress report** that should be submitted to the HWS-REC in December of that particular year, for the HWS-REC to be kept informed of the progress and of any problems you may have encountered.

Kind Regards

Mr. Navindhra Naidoo
Chairperson – Research Ethics Committee
Faculty of Health and Wellness Sciences

Cape Peninsula
University of Technology

HEALTH AND WELLNESS SCIENCES RESEARCH ETHICS COMMITTEE (HW-REC)
Registration Number NHREC: REC- 230408-014

P.O. Box 1906 • Bellville 7535 South Africa
Symphony Road Bellville 7535
•Tel: +27 21 959 6917 • Fax +27 21 953 8490
Email: lebenyat@cput.ac.za

01 December 2016 **REC Approval Reference No: CPUT/HW-REC 2015/H22**

Dear Theresa Binz

Re: Application for Renewal of Ethics Certificate:

Study: A comparison between volumetric modulated arc therapy and 3D Conformal Radiotherapy of stage 3 and 4 Carcinoma of the Larynx.

Your application to the REC for renewal of the ethics clearance on the 29 November 2016 has reference.

Please note that your extension of ethical clearance is **approved** from 01 December 2016 to 01 December 2017. Please annex this extension to your original approval.

We wish you well in your research endeavor.

Navindhra Naidoo
Chairperson: ETHICS RESEARCH COMMITTEE
FACULTY OF HEALTH AND WELLNESS SCIENCES

Cape Peninsula
University of Technology

HEALTH AND WELLNESS SCIENCES RESEARCH ETHICS COMMITTEE (HW-REC)
Registration Number NHREC: REC- 230408-014

P.O. Box 1906 • Bellville 7535 South Africa
Symphony Road Bellville 7535
Tel: +27 21 959 6917
Email: sethn@cput.ac.za

7 May 2019
REC Approval Reference No:
CPUT/HW-REC 2015/H22 (renewal)

Faculty of Health and Wellness Sciences – Biomedical Sciences Department

Dear Theresa Binz

Re: YOUR APPLICATION TO THE HW-REC FOR ETHICS APPROVAL

Approval was granted by the Health and Wellness Sciences-REC to Ms Theresa Binz for ethical clearance. This approval is for research activities related to staff research in the Department of Radiography Sciences at this Institution.

TITLE: A comparison between volumetric modulated arc therapy and 3D conformal radiotherapy of stage 3 and 4 carcinoma of the larynx.

Supervisor: Ms Bridget Wyrley-Birch

Comment:
Approval will not extend beyond 8 May 2020. An extension should be applied for 6 weeks before this expiry date should data collection and use/analysis of data, information and/or samples for this study continue beyond this date.

The investigator(s) should understand the ethical conditions under which they are authorized to carry out this study and they should be compliant to these conditions. It is required that the investigator(s) complete an **annual progress report** that should be submitted to the HWS-REC in December of that particular year, for the HWS-REC to be kept informed of the progress and of any problems you may have encountered.

Kind Regards

Cape Peninsula
University of Technology

HEALTH AND WELLNESS SCIENCES RESEARCH ETHICS COMMITTEE (HWS-REC)
Registration Number NHREC: REC- 230408-014

P.O. Box 1906 • Bellville 7535 South Africa
Symphony Road Bellville 7535
Tel: +27 21 959 6917
Email: simonsy@cput.ac.za

27 September 2020
REC Approval Reference No:
CPUT/HW-REC 2015/H22 (renewal)

Faculty of Health and Wellness Sciences

Dear Ms Theresa Binz,

Re: APPLICATION TO THE HWS-REC FOR ETHICS CLEARANCE - RENEWAL

Approval was granted by the Health and Wellness Sciences-REC to Ms Theresa Binz for ethical clearance. This approval is for research activities related to research for Ms Theresa Binz at Cape Peninsula University of Technology, Department of Radiography Sciences.

TITLE: A comparison between volumetric modulated arc therapy and 3D conformal radiotherapy of stage 3 and 4 carcinoma of the larynx

Supervisor: Ms Bridget Wyley-Birch

Comment:

Approval will not extend beyond 28 September 2021. An extension should be applied for 6 weeks before this expiry date should data collection and use/analysis of data, information and/or samples for this study continue beyond this date.

The investigator(s) should understand the ethical conditions under which they are authorized to carry out this study and they should be compliant to these conditions. It is required that the investigator(s) complete an **annual progress report** that should be submitted to the HWS-REC in December of that particular year, for the HWS-REC to be kept informed of the progress and of any problems you may have encountered.

Kind Regards

M. le Roes-Hill

Dr M Le Roes-Hill
Deputy Chairperson – Research Ethics Committee
Faculty of Health and Wellness Sciences

Western Cape Government
Health

GROOTE SCHUUR HOSPITAL
Enquiries: Dr Bernadette Eick
E-mail : *Bernadette.Eick@westerncape.gov.za*

Dr S. Dalvie
Radiation Oncology
LE34

E-mail: tjvv@gmx.de

Dear Dr Dalvie

RESEARCH PROJECT TITTLE: A Comparison Between Volumetric Modulated Arc Therapy and 3D Conformal Radiotherapy of Stage 3 and 4 Carcinoma of the Larynx (M.Tech Ms T. Binz)

Your recent letter to the hospital refers.

You are hereby granted permission to proceed with your research which is valid until **30 May 2017.**

Please note the following:

a) Your research may not interfere with normal patient care.
b) Hospital staff may not be asked to assist with the research.
c) No additional costs to the hospital should be incurred i.e. Lab, consumables or stationary may be used.
d) **No patient folders may be removed from the premises or be inaccessible.**
e) Please introduce yourself to the person in charge of an area before commencing.
f) Please discuss the study with the HOD before commencing.
g) Please provide the research assistant/field worker with a copy of this letter as verification of approval.
h) Confidentiality must be maintained at all times.
i) Should you require additional research time beyond the stipulated expiry date, please apply for an extension.
j) **On completion of research, please submit a copy of the publication or report.**

I would like to wish you every success with the project.

Yours sincerely

DR BERNADETTE EICK
CHIEF OPERATIONAL OFFICER
Date: 12 August 2016

BE/vms

C.C. Mr L. Naidoo
Professor E. Weimann
Professor J. Parkes
Ms L. Jaftha
G46 Management Suite, Old Main Building,
Observatory 7925

Private Bag X,
Observatory, 7935

Tel: +27 21 404 6288 fax: +27 21 404 6125

www.capegateway.go.v.za

bbb

Western Cape Government
Health

GROOTE SCHUUR HOSPITAL

Enquiries: Dr Bernadette Eick
E-mail : *Bernadette.Eick@westerncape.gov.za*

Dr S. Dalvie
Radiation Oncology
L-BLOCK

E-mail: s.dalvie@uct.ac.za / tjvv@gmx.de

Dear Dr Dalvie

RESEARCH PROJECT EXTENSION: A Comparison Between Volumetric Modulated Arc Therapy and 3D Conformal Radiotherapy of Stage 3 and 4 Carcinoma of the Larynx (M.Tech Ms T. Binz)

Your recent communication to the hospital refers.

The extension of your research has been approved in accordance with UCT Ethics clearance, until **1 December 2017**.

As previously mentioned:

a) Your research may not interfere with normal patient care.
b) Hospital staff may not be asked to assist with the research.
c) No hospital consumables and stationary may be used.
d) **No patient folders may be removed from the premises or be inaccessible.**
e) Please provide the research assistant/field worker with a copy of this letter as verification of approval.
f) Confidentiality must be maintained at all times.
g) Once the research is complete, please submit a copy of the publication or report.

I would like to wish you every success with the project.

Yours sincerely

DR BERNADETTE EICK
CHIEF OPERATIONAL OFFICER
Date: 12 May 2017
BE/vms

C.C. Mr L. Naidoo, Dr H. Aziz, Professor J. Parkes

UNIVERSITY OF CAPE TOWN
Faculty of Health Sciences
Human Research Ethics Committee

Room E52-24 Old Main Building
Groote Schuur Hospital
Observatory 7925
Telephone [021] 406 6626
Email: shuretta.thomas@uct.ac.za
Website: www.health.uct.ac.za/fhs/research/humanethics/forms

30 May 2016

HREC REF: 065/2016

Dr S Dalvie
Radiation Oncology
LE34

Dear Dr Dalvie

PROJECT TITLE: A COMPARISON BETWEEN VOLUMETRIC MODULATED ARC THERAPY AND 3D CONFORMAL RADIOTHERAPY OF STAGE 3 AND 4 CARCINOMA OF THE LARYNX (M.Tech candidate-Ms T Binz)

Thank you for your response to the Faculty of Health Sciences Human Research Ethics Committee received on 26 May 2016.

It is a pleasure to inform you that the HREC has **formally approved** the above-mentioned study.

Approval is granted for one year until the 30th May 2017.

Please submit a progress form, using the standardised Annual Report Form if the study continues beyond the approval period. Please submit a Standard Closure form if the study is completed within the approval period.
(Forms can be found on our website: www.health.uct.ac.za/fhs/research/humanethics/forms)

Approval is granted for one year until the 30th May 2017.

Please submit a progress form, using the standardised Annual Report Form if the study continues beyond the approval period. Please submit a Standard Closure form if the study is completed within the approval period.
(Forms can be found on our website: www.health.uct.ac.za/fhs/research/humanethics/forms)

Please quote the HREC REF in all your correspondence.

Please note that the ongoing ethical conduct of the study remains the responsibility of the principal investigator.

Please note that for all studies approved by the HREC, the principal investigator **must** obtain appropriate institutional approval before the research may occur.

The HREC acknowledge that the student, Theresa Binz will also be involved in this study.

Yours sincerely

PROFESSOR M BLOCKMAN
CHAIRPERSON, FHS HUMAN RESEARCH ETHICS COMMITTEE
Federal Wide Assurance Number: FWA00001637.
Institutional Review Board (IRB) number: IRB00001938
This serves to confirm that the University of Cape Town Human Research Ethics Committee complies to the Ethics Standards for Clinical Research with a new drug in patients, based on the Medical

ddd

Research Council (MRC-SA), Food and Drug Administration (FDA-USA), International Convention on Harmonisation Good Clinical Practice (ICH GCP), South African Good Clinical Practice Guidelines (DoH 2006), based on the Association of the British Pharmaceutical Industry Guidelines (ABPI),and Declaration of Helsinki (2013) guidelines.

The Human Research Ethics Committee granting this approval is in compliance with the ICH Harmonised Tripartite Guidelines E6: Note for Guidance on Good Clinical Practice (CPMP/ICH/135/95) and FDA Code Federal Regulation Part 50, 56 and 312.